495

ANNUAL REPORT

1969

U. S. WATER CONSERVATION LABORATORY
Southwest Branch
Soil and Water Conservation Research Division
Agricultural Research Service
United States Department of Agriculture
Phoenix, Arizona

FOR OFFICIAL USE ONLY

TABLE OF CONTENTS

CHANGES IN PERSONNEL

The Laboratory has been strengthened during 1969 by the addition of eight new members. They are as follows:

C. P. Gerba, Physical Science Technician
B. A. Kimball, Research Soil Scientist
R. S. Linebarger, Physical Science Aid
H. L. Mastin, Physical Science Technician
M. S. Riggs, Laboratory Technician (Salt River Project)
J. A. Schroeder, Physical Science Technician
C. C. Stetter, Laboratory Technician (Salt River Project)
A. Stockton, Biological Laboratory Technician

During 1969 there were seven departures. They are as follows:

G. Ekechukwu, Laboratory Technician (Salt River Project)
D. A. Forstie, Physical Science Aid
J. L. Gale, Physical Science Technician
C. P. Gerba, Physical Science Technician
P. Kuechelmann, Laboratory Technician (Salt River Project)
J. A. Schroeder, Physical Science Technician
A. Stockton, Biological Laboratory Technician

LABORATORY STAFF

Professional:

H. Bouwer, B.S., M.S., Ph.D. P.E., Research Hydraulic Engineer
K. R. Cooley, B.S., M.S., Ph.D., Research Hydrologist
W. L. Ehrler, B.A., M.S., Ph.D., Research Plant Physiologist
L. J. Erie, B.S., M.S., P.E., Research Agricultural Engineer
D. H. Fink, B.S., M.S., Ph.D., Research Soil Scientist
G. W. Frasier, B.S., M.S., Research Hydraulic Engineer
S. B. Idso, B. Phys., M.S., Ph.D., Research Soil Scientist
R. D. Jackson, B.S., M.S., Ph.D., Research Physicist
B. A. Kimball, B.S., M.S., Ph.D., Research Soil Scientist
J. C. Lance, B.S., M.S., Ph.D., Research Soil Scientist
L. E. Myers, B.S., M.S., P.E., Research Hydraulic Engineer and Director
F. S. Nakayama, B.S., M.S., Ph.D., Research Chemist
R. J. Reginato, B.S., M.S., Research Soil Scientist
J. A. Replogle, B.S., M.S., Ph.D., P.E., Research Hydraulic Engineer
R. C. Rice, B.S., M.S., Agricultural Engineer
F. D. Whisler, B.S., M.S., Ph.D., Research Soil Scientist

Technicians:

G. Ekechukwu, Laboratory Technician (Salt River Project)
E. D. Escarcega, Hydraulic Engineering Technician
D. A. Forstie, Physical Science Aid
O. F. French, Agricultural Research Technician
J. L. Gale, Physical Science Technician
C. P. Gerba, Physical Science Technician
L. P. Girdley, Engineering Draftsman
J. R. Griggs, Physical Science Technician
P. Kuechelmann, Laboratory Technician (Salt River Project)
R. S. Linebarger, Physical Science Aid
J. M. R. Martinez, Engineering Aid
H. L. Mastin, Physical Science Technician
J. B. Miller, Physical Science Technician
S. T. Mitchell, Physical Science Technician
K. G. Mullins, Physical Science Technician
J. M. Pritchard, Physical Science Technician
B. A. Rasnick, Physical Science Technician
M. S. Riggs, Laboratory Technician (Salt River Project)
J. A. Schroeder, Physical Science Technician
C. C. Stetter, Laboratory Technician (Salt River Project)
A. Stockton, Biological Laboratory Technician

Administrative, Clerical, and Maintenance:

O. J. Abeyta, Gardener
I. G. Barnett, Janitor
E. D. Bell, General Machinist
E. E. De La Rosa, Maintenance Worker
B. E. Fisher, Library Technician
C. G. Hiesel, General Machinist
R. C. Klapper, Refrigeration and Air Conditioning Mechanic
A. H. Morse, Secretary-Dictating Machine Transcriber
M. E. Olson, Clerk-Stenographer
L. J. Orneside, Clerk-Stenographer
M. A. Seiler, Clerk-Stenographer
M. F. Witcher, Clerk-Stenographer

TITLE: EXPERIMENTAL AND ANALYTICAL STUDIES OF THE FLOW AND OXYGEN REGIMES IN SOIL INTERMITTENTLY INUNDATED WITH LOW QUALITY WATER.

CRIS WORK UNIT: SWC-012-gG-1 CODE NO.: Ariz-WCL 66-1

INTRODUCTION:

The need for this study and the preliminary results are given in the 1966 Annual Report. As reported in last year's Annual Report, the prediction of the volume of drainage with time from soil columns can be made by relatively simple equations; that of Youngs [1] being the best. From the soil columns reported on under Project Code No.: Ariz.-WCL 68-3, comparisons were made between predicted and observed drainage. After some consideration it was discovered that a new set of equations would better predict the volume of drainage with time. This finding was the basis of two papers approved by Division and written by Frank D. Whisler and Ray D. Jackson on "Approximate equations for vertical nonsteady-state drainage." The following is a condensation of those papers.

THEORY:

Consider a column of soil of length L with a water table at the bottom and a height of capillary fringe h. If it is assumed that the height to the transient drainage front is Z and that the hydraulic conductivity, K, averaged over the region h to L in the column corresponds linearly to the average water content over h to L, then the drainage at time t is given by

$$- f A \frac{dZ}{dt} = A K(Z) \frac{Z-h}{Z} \qquad (1)$$

where f is the drainable porosity and A the cross-sectional area. Assuming a linear relationship for K(Z) of the form:

$$K(Z) = \frac{K_o(Z-h)}{L-h} \tag{2}$$

where K_o is the conductivity at zero pressure head, and inserting Equation (2) into Equation (1) and integrating gives

$$\frac{h}{Z-h} - \frac{h}{L-h} - \ln \frac{(Z-h)}{(L-h)} = \frac{K_o t}{f(L-h)} \tag{3}$$

Substituting the total outflow, $Q_\infty = f(L-h)$, the outflow at time t, $Q = f(L-Z)$, and the initial flux, $q_o = K_o(L-h)/L$, into Equation (3) gives

$$\frac{h}{L} \frac{Q/Q_\infty}{1-Q/Q_\infty} - (1-h/L) \ln (1-Q/Q_\infty) = \frac{q_o t}{Q_\infty} \tag{4}$$

At $h/L = 0$, Equation (4) reduces to

$$Q/Q_\infty = 1 - \exp(-\tau) \tag{5}$$

where $\tau = q_o t/Q_\infty$. This is Youngs' [1] equation. At the other limit when $h/L = 1$, Equation (4) reduces to

$$Q/Q_\infty = \tau/(\tau+1) \tag{6}$$

In studying the drainage from laboratory soil columns, it was found that outflow-time data could be statistically fitted by a least-squares technique to a two-parameter equation of the form:

$$Q = \frac{t}{at+b} \tag{7}$$

In the limit as $t \to \infty$, $Q \to Q_\infty$ hence $a = 1/Q_\infty$. Taking the derivative of Equation (7) at $t = 0$ gives the initial flux q_o, and hence $b = 1/q_o$. Thus, Equation 7 becomes

$$Q = \frac{t}{t/Q_\infty + 1/q_o} \tag{8}$$

which when transformed into terms of τ is identical to Equation 6. This equation fits the observed data with a statistical index of determination of 0.99 or better.

As was seen in last year's Annual Report and as will be shown later, Equation 5 fits the data very well for values of $Q/Q_\infty < 0.6$. For higher values of Q/Q_∞ Equation 6 is of a better form. They can be combined in a statistical manner to give

$$Q/Q_\infty = 1 - \exp[-\tau/(A\tau + B)] \tag{9}$$

where A and B are statistical parameters. As will be shown, values of A and B averaged over several soils predict quite well the drainage relationship for most soils.

RESULTS AND DISCUSSION:

Figure 1 shows the relationship between Q/Q_∞ and τ for several different soils reported in the literature. The solid curves are for different values of h/L. It can be seen that the curves for h/L = 0 and h/L = 1 bracket all the measurements.

Figure 2 shows the same relationship as Figure 1. The dashed curve is a plot of Equation 9, using the average values of A = 0.28 and B = 0.8 obtained over several soils. As can be seen, this statistical equation predicts quite well

the bulk of the experimental outflow-time relationships. In the papers more detail is given for individual soils and parameters.

One other advantage of an equation like Equation 8 is that if one measures the outflow-time relationship for a column of soil and has a statistical curve fitting program available, then q_o and Q_∞ can be predicted. These are important parameters in other applications.

SUMMARY:

An equation has been developed from basic flow theory that predicts very well most experimentally observed drainage-time relationships. This equation has as its upper limit Young's equation, which predicts the drainage-time relationship very well over the first 60 percent of the drainage. The lower limit of this equation predicts the shape very well of the last portion of the drainage and can be used to predict the conductivity and total outflow from a soil column. A statistical combination of the two limit equations predicts the drainage-time relationship better than any published equation known to the investigators. There are two statistical parameters in this statistical equation which when given average values from several soils do a very good job of predicting the drainage-time relationship.

REFERENCES:

1. Youngs, E. G. The drainage of liquids from porous materials. Jour. Geophys. Res. 65:4025-4030. 1960.

PERSONNEL: Herman Bouwer, Frank D. Whisler, and Ray D. Jackson

CURRENT TERMINATION DATE: March 1973

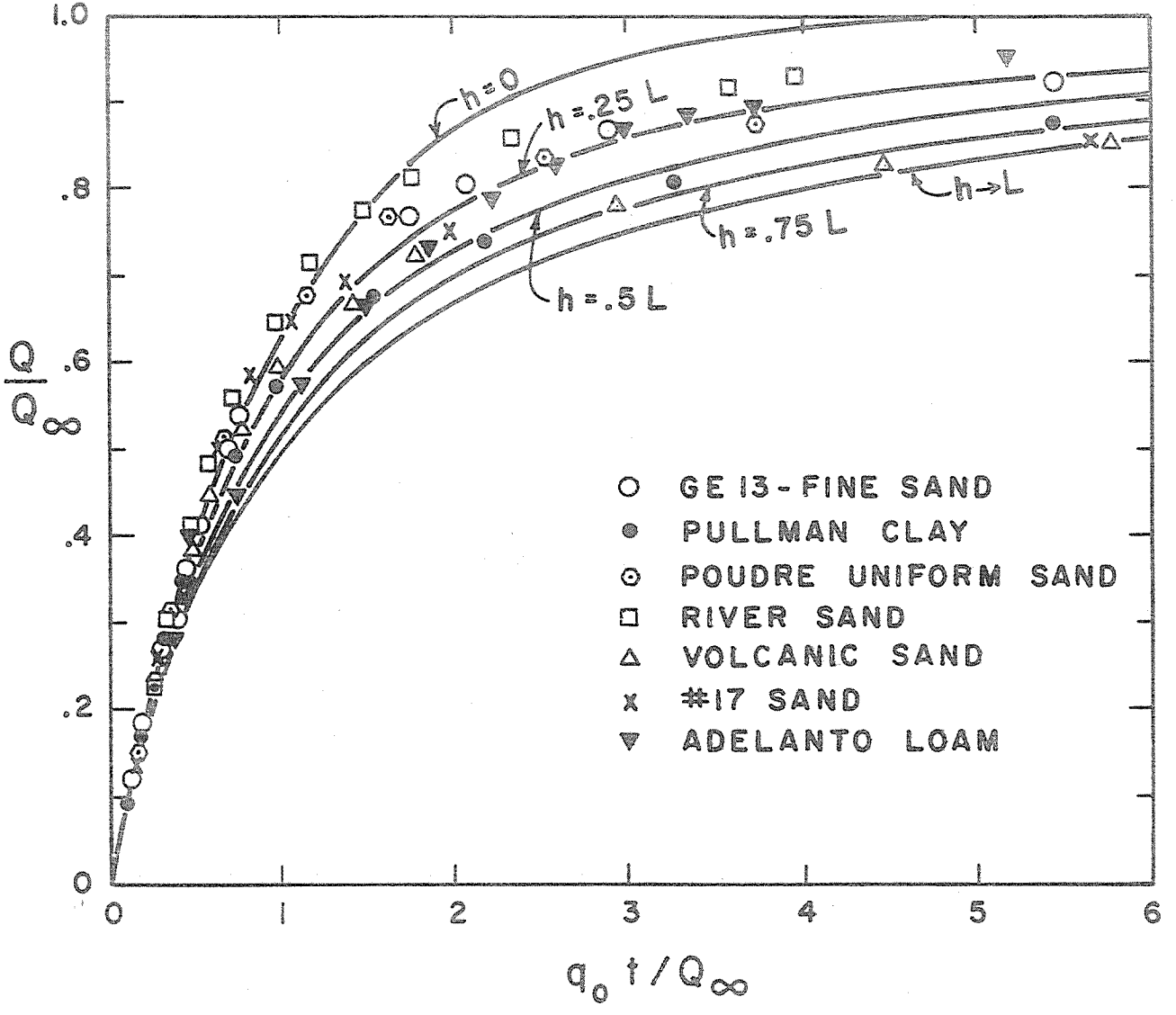

Figure 1. Experimental outflow versus reduced time data for seven porous materials and theoretical outflow curves calculated using

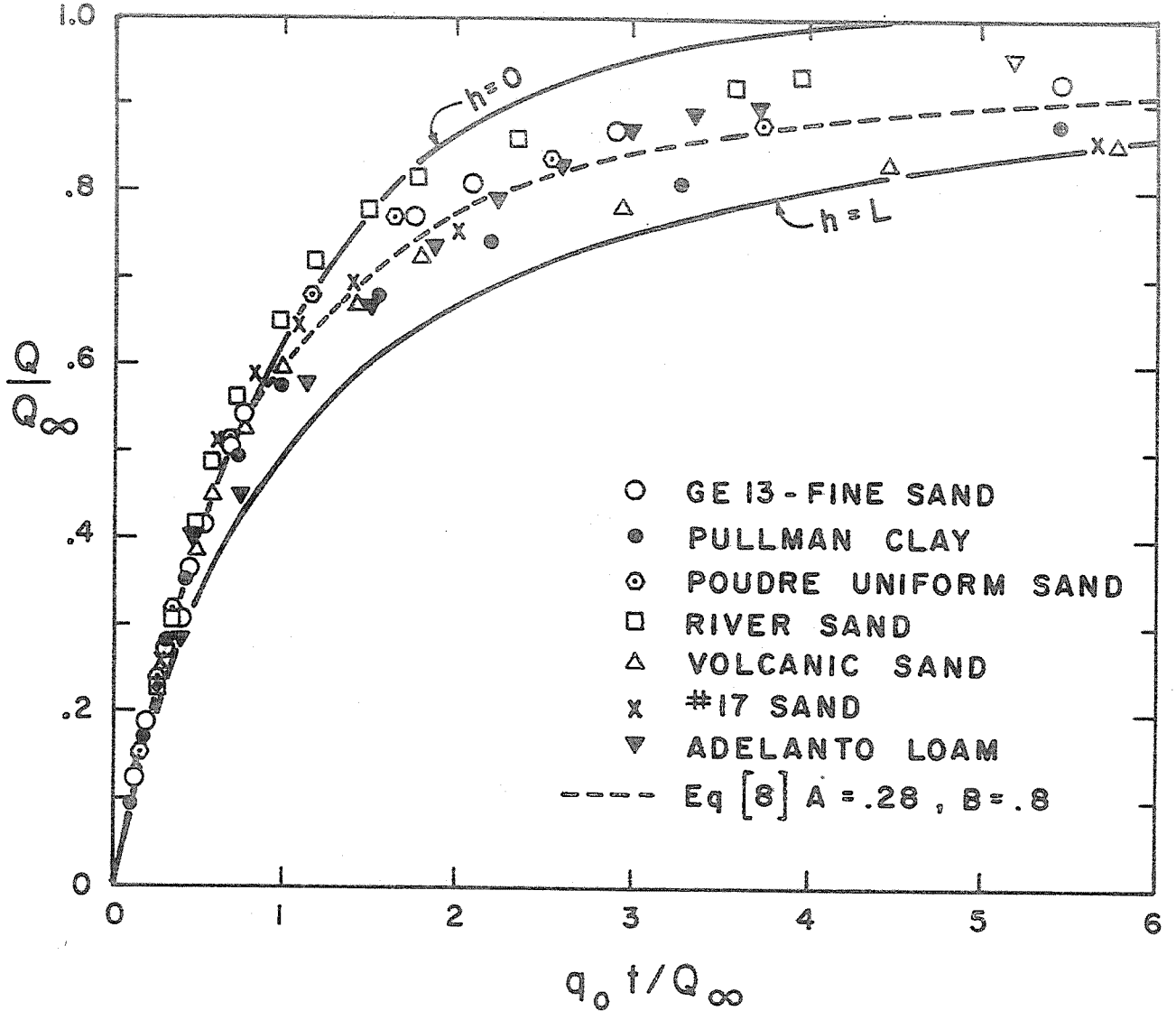

Figure 2. Outflow ratio versus dimensionless flux ratio for seven soil materials. The solid curves are the upper and lower limits of Equation 4, and the dashed curve is the relationship predicted by Equation 9 for A = 0.28, B = 0.8

TITLE: WASTE-WATER RENOVATION BY SPREADING TREATED SEWAGE FOR GROUND-WATER RECHARGE

CRIS WORK UNIT: SWC W4 gG1 CODE NO.: Ariz.-WCL 67-4

INTRODUCTION:

The year of 1969 was the second year of full scale operation of the Flushing Meadows Project, which is an experimental facility for reclaiming water from secondary sewage effluent by ground-water recharge with infiltration basins. In the first half of the year, the effluent had a high suspended solids content, which made it necessary to mostly use long dryup periods and relatively short inundation periods. The effluent cleared up in June-July, so that sequences of long inundation periods could be held in the second half of the year. In two basins, rice was grown on a trial basis. Because horizontal flow through the grass did not have a measurable effect on the quality of the effluent, all basins were operated in parallel for 1969.

Additional construction included a permanent effluent pond and two lined reservoirs which will be filled with reclaimed water from the East Well for fish and algae studies.

The excellent cooperation with the Salt River Project, which received a grant from the Federal Water Pollution Control Administration for partial support of the project, was continued in 1969. The grant terminated at the end of 1969, at which time the financial support for the two laboratory technicians was taken over by the Salt River Project.

To facilitate orderly presentation of the results, the project is divided into five sections: I. Infiltration Studies, II. Water Quality Studies, III. Aquifer Studies, IV. Design of Large Scale Recharge System, and V. Laboratory Filtration Studies. A section with summary and conclusions is listed at the end of the report.

I. INFILTRATION STUDIES

1. Recharge basin management and infiltration rates

A plan of the Flushing Meadows Project is shown in Figure 1. New construction included perforating the East Well (EW) and the installation of one unlined pond and two lined ponds to be supplied with water from the East Well, which yields reclaimed sewage water. The unlined pond will be used to evaluate how "aging" affects seepage in an unlined reservoir. The lined ponds, which have a fiberglas-asphalt lining, will be used to study algae and fish growth in ponds with reclaimed sewage water. Another new construction is the "permanent" effluent pond which is located near the effluent pump. This pond will be kept under continuous inundation with secondary effluent to evaluate infiltration behavior with no dryup periods.

At the beginning of 1969, basin 1 was in bare soil condition, basin 2 had the gravel layer (2 inches of coarse sand topped by 4 inches of 3/8 inch gravel), and basins 3, 4, 5, and 6 had the dead bermudagrass left from the 1968 growing season.

The secondary effluent from the 91st Avenue sewage treatment plant was generally poor in quality from January until July. It had a high suspended solids content which gave it a black appearance and Secchi disk readings of only a few inches. The COD of the effluent after letting it settle for a few days was in the 60 ppm range. In July, the quality of the effluent improved considerably and a clear effluent prevailed for the rest of the year. The COD during the second half of the year was in the 40 ppm range.

The high suspended solids content in the beginning of the year caused a layer of sludge to accumulate in the basins. For the vegetated basins, this sludge blanket formed on top of the dead-grass cover. Because of this, the infiltration rates were relatively low, even when the water depth was 13 inches (open circles in Figure 2). The increase in infiltration rate due to increasing

the water depth from 7 to 13 inches on 15 January exceeded the increase attributable to the increase in depth and width in the basins. This is because the portion of the banks inundated after the depth increase was not covered by sediment, and it had therefore a higher infiltration rate than the bottom of the recharge basins. Two weeks drying at the end of January did not restore the infiltration rates, but after a 2-week dryup at the end of February the infiltration rates were significantly increased. Just before the inundation period starting 3 March, basins 3, 4, 5, and 6 were burned. Only the top layer of the mat of dead bermudagrass, which was about 4 inches thick, was dry enough to burn effectively. The inundation period 3-17 March started with fairly high infiltration rates for the vegetated basins, but because of the high suspended solids content in the effluent the infiltration rates declined rapidly.

In the last week of the dryup period 22 March - 6 April, basin 1 was swept with a power lawnsweeper, which removed most of the dried sludge flakes, and then harrowed with a spike-tooth harrow. Basin 2 was left unchanged because the sludge flakes pulverized and raking or sweeping the gravel surface was not effective. Basins 3, 4, 5, and 6 were burned several times and harrowed in between burnings to loosen up the mat of dead grass. This procedure was fairly effective and when the next inundation period started on 7 April, these basins were essentially in bare soil condition. The inundation period 7-9 April yielded high infiltration rates (2 to 3 ft/day) for basins 3, 4, 5 and 6. The bare soil basin 1 had a rate of 1.5 ft/day and the gravel basin 2 had the lowest infiltration, 1 ft/day.

On 14 April, basin 6 was harrowed and seeded with rice (variety Caloro) using a hand-operated, broadcasting seeder. After seeding, the basin was dragged with a chain and harrowed. All basins were then inundated for two days (14-16 April), employing a water depth

of 7 inches.

On 21 April, basins 1, 3, 4 and 5 were harrowed again and basin 5 was seeded with rice. For the next few months (until July), the inundation periods for basins 5 and 6 were short and frequent (see Figure 2) for germination and growth of the rice. When the rice had grown sufficiently so that it was well above the water, longer inundation periods were used (July, August, and September). Unusually cold weather in April and May delayed the growth of the rice, but excellent growth was obtained thereafter to give a dense, tall vegetation for the summer and fall periods. In the middle of June, the rice was about 1 ft tall, in July it had reached a height of 3 ft.

Because of the continued black appearance and high suspended solids content of the secondary effluent, short inundation periods were also maintained in the other basins for the April-July period. At the start of the inundation period, infiltration rates were relatively high, but then they declined rapidly because of the buildup of a sediment layer on the bottom of the basins (see, for example, the infiltration rates in the first half of June). For May and June, the infiltration rates were generally close to 1 ft/day, except for basin 4, which sometimes reached 2 ft/day at the start of the period. The giant bermudagrass in basins 3 and 4 made a very slow comeback. The Tifway had completely died and there were only sporadic tufts of giant bermudagrass (one tuft for every 2 or 3 yd^2). During the frequent short inundations in May and June, however, the bermudagrass spread rapidly especially from the banks. Also, "native" grasses, mainly Mexican sprangle top (Leptochloa uninervia) and barnyard grass (Echenochloa crusgalli) came in and exhibited a luxurious growth, particularly in basin 1. A third grass, probably blue panicum, also volunteered in basins 1, 3 and 4. Blue panicum was seeded in 1968 in a few strips across several basins and may have reseeded itself. Thus, the condition

of the basins for the summer and fall of 1969 was as follows:

Basin 1, dense stand of sprangle top, barnyard grass and blue panicum

Basin 2, gravel layer

Basins 3 and 4, giant bermudagrass with sprangle top and barnyard grass and some blue panicum

Basins 5 and 6, rice with giant bermuda and some sprangle top, barnyard grass and blue panicum

Because of the accumulation of sludge, basins 1, 2, 3 and 4 were subjected to a 2-wk dryup period in the second half of June. This was effective in restoring infiltration rates and also at this time the effluent improved in quality. Because of this, "normal" infiltration rates were again obtained. In the rice basins, shorter dryup periods were used than in the other basins for the summer months.

On 9 August, a pump failure occurred so that the rice was dry for almost 6 days. This happened during a very hot period and it caused visible damage to the rice. Although the rice seemed to recover fully, not much grain was formed and also because of lodging later on, no attempt was made to harvest the grain.

A sequence of long inundation and dryup periods was started in August, with the rice basins receiving "extra" inundations during the dryup period until 15 October. On 20 November, the vegetation in basins 1, 3, and 6 was mowed, baled, and removed. Basins 4 and 5 were not mowed, so that the effect of mowing on infiltration during the winter and spring seasons could be evaluated. Thus, the condition of the basins at the start of the winter was as follows:

Basin 1, stubble of sprangle top and barnyard grass

Basin 2, gravel layer

Basin 3, stubble of bermudagrass

Basin 4, dead bermudagrass (about a 4-inch thatch layer)

Basin 5, dead rice straw (forming a 2-3 inch thick layer)

Basin 6, rice stubble

The infiltration rates in Figure 2 show that, generally, short dryup periods are not effective in restoring infiltration rates. In the summer, dryup periods should be at least a week, and in the winter, 2 wks, if a significant restoration of the infiltration rate is to be obtained.

Because of the short dryup periods, the infiltration rates in the rice basins 5 and 6 from April to October were about 1 ft/day. Since these basins were inundated for a relatively high percentage of time, however, the accumulated infiltration for the rice basins was still appreciable. Figure 3 shows that the rice basin 5 yielded the highest accumulated infiltration rate for the year.

Most of the reduction in infiltration rate during inundation was caused by clogging of the surface layer of the soil. This is evidenced by the change in infiltration rate due to increasing the water depth in the basins from 7 to 13 inches, as was done on 15 January, and reducing it from 13 to 7 inches as was done on 4 December (Figure 2). On 4 December, for example, the infiltration rate was reduced by an average factor of 0.57 (Table 1). Assuming that the reduction in water depth caused the width of the water surface in the basins to change from 20 ft to 18 ft, the reduction in infiltration rate should be by a factor of $\frac{18}{20} \times \frac{7}{13} = 0.485$ if surface clogging occurred. If the fine sandy top layer, which averages about 3 ft in depth for the basins, would have clogged as a whole, the infiltration reduction factor would have been $\frac{18}{20} \times \frac{36 + 7}{36 + 13} = 0.79$. Since the actual reduction factor is below 0.6 for most of the basins (Table 1) it is concluded that most clogging took place near the surface of the soil.

As regards clogging in the gravel basin, the water depths in this basin refer to the surface of the original soil material.

Since the combined sand and gravel layer is 6 inches thick, the actual water depth above the gravel is about 1 inch for the 7-inch depth, and 7 inches for the 13-inch depth. If clogging in this basin were due to the growth of algae on top of the gravel layer, the infiltration rate would have been reduced seven-fold by decreasing the water depth above the original soil from 13 to 7 inches. The actual reduction was almost two-fold (Table 1), indicating that soil clogging in basin 2 also occurred near the surface of the original soil, and probably at the soil-gravel interface.

When the basins were all in bare soil condition (from September 1967 to April 1968), rain at the end of a dryup period caused the infiltration rate for the ensuing inundation period to be significantly reduced (see Annual Reports 1967 and 1968). On 15 September 1969, however, the basins were covered by a dense vegetation, and 0.6 inches rain fell just before the start of a new inundation period (Figure 2). As shown in Figure 2, this rain had little or no effect on the infiltration rate. Thus, reductions in infiltration rate due to rain when the basins were in bare soil condition must be attributed to the mechanical impact of the rain on the soil surface (translocation of fine particles and sealing).

Accumulated infiltration amounts for each basin in the year 1969 are shown in Figure 3. The average yearly infiltration amount for all basins was 227 ft, which is higher than the 161 ft obtained in 1968. In 1967, a total infiltration of 73 ft was obtained, following the start of the project on 20 September 1967. Thus, as of 31 December 1969, the average accumulated infiltration for all six basins was 461 ft.

The slope of the curves in Figure 3 indicates that the rate of recharge in the second half of the year was much higher than in the first half. This is undoubtedly due to the improvement of the effluent quality in July. Of the total of 227 ft infiltrated

in 1969, 160 ft infiltrated in the second half of the year. Thus, for a good effluent quality with little suspended material and using long inundation and dryup periods, an annual recharge rate of 300 ft should well be attainable.

Figure 3 shows that the rice basin 5 gave the highest infiltration rate, followed closely by grass basin 4. Grass basins 1 and 3 were very close, rice basin 6 was the lowest of the vegetated basins, and the gravel basin 2 was the lowest of all basins. In evaluating the effect of surface condition and basin management on infiltration, the "natural" infiltration capability of the basins due to soil variability should be taken into account. This capability is probably best reflected by the infiltration rates when the basins were flooded for the first time and hence still free from sediment and effects from biological processes. The first inundation period was from 21 to 26 September 1967, at which time the effluent was very clear and the infiltration rates remained fairly constant. Listing the basins in order of decreasing infiltration rates, the following rates were observed for that period:

Basin	Infiltration rate in ft/day
2	4.0
5	3.9
4	3.6
1, 3	3.2
6	3.1

The curves in Figure 3 show that this order was essentially maintained in 1969, with the exception of the gravel basin, which moved from the top to the bottom of the list. Hence, the gravel layer has an unfavorable effect on the infiltration rate, probably because the gravel acts as a mulch and prevents drying of the surface of the underlying soil where most of the clogging occurs.

2. Effect of surface condition on wetting and drying of soil profile.

The (negative) pressure head and content of water in the soil beneath the recharge basins were again measured occasionally with tensiometers and neutron probes in basins 1, 2, 5 and 6. Pressure heads and water contents during drainage were measured in basin 2 from 30 September to 15 October and in basin 6 from 10 October to 15 October. On 15 October all the basins were flooded and remained inundated until after 29 October. The pressure-head profiles for these basins on 15 October before flooding and 17 October after the start of an inundation period are shown in Figure 4. The pressure heads in basin 2 changed little, indicating that little drainage had taken place during the dryup period. Basin 6 had drained to a much lower water content, as evidenced by the increase in pressure due to wetting. The water content profile for basin 6 on 15 October before flooding and on 22 and 29 October in the inundation period are shown in Figure 5. This figure shows that the soil moisture content in basins 2 and 6 both increased after wetting. Thus, there is a discrepancy between the pressure head and water content behavior of basin 2. Perhaps this is caused by slow or plugged tensiometers. Figure 6 shows the water pressures in the soil profile for basins 2 and 6 for 17 and 29 October. They indicate that during inundation little additional soil clogging took place, except basin 2 which might have had some clogging above the 10 cm tensiometer.

II. WATER QUALITY STUDIES

1. Sampling, observation wells, and analytical techniques

A simple, dipstick type sampler was constructed to obtain continuous samples of the secondary effluent (Figure 7). The dipstick consists of ¼-inch metal tubing. The tubing is closed at the dipping end and about 1 inch from this end a hole is cut through which effluent can enter. A wheel, driven by an electric motor, lowers the dipstick into the fluid to be sampled, after which the stick is raised so that it empties at the other end into a bottle. The device collects about 4 ml of effluent every 2 minutes. Over a 24-hour period, about 3 liters of effluent (about 3/4 gal) are obtained. The dipstick is equipped with another hole closer to the end which is normally taped but open for weekend sampling, so that a smaller sample is collected and the sampler can run through the 72-hr weekend period. The volume collected in that time is about 5 liters. The sampler was placed at the headbox of the inflow flume of one of the basins. Samples of the effluent were taken whenever inundation periods were held. Each sample was analyzed for NH_4, NO_3, and COD. P and F were determined monthly, and B bimonthly. Periodically, Kjeldahl N, pH, and salt content were determined. Since the effluent from the sewage treatment plant is the influent for the Flushing Meadows Project, the terms effluent and influent are used interchangeably in this report.

The East Well (EW, Figure 1), which was 250 ft deep and completely cased, was sealed at the bottom with a concrete plug and perforated from 10 to 30 ft depth to pump reclaimed sewage water. A submersible pump was installed in the fall of 1969 and the flow from this well will be used for the study of growth of algae and fish in the two lined ponds.

Well 5-6, which had a very slow response since its installation, was "opened up" at the bottom by driving in a rod and working it

around. Loose material was then bailed out with a hand bailer. This operation, which was done in October, increased the response of the well considerably and enabled better sampling. A summary of the wells at the Flushing Meadows project and the depth from which ground water is obtained is shown in Table 2. The 91st Avenue well is an irrigation well located about 1½ miles east of the Flushing Meadows Project. Wells 8 and 91st Avenue yielded native ground water, the WCW yielded native ground water for the first half of the year (see II.8 Dissolved salts), and the other wells yielded reclaimed sewage water.

Wells 1-2, ECW, and 5-6 were sampled almost daily for NH_4 and NO_3 analysis. COD was determined weekly, P and F monthly, and B bimonthly. BOD_5 was determined about once every 2 months for ECW water. Coliform and fecal streptoccus densities were determined weekly for ECW and well 7. Samples from wells 1, 7, 8, WCW, and 91st Avenue were taken monthly for determination of COD, NH_4, NO_3, P, F, B, TDS, and pH. The analytical methods were the same as reported last year, and dichromate technique for COD, distillation for NH_4, brucine for NO_3, Murphey & Riley method for P, curcumin for B, SPADN for F, and multiple tube fermentation techniques for the coliform and fecal streptococcus counts.

2. Chemical oxygen demand

COD of influent and reclaimed water from ECW, well 1-2, and 5-6, are shown in Figure 8. For the first five months, the COD of the influent was in the 50 to 70 ppm range and for the last six months in the 40-50 ppm range. This drop in COD paralleled an improvement in the appearance of the effluent, which was black and dirty in the first half of the year and clear in the second half. COD of the reclaimed water was generally in the 10 to 20 ppm range. Comparing the 3 wells in Figure 8 shows that well 1-2 yielded a slightly higher COD and well 5-6 a slightly lower COD than ECW. This may be due to the fact that well 1-2 is 20 ft

deep compared to the 30-ft depth of the ECW and that well 5-6 is in finer soil material.

COD values of the reclaimed water from wells 1, 7, and the East Well were generally in the 10 to 20 ppm range (Table 3), the COD of the native ground water (well 8, WCW, and 91st Avenue well) was in the 10 to 30 ppm range.

3. Biochemical oxygen demand

BOD_5 of ECW did not exceed 2 ppm and was less than 0.5 ppm for the summer months. The slightly higher BOD in the spring and fall may have been caused by the decaying vegetation in the basins, which could have added soluble carbon to the influent. The BOD analyses were performed by the laboratory of the 91st Avenue Phoenix sewage treatment plant and the cooperation received is gratefully acknowledged.

4. Nitrogen

The total nitrogen content of the influent, obtained by adding organic N (which runs about 1 ppm) to NH_4-N, is shown in Figure 9, along with the NH_4-N and NO_3-N in the water from ECW. In the first half of the year, influent N was mostly in the 30-35 ppm range, in the second half it was more in the 20-30 ppm range.

As in 1968, the NO_3-N in the reclaimed water from ECW depended on the length of the inundation period with long periods (about 2 wks) yielding low NO_3-N concentrations and short periods (2-4 days) yielding high NO_3-N concentrations. Again a peak in NO_3-N was observed 5 to 11 days after the start of a long inundation period, because of the arrival of nitrified effluent held as capillary water during the preceding dryup period (see also section III.3.). The low NO_3-N concentration after burning grass in basins 3, 4, 5, and 6 on 3 March were slightly higher than those in January and February when the full mass of dead bermudagrass was still present. In the fall months, full vegetation had again developed and low NO_3-N concentrations of essentially 0 were reached.

The NH_4-N concentration in ECW water increased gradually from 4 to 12 ppm during the first half of the year and then decreased gradually after July to reach the 4-5 ppm range again in November. This is an interesting trend and several speculations as to the causes can be made, for example, temporary deactivation of nitrifying bacteria due to antagonistic or other effects, higher COD and N concentrations in the influent for the first half of the year, release of stored NH_4 in the soil, etc. Because of the high NH_4-N concentrations in the period of short, frequent inundations (May-August), the NO_3-N concentrations in that time were not as high as during previous cycles of short inundation periods when almost all the influent N was converted to NO_3-N (see Annual Report 1968). However, NH_4-N + NO_3-N were about equal to the influent N during the May-August period of 1969. It is also interesting to note that as NH_4-N in ECW gradually increased during May-July, the NO_3-N in ECW paralleled the decrease in influent N during that period.

Figure 9 shows that after the appearance of the NO_3-peaks, total N-concentrations of 5-6 ppm prevailed in the reclaimed water of ECW during the fall period. Since the influent N was about 26 ppm, a nitrogen removal of about 80 percent was accomplished. The reclaimed water with the NO_3- peaks could be used for irrigation where a high N-content is desirable. Also, this water could be denitrified by recycling or by adding methanol in anaerobic lagoons or denitrifying stacks. From an air pollution standpoint, denitrification is preferable over ammonia stripping.

The NO_3-N concentration in ECW-water is shown again in Figure 10, along with the NO_3-N concentration in wells 1-2 and 5-6. For the first few months, the NO_3-peaks were much higher in well 1-2, and much lower in well 5-6 than in ECW. This may be due to the fact that well 1-2 is located between basins 1 and 2 which were

nonvegetated during this period. Also, well 1-2 is shallower than ECW (Table 2). Well 5-6 is also 20 ft deep but it is in finer soil material. In the fall, when basin 1 was also vegetated, the NO_3 peaks in well 1-2 were lower and about the same as in ECW. Peaks in 1-2 occurred sooner than in ECW. No samples from well 1-2 were taken during the inundation period November 21-December 8 because the water levels in the wells were measured daily during that period (see section III.1.). From the NO_3-N concentrations in ECW during that period, it seems likely that a NO_3 peak also would have occurred in well 1-2. Thus, the line connecting the NO_3 points for well 1-2 from November to December most likely does not present the true course of the NO_3-concentrations for that period.

The low NO_3-N concentrations in Well 1-2 during long inundation periods were higher in the January-April period, when basin 1 was not vegetated, than in September-December when basin 1 had a dense stand of volunteer grasses.

During the sequence of frequent short inundation periods in April-July, NO_3-N concentrations in all three wells were about the same, with the exception of August when the NO_3-N in well 1-2 was higher than in 5-6 and ECW.

The NO_3-N and NH_4-N concentrations for the other wells are shown in Tables 4 and 5, respectively. The NO_3-N concentrations for wells 1 and 7 dropped in August and September in response to the change from frequent short inundation periods to long inundation periods. Low nitrate concentrations were also observed for the East Well, for which sampling began 28 November. The WCW and 91st Avenue wells, which yielded native ground water, showed NO_3-N concentrations of 2 to 6 ppm. The NO_3-N concentration in well 8, which also yielded native ground water was lower, i.e., 0-2 ppm. Well 8 is 20 ft deep, whereas WCW and 91st Avenue tap the ground water from greater depths (see Table 2). The NH_4-N concentrations

generally ranged from 1 to 4 ppm for the wells yielding reclaimed water and they were essentially 0 for the native ground water (Table 5).

Since the nitrogen removal takes place only for the long inundation periods (10 days or more) when the oxygen supply in the soil is not as plentiful as for the short periods, the nitrogen removal tends to be more complete below vegetated basins than below non-vegetated basins, it is logical to attribute the nitrogen removal at least partly to biodenitrification. Other mechanisms for removing nitrogen from the waste water as it percolates through the soil are ammonium adsorption by clay and organic matter, and nitrogen fixation in bacterial tissue and other living organisms in the soil. Ammonium nitrogen seems to be more easily assimilated by the organisms than nitrate nitrogen. Estimates of how much nitrogen could be removed by these processes are presented below.

a. Ammonium adsorption by clay. Adsorption of NH_4 by the clay fraction in the surface soil and the deeper soil deposits could take place during long inundation periods when oxygen for nitrification may be limiting and most of the nitrogen in the effluent could remain in the form of NH_4. The sandy and gravelly materials at Flushing Meadows, however, contain very little clay. The clay content of the upper 3 ft of fine, loamy sand is not more than 2 percent, whereas the underlying coarse sands and gravels contain essentially no clay. Thus, if for the first 30 ft or 10 m of soil (the depth of ECW) an average clay content of 1 percent is assumed, this will be on the liberal side. Since the NH_4-ion is close to the Na-ion in adsorptive properties, the exchangeable sodium percentage (ESP) can be used for the exchangeable ammonium percentage. To determine ESP, the sodium adsorption ratio (SAR) for the water must be known ($SAR = Na^{+}/\sqrt{Ca^{++} + Mg^{++}})/2$, where ionic concentrations are expressed in meq/l). The value of ESP can then be determined and knowing the exchange capacity of the clay fraction, the amount

of ammonium that will ultimately be adsorbed by the clay can be calculated.

The concentrations of Ca, Mg, and Na in the effluent are 82, 36, and 200 mg/l, respectively, which corresponds to 4.1, 3.0, and 8.7 meq/l. This gives SAR = 4.7, which yields an ESP-value of 5.2 percent, according to Figure IV on page 165 of Water Quality Criteria (1).

The dry density of the soil is about 1.5, so that a 10 m depth contains 1500 gm of dry soil per cm^2 surface area. At 1 percent clay, this would contain 15 gm clay and assuming an exchange capacity of 100 meq/100 gm clay, the total exchange capacity would thus be 15 meq. For an exchangeable ammonium percentage of 5.2 percent, this amount of clay will thus adsorb 15 x 0.052 = 0.78 meq of NH_4, or 0.78 x 14 = 10.9 mg of NH_4-N. Since the NH_4-N concentration of the effluent is about 25 ppm, this amount of NH_4-N is contained in 0.437 liters effluent. Per cm^2 surface area, this corresponds to an accumulated infiltration of 437 cm or about 14 ft, which infiltrates in about 1 wk. Thus, after about 1 wk the ultimate adsorption capacity of the clay for ammonium is reached. The conclusion is therefore that nitrogen removal by adsorption of ammonia on clay is insignificant for the Flushing Meadows Project.

b. Nitrogen fixation in bacterial tissue. As the nutrients in the effluent cause an increase in the bacterial population of the soil and as bacteria and other organisms continually grow and die, some of the nitrogen undoubtedly goes into bacterial tissue. If this would be the major mechanism for nitrogen removal, however, it is difficult to see why it would be effective only for the longer inundation periods and not for the short periods when essentially no nitrogen removal is observed, even though ammonium nitrogen may be more readily assimilated by the bacteria than nitrate nitrogen. Another factor limiting the nitrogen removal by fixation in

bacterial tissue is the soluble carbon content of the effluent. Assuming, for example, that the COD of the effluent, which is about 50 mg/l, is entirely due to carbohydrates, the C-content of the effluent would be 19 mg/l. Assuming a C/N-ratio of 7 in dry bacterial matter, removal of 20 mg N/l as obtained at Flushing Meadows during long inundations, would require 140 mg C/l. This is about 7 times as much as the actual C-content of the effluent, so that the carbon supply in the effluent severely limits the amount of nitrogen that can be fixed in bacterial tissue.

The population of aerobic bacteria in the soil beneath the recharge basins was determined by plate count techniques. The results (Table 6) show that the population ranges from 100 million to 400 million per gram of dry soil, which is about 10 times as much as the 1 to 50 million range usually reported for agricultural soil (2, 4). Since the plate count tends to yield only a small fraction, for example, a few percent of the entire bacterial population, the actual population in the soil can be expected to be about 2 orders of magnitude higher.

Lyon, et al (2), indicate that a furrow slice of soil may contain 1000 lbs of fungi, 500 lbs of actinomycetes, and 500 lbs of bacteria, all per acre. This amounts to a total of 0.02 gr/cm^2 of soil. Since a furrow slice is about 15 cm deep, and the fine loamy sand layer of the Flushing Meadows profile is about 90 cm deep, this figure would have to be multiplied by 90/15 = 6 for the Flushing Meadows profile. The assumption will be made that the bacterial population in the coarse sands and gravels below the 90 cm fine loamy sand is negligible. Also, because bacterial populations tend to decrease with depth, it will be assumed that the total microflora in the Flushing Meadows profile is 10 times that of an agricultural soil. Thus, the total weight of fungi, actinomycetes, and bacteria in the Flushing Meadows profile can be calculated as 6 x 10 x 0.02 = 1.2 gm per cm^2 of surface area.

Assuming 20 percent dry matter content and 12 percent N in the dry matter of the microflora, the nitrogen in the 1.2 gm of bacteria, etc., is 0.2 x 0.12 x 1.2 = 0.0288 gm. This amount of nitrogen is contained in about 1.2 l of effluent, which per cm^2 is equivalent to a total infiltration of 1200 cm or about 40 ft, which occurs in about 20 days of inundation. Thus, the nitrogen in the bacteria and other microflora in the soil is small compared to the amounts of nitrogen removed from the effluent.

c. Ammonium adsorption by organic material. Another mechanism for nitrogen removal would be nitrogen fixation in relatively stable organic material formed by bacterial debris, and adsorption of ammonium thereon. To get an estimate of the amount of nitrogen that may be held in the soil in this manner, total nitrogen in the soil from the recharge basins was measured and compared with that in the virgin soil outside the project area. The soil nitrogen was determined with the Kjeldahl technique using the salicylic acid modification to obtain total nitrogen. The results (Table 7) indicate that the soil beneath the recharge basins contains about 1 mg N more per gr of dry soil than the natural soil outside the basins.

Assuming that nitrogen is primarily fixed in the fine sandy top layer, (which averages about 90 cm in thickness), and not in the underlying coarse sands and gravels, the total nitrogen increase in the soil beneath the recharge basins would be 90 x 1.5 x 1 = 135 mg per cm^2 surface area. The factor 1.5 in this product is the density of the dry soil. This amount of nitrogen is contained in about 5 liters of sewage effluent, which per cm^2 surface area corresponds to a total infiltration of 5000 cm or 170 ft. Since the total infiltration by the end of December 1969 is about 460 ft, and since high rates of nitrogen removal were obtained only when long inundation periods were employed, it

can be concluded that nitrogen fixation in the soil may play an important role in the nitrogen removal process.

The above analyses show that adsorption of ammonia on clay and fixation of nitrogen in live bacterial tissue can remove a small quantity of nitrogen only. Thus, the main mechanisms for nitrogen removal must be fixation in and adsorption to stable organic matter and biodenitrification. Continuation of the research to determine the maximum nitrogen storage capacity in the soil and how much nitrogen is removed by denitrification once this maximum capacity is reached, will be desirable.

5. Phosphates

The phosphate concentrations, expressed in mg P/l in Figures 11 and 12, show the P-concentration of the influent ranged from 18 to 32 mg/l. Figure 11 shows that this concentration is reduced by more than 50 percent in the reclaimed water from ECW and well 1-2. P-concentrations in the 5-6 well are lower, probably because the soil at the bottom of this well is of much lower permeability, and hence of finer texture, than at the other wells.

Figure 12 shows that the P-concentration in wells 1 and 7 was generally below 5 ppm, which is lower than that in ECW and well 1-2. Thus, the additional lateral movement of reclaimed water below the water table yielded additional removal of P. The same is true for the East Well, which had a P content of 3.5 ppm in December (see Table 8). The P-concentration in the native ground water ranged from 0 to 1 ppm (well 8 in Figure 12, WCW and 91st Avenue well in Table 8).

The phosphate removal will probably mainly be due to precipitation in the soil, some as fluor-apatites, but probably mostly as oxy-apatites. Taking the formula for oxy-apatite as $3Ca_3(PO_4)_2.CaO$ and the density as 3.2, 1 cm^3 of oxy-apatite will contain 604 mg P.

Assuming that 20 mg P are removed per liter of effluent, 1 cm^3 of oxy-apatite would thus contain the P removed from 604/20 or about 30 liters of effluent. Per cm^2 surface area, this volume corresponds to a total infiltration of 30 x 1000 cm or 300 m, which would take about 3 years. Thus, in 60 years, the volume of oxy-apatite per cm^2 of recharge basin would be 60/3, or 20 cm^3. Assuming that this volume would be spread out over a depth of 10 m and a horizontal area 4 times as wide as the width of the area in recharge basins, 20 cm^3 apatite would occupy 0.5 percent of the total soil volume. Assuming a pore space of 20 percent, the apatite would occupy 2.5 percent of the pore space in this volume. This is small and will most likely not have a significant effect on the hydraulic conductivity.

Phosphorus is the only major element in the renovation process that is removed by precipitation. Most of the other end products of the reclamation process are gaseous or water-soluble. The above analysis shows that it will be a very long time, in the order of 100 years, before accumulation of phosphate precipitates in the soil could begin to have an adverse effect on the operation of the system.

6. Fluorides

The fluoride concentration in the effluent was generally between 4 and 5 ppm (Table 9). The F-concentration in the reclaimed water was lower for the wells outside the basin area (wells 1 and 7) than for the wells inside the basin area (wells 1-2, ECW, and 5-6). This indicates that F-removal continues as the reclaimed water moves laterally below the water table. The average F-concentration for well 1, which is 90 ft from basin 1 (Figure 1), is 62 percent less than that in the effluent. The F-concentration in the native ground water varied generally between 0.6 and 0.8 ppm.

7. Boron

The boron concentrations, shown in Table 10, generally range between 0.4 and 0.5 ppm for the effluent and the reclaimed water. Movement of the effluent through the soil profile again did not cause a decrease in the boron content. The boron content in the native ground water was about the same as that in the effluent water. The boron concentration again remained generally below the 0.5 ppm value whereby the yield of the more boron-sensitive crops, such as citrus, may be adversely affected.

8. Dissolved salts

The salt content for the effluent and the reclaimed water continued to hover around the 1000 ppm mark (Table II) with the average for the effluent at 1021 ppm and for the reclaimed water from ECW at 1063 ppm. This is an increase about 4 percent, which is probably mostly due to evaporation from the recharge basins. The average annual evaporation from a free water surface in the Salt River Valley is about 6 ft. Since the total annual infiltration in 1969 was 226 ft, the salinity increase calculated on this basis would be about 3 percent. The evaporation in 1969 may have been above average because of above average summer temperatures. Also, because of the location of the basins in the dry surroundings of the river bed, advective energy may have been significant and actual evaporation may have been higher than the 6 ft. A salinity increase of 4 percent would correspond to an annual evaporation of 9 ft. Even though the basins are regularly dried, the annual evaporation rate is probably the best estimate of the evaporation losses, because when the basins are not inundated, the bottom is still wet and evaporating at near potential rates for most of the dryup period.

The salinity of the ground waters indicate that wells 1, 7, and the East Well are yielding reclaimed water (as do wells 1-2, ECW,

and 5-6, of course). Well 8 continued to yield native ground water.

The salt content of the WCW water, which was about 2200 ppm in the fall of 1967 and then gradually increased during 1968 to about 3800 ppm is shown in Figure 13 for 1969. In the first 3 months of 1969, the salt content dropped to about 3200 ppm, then increased to a 3800-4000 range in April and May. In the beginning of August, the salt content started a sustained decline to about 2000 ppm at the end of the year. This drop continued in January, and 1500 ppm were measured on 13 January 1970. The possibility of the reduction in the salt content signaling the arrival of reclaimed water at the bottom of WCW is discussed in section III.3. Arrival times of renovated water.

9. pH

Most of the pH-values of the effluent were in the 7.7-8.1 range (Table 12). The pH for the wells yielding reclaimed water was somewhat lower and ranged between 7 and 8. This was also true for the native ground water from well 8, WCW, and the 91st Avenue well (Table 12).

10. Coliforms and streptococci

Coliform and fecal streptococcus densities were obtained for the water from ECW with the multiple tube fermentation technique. Confirmed MPN-values, which were determined occasionally, were generally the same as the presumptive values for the coliform densities. Fecal streptococci densities were determined using azide-dextrose broth at 35 C, then EVA broth at 35 C for the positive tubes.

The results (Figure 14) show that the presumptive MPN-values of coliform bacteria were lowest in the summer period, when the inundation periods were short and frequent, and aerobic conditions prevailed in the percolation zone. In the first few and the last few months of the year, long inundation periods were held and

higher presumptive MPN-values were observed. The presumptive MPN-value usually rose after the start of an inundation period with the arrival of newly infiltrated water at the well. The MPN then dropped after the end of the inundation period when movement of reclaimed water below the water table had essentially come to a halt. For example, the presumptive MPN of coliforms rose from about 10 to about 260 per 100 ml for the inundation period of 15-30 October, then dropped to 8 per 100 ml 3 wks after the start of the ensuing dryup period. A similar behavior was sometimes observed for the fecal coliform counts, particularly in the first months of the year. After June, fecal coliform counts were mostly zero. The MPN values of fecal streptococci, which were included on a routine basis after May, were rather erratic. Sometimes they followed a pattern similar to that of the presumptive MPN of the coliforms. Because the bacterial density usually started to decrease after the end of an inundation period, it is anticipated that 3 or 4 wks of additional underground detention time will reduce bacterial counts to essentially zero.

11. Temperature of surface and ground water

The yearly temperature course for various surface and ground waters is shown in Figure 15. The influent temperature was measured at one of the inflow flumes and the temperature of the runoff water at the outflow flume from basin 1. The average of the influent and the runoff temperature is probably a good indication of the temperature of the water in the recharge basins. The temperature of ECW and WCW water was measured at the faucet above the ground after the pump had run a while.

The temperature range of the water in the basins appears to be about 17-32 C. This is of interest because it almost coincides exactly with the 18-30 C range wherein the rate of polysaccharide decomposition was approximately equal to the rate of polysaccharide formation as reported by Nevo and Mitchell (3). These investigators

also found that above 30 C, the rate of polysaccharide decomposition exceeded the rate of production, and that below 18 C, the reverse was true. This may explain why the polysaccharide concentrations in the soil below the recharge basins at Flushing Meadows were about the same at the end of an inundation period as at the end of a dryup period, and not much different from the polysaccharide content in the natural soil outside the recharge basins (see Annual Report 1968).

III. AQUIFER STUDIES

1. Response of water table to ground-water recharge

Well 5-6, which heretofore could not be used for measuring elevations of the ground water level because of its slow response, was deepened about .5 ft by driving in a rod and removing loose material with a bailer. After this operation, which was done in October 1969, the response of the well was greatly improved, and although not as fast as that of the other wells, sufficient for obtaining meaningful data on ground water levels.

The response of the water level in the observation wells to recharge is illustrated in Figure 16, which shows the water level in ECW during and following the recharge period 21 November - 8 December. In conformance with the theory and previous observations, the water level in this well rose rapidly after the start of the inundation and reached a pseudo-equilibrium level in about 5 days. The water level then dropped as the average infiltration rate decreased. On 4 December, the water depth in the recharge basins was reduced from 13 to 7 inches which caused a drop in the infiltration rate and hence also in the water level in ECW. Following the start of a dryup period on 8 December, the water level in ECW fell, and on 15 December it had reached essentially the same level as before the start of the inundation period. The water levels in the other observation wells behaved in similar fashion.

Profiles of water levels in the observation wells for the same recharge period are shown in Figure 17. Since wells 1, 1-2, 5-6, 7, and 8 are all 20 ft deep, the water level readings from the 30-ft deep ECW were converted so that they would also apply to the 20-ft depth. According to the equipotentials in the flow system as determined by resistance network analog (Figure 13 in Annual Report 1968), this correction could be made by multiplying

the water level rises in ECW by 83/66, or 1.26. Thus, the water level rises due to recharge as shown in Figure 17 all apply to the 20-ft depth level. The static ground water level is about 10 ft below the bottom of the recharge basins.

The water level profile on 21 November, prior to the inundation period, is essentially horizontal (Figure 17), indicating static ground water conditions in the north-south direction. The horizontal profile also indicates negligible effect of seepage from the effluent stream north of the project area (Figure 1) on the ground water flow system. The next profile in Figure 17 (1 December) shows the water levels at their highest positions, which is also the pseudo-equilibrium level. Because basins 3 and 4 exhibited the highest infiltration rates (see Figure 2), the water level in ECW is probably higher than it would have been in case the infiltration rate were the same for all basins. The profile on 8 December shows the water levels in the wells at the end of the inundation period, after the water depth in the recharge basins was changed from 13 to 7 inches on 4 December. On 11 December, 3 days after the flow into the basins was stopped, the water level profile in the observation wells was essentially horizontal, and, on 15 December it had returned to about the same position as before the start of the inundation period.

Comparing the profiles on 1 and 8 December shows that the water level in well 5-6 is slower to rise and slower to fall than, for example, the water level in well 1-2. This is because of the slower response of well 5-6.

The rise of the water levels to semiequilibrium positions and the relatively rapid decline to original levels after inundation is stopped is typical for the Flushing Meadows case where the aquifer is of considerable lateral extent and has a high hydraulic conductivity in horizontal direction.

2. Hydraulic conductivity of aquifer

The relationship between the average infiltration rate in the basins and the rise of the water level in the observation wells from static to pseudo-equilibrium position is a direct function of the hydraulic conductivity of the aquifer, which was evaluated as 282 ft/day in horizontal direction and 17.6 ft/day in vertical direction by resistance network analog (see Annual Report 1968).

Figure 16 shows that the water level in ECW at pseudo-equilibrium conditions was 1.8 ft higher than at static conditions. The pseudo-equilibrium level was reached on 26-27 November, when the average infiltration rate was about 2.5 ft/day (Figure 16). Thus the water level rise in ECW per unit infiltration rate was 1.8/2.5 = 0.72 days. If the hydraulic conductivity of the aquifer does not change, this ratio should be constant and should also apply to other infiltration rates. In the fall of 1968, the water level in ECW rose 1.0 ft above static level for an average infiltration rate of 1.4 ft/day. At that time, the water level rise per unit infiltration rate was 1.0/1.4 = 0.71 days (see Annual Report 1968), which is essentially the same as in 1969. Thus, it is concluded that the hydraulic conductivity of the aquifer has not changed.

The rise in WCW to pseudo-equilibrium level for the same period as in Figure 16 was 0.7 ft.

3. Arrival times of renovated water

The time it takes the water to travel from the recharge basins to the 30-ft deep ECW, as evidenced by the time between the start of an inundation period and the arrival of a nitrate peak in the water from ECW, varied from 5 days for a period with an average infiltration rate of 2.5 ft/day to 11 days for a period with an infiltration rate of 0.83 ft/day (Table 13). The product of travel or detention time and average infiltration rate should be constant, and the experimental data as shown in the last column of Table 13 bring this out reasonably well. The average value of the product

is 11.5 ft. In Annual Report 1968, the value of the product was predicted to be 16 ft if the soil porosity was 33 percent, based on analysis of the underground flow system by resistance network analog. Since the actual value of the product is 11.5 ft, a better value for the porosity of the sand and gravel strata is 11.5 x 33/16 = 24%.

The analog analyses also indicated that reclaimed effluent water would reach the bottom of the 100-ft deep WCW after a total of 315 ft of effluent would have infiltrated into the soil (based on a soil porosity of 33 percent, see Annual Report 1968). The accumulated infiltration data show that this infiltration was reached on 19 July 1969. As shown in Figure 13 and discussed in Section II.8, Dissolved salts, the salt content in WCW did indeed show a sustained decline starting in the beginning of August. After penetration to the 100-ft depth level, which required about 660 days, the reclaimed water "front" can be expected to be quite disperse and the salinity reduction and displacement of native ground water by reclaimed water will be extremely gradual. If the reduction in salinity as shown by Figure 13 is due to the arrival of reclaimed water, an increase in NO_3 and PO_4 would ultimately be expected. An increase in PO_4 may indeed have occurred (see Table 8), but nitrogen increases have not yet been observed. It could be that the first reclaimed water to arrive is relatively pure, similar to water that has been passed through an ion exchange column!

IV. DESIGN OF LARGE-SCALE RECHARGE SYSTEM

1. Calculation of underground travel times

The calculation of water table positions in a recharge system consisting of two parallel strips with infiltration basins and wells midway between the strips to pump up the reclaimed water, was presented in Annual Report 1968. A plan and cross section of this system are shown in Figure 18. Since sufficient time and distance of underground travel (for example, at least 1 month and 500 ft) are important for obtaining high quality reclaimed water, a procedure for calculating the underground travel time was developed. The shortest underground detention time, and hence the time that will be of most interest, will be associated with water that has infiltrated at A, since this point is closest to the well.

To calculate the travel time below the water table from A to the well, equipotentials and streamlines in the region ABEF must be known (see Figure 19). The flow rate in the stream tube between AF and the next streamline is then calculated by multiplying the width of the tube along AB by IW (I is the average infiltration rate for the recharge strip and W is the width of the recharge strip). This flow rate is then divided by the cross-sectional area of the tube (width of tube x height of aquifer) and by the porosity of the aquifer material to yield the macroscopic velocity. This velocity can be computed for each section of the stream tube between successive equipotentials. Dividing the distance between these equipotentials by the macroscopic velocity for the section in question then yields the travel time increment for that section. Summing the time increments for each section in the stream tube yields the total travel time from A to F.

To enable calculation of travel times for different system geometries, equipotentials for the region ABEF are shown in Figure 20 for different ratios of L/S. These equipotentials are expressed in percent head loss between A and F and they were evaluated by

resistance network analog. Streamlines can be sketched as orthogonals to these equipotentials.

2. Example

To illustrate the use of the procedures for calculating water table positions and minimum underground travel times in a system of two parallel recharge strips with wells midway in between, an example will be presented. The following values were selected:

T_e = 20,000 ft^2/day for the recharge-flow system in region ABCD

T_e = 30,000 ft^2/day for the well-flow system in region ABEF

L = 500 ft

W = 600 ft

I = 0.8 ft/day, and

Q_w = 768,000 ft^3/day (or almost 4000 gal/min)

The symbol T_e refers to the effective aquifer transmissibility, L is the distance between the recharge strip to the well, and Q_w is the discharge per well.

Assuming an equilibrium condition with the well discharge equal to the recharge rate, the distance between the wells, S, can be calculated as 800 ft, using equation 4 on page 33 of Annual Report 1968. This gives L/S = 0.625, so that according to Figure 20 in Annual Report 1968, $2\ WSI/T_e\Delta H_{A-F} = 1.38$. In this parameter, ΔH_{A-F} is the elevation difference between the water table levels at A and F (adjacent to the well). Substituting the values for W, S, I, and T_e for the well-flow system into this parameter yields ΔH_{A-F} = 18.6 ft. Figure 21 in Annual Report 1968 shows that for L/S = 0.625, $\Delta H_{B-F}/\Delta H_{A-F} = 1.02$, so that the elevation difference, ΔH_{B-F}, between the water table levels at B and F is 18.9 ft. The next step is to calculate the elevation difference, ΔH_{C-B}, between the water table levels at C and B with equation (5) in Annual Report 1968, which yields ΔH_{C-B} = 7.2 ft. Thus, the elevation difference between the water table levels at D and F, ΔH_{D-F}, is equal to 18.6 + 7.2 = 25.8 ft, and that at C and F, ΔH_{C-F}, is

equal to 18.9 + 7.2 = 26.1 ft. The water table beneath the outside edges of the recharge strips is thus essentially at uniform depth and about 26 ft higher than the water table adjacent to the well.

Equipotentials and streamlines for the flow system of this example are shown in Figure 19. The equipotentials for the recharge flow system in region ABCD were calculated with equation (5) on page 34 of Annual Report 1968, using different values for W. The equipotentials for the well-flow system in section ABEF were obtained from Figure 20. The streamlines were sketched as orthogonals to the equipotentials.

To calculate the minimum travel time, K_h will be taken as 282 ft/day, as evaluated by resistance network analog for the Flushing Meadows site (see Figure 2, Annual Report 1968). Thus, the effective height of the aquifer for the well flow system is 30,000/282 = 106 ft. Assuming a porosity of 30%, the macroscopic velocity between the 18-ft and 16-ft equipotentials in the stream tube between AF and the next streamline can be estimated as 0.8 x 600 x 100/123 x 100 x 0.3 = 13 ft/day. In this calculation, the numerator is a product of recharge rate and recharge area feeding the stream tube, the factor 123 is the average height of the aquifer between the 18-ft and 16-ft equipotentials (106 + (16 + 18)/2), the factor 100 in the denominator is the average width of the stream tube between the 18-ft and 16-ft equipotentials, and the factor 0.3 represents the porosity. Dividing the average distance between the two equipotentials, which is 115 ft, by the macroscopic velocity, yields a travel time of 8.8 days. Applying this procedure to the rest of the potential intervals of the stream tube and summing the time increments yields a total travel time of 4 weeks from A to the well. If longer minimum travel times are desired, S can be decreased, L increased, I decreased, and/or W decreased.

To get the total underground detention time, the time for vertical movement from the recharge basin to the water table must

be added to the time for lateral movement. The time for vertical movement can be calculated from the depth of the water table, the infiltration rate, and the volumetric water content in the percolation zone.

V. LABORATORY FILTRATION STUDIES

Because a high suspended solids content in the effluent has such adverse effects on the infiltration rates, a laboratory study was set up to investigate more closely the relationship between suspended solids and infiltration rate, and to evaluate the feasibility of filtering the effluent prior to admitting it into the recharge basins. If the cost of filtering would be less than the value of the increased reclaimed water obtained per unit area of recharge basin, filtration would be economical.

The filter selected for this study was a mixed media filter column by Neptune MicroFloc.[1] This filter consists of three different materials that are graded both for size and density. The coarsest material had the lowest density while the finest material had the highest density. Thus, after backwashing, the heavy, fine material settles out first and the light, coarse material last. The particle size in the resulting column thus decreases with depth, which causes the column to filter over its entire length and to be thus more efficient than a uniform column which filters only at the top. The materials were coal, sand, and garnet with densities of 1.6, 2.6, and 4.0, respectively. The resulting particle size gradation in the filter ranged from 1 mm at the top to 0.15 mm at the bottom.

Twelve columns, 61 cm long and made from 10-cm ID white opaque polyvinyl chloride pipe, were packed with 50 cm of loamy sand from one of the recharge basins. Tensiometers were installed in each column at 1, 4, 10, and 30 cm from the soil surface. Construction details of the tensiometers are shown in Figure 21. The tensiometers were connected to a manometer for reading. Six

of the columns received filtered and the other six unfiltered effluent from the 91st Avenue sewage treatment plant.

A sketch of the experimental setup is shown in Figure 22. A recirculating system was used to apply the water to the columns. Water levels were maintained in the recirculatory reservoirs with the use of float-activated solenoid valves connected to the main supply reservoir. The main supply and unfiltered supply reservoirs were equipped with agitators to prevent the suspended material from settling out. Algae growth was avoided by covering all light transmitting components with tape.

The columns were initially saturated from the bottom and run for a period of time with tap water. Effluent was then applied to the columns and an inundation schedule of 2 wks wet and 1 wk dry was followed. Turbidity and chemical oxygen demand (COD) of the filtered and unfiltered effluent were routinely measured. The COD was also measured on the water coming out of the columns. Suspended solids greater than 4 microns were also determined.

During inundation with tap water the hydraulic conductivity (K) of the sand was measured. This value can be considered as the maximum or reference hydraulic conductivity. The average of the K-values of the 6 filtered and the 6 unfiltered columns is shown in Table 14 for the different depth intervals. These values are for the period immediately before sewage effluent was applied for the first time to the columns. The infiltration rate is also shown. When the sewage water was applied to the column, the infiltration rate started to decrease immediately. The hydraulic conductivity also decreased throughout the column as shown in Figure 23 where the average K-values of the different depths is shown in relation to time. There is no significant difference between the K-values of the columns receiving filtered and unfiltered effluent except at the 0 to 1-cm depth where the unfiltered K-values are lower. This indicates that more surface plugging is occurring in the

columns receiving unfiltered effluent. The surface plugging is also illustrated in Figure 24 where the pressure profiles for the filtered and unfiltered columns are shown for a number of days after inundation. Although there is plugging in both cases, the gradient in the 0 to 1-cm depth is higher and increased faster in the unfiltered columns.

The decrease of K and infiltration rate after 2 months is shown in Table 15. These values are referenced to the hydraulic conductivity and infiltration rates obtained with the tap water. After three cycles of 2 wk inundation-1 wk dryup periods, the decrease in infiltration rate was 88% for the unfiltered columns and 47% for the filtered columns.

The turbidity of the unfiltered effluent was somewhat variable and ranged between 1 and 8.2 with an average of 3.7. Jackson turbidity units (JTU). The filtered effluent ranged between 0.9 and 2.4 with an average of 1.5 JTU. The COD measurements did not show any difference. The average for the 2-month period was 36 ppm in both cases. The COD of the outflow from the columns was 31 ppm for the filtered and 28 ppm for the unfiltered. The amount of COD in the suspended solids is evidently small compared to that in the clear effluent.

The suspended solids content was determined by filtering the water through a 4-micron filter and weighing the residue. In the only determination made with this method, the filtered effluent had 2.1 mg solids per liter, and the unfiltered water 22.3 mg per liter. The turbidity was 1.5 and 3 JTU, respectively.

The results so far show that suspended solids removal by mixed media filtration or other techniques can significantly increase the infiltration rates. Further studies using different soils, infiltration gradients, and suspended solids concentrations are planned so that the impedance of the clogged layer can be related to the total solids load for different soils and gradients.

SUMMARY AND CONCLUSIONS:

The sewage effluent at the pump intake of the Flushing Meadows Project, which is an experimental facility for reclaiming sewage water by ground-water recharge with infiltration basins, was of poor quality (high suspended solids content) for the first half of 1969. In June-July, the effluent cleared up completely and maintained a low suspended solids content for the rest of the year.

Of the six recharge basins in the project (each basin is 20 x 700 ft in size and the basins are spaced 20 ft apart), two were planted to rice, giant bermudagrass grew back in two other basins, the bare-soil basin was allowed to become overgrown with volunteer grasses, and the gravel basin remained without vegetation. The rice made an excellent vegetative growth, but yielded little grain, probably because of high summer temperatures and a pump failure in August which caused a dry period of a week.

The accumulated average infiltration for the 6 basins during the last 6 months of 1969 was 160 ft, thus corroborating the earlier estimates of an annual infiltration of 300 ft. Referring the infiltration rates of the individual basins to the natural infiltration capacity of the basins as measured during the first inundation period for the project when soil clogging and biological processes had not yet taken place, it appeared that the vegetated basins had the highest infiltration rates. Setting the infiltration behavior of the vegetated basins at 100 percent of the natural capacity, the bare soil basin infiltrated at 80 percent of its natural capacity, and the gravel basin only at 40 percent. Thus, a gravel layer has an adverse effect on the infiltration rate (probably due to poor drying) and maximum infiltration rates can be obtained with vegetated basins (probably because the vegetation prevents algae growth on the bottom of the basins). The infiltration rate in the basins appeared to vary almost directly with the water depth, indicating that most soil clogging took place at the surface. For the gravel-

covered basin, clogging occurred at the gravel-soil interface. A desirable inundation schedule for maximizing both quantity and quality of the reclaimed water appeared to be about two weeks inundation followed by 10 days dryup in the summer and 17 days dryup in the winter.

As the waste water percolates downward to the ground-water table, which at the Flushing Meadows Project is at a depth of about 10 ft, it undergoes a drastic quality improvement so that it joins the ground water as reclaimed water. Analysis of this water pumped by the 30-ft deep well in the center of the basin area showed that 5 to 11 days after the start of a new inundation period a nitrate peak of 20-30 ppm NO_3-N occurred. Before and after passage of this peak, which is due to the arrival of nitrified effluent held as capillary water during the preceding dryup period, NO_3-N concentrations of about 0.2 ppm prevailed. Since NH_4-N concentrations were about 5 ppm (after an unexplainable peak reaching 10 ppm in the summer) and the total N concentration in the effluent was about 25 ppm, a nitrogen removal of about 80 percent was obtained. This removal did not occur during cycles of short inundation periods (2 or 3 days), when all the nitrogen in the effluent was converted to nitrate in the reclaimed water.

The main mechanisms for the nitrogen removal appeared to be fixation in relatively stable organic matter and adsorption of ammonium thereon, and biodenitrification. This was indicated by laboratory column studies (described elsewhere in this report) and by nitrogen analyses of the soil from the recharge basins, which had about 1 mg N more per dry gram of soil than the virgin soil outside the basins. After about 3 weeks continuous inundation, the ammonium can be expected to increase in the reclaimed water, and after 3 months continuous inundation nitrogen removal no longer takes place.

Biochemical oxygen demand and fecal coliform density in the reclaimed water from the 30-ft deep center well was essentially zero (compared to a BOD of 20 mg/liter and an MPN of 10^6 in the effluent). The chemical oxygen demand of this water was about 15 ppm, as compared to 50 ppm for the sewage effluent. Phosphates and fluorides continued to be removed from the reclaimed water as it moved laterally below the water table. Reclaimed water pumped at a distance of 100 ft from the recharge basins had P and F concentrations of 3 and 2 ppm for a reduction of 90 percent and 60 percent, respectively. Assuming that all P-removal is by formation of the insoluble apatites, this process can continue for more than a hundred years before adverse effects on the hydraulic conductivity of the aquifer could be expected.

The boron concentration in the sewage effluent was about 0.4 ppm. This did not change as the water percolated through the soil because the profile consists almost entirely of sands and gravels and contains little or no iron or aluminum oxides. A concentration of 0.4 ppm is below the range where injurious effects on crops will occur, even on the more sensitive plants.

The salt concentration of the reclaimed water was 1060 ppm. This is 4 percent higher than in the sewage effluent, which can be entirely attributed to evaporation from the effluent in the recharge basins. The pH of the reclaimed water was in the 7.2-7.7 range, which is somewhat lower than the average pH of 7.9 for the sewage effluent.

In Annual Report 1968, the prediction was made (based on analysis with an electric analog) that native ground-water would be replaced by reclaimed sewage water at the bottom of the 100-ft deep well in the center of the basin area after a total of 315 ft of effluent had infiltrated into the soil. This infiltration amount was reached on 19 July 1969 and in August the salt content in the water from the 100-ft well, which had been in the 3000-4000 ppm

range, started a steady decline to reach 1500 ppm in January 1970. This may signal the arrival of reclaimed water.

Studies of the rise of the water level in the observation wells in response to the infiltration rates showed that the hydraulic conductivity of the aquifer had not changed.

Analog analyses were performed to predict underground detention times of sewage water in a system of parallel recharge strips with wells midway between the strips. An example applying to the hydrogeological conditions of the Salt River bed showed that detention times of at least one month could be obtained.

Laboratory studies on using filtered and unfiltered secondary sewage effluent on soil columns showed that filtration with a mixed media filter could double the infiltration rates, even with effluent that appeared very clear to the naked eye.

After 2½ years of intensive operation of the Flushing Meadows Project, there are no indications of decreasing infiltration rates, decreasing hydraulic conductivity of the aquifer, or a decline in the quality improvement as the sewage water moves through the ground. Thus, as observed elsewhere, ground-water recharge systems for renovating waste water should have a long, useful life.

REFERENCES:

1. Fed. Water Pollut. Control Admin. Water Quality Criteria. Report of Natl. Tech. Advisory Com. to Sec. of Int. April 1968. Washington, D. C.

2. Lyon, T. L., Buckman, H. O., and Brady, N. C. The nature and properties of soils, Fifth Edition. MacMillan Company, New York. 1952.

3. Nevo, Z., and Mitchell, R. Factors affecting biological clogging of sand associated with ground water recharge. Water Research 1: 231-236. 1967.

4. Waksman, S. A. Soil microbiology. John Wiley & Sons. 1952.

PERSONNEL: Herman Bouwer, J. C. Lance, R. C. Rice, F. D. Whisler, and E. D. Escarcega.

Salt River Project: M. S. Riggs and C. C. Stetter.

CURRENT TERMINATION DATE: 1972.

Table 1. Infiltration reduction on 4 December 1969 due to changing the water depth from 13 in. to 7 in.

Basin	Infiltration rate in ft/day		
	13 in.	7 in.	Reduction factor
1	3.25	1.82	0.56
2	1.80	0.95	0.53
3	2.90	1.40	0.48
4	2.90	1.90	0.65
5	2.25	1.30	0.58
6	1.40	0.85	0.61
		Avg.	0.57

Table 2. Sampling depths for Flushing Meadows wells and 91st Avenue well.

Well	Depth in ft
1	20
1-2	20
ECW	30
WCW	100
5-6	20
7	20
8	20
East Well	10-30
91st Avenue	100-200

Table 3. COD in mg/liter for various wells (1969).

Date	1	7	EW	WCW	8	91st Avenue
23 Jan	12	12		31	11	
20 Feb	12	10		22	12	24
12 Mar	12	16		19	16	14
26 Mar	6	6		24	8	14
2 May	12	7		20	7	11
6 Jun	17	12			8	
16 Jul		16		35	27	
15 Aug	16	12		37	22	
10 Sep	25	25		29	30	
10 Oct	23	18		29	26	29
14 Nov	16	16	15	21	20	
18 Dec	8	13	13	13	17	21

Table 4. Nitrate nitrogen concentrations in mg N per liter for various wells (1969).

Date	1	7	8	EW	WCW	91st Avenue
23 Jan	14.2	7.6	2.0		3.5	6.0
20 Feb	16.0	15.6	2.1		4.1	
12 Mar	14.0	18.4	0.3		4.7	5.8
26 Mar	11.5	11.8	0.3		1.8	5.9
2 May	23.2	4.2	0.2		2.2	4.3
6 Jun	21.6	10.8	0.2		2.8	
16 Jul	22.4	17.6	0.1		3.5	5.4
15 Aug	2.0	14.8	0.5		3.5	
10 Sep	1.3	5.0	0.3		3.3	
10 Oct	0.3	3.4	0.1		2.5	6.4
14 Nov	0.2	0.0	0.3		3.7	
18 Dec	0.2	0.5	0.5		4.4	5.5
28 Nov				8.5		
3 Dec				6.4		
9 Dec				3.3		
17 Dec				0.2		
22 Dec				4.8		
29 Dec				8.3		

Table 5. Ammonium nitrogen concentrations in mg N per liter for various wells (1969).

Date	1	7	8	EW	WCW	91st Avenue
23 Jan	3.3	1.1	0.2		0.1	0.1
20 Feb	2.8	1.2	0.2		0.4	
12 Mar	2.9	0.9	0.2		0.0	0.0
26 Mar	2.8	0.7	0.1		0.0	0.1
2 May	3.4	0.4	0.2		0.0	0.0
6 Jun	2.8	1.3	0.0		0.0	
16 Jul	2.9	0.2	0.0		0.5	
15 Aug	2.0	1.2	0.4			
10 Sep	3.8	1.5	0.1		0.0	
10 Oct	4.1	1.5	0.1			0.0
14 Nov	3.8		0.1		0.1	
18 Dec	2.8	1.1	0.1		0.1	0.0
28 Nov				2.2		
3 Dec				2.8		
9 Dec				3.6		
17 Dec				4.9		
21 Dec				3.5		
29 Dec				5.6		

Table 6. Aerobic bacteria counts in recharge basin soil (1969).

Date	Basin	Depth inches	Population per gram of dry soil
2 July	4 (grass)	0-1	9.2×10^7
	5 (rice)	0-1	3.7×10^8
21 July	6 (rice)	0-1	4.2×10^8
	6 (rice)	12	4.3×10^8
	6 (rice)	36	4.0×10^6
21 July	1 (bare area)	0-1	1.9×10^8
	1 (bare area)	36	2.2×10^7

Table 7. Total N in soil from recharge basins and in natural soil adjacent to project area (1969).

Date	Depth inches	Total N in mg per gram of dry soil	
		Basin 4	Natural soil taken from SW corner
8 Dec	0-12	2.08	0.77
	12-24	1.27	0.67
		Basin 1 (East end)	Natural soil taken from NE corner
22 Dec	0-12	1.92	0.77*
	12-24	1.85	0.68
	24-36	1.56	0.58
	36-48	0.89	0.39
	48-60	1.18	0.49

*Sample lost but because N at 12-24 inch depth agreed with that in soil from SW corner, 0.77 mg/g from SW corner was repeated here.

Table 8. Phosphate concentration in mg P/liter for various wells (1969).

Date	WCW	EW	91st Avenue
23 Jan	0.2		
10 Feb	0.0		0.0
11 Mar	0.0		0.1
8 Apr	0.0		0.0
6 May	0.0		
13 May	0.2		0.3
26 May	0.4		
9 Jun	0.4		
7 Jul	0.0		
22 Jul	0.2		0.0
8 Sep	0.0		
13 Oct	0,7		0.6
12 Nov	0.2		
15 Dec	0.5	3.5	0.4

Table 9. Fluoride concentration in mg F/liter for effluent and wells (1969).

Date	Effl.	Date	1	1-2	ECW	5-6	7	8	EW	WCW	91st Ave.
27 Jan	2.7	23 Jan	1.3	3.5	1.9	1.4	2.0	0.8		0.8	
26 Jun	5.6	20 Feb	1.3	3.1	2.1	1.6	1.9	0.8		0.8	0.6
4-5 Sep	4.9	26 Mar	1.5	2.9	2.6	1.8	1.5	0.8		0.9	0.6
8-12 Sep	4.3	6 Jun	1.5	2.6	2.3	1.8	1.2	0.6		0.8	
15-19 Sep	4.4	10 Sep	2.1	2.4	2.6	2.6	2.7	0.8		0.8	
16-17 Oct	5.3	10 Oct	2.0	2.3	2.6	2.6	2.9	0.7		0.6	0.6
17-24 Oct	4.9	14 Nov	1.8	2.5	2.7	2.8	2.3	0.8		0.6	
26-30 Oct	4.5	18 Dec	2.2	2.8	3.1	3.0	2.7	0.8	2.6	0.7	0.6
24-28 Nov	4.1	Avg.	1.7	2.8	2.5	2.2	2.1	0.76	2.6	0.75	0.6
1-5 Dec	4.5										
5-8 Dec	4.5										
23-24 Dec	5.0										
29-31 Dec	3.6										
Avg.	4.5										

Table 10. Boron concentration in mg B/liter for effluent and wells (1969).

Date	Effl.	1	1-2	ECW	5-6	7	8	EW	WCW
23 Jan	0.40	0.38	0.39	0.39		0.38	0.38		0.50
26 Mar		0.45				0.41	0.35		
25 Apr	0.50		0.45	0.40	0.39				
16 Jul						0.50			
15 Aug	0.50	0.50	0.50	0.50	0.50		0.50		
14 Nov		0.46	0.45	0.40		0.44			0.58
18 Dec	0.36		0.44	0.46	0.45	0.44		0.47	

Table 11. Total salt concentration in effluent and in water from wells, mg/liter (1969).

Date	Effl.	1	1-2	ECW	5-6	7	8	EW	91st Ave.
13-14 Jan	1056		1216	1088	1011				
23 Jan		1152	1088	1024	960	1056	1984		
10-11 Feb	922		1120	1088	1024				
14-17 Feb	1088	1152	1088	1024	1056	1120	2048		
10-11 Mar	1024	1152	1152	1120	992	1152	1856		2560
26 Mar		1056	960	992	1037	1216	1664		2432
14-15 Apr	979		1011	1024	1024				
28-29 Apr	1024		1216	1088	960				
6 May	1088	1203	1152	1216	1120	1792	1677		2624
26-27 May	1024		1216	1184	1152				
6 Jun		1216	1280	1248	1248	1696	1798		
30 Jun	966		1152	1210	1184	1613			
8-9 Jul	966	1152	1184	1184	1152	1408	1920		
28-29 Jul	960		1056	1024	1088	1120			2560
5-6 Aug	973		1030	1024	1030	1050			
19-20 Aug	960	992	1043	1018	1082		2048		
9-10 Sep	1152	1024	992	896	960	992	2048		
25-26 Sep	1152		1088	1152	1088				
8-10 Oct	1216	1088	1056	1088	1056	1024	1948		2720
25-26 Oct	1056		1056	992	1024				
14 Nov		992	845	928	896	1024	1888		
24 Nov	864		960	960	960			1152	
5-8 Dec	960	960	1024	896	992	960		1024	2528
29-30 Dec	928		992	1043	947		1856	960	

Table 12. pH of effluent and water from wells (1969).

Date	Effl.	1	1-2	ECW	5-6	7	8	EW	WCW	91st Ave.
13-14 Jan	7.25									
27 Jan	8.1	7.9	7.6	8.1	8.0	7.8	8.0		7.6	
20 Feb		7.8	7.2	7.2	7.7	7.4	7.7		7.9	
10-11 Mar	7.8		7.4	7.3	7.8				7.4	7.8
20 Apr									7.4	
6 May	7.7	7.6	7.1	7.1	7.8	7.5	7.7		7.4	
9-10 Jun	7.7	7.3				7.9	7.8			
26-27 Jun	8.1		7.1	6.9	7.6				7.3	
8-9 Jul	8.0	7.4	7.0	7.0	7.7	7.0	7.1		7.4	
22-23 Jul	7.6		7.3	7.2	7.7	7.4			7.2	7.5
4-5 Aug	8.0			7.1	7.6	7.2			7.1	
19-20 Aug	8.1	7.6	7.1	6.9	7.4		7.5		7.3	
9-10 Sep	8.1	7.7	7.2	7.1	7.4	7.2	7.5		7.3	
25-26 Sep	8.1		7.3	7.2	7.5					
8-10 Oct	8.2	7.9	7.6	7.4	7.7	7.4	7.6			7.4
23-24 Oct	7.8		7.1	7.0	7.3				7.3	
14 Nov		7.8	7.2	7.3	7.5	7.5	7.4		7.4	
24 Nov	8.1		7.2	7.3	7.4			7.4	7.4	
5-8 Dec	8.0	7.7	7.4	7.2	7.4	7.5		7.5	7.5	7.3
29-30 Dec	7.8		7.6	7.2	8.0		7.6	7.2	7.5	

Table 13. Occurence of distinct nitrate peaks in ECW in relation to start of inundation period and average infiltration rate (1969).

NO_3-peaks	Number of days after start of inundation	Average infiltration rate, ft/day	Number of days times infiltration rate
17 Jan	11	0.83	9.1
12 Feb	9	1.12	10.1
13 Mar	10	1.00	10.0
25 Sep	8	1.65	13.2
21 Oct	6	1.98	11.9
26 Nov	5	2.50	12.5
30 Dec	7	1.94	13.6
		Avg.	11.5

Table 14. Average hydraulic conductivity and infiltration rates for filtered and unfiltered columns before sewage water was applied.

	K, cm/min Depth, cm				I, cm/min
	0-1	1-4	4-10	10-30	
Unfiltered	.093	.084	.097	.092	.096
Filtered	.087	.076	.100	.090	.096

Table 15. Percent reduction in hydraulic conductivity and infiltration rates after sewage water was applied to columns.

	Unfiltered					Filtered				
	K, cm/min				I	K, cm/min				I
	0-1	1-4	4-10	10-30		0-1	1-4	4-10	10-30	
2 Oct	86	65	68	77	79	40	45	75	78	69
7 Oct	8	39	68	71	50	28	47	62	75	74
24 Nov	10	44	60	70	54	29	41	58	71	59
4 Dec	3.4	38	61	77	45	16	30	62	71	60
16 Dec	4.3	39	52	68	45	25	41	59	64	60
24 Dec	0.3	30	61	66	12	12	30	55	63	53

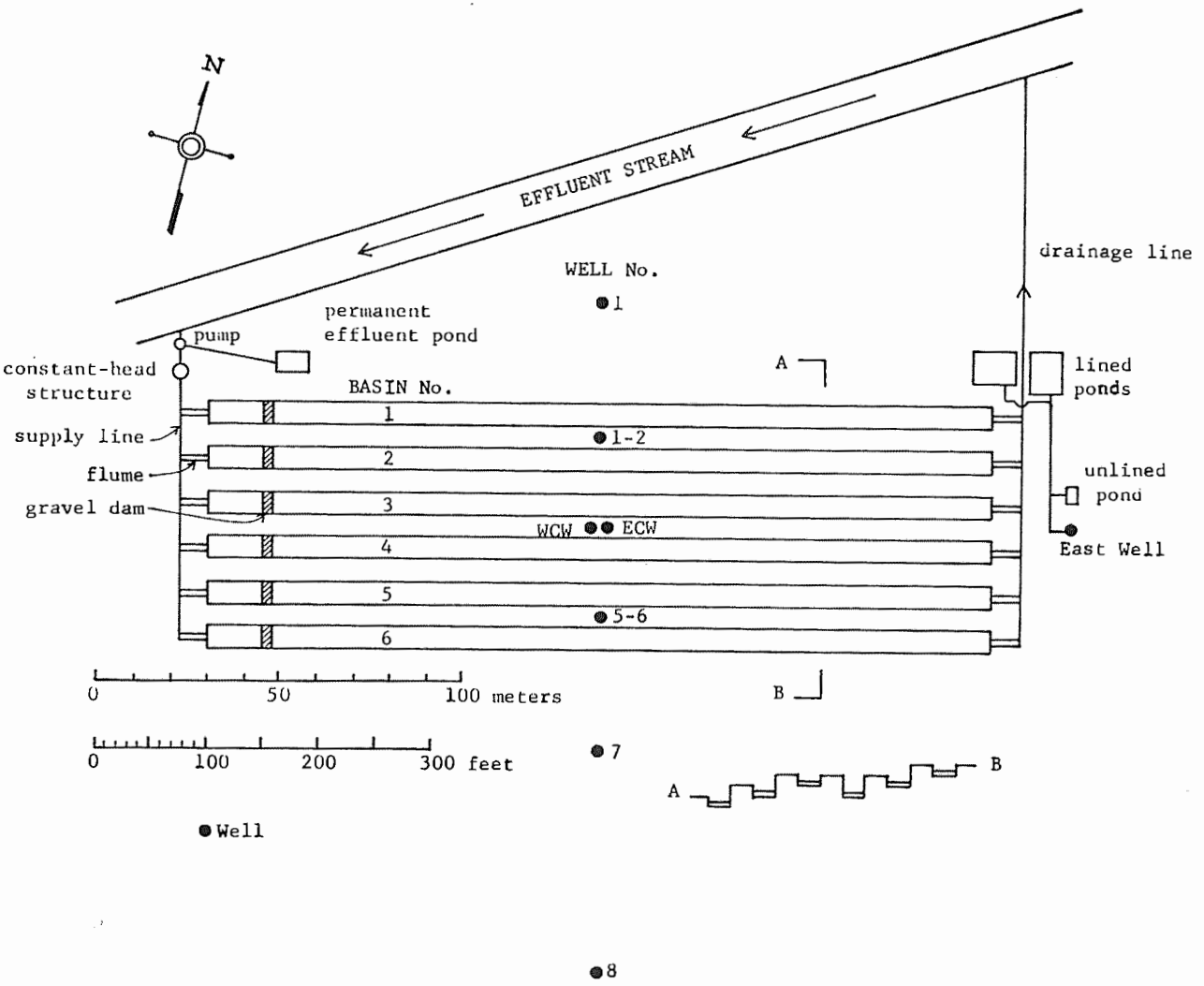

Figure 1. Plan of Flushing Meadows Project.

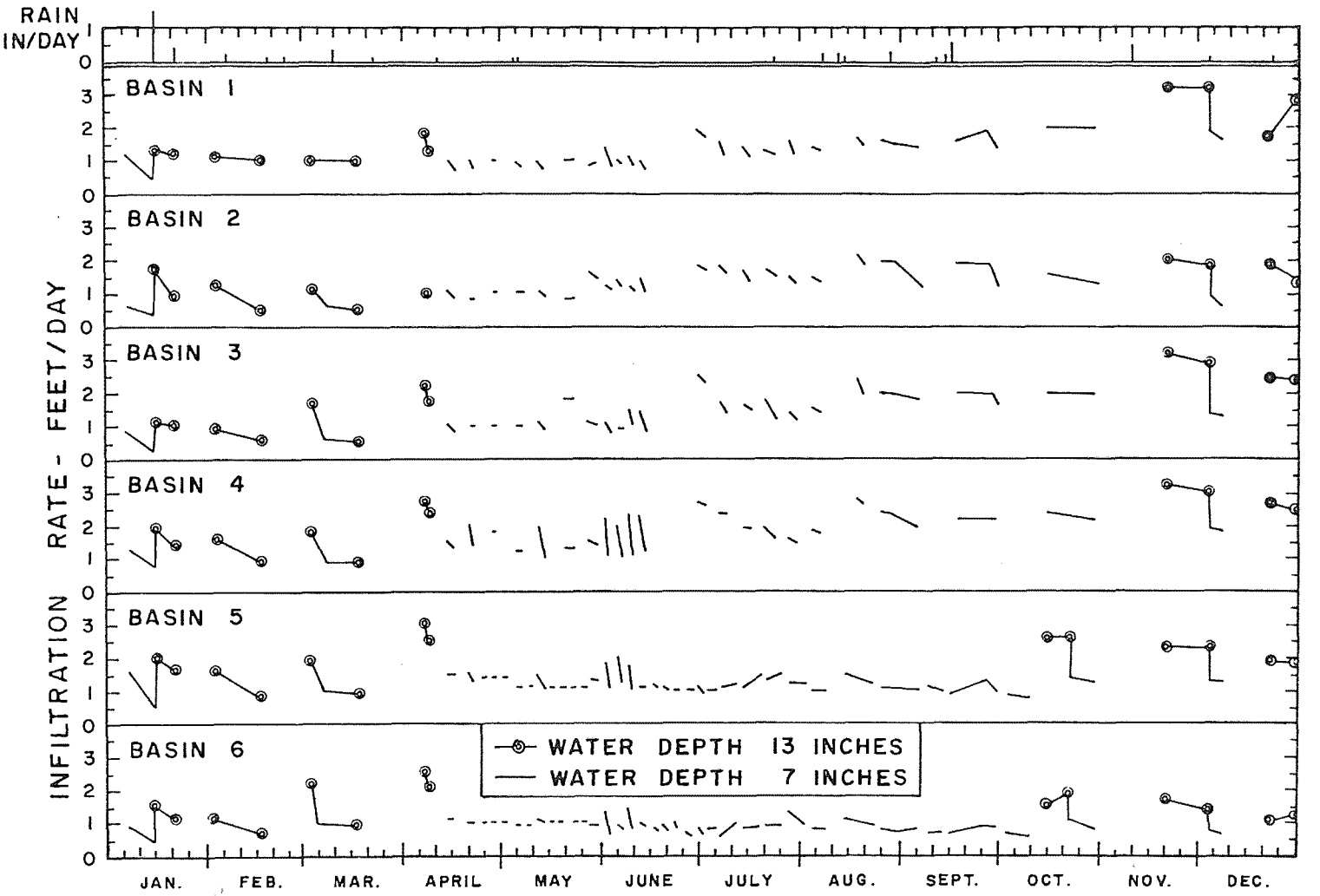

Figure 2. Infiltration rates in basins and rainfall for 1969.

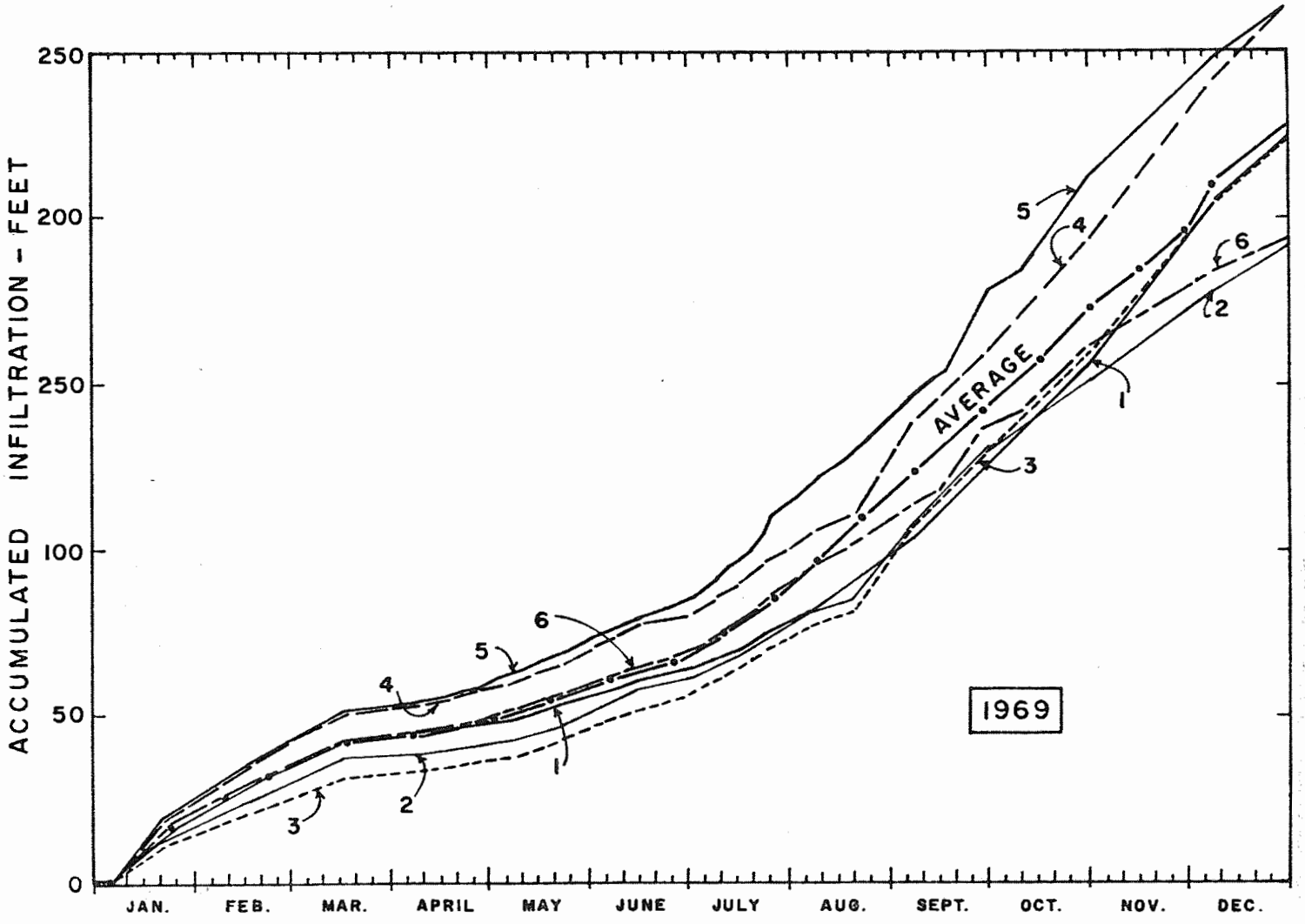

Figure 3. Accumulated infiltration in basins for 1969.

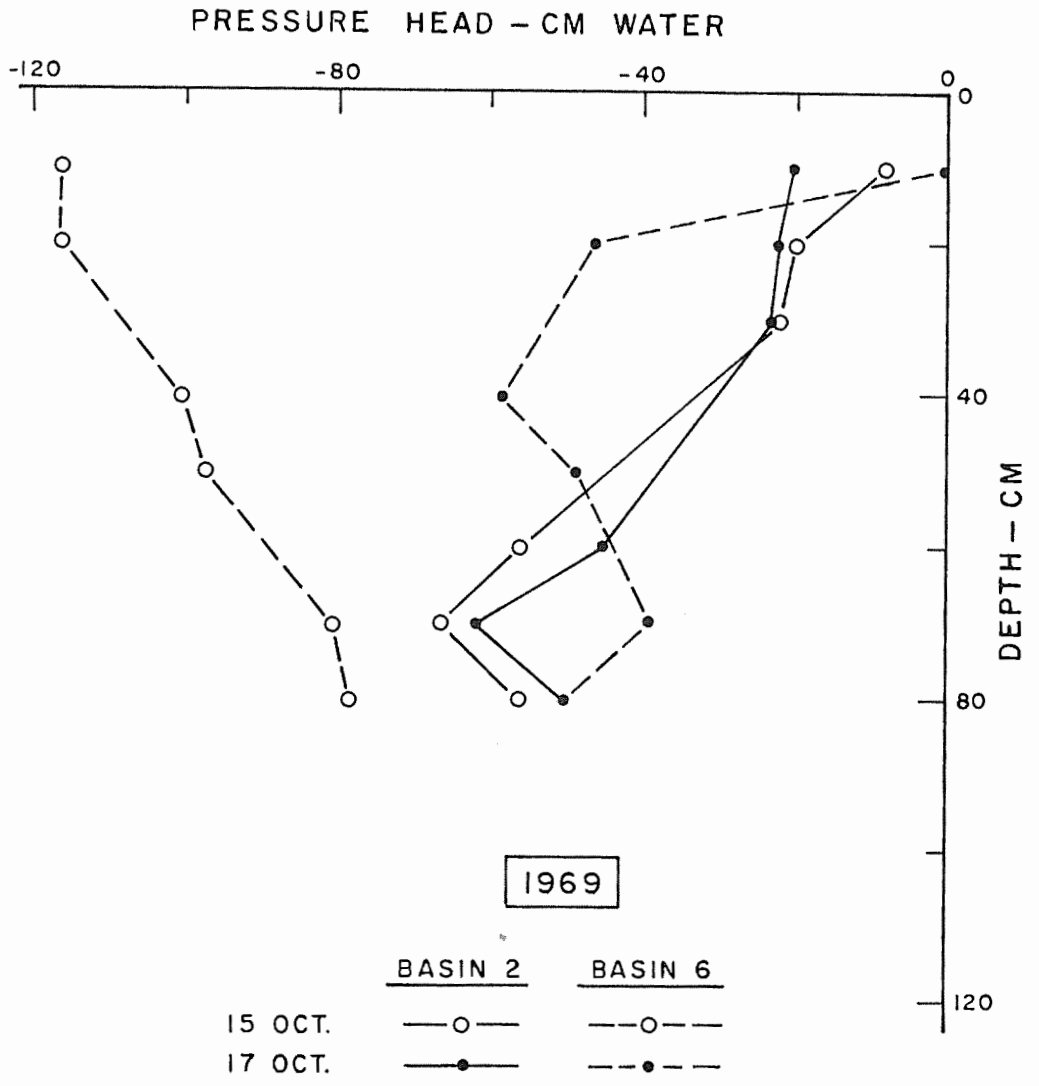

Figure 4. Profiles of soil-water pressure head in basins 2 and 6.

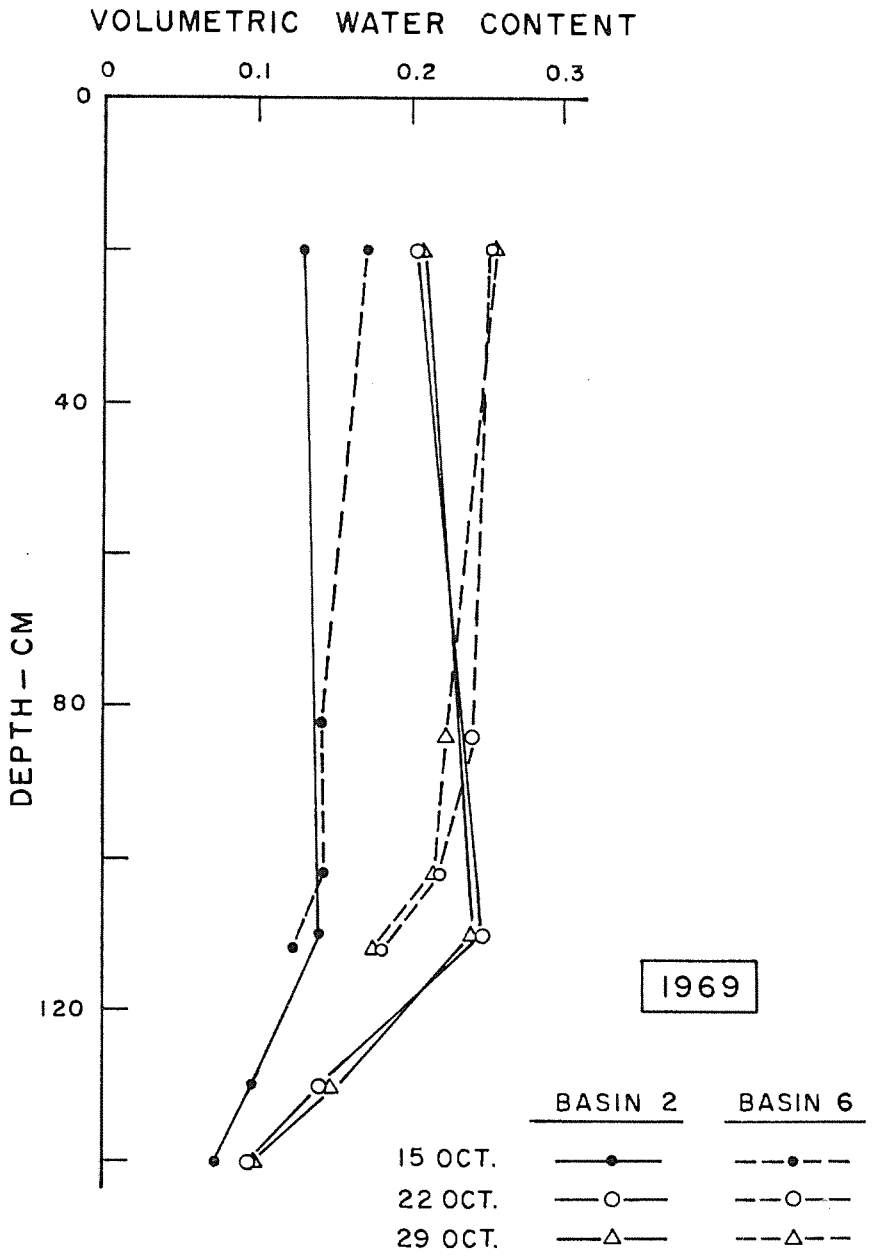

Figure 5. Profiles of soil-water content in basins.

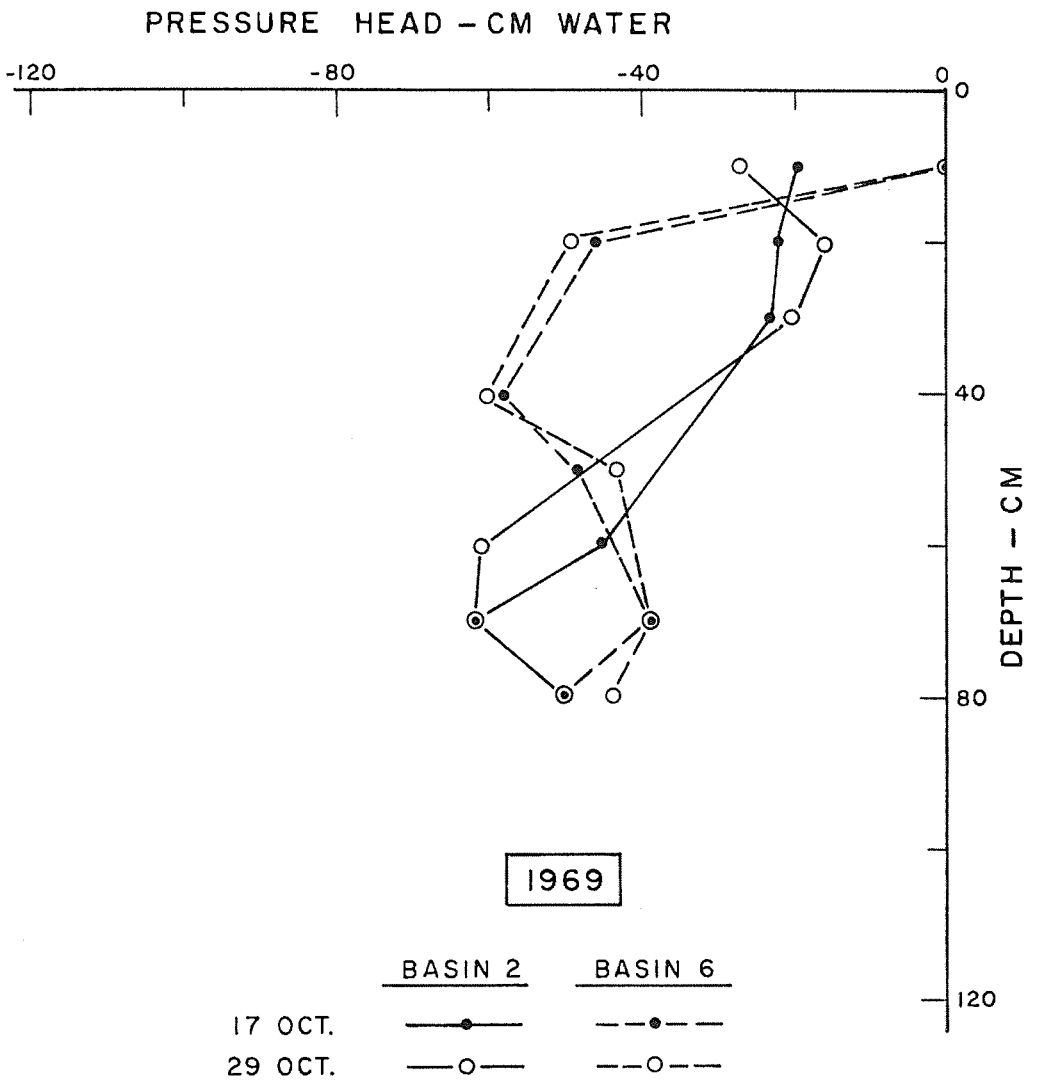

Figure 6. Profiles of soil-water pressure head in basins 2 and 6.

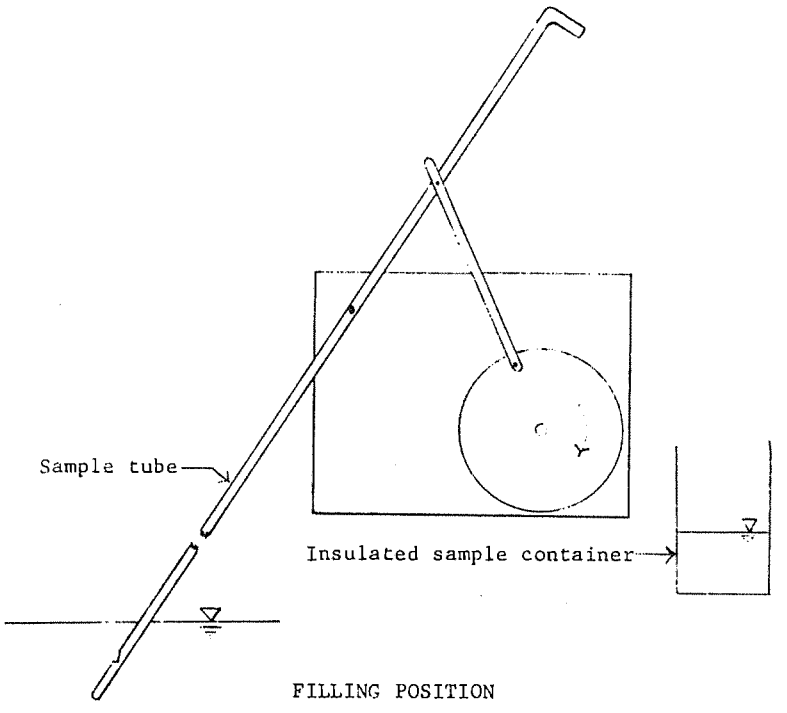

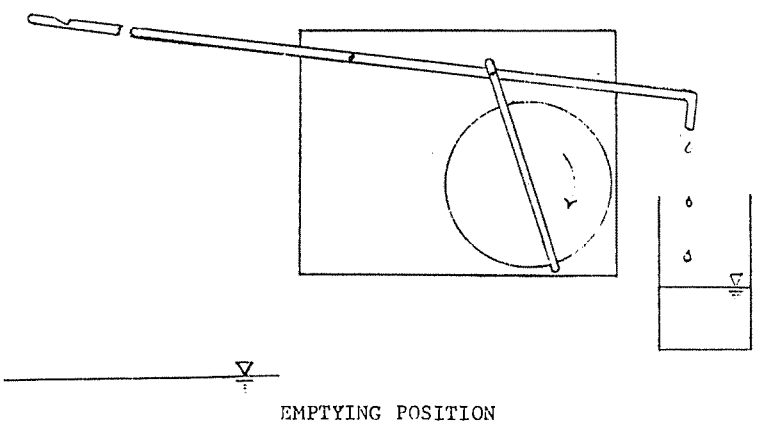

Figure 7. Schematic of continuous sampler.

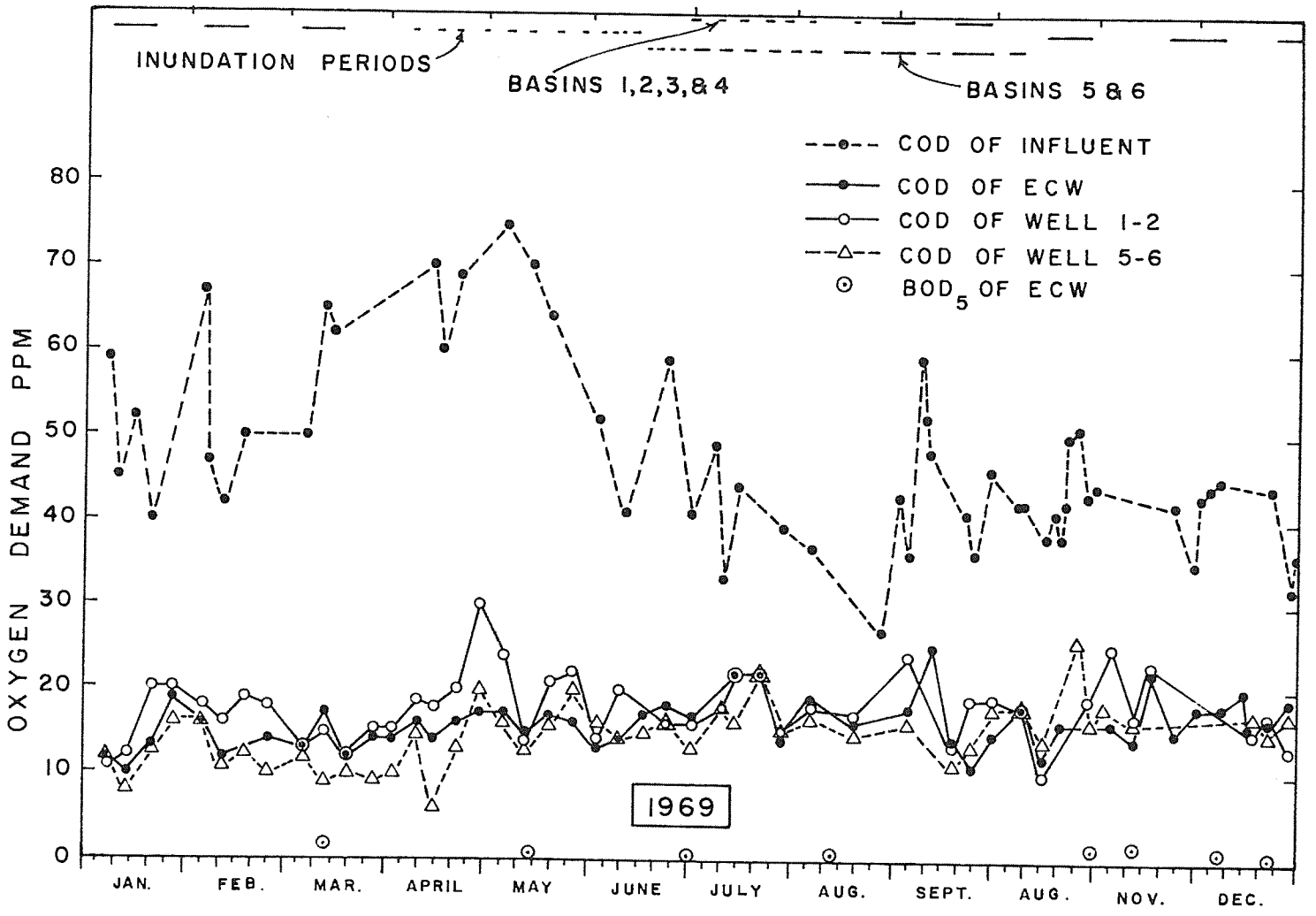

Figure 8. COD of influent and reclaimed water.

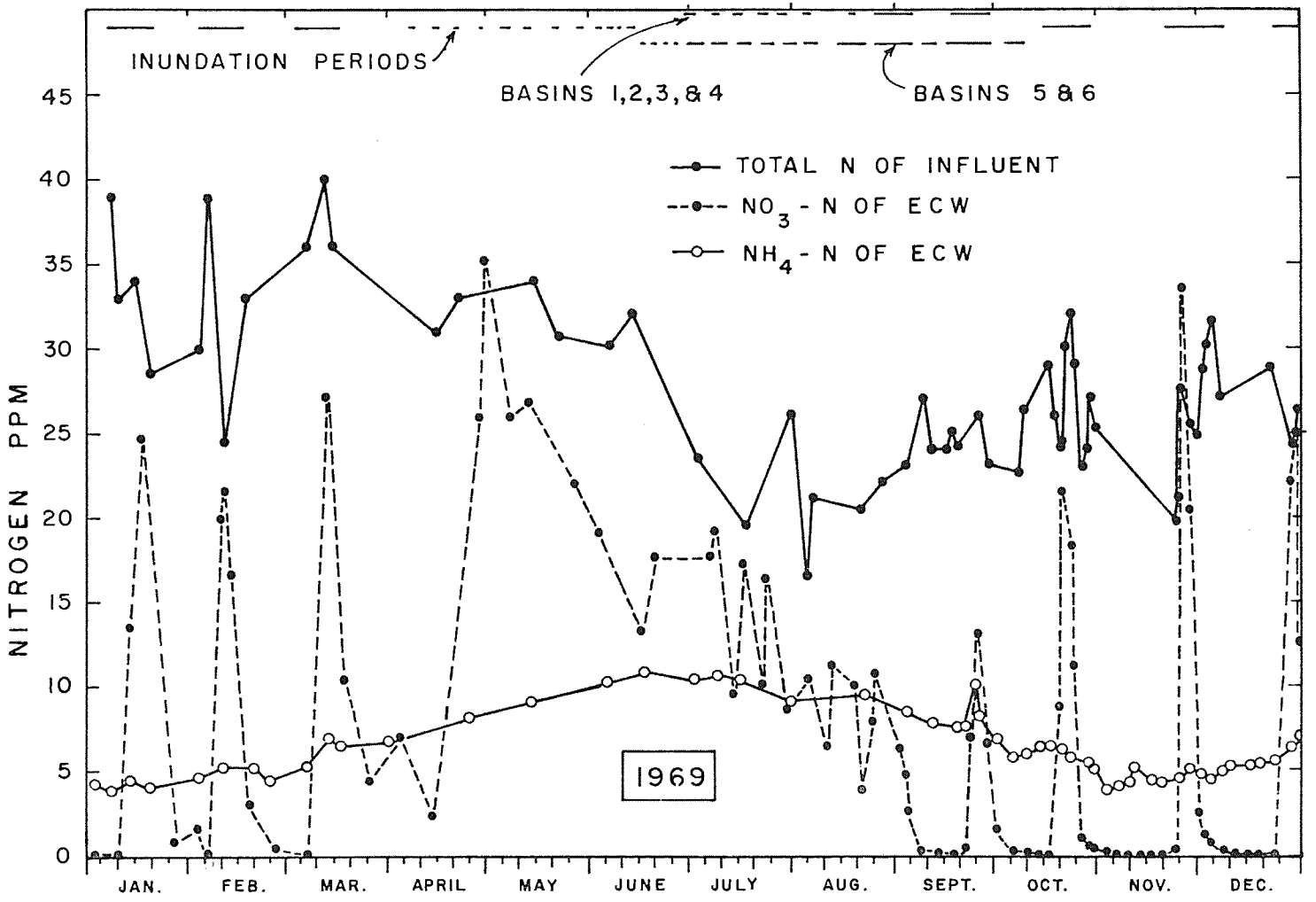

Figure 9. Nitrogen in influent and reclaimed water from ECW.

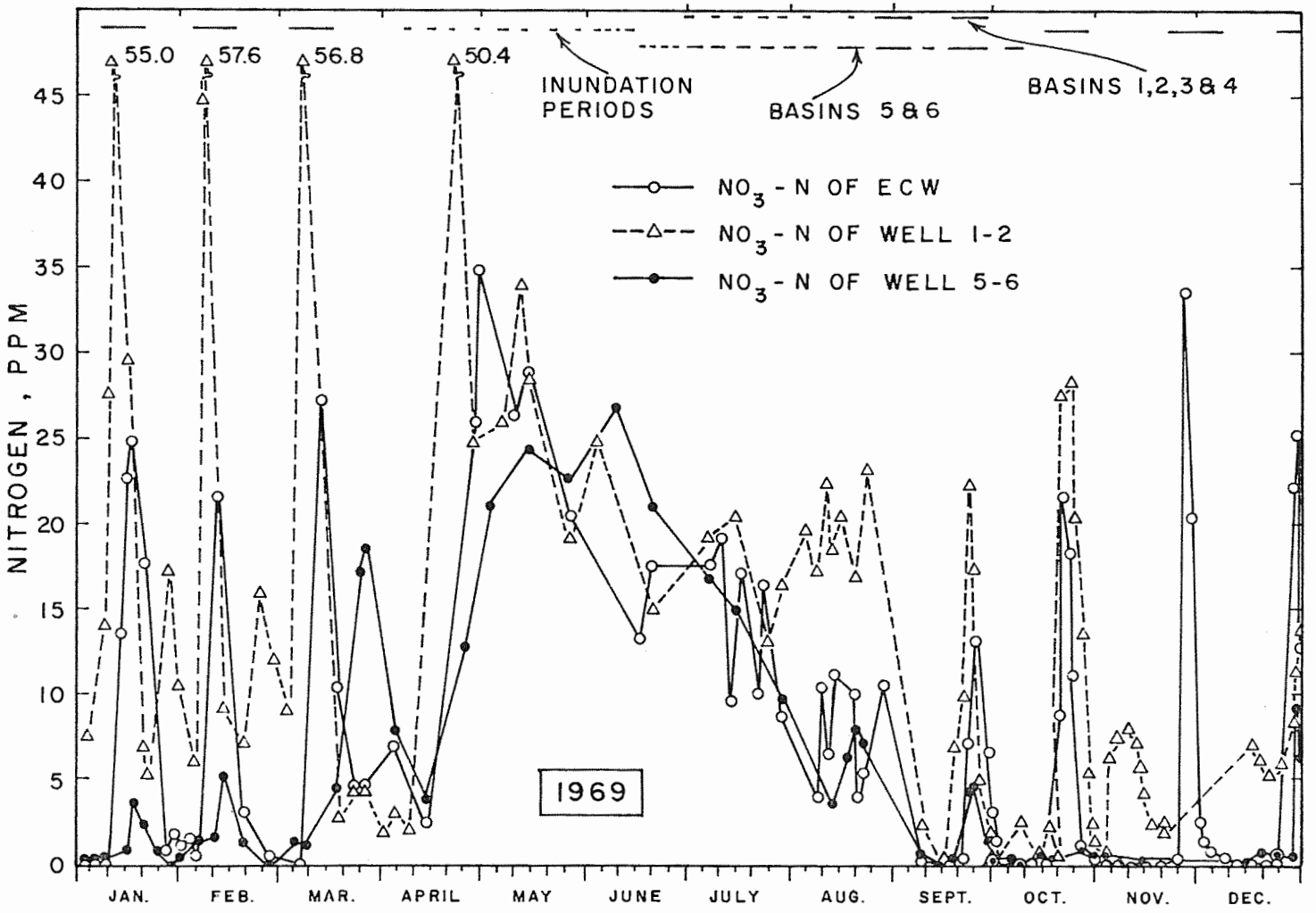

Figure 10. Nitrate nitrogen in reclaimed water.

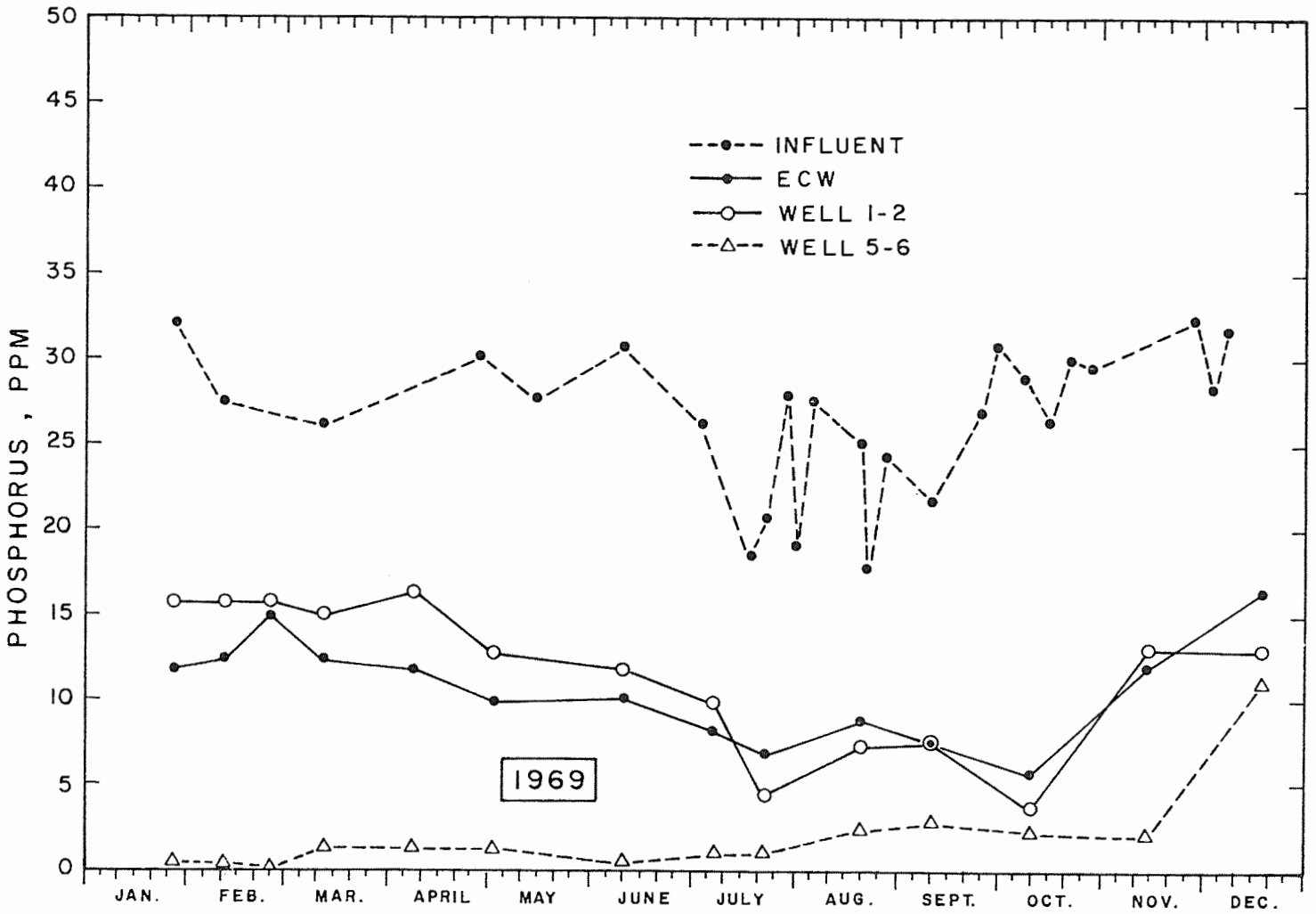

Figure 11. Phosphates in influent and reclaimed water.

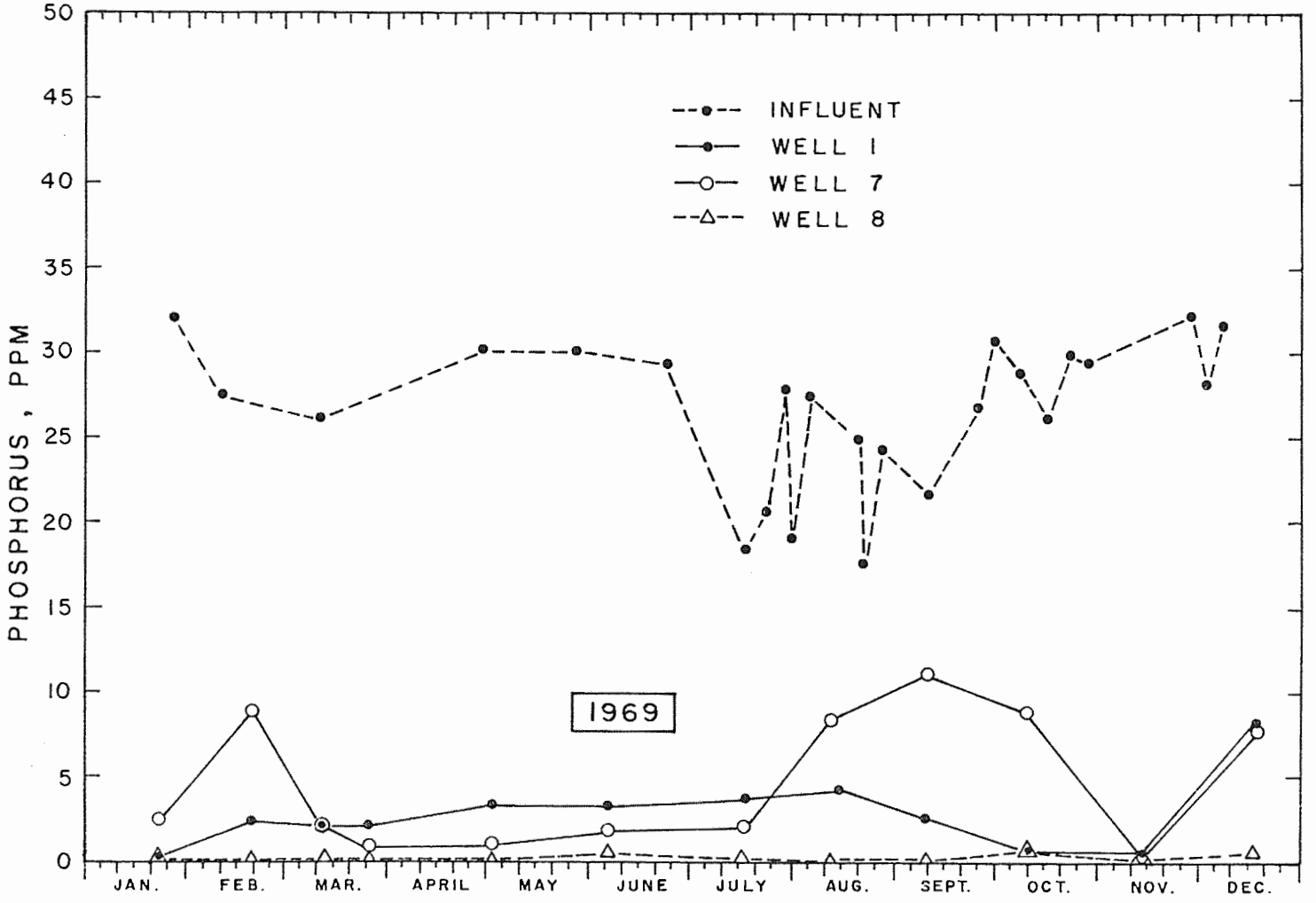

Figure 12. Phosphates in influent, reclaimed water, and native ground water.

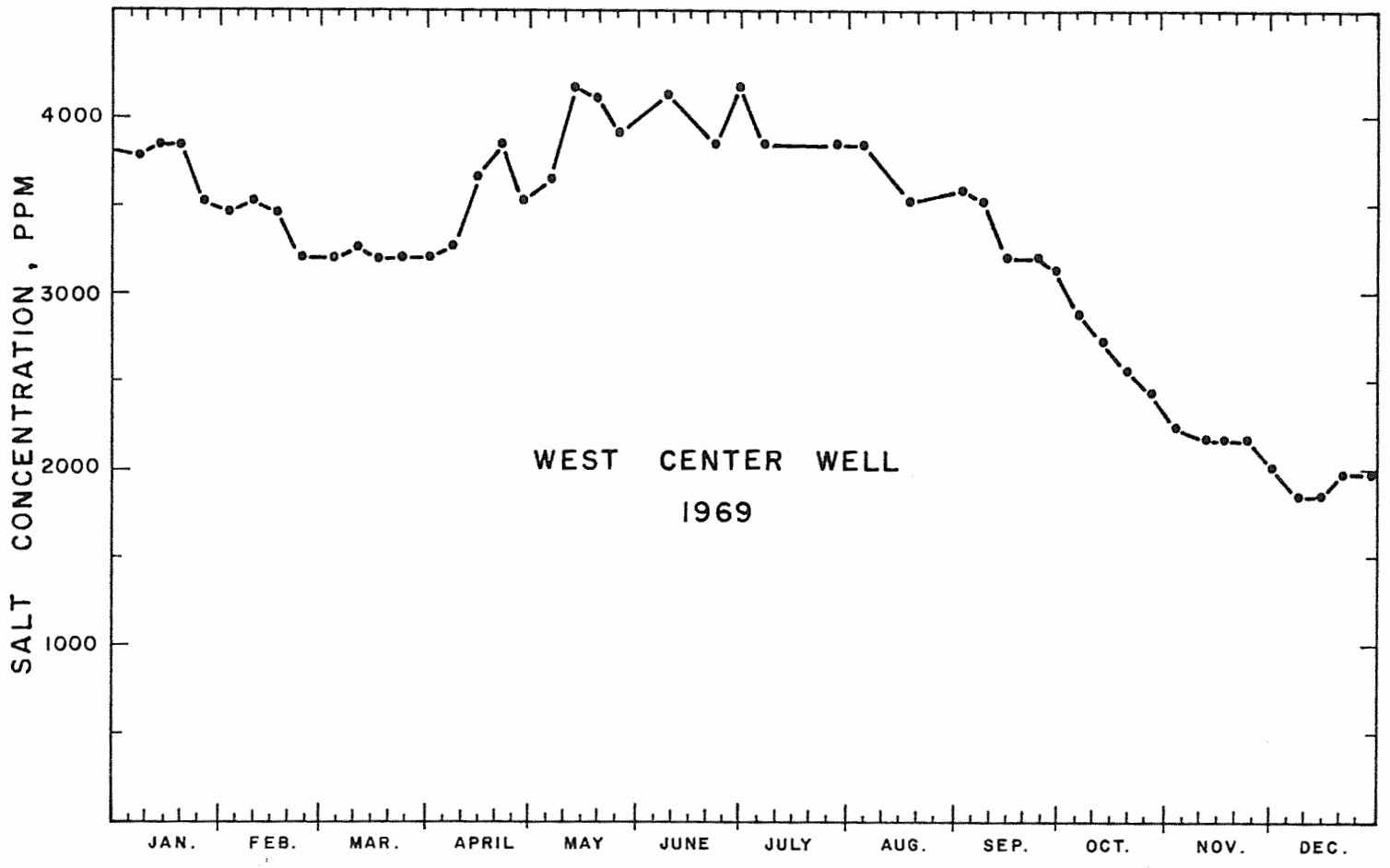

Figure 13. Salt concentration of WCW water.

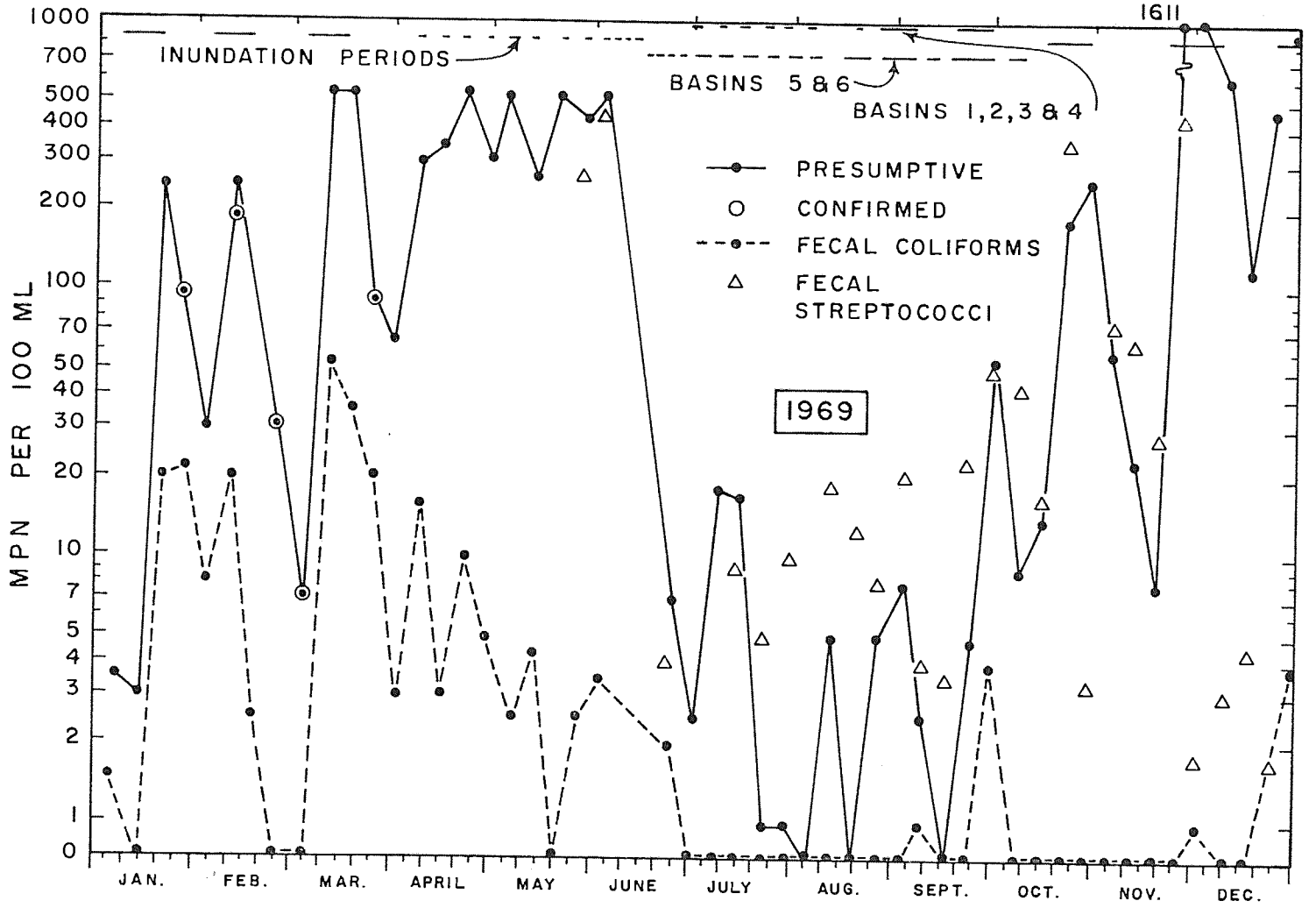

Figure 14. Coliform and streptococci densities in reclaimed water from ECW.

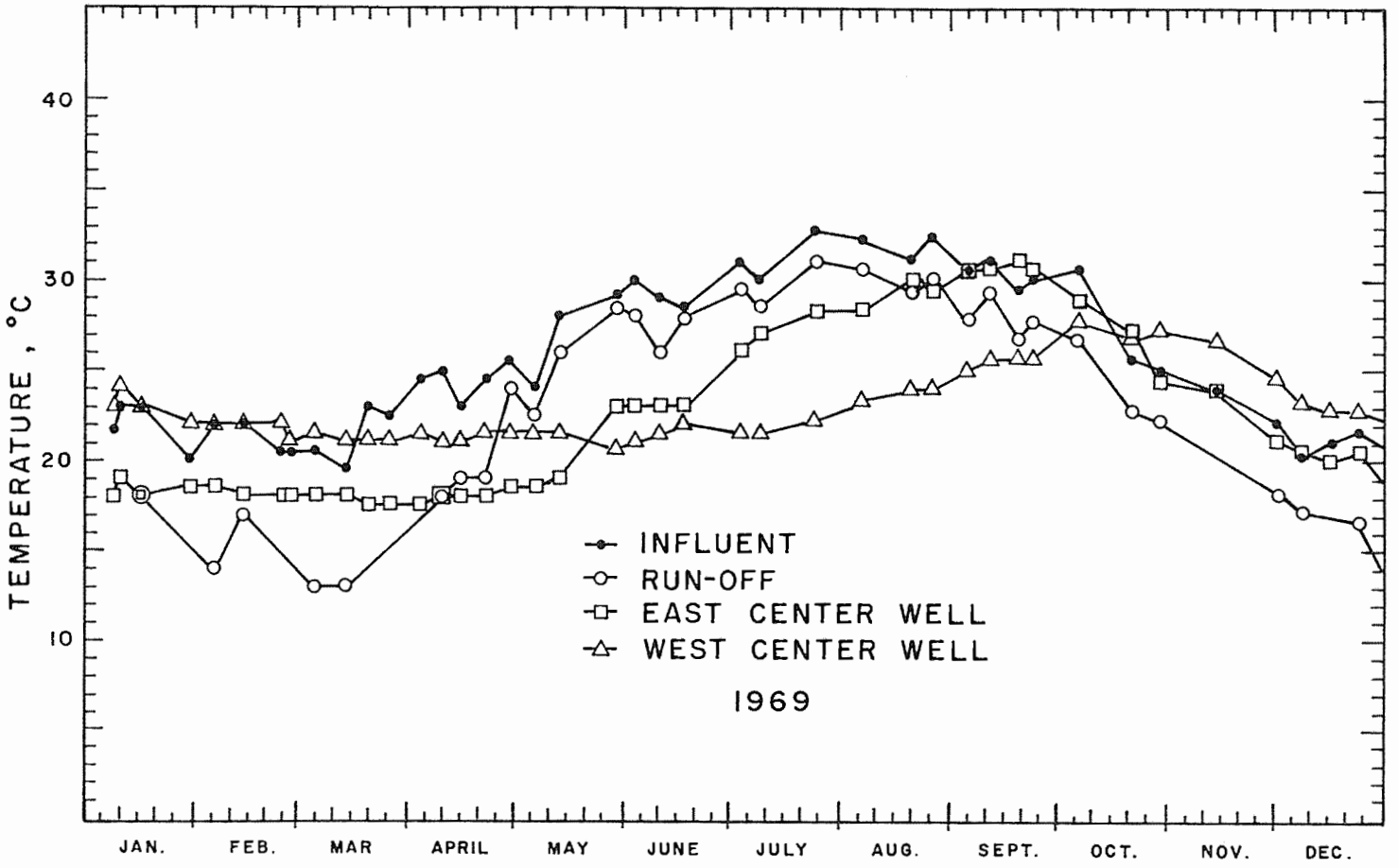

Figure 15. Temperature of influent and ground water.

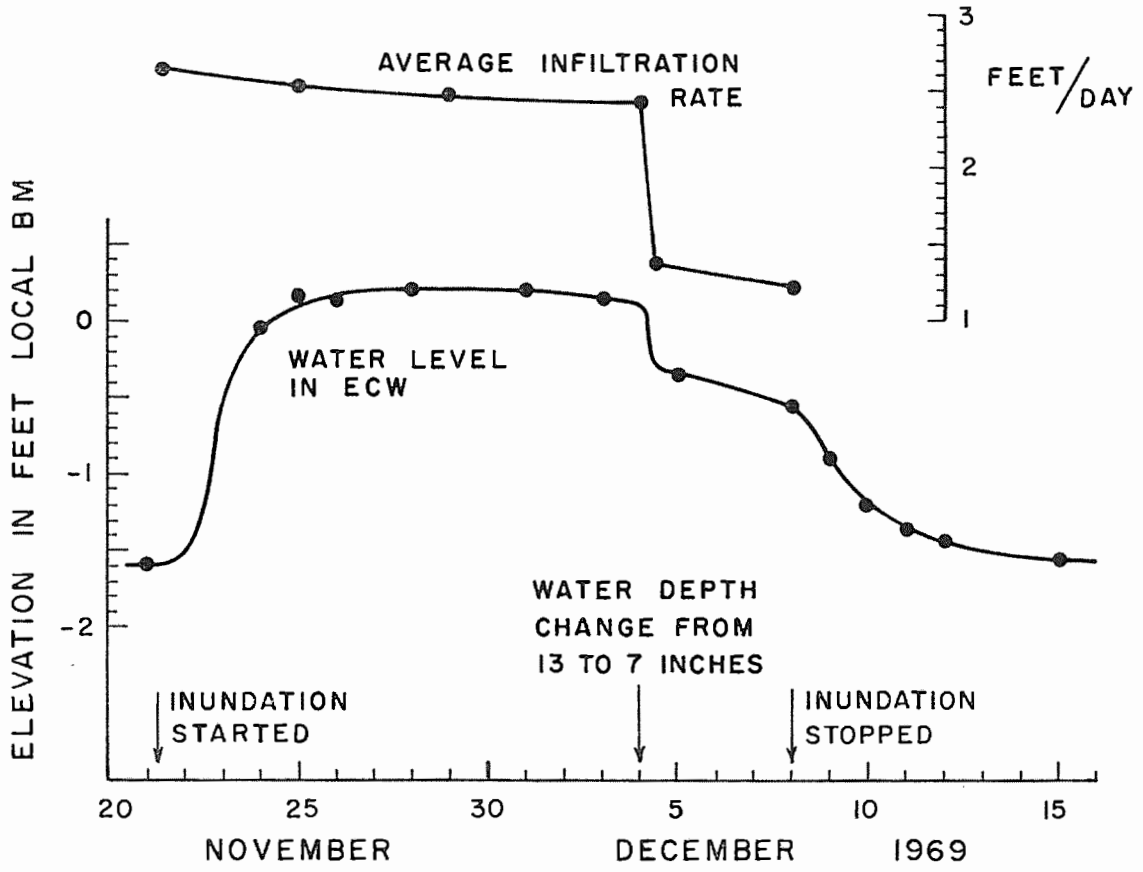

Figure 16. Response of water level in ECW to infiltration.

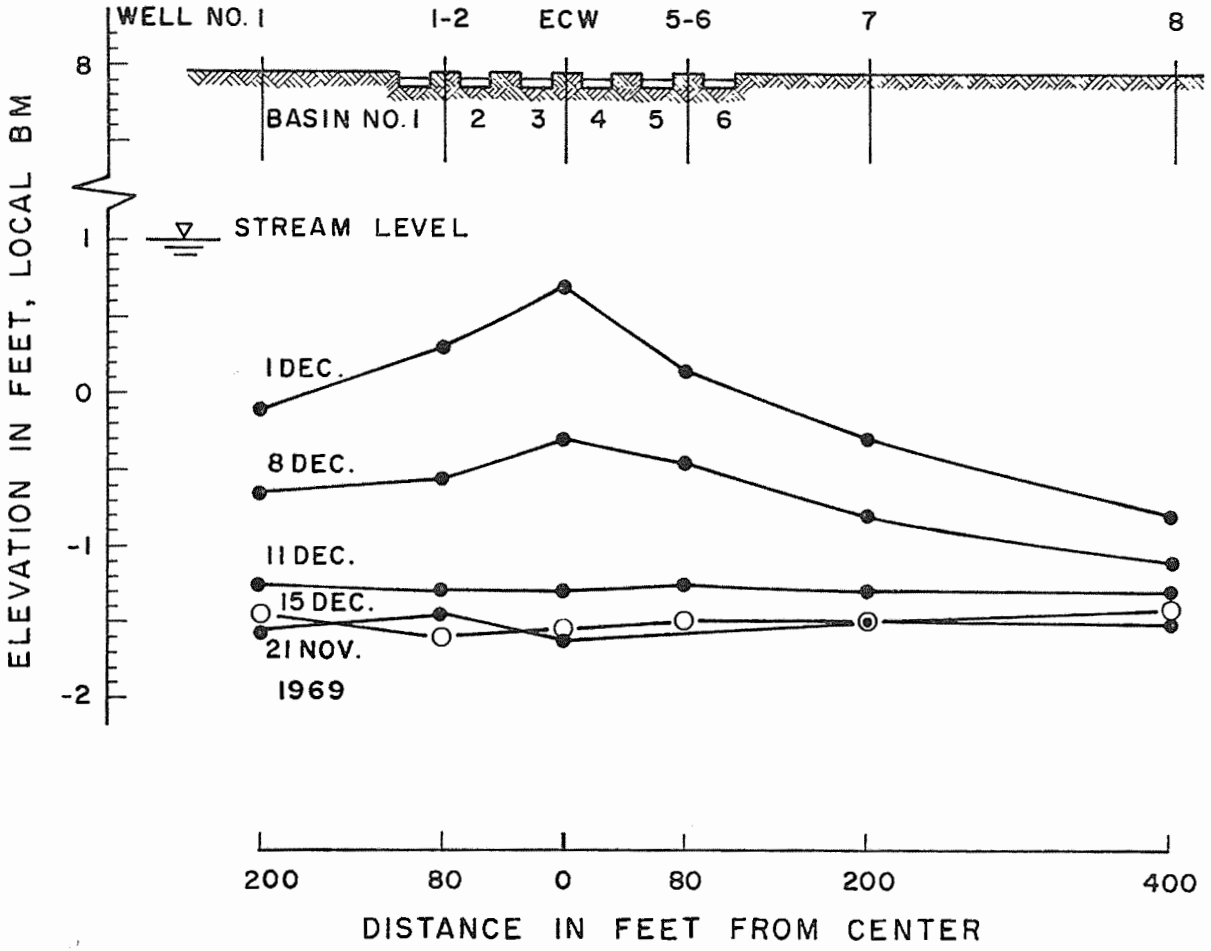

Figure 17. Water level profiles in observation wells.

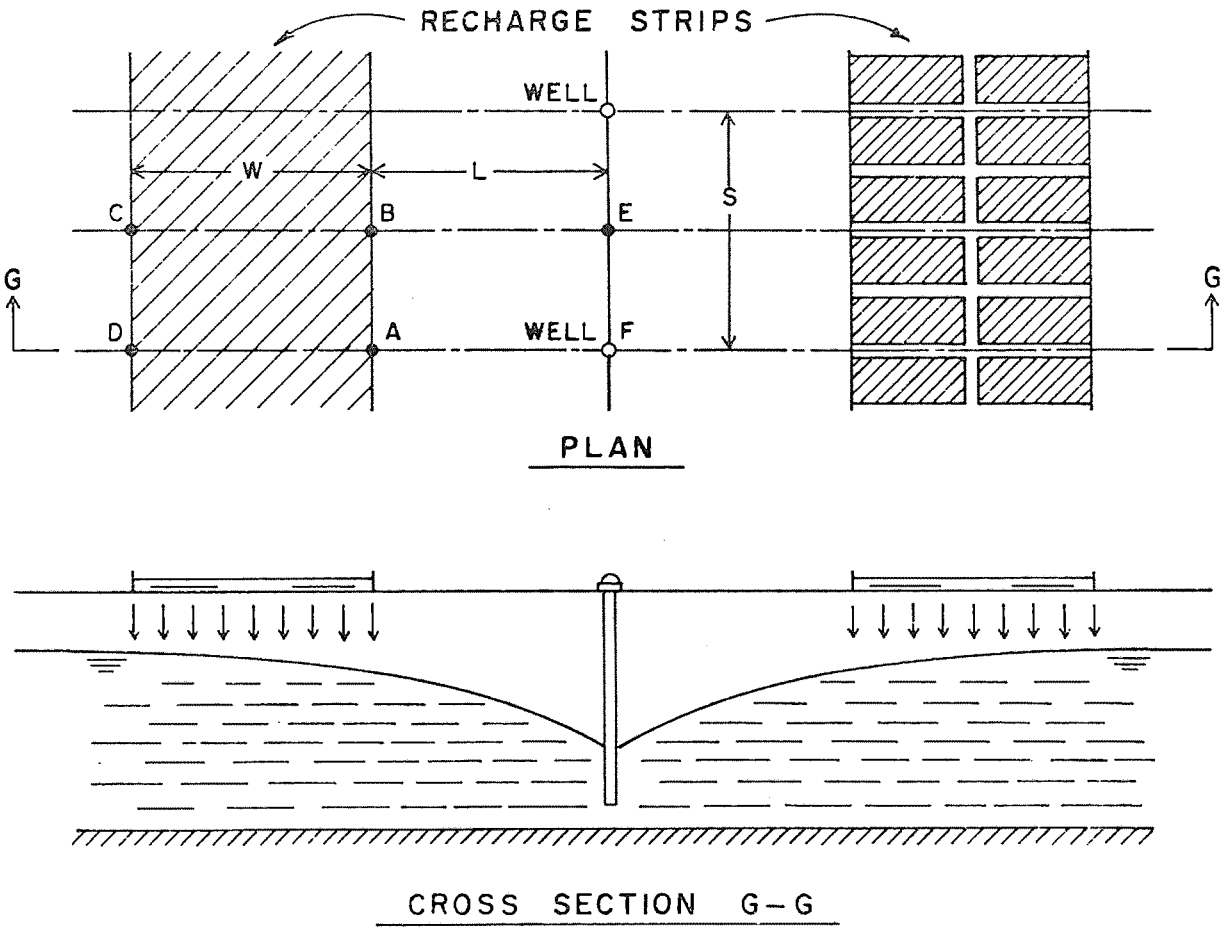

Figure 18. Plan and cross-section of two parallel recharge strips with wells midway between strips.

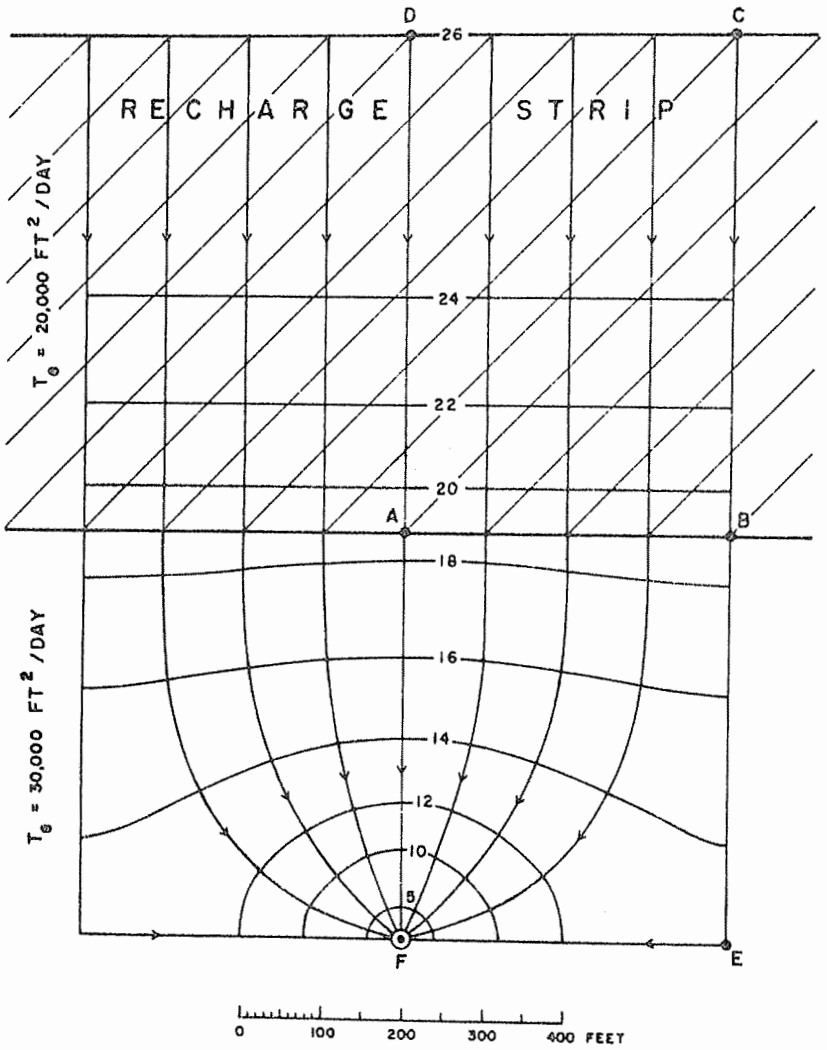

Figure 19. Streamlines and equipotentials (feet above water table adjacent to well) for parallel recharge strips with wells midway between strips.

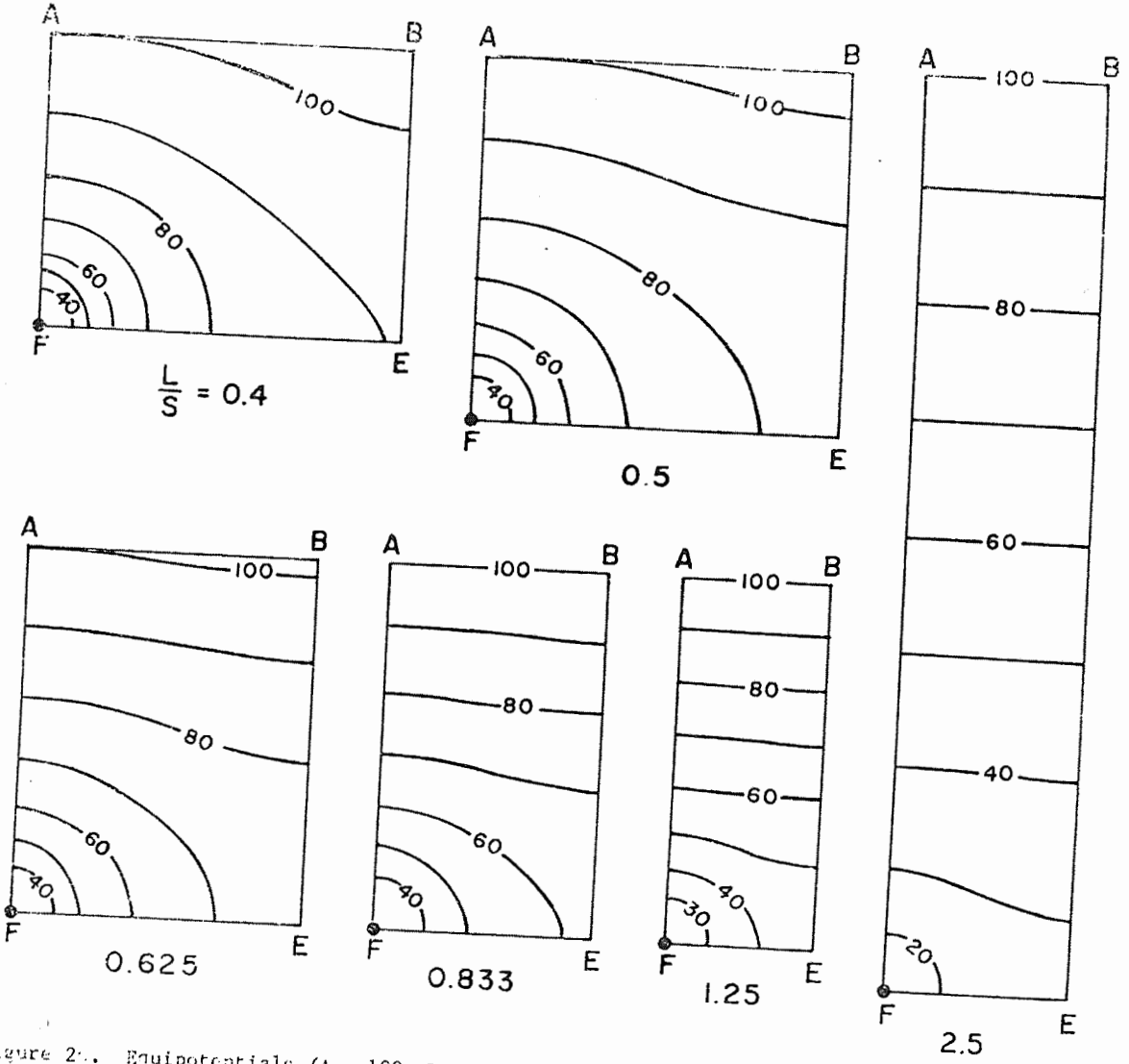

Figure 2-. Equipotentials (A = 100, F = 0) in region ABEF for different values of L/S.

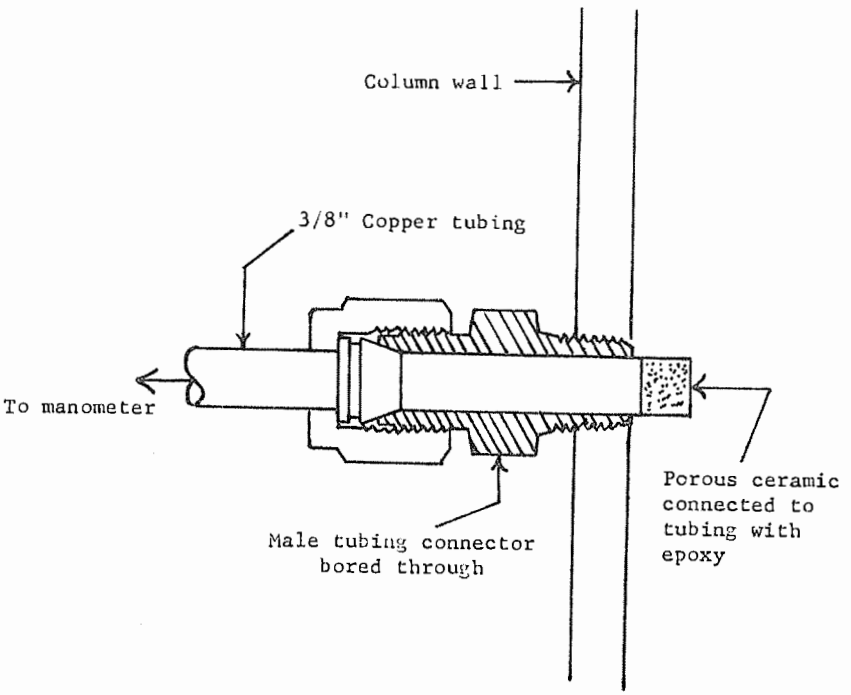

Figure 21. Schematic of tensiometer.

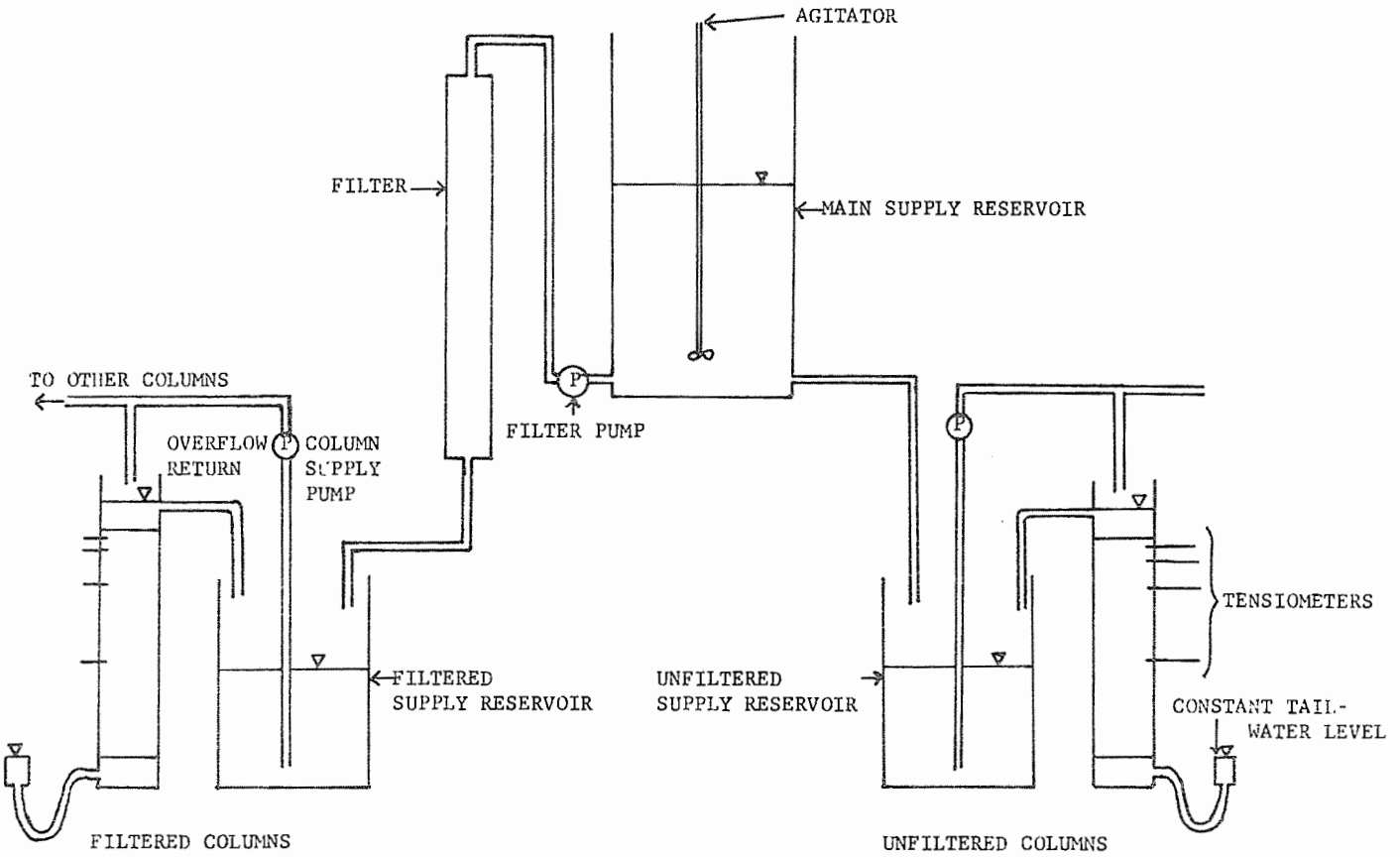

Figure 22. Schematic of filtration experiment.

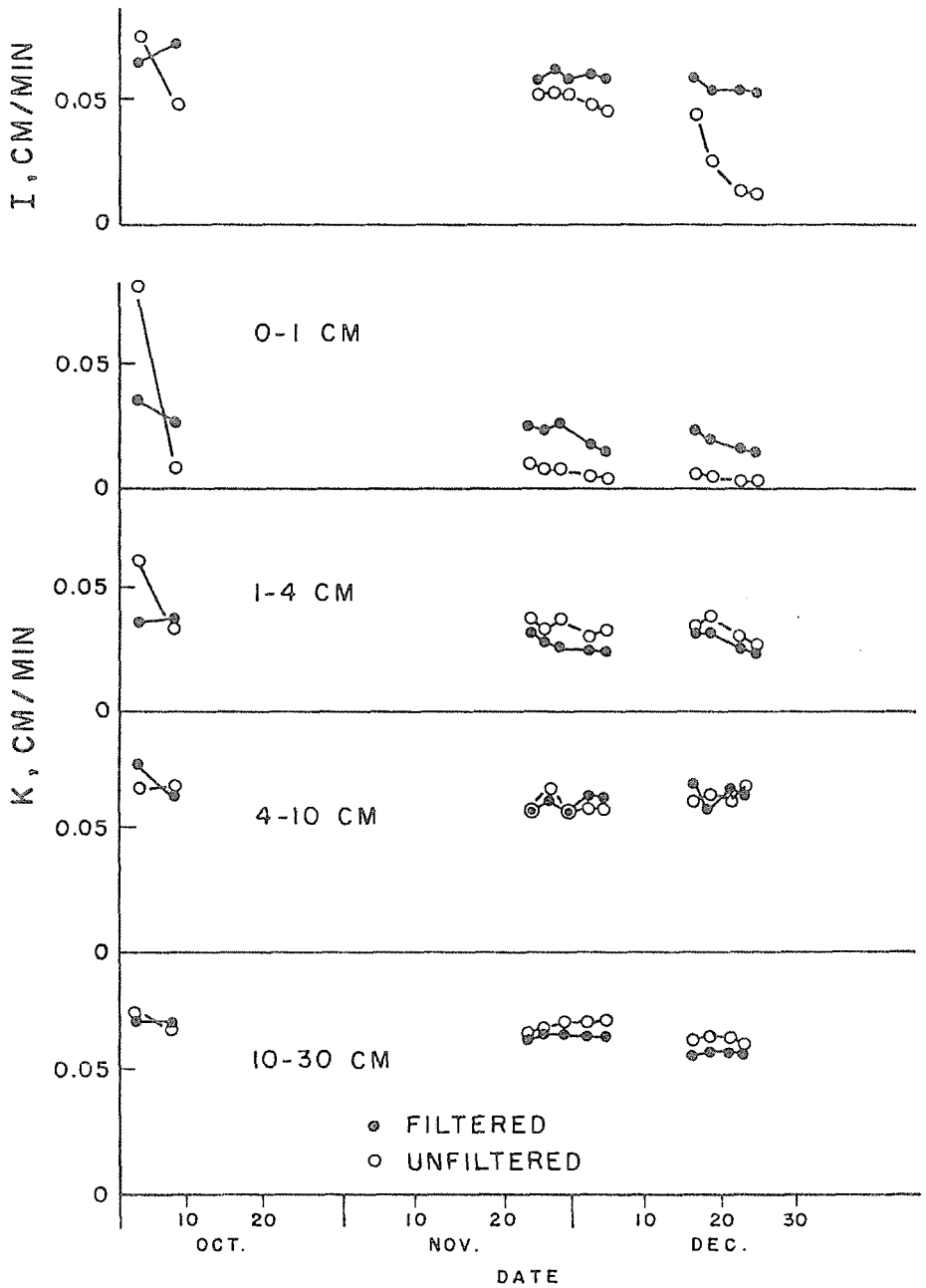

Figure 23. Hydraulic conductivity at different depths and infiltration rates for filtered and unfiltered columns.

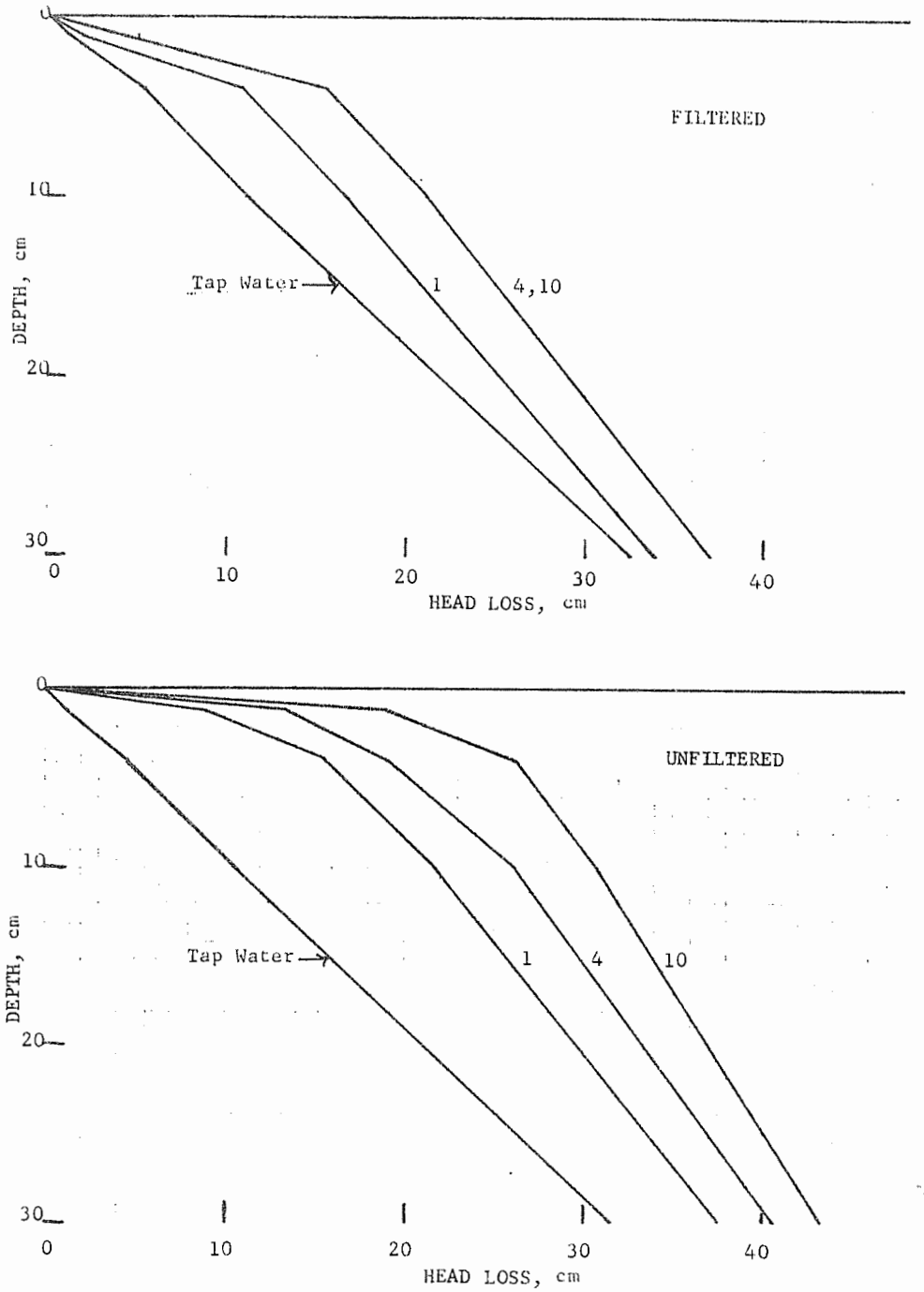

Figure 24. Head loss in columns for tap water and filtered and unfiltered effluent (curve parameter days after start of inundation period).

TITLE: COLUMN STUDIES OF THE CHEMICAL, PHYSICAL AND BIOLOGICAL PROCESSES OF WASTEWATER RENOVATION BY PERCOLATION THROUGH THE SOIL

CRIS WORK UNIT: SWC-012-gG-1 CODE NO.: Ariz-WCL 68-3

INTRODUCTION:

The soil columns described in the 1968 Annual Report were intermittently flooded with secondary sewage effluent from the 91st Avenue treatment plant in Phoenix, Arizona, during all of 1969. The research emphasis during this period was on oxygen use and movement and nitrogen removal from the sewage during flooding periods of varying lengths of time. Two major objectives were to determine the most important mechanisms of oxygen movement into the soil and nitrogen removal from the sewage water.

PART I. CHEMICAL AND BIOLOGICAL PROCESSES DURING RENOVATION

PROCEDURE:

Six columns of material from the basins at Flushing Meadows were packed in the laboratory. Effluent collected at Flushing Meadows from the 91st Avenue treatment plant was passed through the columns. Each column consists of a 2.75-meter length of 10-cm (I.D.) polyvinyl chloride pipe filled with 6 cm of pea gravel at the bottom and 250 cm of fine sand above that. The air-dry soil was packed to an average bulk density of 1.6 g/cc.

A constant head of 8 cm of water was maintained above the soil by means of a Mariotte siphon. The pipe was capped 10 cm above the level of this constant head. This space above the level of the head was filled with water at the beginning of the flooding period in order to provide a volume of water held at a slight negative pressure when the pipe was sealed (Figure 1). The air bubbling from the top of the soil column during flooding was collected when it displaced this water and pushed it back through the siphon tube. This air volume was sampled and measured by

withdrawing it through a serum cap in the top of the column with a syringe. A constant water level was maintained 5 cm above the lower end of the column, and air forced out the bottom was collected through a tube inserted into the gravel layer just above this water "table." This air was collected by displacement of water from a bottle connected to a constant head device. The air was sampled through a serum cap in the bottle, and its volume was measured by weighing the water displaced from the bottle.

The flow rate and cumulative flow through the columns were measured by weighing the column effluent at regular time intervals. The sewage water and column effluent were analyzed periodically for NO_3^-, NH_4^+, COD, and organic N. The air collected from the columns was analyzed for O_2, N_2, N_2O, and CH_4 with a model 900 Perkin-Elmer gas chromatograph equipped with a precision sampling valve, a molecular sieve column, and a Poropak Q column. Standard curves were prepared using purchased standard gas mixtures.

The columns were operated for 8 consecutive cycles of 2-days flooding and 5-days drainage, 6 cycles of 9-days flooding and 5-days drainage, and 4 cycles of 16-days flooding and 5-days drainage. Two columns were flooded continuously for 115 days and two others for 30 days.

Oxygen movement into the columns by mass flow was calculated by assuming that the water drained from the columns during the drainage or dry periods was replaced by an equal volume of air. Oxygen movement into the columns by diffusion was measured by stopping the column drainage for periods of 1 to 3 hours while the top of the column was capped. The oxygen depletion in the air space above the soil was measured by chromatographic analysis of samples taken at the beginning and end of this time. The oxygen diffusion rate was determined in this manner for several points during the 5-day drainage periods and plotted

vs. time (Figure 2). The area under the curve represented the total amount of oxygen diffusing into the column for the 5-day periods.

RESULTS AND DISCUSSION:

A. Two-day flooding cycles. A large nitrate "wave" was produced by the columns soon after the beginning of the flooding cycle (Figure 3). The NO_3^- content declined to almost zero near the end of the 2-day flooding period and remained low during the drainage period. This pattern was repeated for each of these cycles while the NH_4^+ and organic N remained at a low level (< 0.5 ppm). About 90 percent of the nitrogen entering the columns in the sewage water was in the NH_4^+ form, but almost all of this was oxidized to NO_3^- and passed through.

Nitrogen was apparently removed from the water during the last half of the flooding period and stored in the column. This could be tied up in microbial cells and/or held by the soil in some weakly adsorbed form. This nitrogen was nitrified during the drainage period and emitted from the column as NO_3^- when the columns were subsequently flooded. The nitrogen balance indicated that the total amount of nitrogen in the column effluent was about the same as the total amount of nitrogen entering the column in the sewage water (Table 1). The total amount of nitrogen in the air forced from the columns during flooding was also about equal to the nitrogen in the air which entered the column during drainage (Table 2).

B. Nine-day flooding cycles. When the columns were flooded for 9-day periods, the pattern of nitrate peaks was similar to that of the 2-day periods, but the peaks were farther apart (Figure 4). Consequently, more low-nitrate water was collected from the columns. The NH_4^+ also reached a peak soon after flooding and gradually declined throughout the flooding period. The total

amount of nitrogen in the column effluent was about 30 percent less than the total nitrogen of the incoming sewage water (Table 1). The amount of nitrogen in the air forced from the columns was about the same as the amount entering in the air (Table 2). It is possible that some nitrogen was produced in the columns during flooding and then diffused out during the dry period. This amount would have to be small, however, because nitrogen gas in large quantities would either bubble out through the water or cause the columns to clog.

C. Sixteen-day flooding cycles. The NO_3^- and NH_4^+ followed about the same pattern for the 16-day flooding cycles as for the 9-day cycles (Figure 5). The total amount of nitrogen in the column effluent was about 50 percent of the incoming nitrogen of the sewage water for the first cycle. When several cycles were run consecutively, the percentage nitrogen removal was considerably reduced (Table 1). The amount of nitrogen in the air forced from the columns was slightly greater than the amount of nitrogen in the incoming air (Table 2). This indicates some denitrification, but does not account for very much nitrogen loss.

D. Continuous flooding. Under continuous flooding the greatest nitrogen removal occurred from 2 to 20 days; it then decreased rapidly from 20 to 35 days and gradually decreased from 35 to 80 days when removal ceased (Figure 6). The infiltration rate was steady for about 30 days and then gradually decreased through the end of the year until the present time (Figure 8). Two other columns which were flooded for 30 days showed the same trend to that point (Figure 7).

E. Nitrogen removal from sewage water. About one half of the water collected from the columns during the 2-day flooding periods was low in nitrogen, even though the nitrogen removal for the whole cycle was zero. This was due to the concentration

of most of the nitrogen from the sewage water into about one half of the volume of the water leaving the columns (Figure 3). From 30 to 50 percent of the nitrogen was removed from the incoming sewage water during the long flooding cycles, and about one half of the remaining nitrogen was concentrated in about 10 percent of the total volume of water leaving the columns (Figures 4 and 5). Consequently, most of the water collected during the long cycles contained less than 10 ppm total nitrogen while the incoming sewage water contained about 25 ppm total nitrogen.

Much of the nitrogen removed from the sewage water was held by the soil in a form which could be nitrified during the dry periods, as evidenced by the very high nitrate concentrations of the water collected from the columns soon after flooding.

F. Nitrogen removal processes. The following processes were considered in attempting to account for the nitrogen removal by the soil columns: (1) denitrification, (2) volatilization of NH_3, (3) incorporation into microbial tissue, (4) adsorption of NH_4^+ by the clay fraction, and (5) adsorption of NH_3 by organic matter.

Gas was emitted from the columns several days after the flooding began in some cases. It was difficult to tell, however, if this was release of entrapped air or production of nitrogen. The amounts of gas released during the 9-day flooding periods were small and the nitrogen balance for the air indicated no N_2 production by the columns (Table 2). The nitrogen balance of the air forced from the columns during the 16-day flooding periods did indicate some N_2 production. The nitrogen accounted for by this N_2 would amount to only 10 to 20 percent of the total amount of nitrogen removed by the first two 16-day flooding cycles, however. Analyses of air samples taken near the end of

the first day of flooding showed an O_2 content of 1 to 2 percent, indicating that the columns had already been depleted of O_2. This means that most of the NH_4^+ entering the columns after the first day could not be nitrified and, consequently, could not be denitrified. Figures show that nitrogen removal occurs after the first day and is therefore due to some reaction involving NH_4^+ in an anaerobic environment. The sewage water does contain about 1 ppm NO_3 and 2 ppm dissolved oxygen. Some nitrate then can be produced and reduced to N_2. Large amounts of gas were not emitted from the columns even when they were flooded for more than 100 days and large amounts could not have collected in the columns without causing clogging.

Some NH_3 could be volatilized since the sewage water enters the columns at a pH of 7.8 to 8.2. The air forced from the columns was bubbled through boric acid, however, and no ammonia loss was detected. NH_3 loss by diffusion was also not detected during the dry period.

The incorporation of nitrogen into microbial cells undoubtedly occurs, but the extent of this removal is limited by the available carbon. The COD of the sewage water is reduced from about 40 ppm to 20 ppm, which is equivalent to the removal of about 8 ppm carbon. Since the C:N ratio of microbial tissue varies from 5:1 to 10:1, a maximum of 1 ppm nitrogen could be incorporated into microbial tissue. The actual amount is less than 1 ppm because some of the carbon is evolved as CO_2.

The soil used in the columns was removed from the recharge basins at Flushing Meadows where the clay content is 2 to 3 percent. The NH_4^+ absorbing capacity of the soil was probably saturated by the 200 feet of sewage water previously infiltrated through it during field experiments. Also, the NH_4^+ would have to compete with other ions such as Ca^{++}, Mg^{++}, and

Na^+ for any absorption sites which might be available. Therefore, nitrogen removal by this mechanism was probably very slight.

The chemical adsorption of NH_3 on organic matter could account for the removal of a large amount of nitrogen from the sewage water. This reaction occurs under both aerobic and anaerobic conditions, but primarily above pH 7. Broadbent et al. (1) has suggested that quinones produced by the oxidation of polyphenols are normally present in soils and may account for NH_3 fixation under anaerobic conditions. He further suggests that, when these active groups have been consumed, this reaction will continue only when new groups are produced by oxidation. This could explain why the nitrogen removal ceases after long periods of flooding (Figure 6). Further research will be needed to determine if the nitrogen removal can be rejuvenated by oxidation and to study the extent and form of the nitrogen retained in the soil.

G. Oxygen movement into soil columns. The amount of O_2 entering the columns by diffusion was about 1.5 times as much as by mass flow for 5-day periods following 2 days of flooding and twice as much as mass flow for 5 days following a 9-day flooding period (Table 3). The amount of oxygen entering by the two mechanisms would be about the same for a 3-day dry period.

The long flooding periods evidently built up a larger oxygen "sink" in the columns than did the short periods. Most of the oxygen entering the column is utilized in the oxidation of NH_4^+ to NO_3^- (Table 4). This produces the high nitrate concentrations emitted from column during the first 2 days of flooding. The oxygen utilization during the 9-day flooding periods appears to exceed the oxygen entry. This is probably due to a reduction in COD by anaerobic bacteria without the utilization of atmospheric oxygen. There may also be some experimental error in the nitrate

analyses due to oxidation of NH_4^+ while the columns effluent was being collected.

PART II. PHYSICAL PROCESSES DURING RENOVATION

PROCEDURE:

In addition to the six columns reported in last year's Annual Report, two more columns were constructed in which eight tensiometers and black platinum electrodes were installed. Figure 9 shows the relative positions of the tensiometers and electrodes. The grouping of four sets between 30 and 60 cm was made because, from independent measurements, it was determined that the height of capillary rise, or fringe, would be about 50 cm. It seems desirable to get measurements both above and below the capillary fringe, since this zone is essentially saturated during both drainage and infiltration.

The black platinum electrodes were made by drilling a small hole in the end of a 2-inch piece of brazing rod, into which about a 1-cm piece of #22 platinum wire was soldered. A piece of shrinkable plastic insulation was heated over the outside of the rod, and epoxy was smoothed over the soldered end as a final insulation. The probes were platinized after the manner of Quispel (2). They were standardized over a pH 4 buffer, using a Beckman Expandomatic SS-2 pH meter. Any probe which was off by more than $\pm$ 10 mv was discarded.

The tensiometers were made from either 150- or 300-cm H_2O bubbling pressure ceramic. This ceramic was epoxied onto the end of a piece of copper tubing. The higher bubbling pressure ceramic was used at the top of the column. The tensiometers were all filled with water and connected to a pressure transducer by means of a Scanivalve. The transducer output was recorded on a H Azar Leeds and Northrup recorder.

These columns will be referred to as columns 7 and 8 in this report.

RESULTS AND DISCUSSION:

Several cycles of 1-, 2-, and 3-week duration in which a drainage time of 5 days is kept constant have been run for columns 1 - 6. The results are given in another section of this report. The findings point out that during the 3-week cycle there is perhaps something happening to the nitrogen that we cannot account for. Columns 7 and 8 were run for several 3-week cycles and finally a 4-week cycle. The results of the last two cycles will be discussed.

On 25 November columns 7 and 8 were inundated. Figures 10 and 11 show the redox potential for several positions in the columns for 26 November to 11 December when the columns were drained. The influent had a pH of about 8; therefore, a value of +300 mv was added to all the millivolt readings to correct to a pH of 7 and a hydrogen electrode. It is obvious from comparing these two figures that columns 7 and 8 act differently. In general, the redox potential dropped at all points in column 7 during the entire inundation period. (The results for the positions not shown are similar to those shown and are left out for clarity's sale.) In column 8 after 1 December the potential at 60 cm started to rise; then after the 5th the potential at 50 cm started to rise. This zone spread downward to the 30-cm tensiometer by the 11th. No gaseous losses were detected at either end of the column.

The fluxes of water through these columns are shown in Figure 12. As can be seen, the flux in column 8 started out higher than column 7, but ended up lower by 11 December. This would lead one to suspect that something, perhaps denitrification with the N_2 trapped in the column, was responsible for the

decrease in fluxes in column 8 and the increase in redox at the bottom of column 8.

The change in tension within the columns during the inundation is shown in Figure 13. These data indicate that the tensions were positive during the early part of the flooding, but had become negative by the end of this inundation. The change most probably is due to surface clogging.

On 11 December the columns were both allowed to drain. Figures 14 and 15 show the change in redox potential over the drainage period. During this time both columns acted alike in that the redox potential increased above the 180-cm level, but decreased at all other positions. The potentials that had increased toward the end of the inundation period in column 8 decreased during drainages. The sections of the column below 180 cm then remained in a reduced status even during drainage.

Figures 16 and 17 show the tension profiles during drainage. As can be seen, the tension below 60 cm reached equilibrium during this period, but did not at the higher elevations. During the drainage the cap was removed and may have allowed loss of water by evaporation. In column 8 the evaporation may have caused some shrinkage and cracks so that the upper part of the column was separated from the rest of the column; thus, the change in tension at the top between 13 and 15 December.

On 16 December the columns were again flooded. The results in terms of the redox potentials are shown in Figures 18 and 19 and agree with those of the previous cycle. This cycle, however, was allowed to run for 4 weeks. Over the first day the two columns acted similarly in that the top potentials declined while those at 50 cm and below rose. This was probably due to the water which had been at the top of the column and in contact with the air and thus oxidized being pushed down

the column ahead of the new influent, and thus raising the lower potentials. The potentials in column 7, for the most part, all declined after the first day. Column 8 behaved as previously, with the potentials at 60, 50, 40, and 30 cm increasing in order as the zone spread. This time, however, on 2 January 1970 and following, gas was collected at both the top and bottom of the column. The gas contained about 98 percent N_2, 1 percent O_2, 1 percent CO_2, and traces of N_2O and CH_4. The O_2 could be due to contamination during sampling.

The fluxes in the columns are shown in Figure 20 for the inundation period. Column 7 behaved as before, but column 8 showed a sharp drop and then rise on 2 January. It is believed that the increase in redox potential, bubbling of gases, and increase of flux were all due to denitrification at the bottom of the column and subsequent release of the gases.

The tension profiles at the beginning of infiltration, the end of infiltration, and at the lowest flux are shown in Figure 21. These also indicate surface clogging of the soil during infiltration, especially of column 7. The fact that the profile in column 8 is almost the same at the end as at the beginning shows that the disruption of the surface by gaseous bubbles when the N_2 was released restores the infiltration rate all along the profile. The changes in tension with time for different positions in the profile in column 8 are shown in Figure 22. The tensions were most negative above the zone of highest redox around 31 December to 2 January; then, when the air was released, the tensions increased (algebraically).

As to why column 8 shows denitrification and not column 7 (or any of the others for that matter) will be the subject of further investigation.

SUMMARY AND CONCLUSIONS:

Six columns filled with 250 cm of soil from the Flushing Meadows recharge basins were intermittently flooded with secondary sewage effluent during 1969. The columns were operated on schedules of either 2-, 9-, or 16-days flooding, followed in each case by a 5-day drainage or dry period. Two columns, however, were continuously flooded for 115 days. The incoming sewage water and the column effluent were analyzed for NO_3^+, NH_4^+, COD, and organic N, and the gases forced out of the columns were collected and analyzed for N_2, O_2, CO_2, N_2O, and CH_4.

Nitrogen and oxygen balances were calculated for the various cycles. The total amounts of nitrogen entering and leaving the columns were about the same for the 2-day flooding cycles. About 30 percent of the total nitrogen of the sewage water was removed during the 9-day flooding cycle, while the 16-day cycles effected a 50 percent removal. The amount of removal during the 16-day cycles declined to about 25 percent, however, when several cycles were run consecutively. The continuously flooded columns showed a steady rate of nitrogen removal for 25 days, but then declined until about 80 days when the nitrogen removal reached zero.

The nitrogen balance of the column air indicated that nitrogen was lost as a gas only after the columns had been flooded for more than 9 days, and this gaseous loss was usually less than 20 percent of the total amount of nitrogen removed from the sewage water.

Denitrification did not seem to be the primary mechanism of nitrogen removal because gas production was low and the oxygen available to oxidize NH_4^+ to NO_3^- before denitrification was limited. The volatilization of NH_4^+ could not be detected by chemical tests, and the incorporation of nitrogen into organic matter was limited by the small concentration of carbon in the sewage water. Fixation of NH_4^+ by the clay fraction of the soil was limited by the low

clay content of the soil, which had probably been previously saturated during recharge of sewage water in the field. The adsorption of nitrogen by the organic fraction of the soil could account for much of the nitrogen removal. Most of the nitrogen removal is effected by some reaction of NH_4^+ in an anaerobic environment, but more research will be needed in order to describe this reaction.

A groundwater recharge system could be operated to produce reclaimed water with varying nitrogen concentrations in accordance with the intended use of the water. Short, frequent flooding periods would provide a high-nitrate water for grain or forage crops. During long flooding cycles, large quantities of low nitrogen water can be produced because much of the nitrogen is removed and about half of the remaining nitrogen is concentrated in 10 to 15 percent of the total volume of reclaimed water.

The ratio of oxygen entering the columns by diffusion to that entering by mass flow was 1.5 to 1 and 2 to 1 for 5-day drainage periods following 2-day and 9-day flooding periods, respectively. Both mass flow and diffusion are therefore important mechanisms of oxygen entry. Most of the oxygen is utilized in oxidizing NH_4^+ to NO_3^-, as evidenced by the NO_3^- wave produced soon after flooding.

Two other columns were constructed late in the year in which eight tensiometers and black platinum electrodes were installed. Soon after flooding, the oxidation-reduction potential at most of the electrodes dropped to a negative value. During a 23-day flooding period, a rise in the oxidation-reduction potential and the bubbling gas from out of the columns near the end of the period indicated that denitrification had taken place in one column. The flux decreased before the gas was evolved, and the tensiometers showed a negative pressure throughout the column. The flux

increased, and the tensiometer showed a positive pressure after the gas was evolved. During other parts of the flooding period the tensiometers indicated surface clogging, while tensiometers in the other column indicated surface clogging throughout the flooding period.

REFERENCES:

1. Broadbent, F. E., W. D. Burge, and T. Nakashima. Factors influencing the reaction between ammonia and soil organic matter. Trans. 7th Intern. Congress Soil Sci. 2:509-516. 1961.

2. Quispel, A. Measurement of the oxidation-reduction potentials of normal and inundated soils. Soil Sci. 63:265-275. 1947.

PERSONNEL: J. C. Lance, F. D. Whisler, Herman Bouwer, R. C. Rice, E. Escarcega

CURRENT TERMINATION DATE: October 1971

Table 1. Nitrogen removal from secondary sewage effluent by soil columns during flooding periods of different lengths.

Nitrogen content	CYCLE A	B	C	D	E	F	Total
			2 Days Flooded				
N influent	340.0	261.5	226.1	258.0	277.4	278.5	1641.5
N effluent	295.7	294.7	305.7	286.3	260.0	272.4	1714.8
% removal	-13%	+11%	-26%	+10%	+6%	+2%	-4%
			9 Days Flooded				
N influent	1100.0	1236.0	1146.4	815.7			4298.1
N effluent	857.3	862.7	837.9	551.0			3108.9
% removal	22%	30%	27%	32%			28%
			16 Days Flooded				
N influent	1516.2	1753.0	1826.7	1715.3*			-
N effluent	764.7	1039.2	1596.9	1146.5			-
% removal	50%	41%	20%	33%			-

*Column 1 only

Table 2. Nitrogen balance of air from soil columns during intermittent flooding with secondary sewage effluent.

Days flooded	N in	N out
	mg	mg
2	2289	2204[1/]
9	2360	2324[2/]
16	2404	2517[3/]

[1/] Data are averages for 8 flooding cycles.

[2/] Data are averages for 3 flooding cycles.

[3/] Data are averages for 2 flooding cycles.

Table 3. Comparison of oxygen entry into soil columns by diffusion and mass flow during intermittent flooding cycles with secondary sewage effluent.

Oxygen entry during 5 days following 2-day flooding periods				Oxygen entry during 5 days following 9-day flooding periods			
Column number	Mass flow	Diffusion	Diffusion / Mass flow	Column number	Mass flow	Diffusion	Diffusion / Mass flow
	mg	mg			mg	mg	
4	758.9	1030.0	1.36	1	657.6	1489.7	2.27
4	723.7	1226.7	1.70	2	663.7	1398.2	2.11
3	767.3	1205.5	1.57	1	753.5	1410.6	1.87
				5	780.5	1348.6	1.73
Average	750.0	1154.1	1.5	Average	713.8	1411.8	2.0

Table 4. Oxygen balance of soil columns intermittently flooded with secondary sewage effluent.

Time flooded	Oxygen utilization			Oxygen entry			Difference
	NH_4^+ oxidation	COD reduction	Emitted from column	Mass flow[2]	Diffusion	NO_3 of sewage	
days[1]	mg	mg	mg	mg	mg	mg	mg
2	1288.7	170.4	344.7	758.9	1030.0	60.8	+46.0
2	1346.5	239.5	305.6	723.7	1226.7	12.3	+81.1
2	1310.5	252.8	344.5	767.3	1205.5	11.6	+76.6
9	1917.9	780.7	164.7	657.6	1489.7	9.6	-706.4
9	1960.7	671.4	98.8	663.7	1398.2	8.8	-660.2
9	1773.3	924.4	160.0	753.5	1410.6	18.2	-665.4
9	1779.9	1121.0	203.8	780.5	1348.5	21.4	-944.3

[1] Entries are for different columns and/or flooding periods.

[2] The drainage period was 5 days in each case.

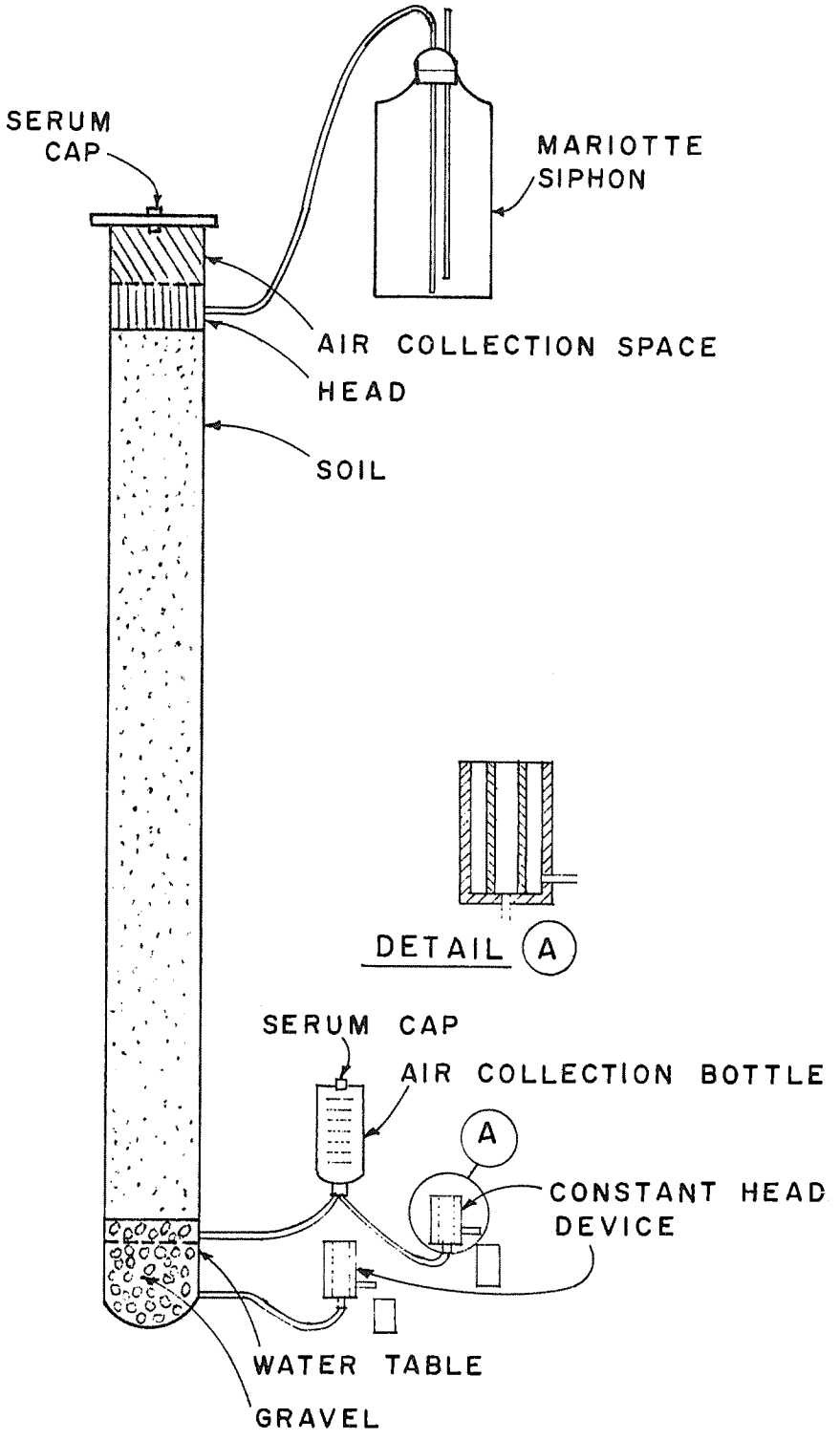

Figure 1. Soil column for wastewater renovation studies.

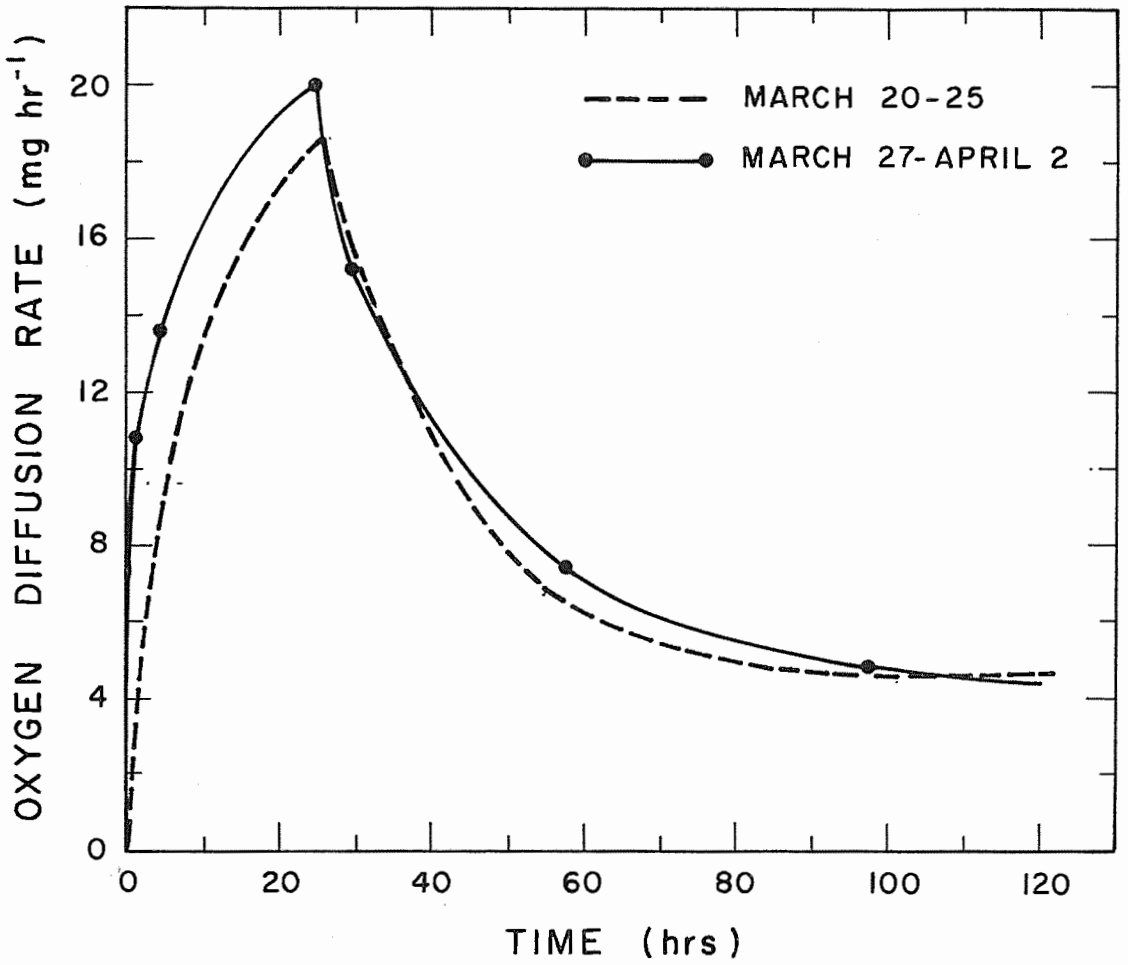

Figure 2. The oxygen diffusion rate during 5-day drainage periods following 2 days of flooding.

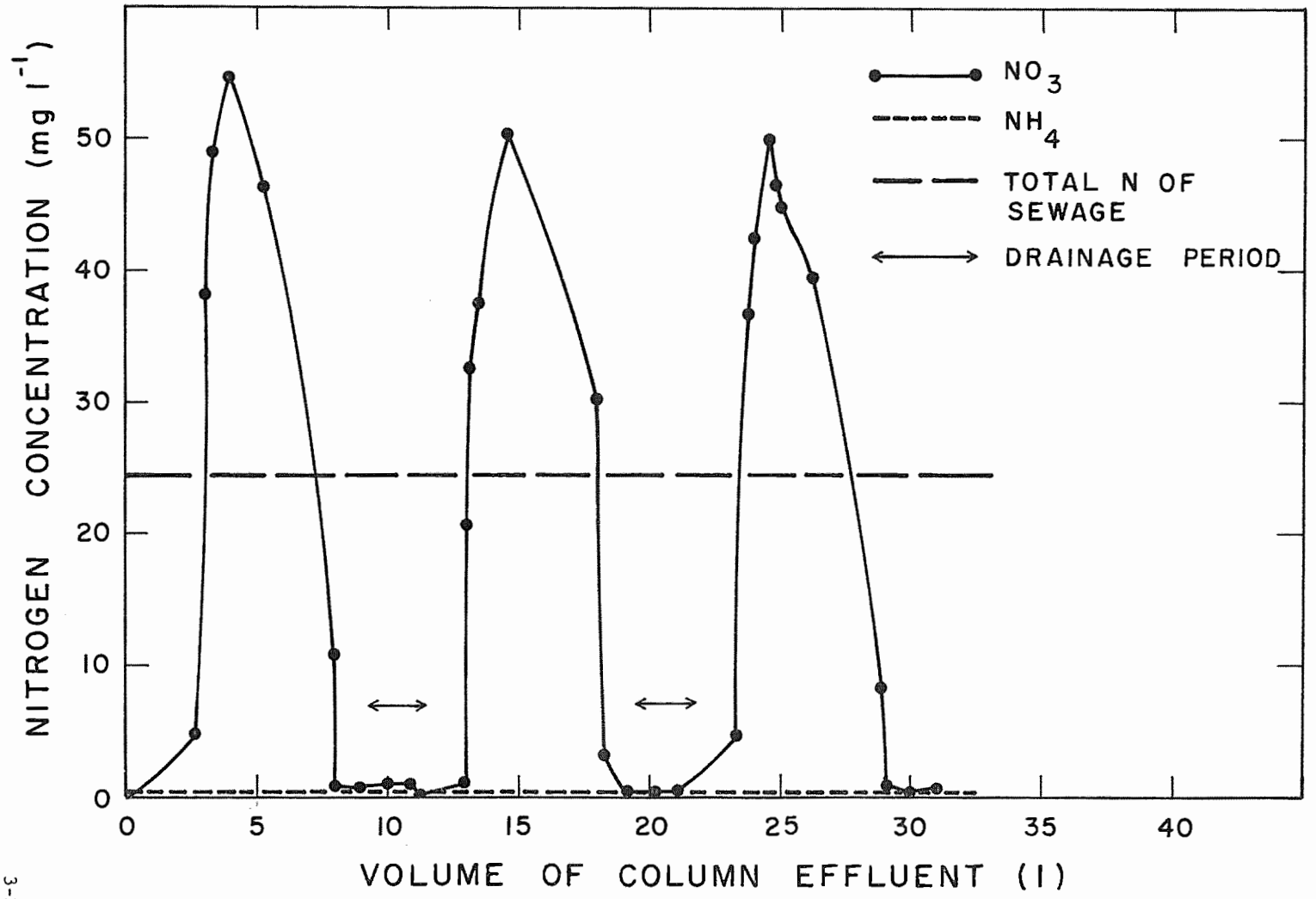

Figure 3. The change in nitrogen content with volume of column effluent during 3 cycles of 2 days flooding and 5 days dry.

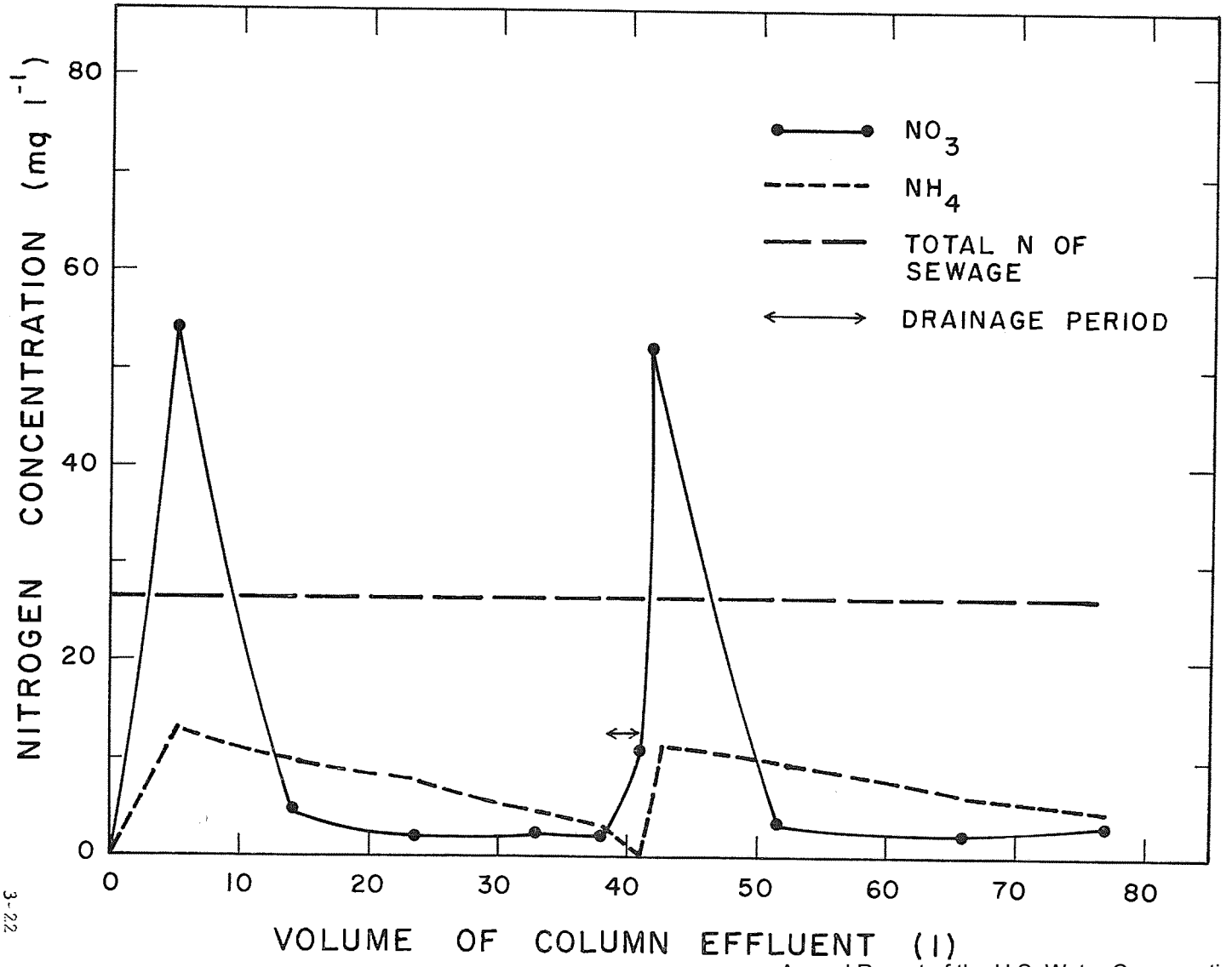

Figure 4. The change in nitrogen content with volume of column effluent during 2 cycles of 9 days flooding and 5 days dry.

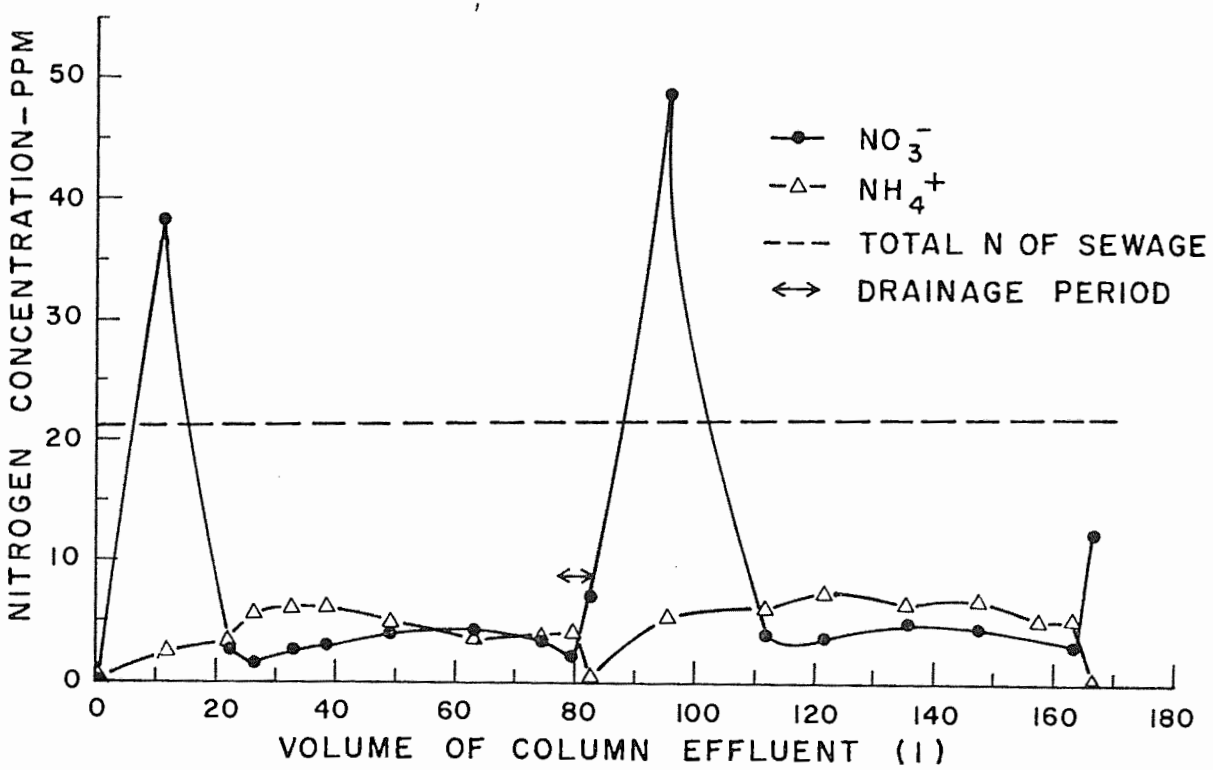

Figure 5. The change in nitrogen content with volume of column effluent during two cycles of 16 days flooding and 5 days dry.

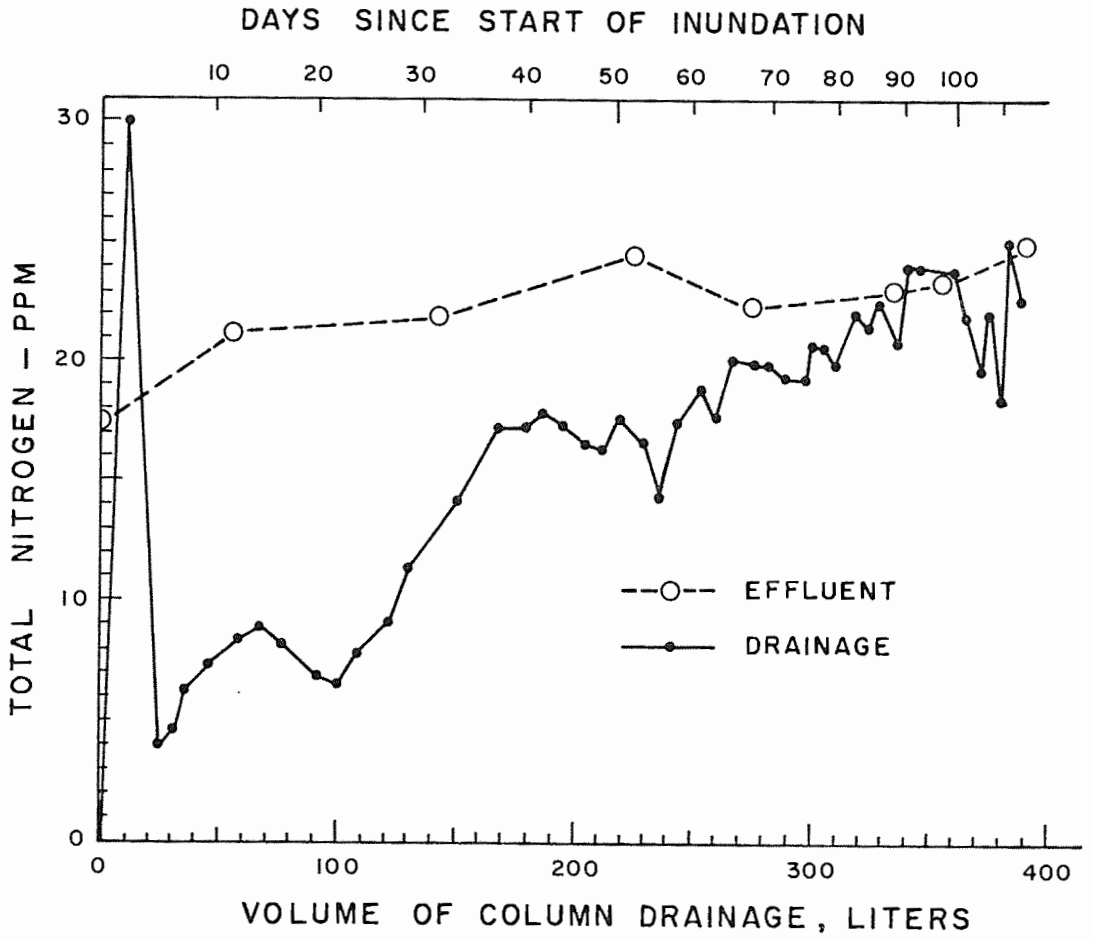

Figure 6. The change in total nitrogen content of secondary sewage effluent during continuous flooding of a soil column.

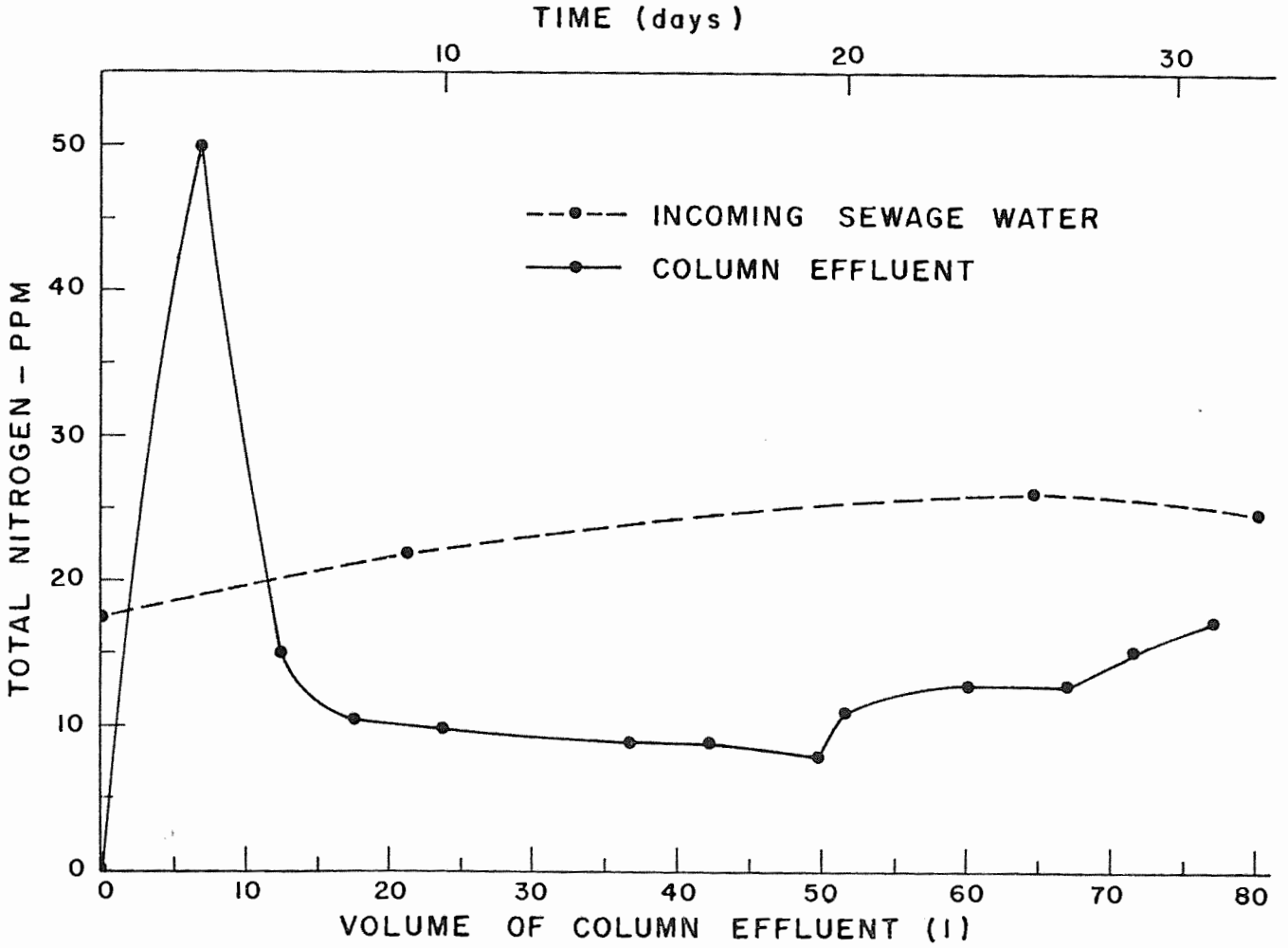

Figure 7. The change in nitrogen content with volume of column effluent during a 30-day flooding period.

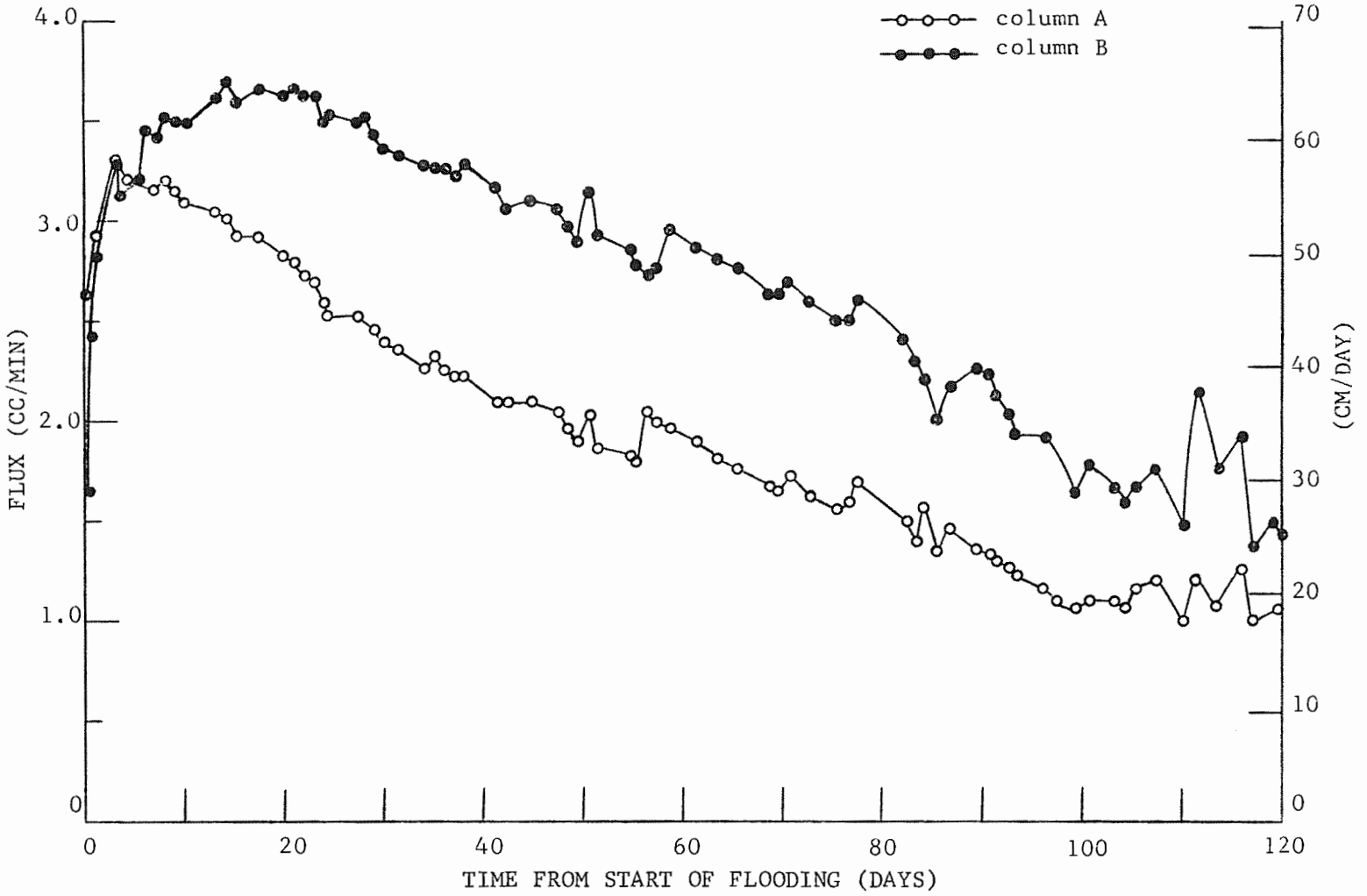

Figure 8. The change in flux with length of flooding time for two continuously flooded soil columns.

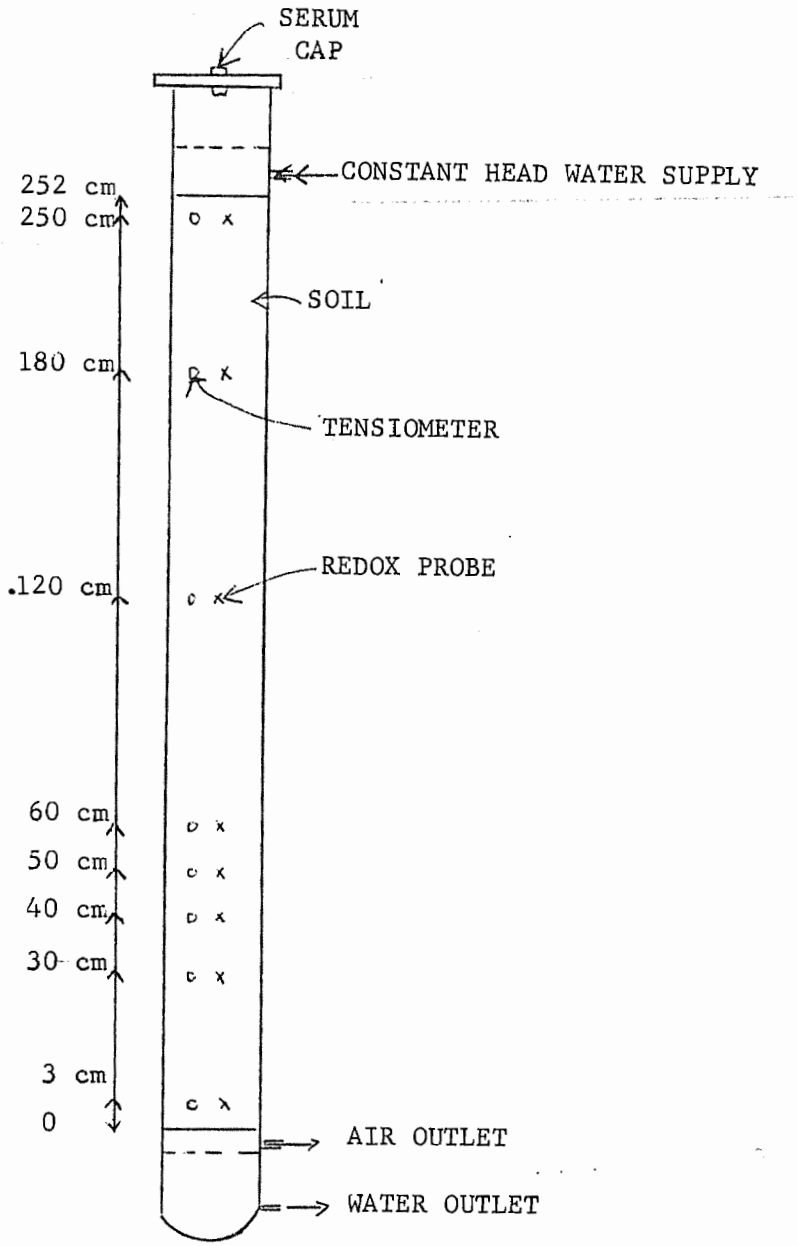

Figure 9. Schematic diagram of the soil columns with tensiometers and redox potential probes.

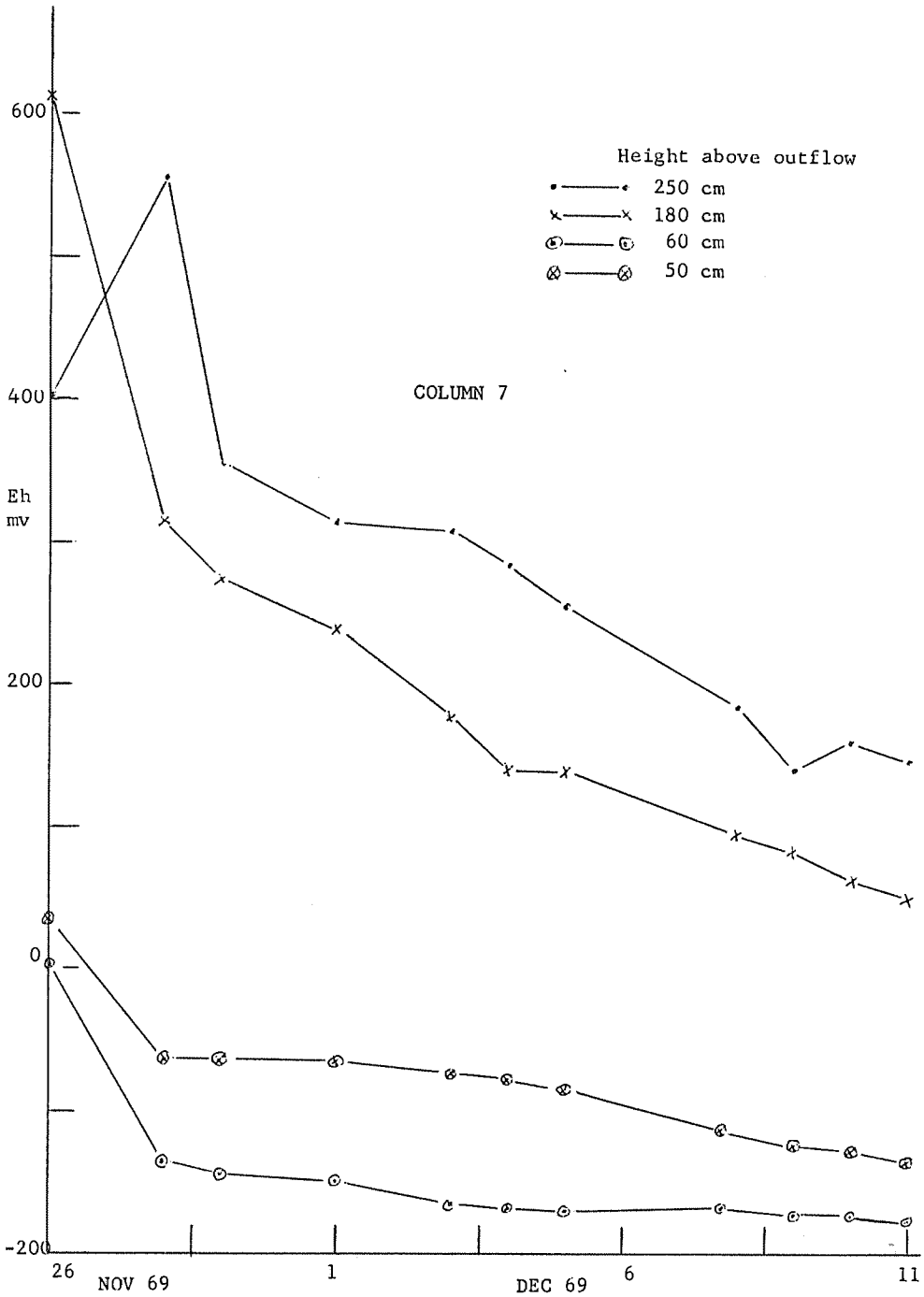

Figure 10. Redox potential versus time for column 7 during 16-day inundation.

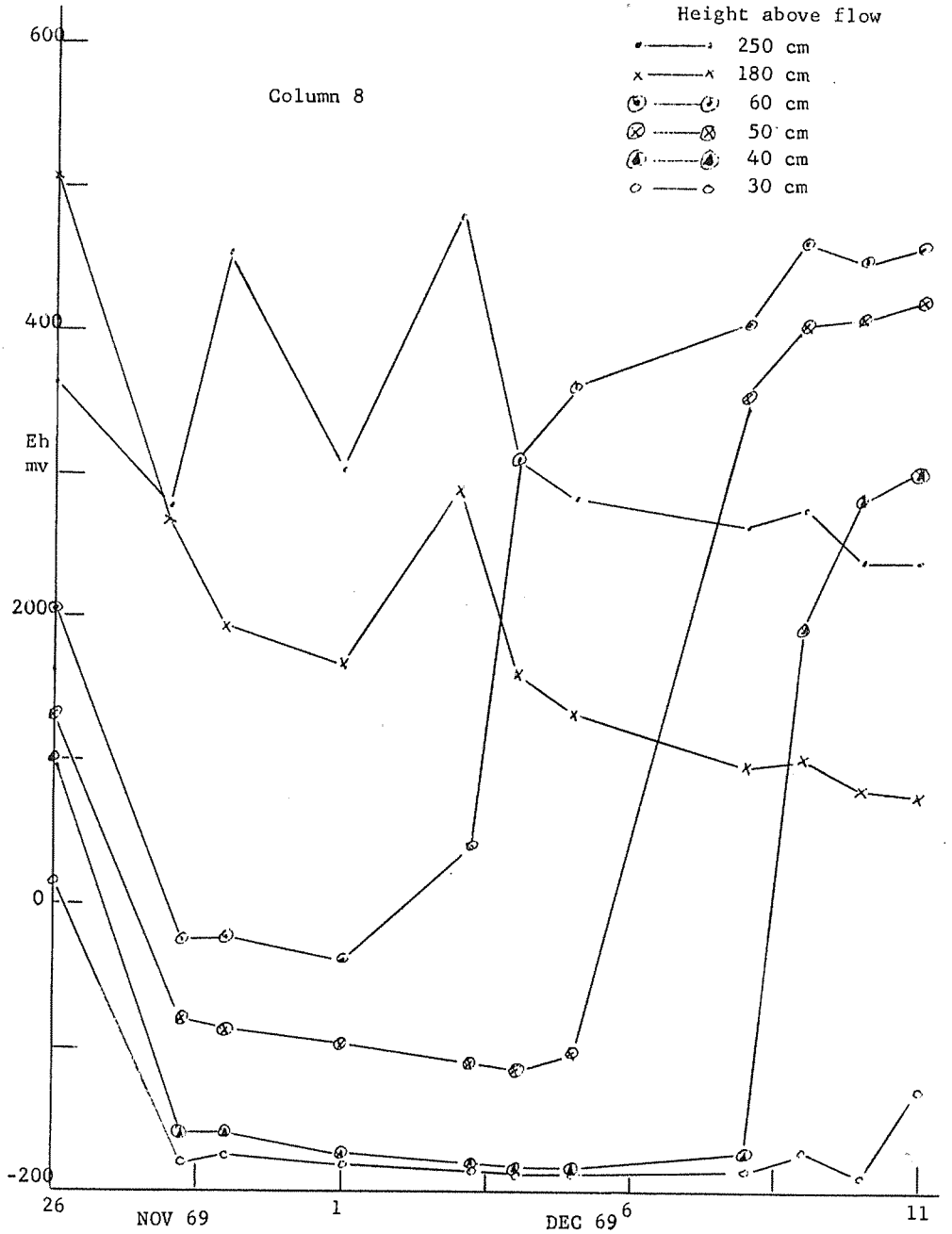

Figure 11. Redox potential versus time for column 8 during 16-day inundation.

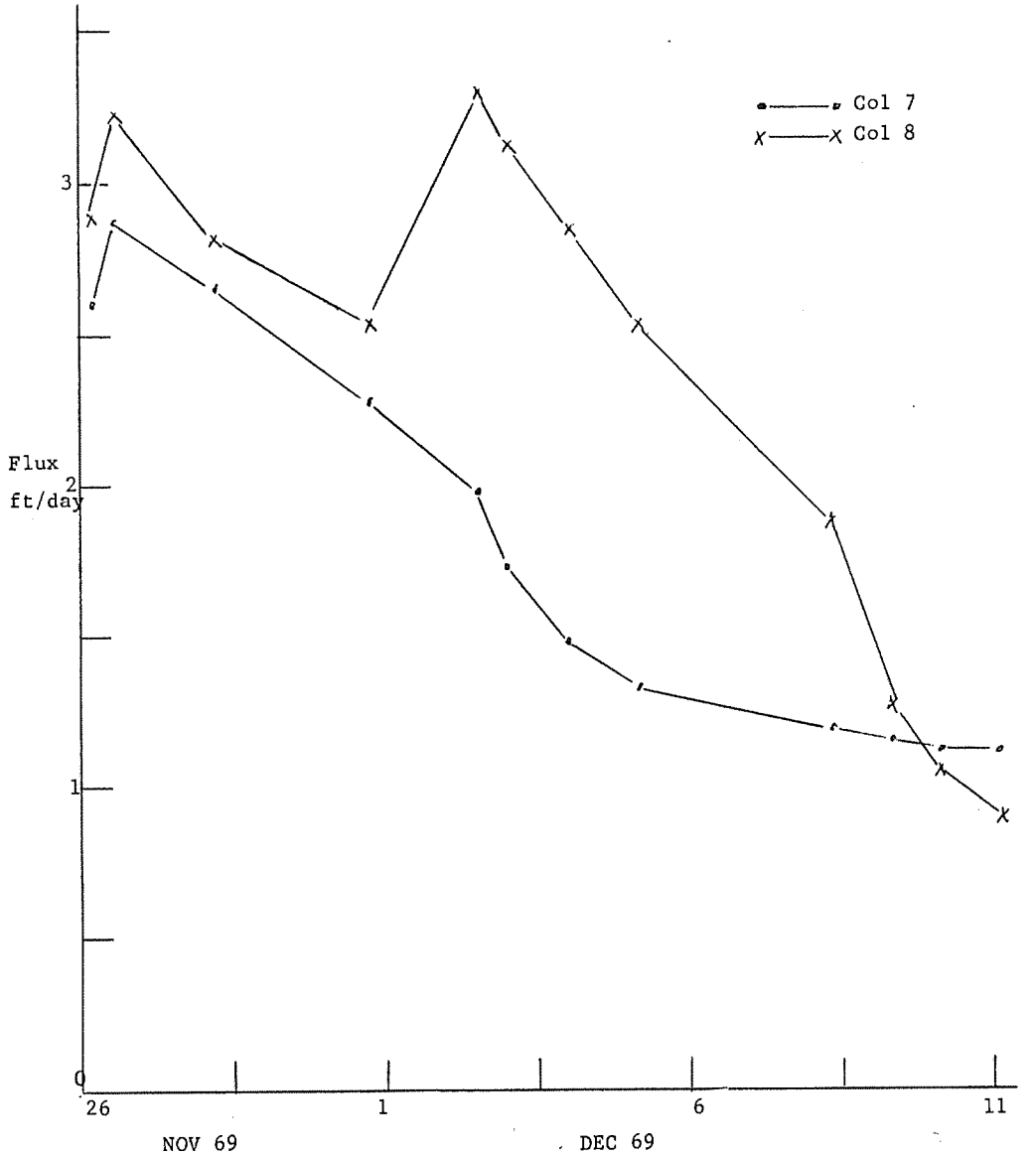

Figure 12. Flux of water versus time into columns 7 and 8 during 16-day inundation.

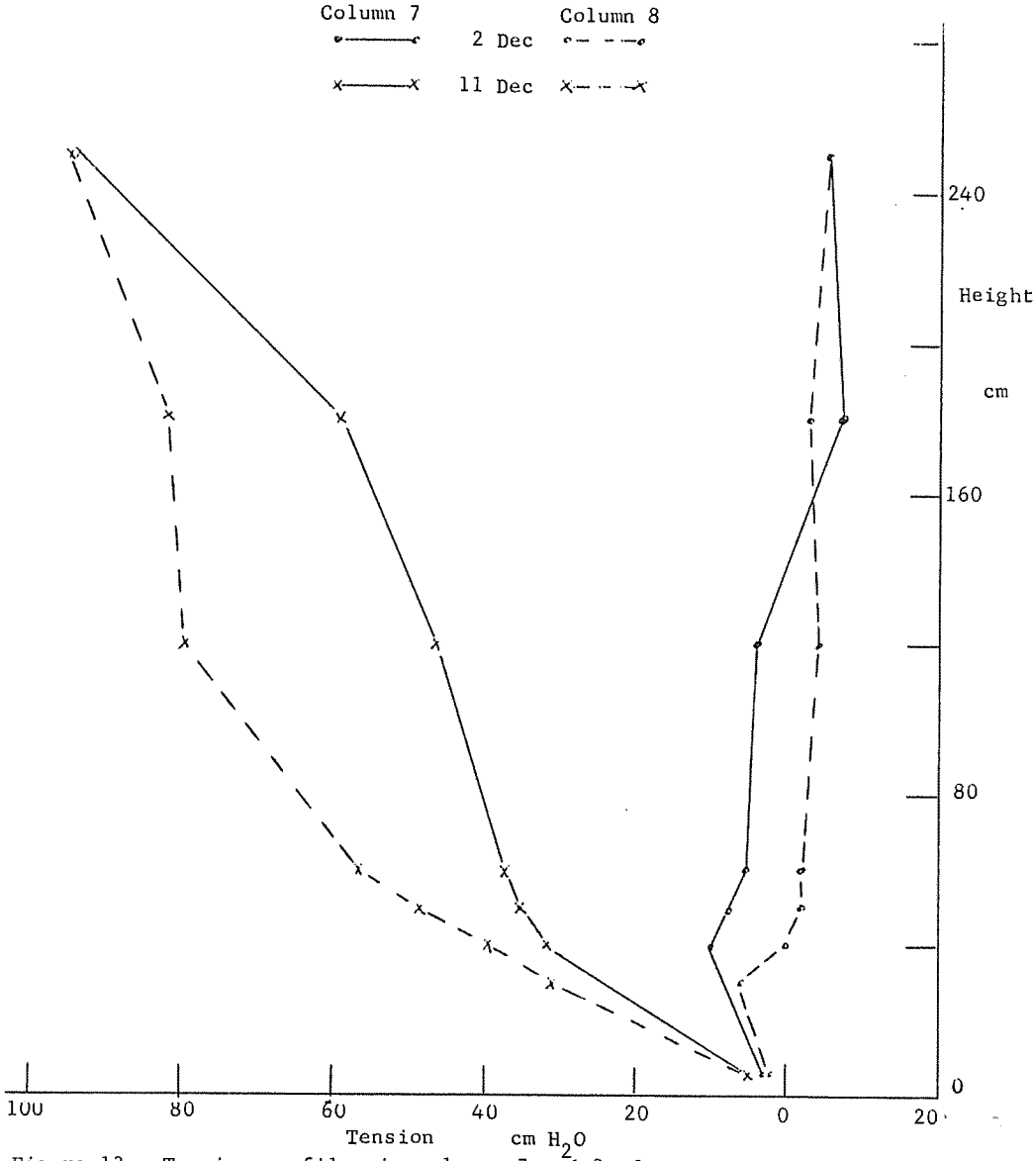

Figure 13. Tension profiles in columns 7 and 8 after one week of inundation and at the end of the 16-day inundation.

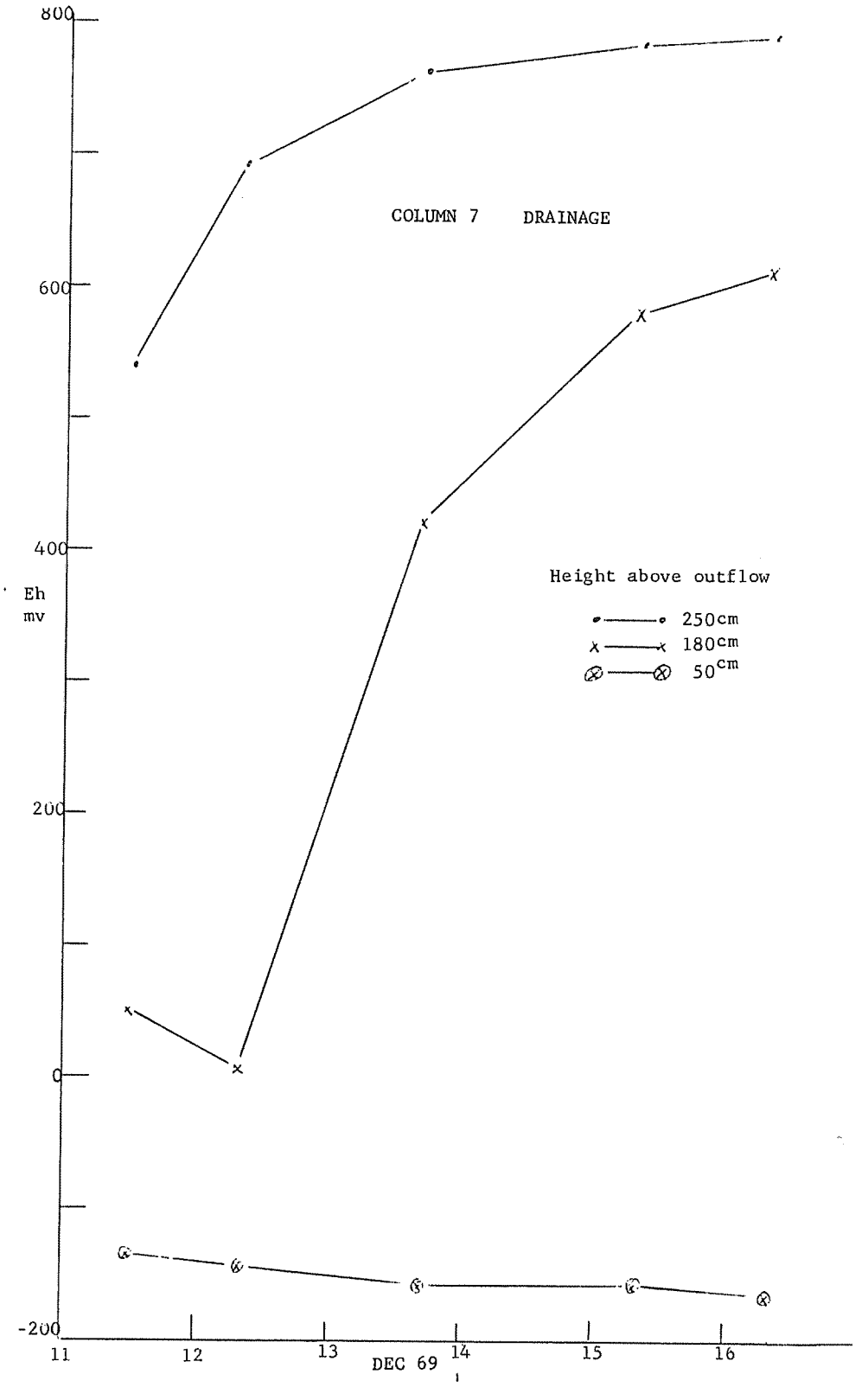

Figure 14. Redox potential versus time for column 7 during drainage.

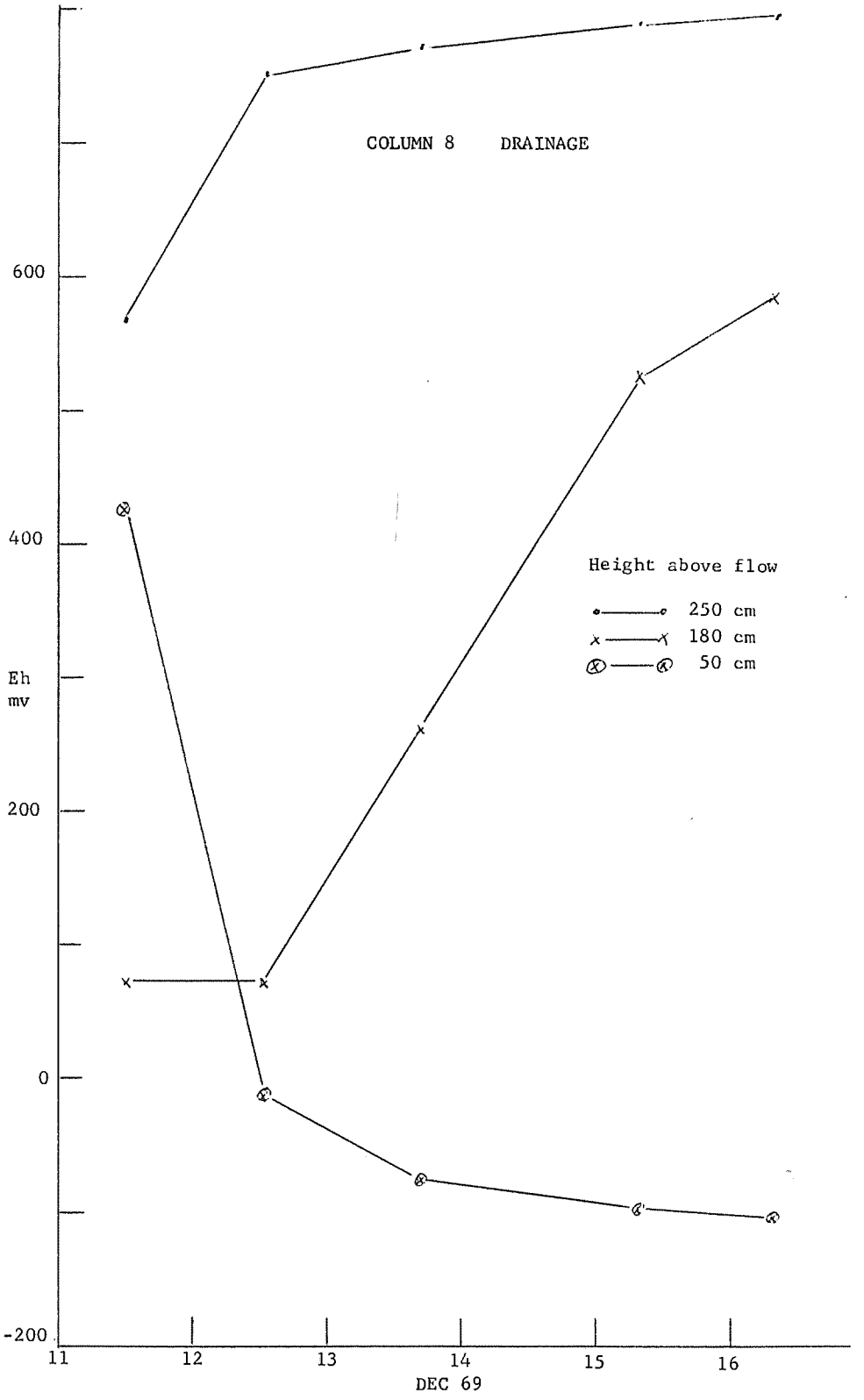

Figure 15. Redox potential versus time for column 8 during drainage.

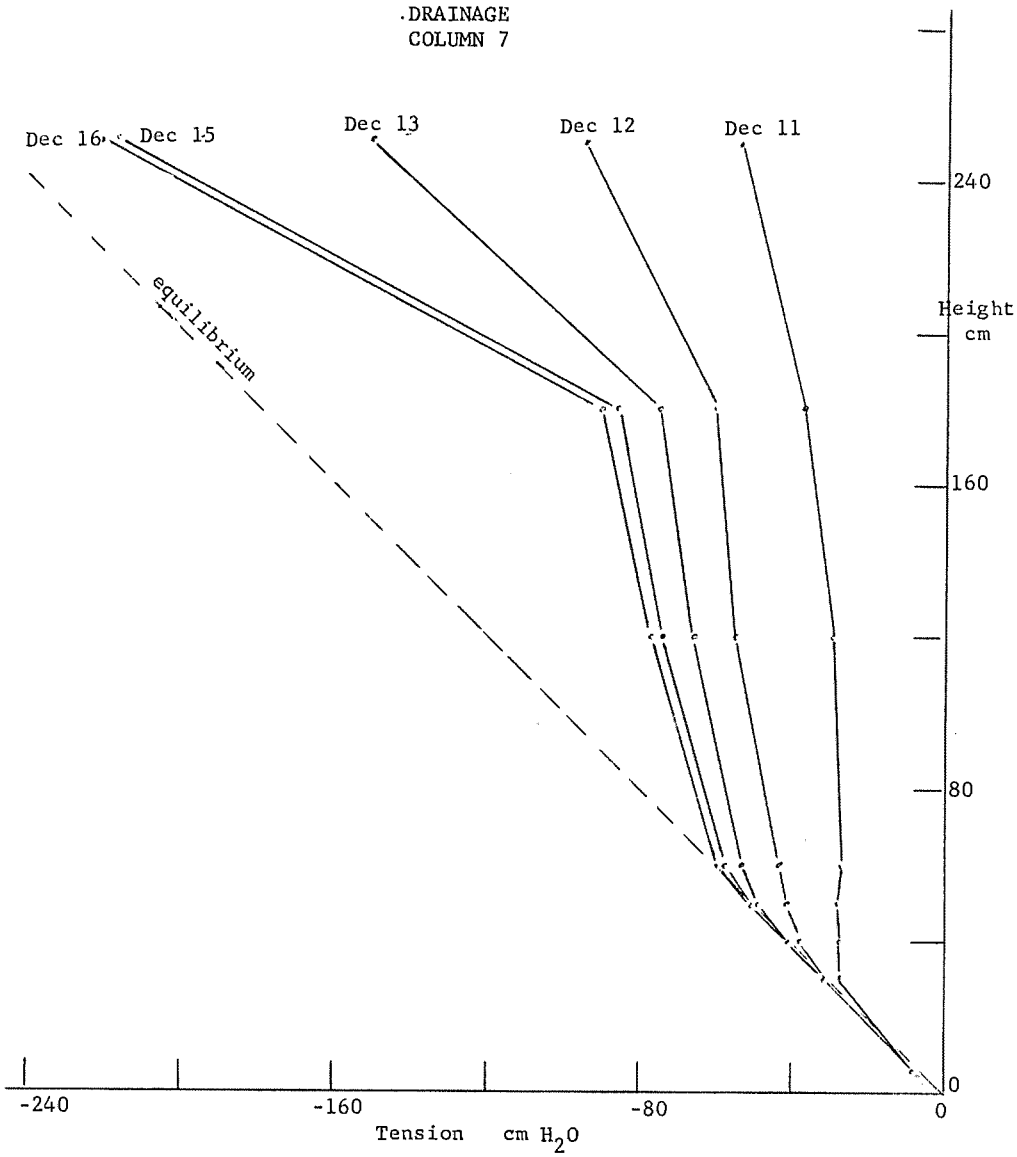

Figure 16. Tension profiles for column 7 during drainage.

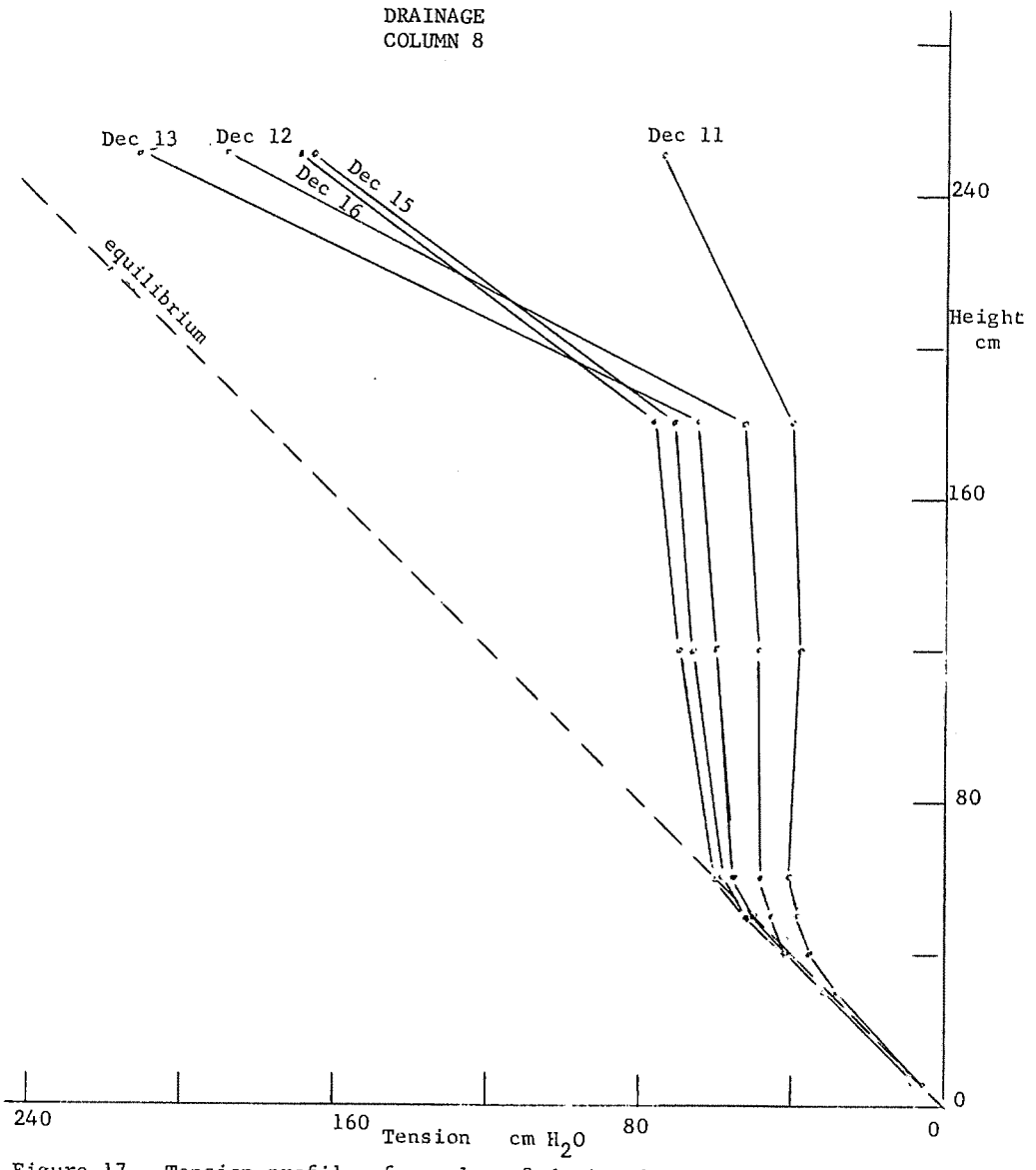

Figure 17. Tension profiles for column 8 during drainage.

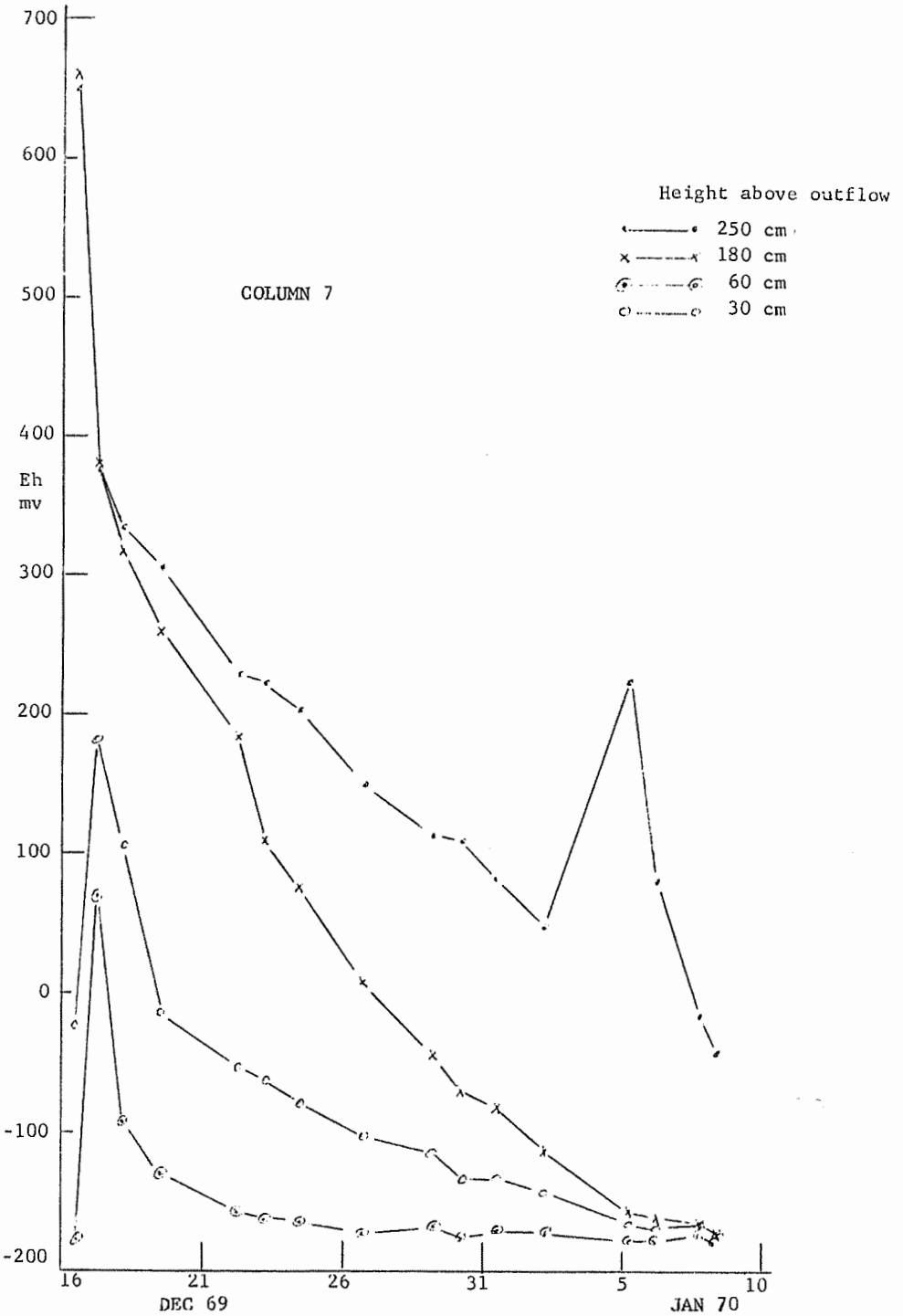

Figure 18. Redox potential versus time for column 7 during 23-day inundation.

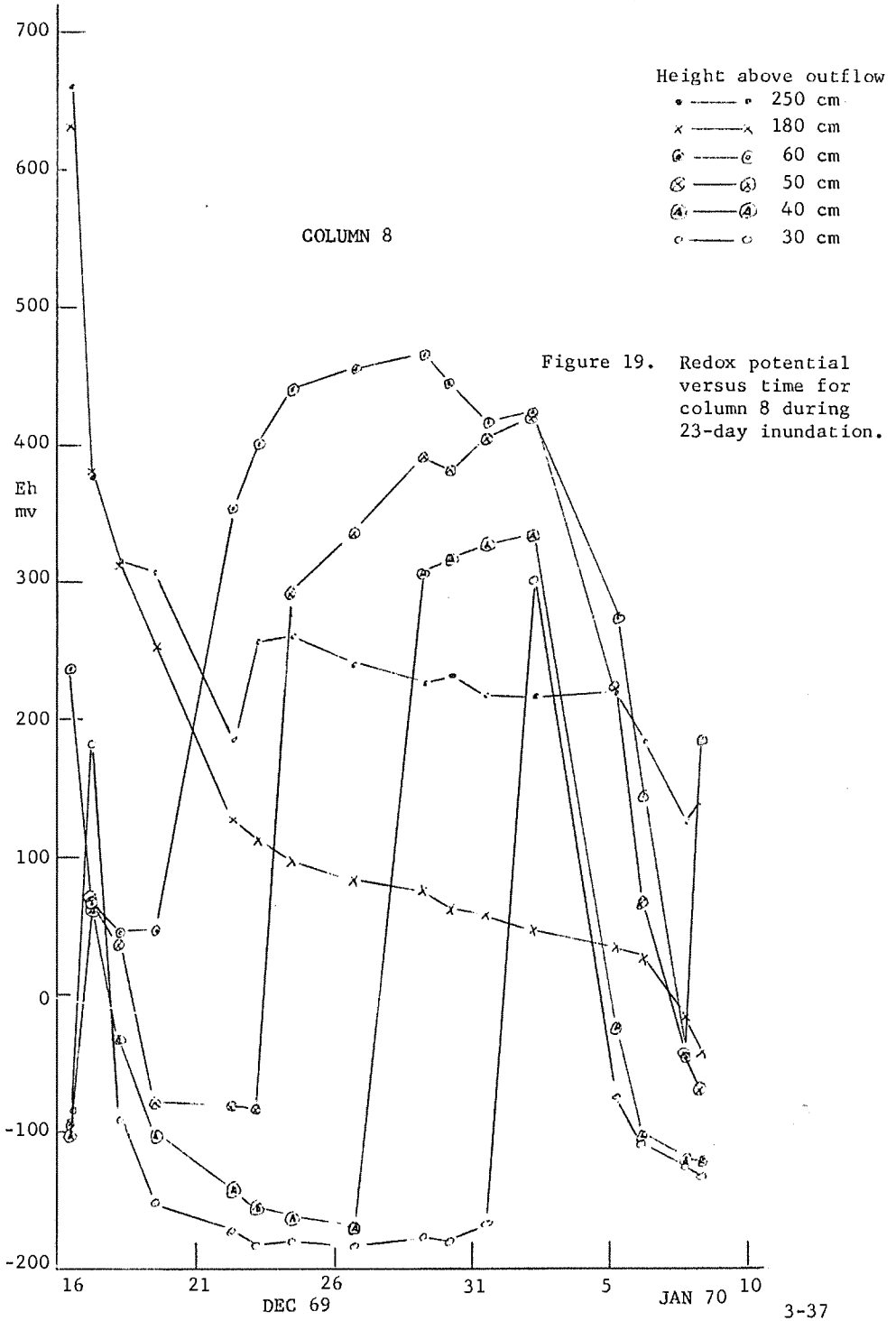

Figure 19. Redox potential versus time for column 8 during 23-day inundation.

Figure 19. Redox potential versus time for column 8 during 23-day inundation.

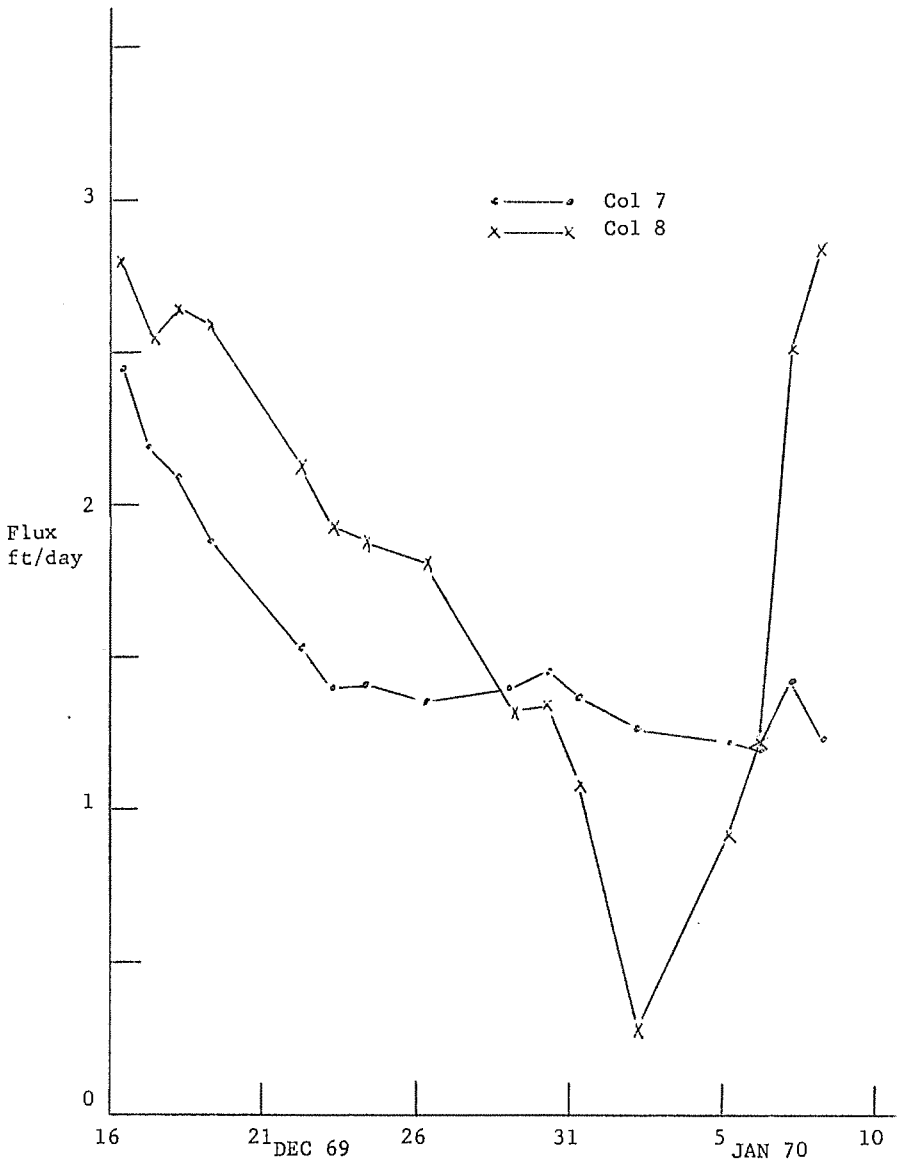

Figure 20. Flux of water versus time into columns 7 and 8 during 23-day inundation.

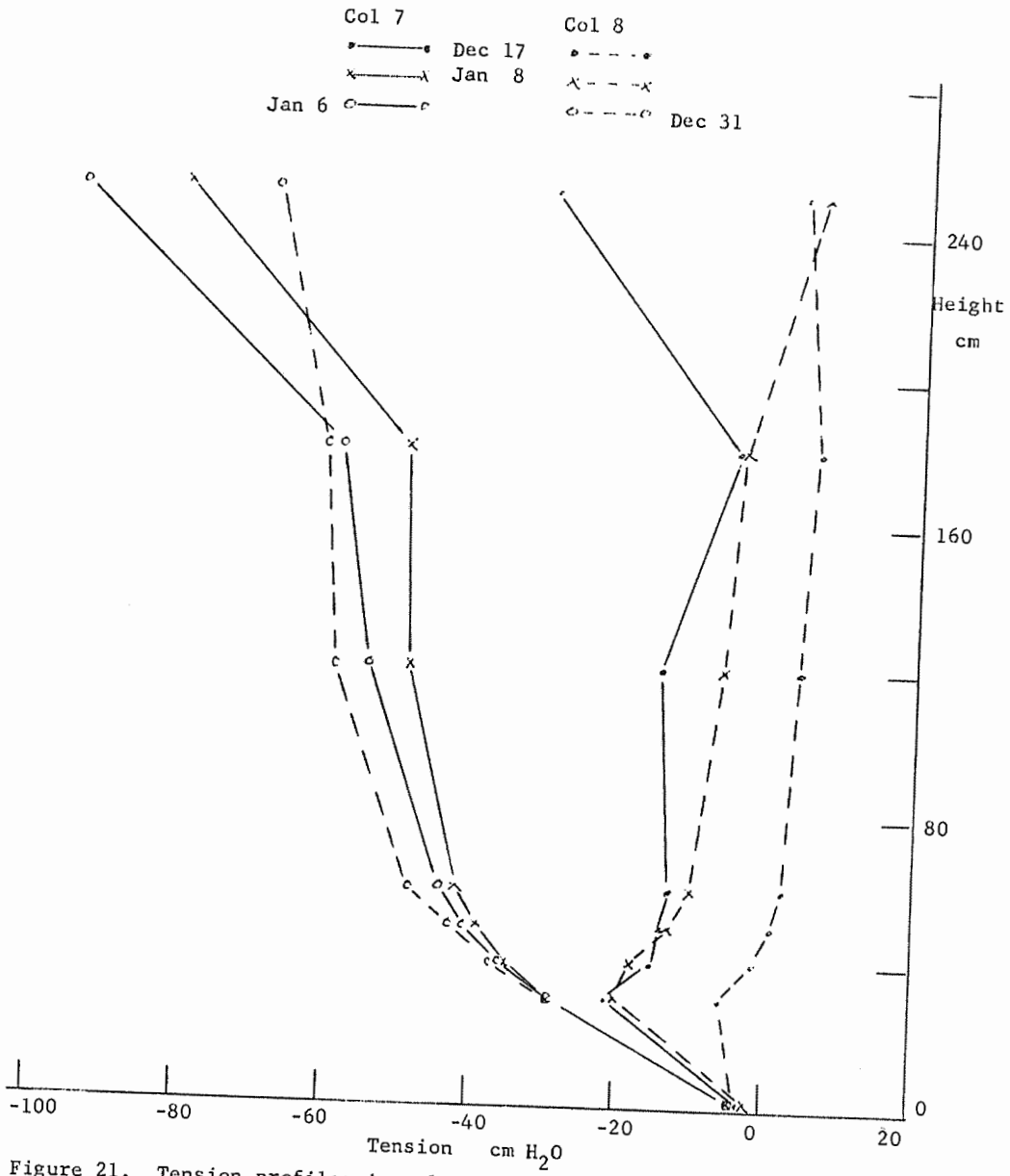

Figure 21. Tension profiles in columns 7 and 8 at the beginning, intermediate and end of the 23-day inundation.

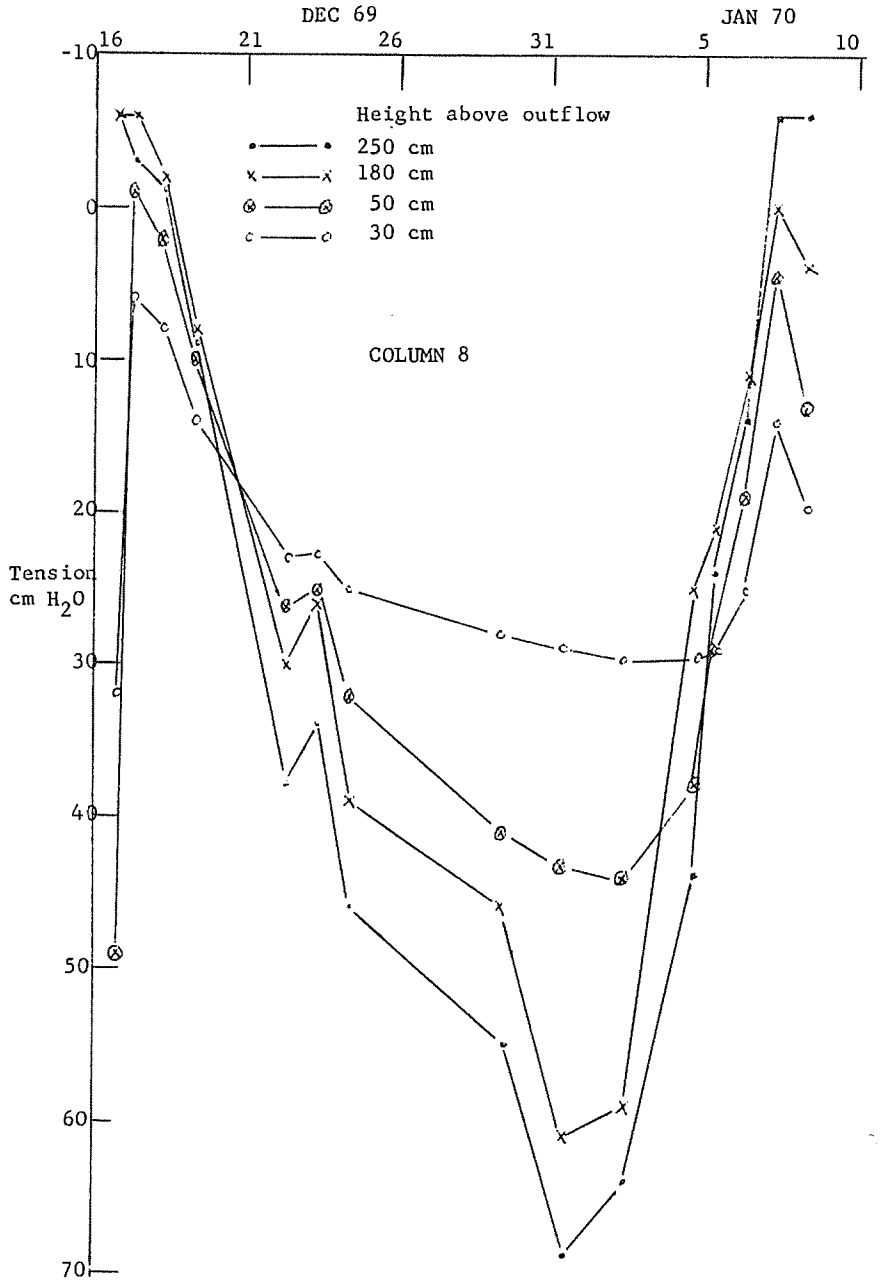

Figure 22. Tension versus time in column 8 during the 23-day inundation.

TITLE: SOIL TREATMENT TO REDUCE INFILTRATION AND INCREASE PRECIPITATION RUNOFF

CRIS WORK UNIT: SWC-018-gG-2 CODE NO.: Ariz.-WCL 60-7

INTRODUCTION:

Observations and measurements were continued on plots at the Granite Reef testing site. Laboratory studies were concerned with evaluation of low-cost soil stabilizer - water repellent treatments. A computer program was written to assist in the rational design of combined catchment and storage units.

Measurements of rainfall and runoff were continued at the Monument Tank testing site in the pretreatment phase of the study to evaluate water harvesting techniques on large areas. Preliminary analysis of the data was started. The Seneca catchment was re-treated and measurements of rainfall-runoff continued.

PART I. OPERATIONAL FIELD CATCHMENTS.

Metate Catchment: The Metate catchment was treated 18 June 1968 with asphalt-fiberglass. On 9 April 1969 additional asphalt-fiberglass was installed to increase the catchment width. Shortly after starting the repair work, a shaft was broken on the asphalt pump. The remainder of the asphalt was poured on with buckets and spread with cedar branches. A final sealcoat of asphalt-clay emulsion was applied on 8 October 1969. The catchment storage reservoir is still in excellent condition.

Seneca Catchment: The grass on the Seneca catchment was burned during March and April 1969. On 10 April 1969 the area was treated with 50 lbs. Telvar soil sterilant in 600 gal. water. Inspection of the plot on 3 June 1969 showed the sterilant had only stunted the plant growth.

Prior to retreatment, various combinations of soil stabilizers and water repellents were applied to samples of soil from the Seneca catchment. These tests indicated that the soil could be

waterproofed by applying a water solution containing 3 percent silicone water repellent and 2 percent plastic stabilizer at a rate of 2.3 liters per square meter. This treatment was applied on 17 June 1969. Prior to treatment the plants not killed by soil sterilant were pulled by hand. The solution was mixed in a 1000 liter tank and sprayed with a centrifugal pump through deflector nozzles. The treatment was in good condition two months later, but there had been very little rain. Inspections during the last 4 months in 1969 showed that the plastic stabilizer was starting to deteriorate, but the water repellency was still good. Runoff data from the plot have not been analyzed, but a preliminary examination shows that there is considerable retention of water on the plot.

Problems were encountered during the year with deer walking into the reservoir to drink and, upon climbing out of the pit, cutting the butyl lining with their hooves. Over 50 holes were patched in 1969. From 7 January through 3 December 1969, a total of 316 mm of rainfall was measured at the site. The butyl reservoir alone would have collected over 300,000 liters. On 3 December 1969 there was less than 5000 liters of water in the reservoir. The rest of the water had been lost through holes in the butyl lining, incorrect setting of float on the watering trough, and evaporation.

Guthrie Peak Catchment: This catchment was installed in May 1968, in cooperation with the Bureau of Land Management, using a combination of water repellent and soil stabilizer on half the catchment. The catchment was inspected on 6 July 1969. No evidence of either the water repellent or stabilizer was found. The rapid deterioration of the treatment probably resulted because the treatment solution did not soak into the soil. Butyl on the other half of the catchment was in poor condition at all locations where it was laid over rocks.

PART II. MONUMENT TANK TESTING SITE

Pretreatment measurements of rainfall and runoff continued during 1969 for calibration purposes.

Analysis of the data collected during previous years was initiated to determine the relationships between rainfall and subsequent runoff for three selected storms. The storms selected for investigations were those occurring as isolated events between monthly recording periods, since only total volume of rainfall is recorded in all but one recording raingage.

PROCEDURE:

The total volume of rainfall collected in each raingage, for each of the three isolated storms, was plotted on maps of the Monument Tank watershed area. A study of these rainfall plots revealed considerable variation in the areal distribution of rainfall over the watershed area. This variation was taken into account when determining the average depth of rainfall over the individual watersheds by using the Thiessen polygon method of weighted averaging.

Runoff from each watershed area was determined from the water-stage chart record, utilizing a computer program developed to convert depth of water in the critical depth flumes to volume of water flowing through the flumes. The percent of runoff from each watershed, for each storm, was determined by comparing the average rainfall over the basin to the total runoff from the basin, expressed as an equivalent depth. In the case of watersheds 2 and 3, the amount of runoff from the lined ditches was assumed to be 80 and 85 percent of the rainfall respectively. These values of percent runoff were based on observation and past experience with asphalt catchments. The volume of runoff attributed to the lined ditches was computed, and subtracted

from the total runoff. The remainder was then divided by the natural watershed area and the percent of runoff for the natural surface determined by comparing this value to the average rainfall.

RESULTS:

Monthly data collected from the network of 14 raingages showed slightly more variation than noticed on previous years. The maximum monthly variation was about 20 percent. Totals for the year varied by 10 percent.

Total rainfall recorded for the year was 274 mm, which is slightly less than the previous two years. The three year average now stands at 360 mm per year.

The rainfall directional pattern for the year, as determined from vector pluviometer readings, was essentially the same as the previous year. The percent of the total collected by the four pluviometer openings, for the past year, are: North - 26, East - 22, South - 15, West-37.

Estimates of various watershed characteristics were made from the maps of the watershed area. These characteristics are presented in Table 1. Revision of this table may be necessary after a field survey is conducted to locate specific points on the maps, since they are based on aerial photography and do not show all of the details necessary for exact values to be determined.

The average rainfall for each storm investigated and for each watershed, along with runoff data for each event, are presented in Table 2. Results for watershed 4 are not included since runoff did not occur from this watershed during the three storms under consideration, and raingages were not in continual operation.

The results presented in Table 2 are interesting from three standpoints, these being: (1) response of the different watersheds to storms of different types and intensities, (2) comparison of

volume and percent of runoff from natural and lined-channel watersheds, and (3) comparison of runoff from the natural portion of the three watersheds.

The three storms under investigation vary from a general and rather uniform storm of two days duration to a high intensity thunderstorm of only a few minutes duration. All three watersheds experienced the greatest percentage of runoff from the storm of 31 October, even though total rainfall was only one-tenth that of the large 13-15 November storm. This high runoff was due to the relatively high intensity of the 31 October storm which deposited approximately 3 mm of rain in a 6 to 8 minute period.

Percent of runoff varied among watersheds even more than among storms. The range for the different storms being: from 2 - 19 percent for the natural watershed (1), from 60 - 68 percent for the partially lined-channel watershed (3), and from 44 - 72 percent for the completely lined-channel watershed (2). The increase in average runoff produced by lining a portion, or all, of the watershed channel varied from 3.5 to 30 times depending on the type and intensity of storm. The greatest increase occurring in the case of the longer duration, higher rainfall storms.

Response of the watersheds to the storm of 2-3 October is presented in Figure 1. The response of watersheds 2 and 3 is seen to be very similar, but watershed 3 is more sensitive. In this case, seven distinct showers are noted for watershed 3, while only six are indicated for watershed 2. Watershed 1 is seen to be much less sensitive in that less water runs off of the natural watershed and the hydrograph peaks, after runoff does occur, are much less descriptive. Only three showers are noted for watershed 1, the first four showers being used to fill the watershed channel and stilling basin. For this particular storm almost all of the runoff occurring from watershed 2 was derived from the lined channel

itself. It would seem that watershed 2 would therefore be more sensitive than watershed 3, since half of the channel on watershed 3 is unlined. Watershed 3 is considerably steeper than watershed 2, and has a slightly sandier soil, although the soil on both is quite shallow. The fact that the lined channel on watershed 3 is in better condition and slightly steeper may also account for the difference.

The direction of storms, as determined from the vector pluviometer, did not appear to have any effect on runoff. The distribution of rainfall on the watershed and the intensity of rainfall were much more important.

Runoff from the unlined or natural watershed areas is also noted to be considerably different. As previously noted, runoff from watershed 1 varied from 2 - 19 percent, runoff from the natural area of watershed 2 varied from 1 - 30 percent, and that from the natural area of watershed 3 varied from 34 - 42 percent. The difference in slope and soil could again account for these variations. The response of watersheds 1 and 2 was very similar for the three different storm situations; the percent runoff being greater for the 31 October thunderstorm, and much smaller for the two more general storms. Watershed 3, on the other hand, produced essentially the same percent of runoff (34 - 42 percent) for all three storms.

PART III. GRANITE REEF TESTING SITE

A total of 232.2 mm of rainfall was measured on 32 separate storms. The following discussion compares test plot runoff measurements for the different storms to rainfall measured in a standard U. S. Weather Bureau storage raingage.

Esso Plots. This is the concluding year of the five year study in cooperation with Esso Research Corporation of Linden, New Jersey, in the evaluation of a single-phase application of Venezuelan asphalt as a soil treatment. Runoff has continued to

decrease but is still a significant portion of the rainfall. During 1969, Plot E-1 averaged 54 percent runoff, Plot E-2 averaged 45 percent, and E-4 averaged 51 percent. This compares to 20 percent runoff from the smoothed untreated Plot E-3.

A summary of the average annual runoff for the five years of the study is presented in Table 3. The treatments are still in fair condition and have lasted much longer than would similar applications of locally available California asphalt.

The cost of the single phase asphalt treatments is approximately 16.6 cents m^{-2}. Over the five year study period, the asphalt plots each collected a total of approximately 950 liters of water per m^2, which was 720 liters m^{-2} more than an adjacent undisturbed watershed collected. The average cost of the increased runoff water is approximately 23.1 cents per 1000 liters, or 87 cents per 1000 gallons.

Paved Plots: Treatments applied to the paved plots are listed in Table 4 and the runoff results presented in Table 5.

Plot L-1, 30-mil chlorinated polyethylene bonded to the soil, averaged 96 percent runoff for the year. The sheeting is in excellent condition with no signs of asphalt migration through it. The sheeting is slightly water repellent, has few wrinkles, and as a result has very little retention.

Runoff from Plot L-4, 15-mil butyl sheeting, averaged 89 percent for the year. The sheeting is severely chalking and may be partially porous. The sheeting is not water repellent, has few wrinkles, and as a result has very little retention.

Plots L-5 and L-6, two-phase asphalt treatments, averaged 83 percent and 89 percent respectively, for the year. Cracks and numerous small pock marks have developed in the pavement surfaces.

Loss of water through the cracks and retained in the pock marks has significantly reduced runoff from the pavements. Actual retention will be measured on the plots in 1970.

Runoff from Plot L-7, 1-mil bonded aluminum foil, averaged 81 percent runoff for the year. Pinholes are starting to develop in the foil. These apparently result from corrosion by salty soil and pebbles blown onto the plot by wind.

The vinyl-coated asphalt-fiberglass Plot A-1 averaged 85 percent runoff for the year. The treatment is in excellent condition and the surface is slightly water repellent. Runoff should approach 100 percent of rainfall. The reason for the 15 percent loss in runoff has not yet been identified.

Plot A-2, standard gravel roofing covering, averaged 74 percent for the year. The gravel retains an average of 2 mm of rainfall per storm before runoff occurs. This retained water is lost by evaporation after the storm. For 32 separate storms in 1969, the total runoff was 60 mm less than the rainfall.

In September 1968, a 3.05 x 36.59 meter Plot A-5 was constructed by pouring a continuous slab of 10 cm thick concrete. The slab has a longitudinal slope of 3 percent and drains laterally toward the longitudinal center line. Runoff from the plot averaged 71 percent for the year. Several lateral cracks occurred in the concrete approximately 6 months after construction. Runoff has decreased significantly, especially in the winter months when the cracks are the widest.

Bare Soil Plots. The bare soil plots include all treatments where the soil is not completely covered or paved. A description of the treatments is presented in Table 6 with the runoff results presented in Table 7.

Ridge and furrow Plot R-4 treated with sodium carbonate in May 1966, averaged 18 percent runoff for 1969. A similar plot, R-2,

averaged 20 percent for the year. Using runoff from R-2 as a base, runoff from R-4 was 148 percent in 1966, 138 percent in 1967, 128 percent in 1968, and 91 percent in 1969. This shows that the plot has lost all effect of the salt treatment in 3 years.

Watershed W-3, hand cleared of brush in 1963, is still yielding more runoff than the uncleared watershed W-1, even though brush is growing back on the plot. Runoff from W-3 in percent of runoff from W-1 for the last 6 years was: 1964 - 145, 1965 - 123, 1966 - 131, 1967 - 143, 1968,- 131, and 1969 - 117. It is believed the regrowth of brush is starting to make its presence felt.

The three smoothed untreated Plots L-2, E-3, and A-3 averaged 15.9, 20.2, and 21.9 percent rainfall runoff respectively. It was thought that runoff was declining with time as wind and water erosion caused a gravelly desert pavement to develop on the soil surface. A regression analysis of runoff from L-2 vs runoff from untreated watershed W-2 indicates that the rainfall-runoff relationship between the two plots has not changed significantly with time.

Plot L-3, treated with a water repellent in August 1965, was retreated on 6 November 1969. From 1 January to 6 November 1969 the plot had averaged 40 percent runoff of 186 mm rainfall. After retreatment the plot averaged 86 percent runoff from 46 mm during the remainder of the year. On 28 October 1969 detailed study of the degree of water repellency was made as described in the 1966 Annual Report. The following criteria were used for defining the degree of repellency.

Zero - water soaked rapidly into soil.

Slight - soil surface wetted but infiltration slow.

Fair - surface wetted but water did not soak into underlying soil.

Good - Soil surface highly water repellent.

In November 1966, one year after treatment, the plot areas in the various categories were: zero - 8, slight - 19, fair - 44, and

good - 29 percent. In October 1969, 4 years after treatment, the plot areas in the various categories were: zero - 69 percent, slight - 18 percent, fair - 14 percent, and good - 0 percent. On the basis of the last study, the decision was made to retreat the plot. During a 52 month period, the original treatment produced 846 mm of rainfall runoff from a total of 980 mm of precipitation for an average effectiveness of 86 percent. The materials and application cost for the treatment was 6.3 cents per m^{-2}. The water collected from the original treatment cost 7.5 cents per 1000 liters, or 28 cents per 1000 gallons.

PART IV. SOIL STABILIZATION

Preliminary examination of soil stabilizers continued, utilizing procedures described in the 1967 Annual Report. In addition, the water-soil contact angle was measured and penetration of materials into soil was observed. Materials included were

1. polyvinyl acetate emulsion
2. vinyl acrylic terpolymer emulsion
3. polyvinyl alcohol-high molecular weight
4. alkyl resin emulsion
5. unknown resin emulsion
6. unknown elastomer emulsion

These are commercially available materials that imparted reasonable stability to soil surfaces. A number of rosin-derived materials were also examined that did not stabilize the soil.

Water-soil contact angles were calculated from the thickness of a "drop" of water on the treated soil surface. Soil was packed into a petri dish per the 1967 procedure and was treated. The dish was placed on a machinist's surface plate and readings of soil surface position were made with a vertical probe on a machinist's height gage. A drop of water large enough so that adding water did not increase water depth (3 to 4 cm diameter) was placed on the soil surface and a reading of water surface

position was made with the height gage. Drop thickness was the difference between the two height gage readings. Contact angle θ was calculated with the equation

$$\cos \theta = 1 - \frac{\rho g \ell^2}{2v}$$

where ρ = density of water in g cm^{-3},

g = gravitational acceleration in cm sec^{-2},

ℓ = drop height in cm, and

v = surface tension of water in dynes cm^{-1}.

This boils down to: $\cos \theta = 1 - 6.73\ell^2$.

The time required for various concentrations and amounts of materials to soak into the soil and the depth to which soil was stabilized was measured under three conditions.

1. Materials applied to soil packed in petri dishes per the 1967 procedure.

2. Materials applied as a coarse spray to Granite Reef soil in 12 x 38 x 5 cm-deep boxes. Dry soil, sieved through a 3 mm screen, was poured into the box until it overflowed and was screeded off level with the top of the box. The loose, dry soil was sprayed with water at a rate of 2.4 liters m^{-2}, dried, sprayed with water and dried again before treatment.

3. Materials applied to undisturbed, natural soil at the Granite Reef test site.

The dripper erosion test was modified to apply 1000 drops in a period of 10 minutes. The petri dish was placed inside a 500 ml beaker which gradually filled with the water being applied. During the last one minute of the test the soil sample was submerged and the drops impacted on the soil surface through a layer of water 2 mm thick. Under these conditions, materials 1, 2, 5,

and 6 stopped all erosion when applied at a rate of 236 g solids m^{-2} in a 10 percent concentration without including a water repellent in the application. Material 4, without water repellent, stopped erosion when 165 g solids m^{-2} were applied in a 6 percent concentration. Material 3 was ineffective alone, but with the inclusion of 3 percent by weight of applied fluid of SMS (sodium methyl siliconate) stopped erosion when 47 g solids m^{-2} were applied as a 2 percent solution.

Without including a water repellent in the treatment, contact angles for the materials were: 1 - 114°, 2 - 93°, 3 - 0°, 4 - 110°, 5 - 130°, and 6 - 136°. Material 6 has not yet been checked with water repellent included. When SMS at 3 percent by weight of applied fluid was included, contact angles were: 1 - 128°, 2 - 144°, 3 - 128°, 4 - 110°, and 5 - 104°. Emulsions include a surfactant that may also be a water repellent. Materials 4 and 5 were not improved by SMS and 6 probably will not be. SMS reduced the contact angle for material 5, probably because of an unfavorable reaction with the surfactant used as an emulsifier. SMS appreciably improved contact angles for materials 1, 2, and 3.

All materials applied in concentrations of 10 percent or less immediately soaked into Granite Reef soil compacted into petri dishes per the 1967 procedure. Soil was stabilized to a depth of 6 mm or more. However, none of the materials penetrated the surface of the same soil compacted by two cycles of wetting and drying as described in the above section on Procedure. Subsequent application to undisturbed, natural soil at the Granite Reef test site showed that penetration could be achieved but the infiltration rate was slow. Time in minutes for infiltration of 1.8 liters m^{-2} of 10 percent concentrations was: 1 - 2.5, 2 - 2.5, 5 - 5.5, and 4 - 2.5. Infiltration time for 1.8 liters

m^{-2} of material 3 in 2 percent and 1 percent solutions was 1.5 and 0.5 minutes respectively. Except for the 10 percent concentration of material 5, where the resin remained on the surface, the soil was stabilized to depths ranging from 5 to 10 mm.

All of the materials 1 through 6 are capable of stabilizing soil against raindrop erosion and all of them are water repellent. The infiltration rates are too low for satisfactory field application. Slow infiltration means that the applied fluid will collect in micro-depressions so that application will not be uniform. Infiltration rates are a function of the effective pore size of the soil surface, diameter of emulsified resin particles, electrical charges on the particles, and viscosity of applied fluid. These factors will be examined in pending investigations.

PART V. WATER REPELLENTS

Soil can be made water repellent by treating it with solutions of soluble stearates and metallic salts. Work done in 1960 indicated that potassium stearate and aluminum chloride were suitable materials. The studies indicated that the soil should dry between applications of soap or salt solutions, which posed a potentially serious problem for field applications. During 1969 it was decided that the cost of soap-salt treatments was so low that additional work should be done with these materials. The 1969 studies indicate that the 1960 findings were in error and that soil treatment with soap and salt solutions offers promise of low cost water harvesting.

PROCEDURE:

Granite Reef soil was compacted in petri dishes, treated and evaluated in accordance with procedures described in the 1967 Annual Report, plus measurement of time required for solutions to soak into the soil.

RESULTS:

Treatments included all possible variations of the following:

1. $AlCl_3$ solutions of 0.5 percent and 1.0 percent.
2. K-soap solutions of 0.5 percent and 1.0 percent.
3. 2 percent polyvinyl alcohol in either $AlCl_3$ or K-soap solutions.
4. Either $AlCl_3$ or K-soap applied first.
5. Drying or no drying between solution applications.

All solutions were applied at a rate of 1.7 liters m^{-2}.

The tests indicate the following:

1. Solutions of 0.5 percent concentration were effective.
2. Polyvinyl alcohol could be applied in either the $AlCl_3$ or K-soap solution if the K-soap concentration was 0.5 percent.
3. With 0.5 percent concentrations, the order of applying K-soap or $AlCl_3$ solutions did not seem to make any difference.
4. Drying soil after applying the first solution resulted in all cases in slow infiltration of the second solution.

The best treatment appeared to be 0.5 percent K-soap + 2 percent PVA followed by immediate application of 0.5 percent $AlCl_3$. Erosion was light, about 2 mm after 1000 drops. Soil stability and water repellency was evident to a depth of 1 cm. The soil-water contact angle was 145^{o}.

These results are preliminary. Considerable evaluation under different conditions and on other soils is necessary before any definite conclusions can be reached.

PART VI. OPTIMUM DESIGN OF CATCHMENT AND STORAGE

In the past, the sizes of catchment and storage units for livestock water have usually been determined by precedent, irrespective of rainfall or actual water requirements. The

standard unit has ordinarily had a catchment area of approximately 950 m^2 (10,000 ft^2) and a storage of 75,000 to 150,000 liters (20,000 to 40,000 gallons) without regard to relative unit costs of catchment and storage.

For each water harvesting catchment there can be at least two combinations or catchment and reservoir sizes which will provide an adequate water supply. These can consist of a relatively small catchment area and a large reservoir for storing water during periods of low precipitation; or a smaller reservoir and a large catchment which collects more water during low precipitation periods. The lowest cost design will be determined by the relative unit construction costs of catchment and storage.

The computations necessary for determining the relative sizes of catchment and storage for lowest cost are not difficult, but are tedious and time consuming when considering all possible combinations of rainfall, water requirements, and unit construction costs. A computer program was written which determines the combination of catchment and reservoir size with the lowest total cost when supplied with information on the quantity of water required by months or weeks, the amount of precipitation by months or weeks, and the unit construction costs of catchment and storage. The program and examples of its use will be published in 1970.

SUMMARY AND CONCLUSIONS:

The Metate catchment was widened by installation of additional asphalt-fiberglass along one edge. It was discovered that very simple equipment can be used during installation. After failure of the asphalt pump, the asphalt was bucketed on and spread with cedar branches. A sealcoat of clay emulsion was applied and the catchment is in excellent condition. The asphalt-fiberglass reservoir lining shows no signs of deterioration after 6 years.

The grass was burned on the Seneca catchment and soil sterilant applied in the spring of 1969. In June 1969 a combination soil stabilizer-water repellent treatment was applied. Inspection 4 months later showed the stabilizer was starting to deteriorate but the water repellency was still good. Considerable damage to the butyl lining in the reservoir has been caused by deer. Because of holes in the lining, improper float settings on the water trough valve, and evaporation, over 290,000 liters of water have been lost.

The soil stabilizer-water repellent treatment on the Guthrie Peak catchment completly failed during the year because the treatment solution did not penetrate into the soil. The other half of the catchment, which was covered with butyl sheeting, shows advanced signs of deterioration. This is a classic example of problems associated with installation of butyl over rocks without adequate plot preparation.

Pretreatment or calibration measurements of rainfall and runoff were continued at the Monument Tank test site. Rainfall was found to be somewhat more variable than in previous years, the monthly totals varying by 20 percent and the annual values by 10 percent. Data collected during the past three years indicate an average annual rainfall of 360 mm for the area.

Analysis of the data was initiated, and consisted of an investigation of the rainfall-runoff relationships for the various watersheds during three isolated rainstorms. This preliminary analysis indicated considerable increase in runoff from the lined-channel watersheds. The average runoff from the watershed areas during the three storms varied from: 2 - 19 percent for the small natural watershed (1), 60 - 68 percent for the partially lined-channel watershed (3), and 44 - 75 percent for the completely lined-channel watershed (2). There was no runoff recorded from the large natural watershed (4) during these particular storms.

The runoff from only the untreated watershed portions of watersheds 2 and 3 can be estimated by assuming a certain percentage of the rain falling on the lined channels runs off, and then subtracting this portion from the total runoff observed. Using values of runoff from the lined channels of 80 or 85 percent, the runoff from the natural area of watersheds 2 and 3 was calculated to be 1 - 30 percent and 34 - 42 percent respectively. These calculations indicate that watersheds 1 and 2 respond similarly and suggest that channel losses are not significantly large on watershed 1. Watershed 3 also has little channel loss and the type and intensity of the storm did not have much effect on the percent runoff. The steeper slope and different soil type on watershed 3 could cause the noted stability of runoff. Watershed 3 was also found to respond rapidly to rainfall events and thus produce the most descriptive water stage trace.

Runoff from the three plots with single applications of Venezuelan asphalt at the Granite Reef testing site has continued to decrease, but still exceeds 45 percent of the rainfall. This was the final year in the five-year study. The treatments are still in fair condition and have lasted much longer than similar applications of locally available California asphalt. The cost of water collected from the treatments since installation is approximately 87 cents per 1000 gallons. The two plots of two-phase asphalt averaged less than 90 percent runoff. Cracks and numerous small pock marks have developed in the pavement surfaces, causing increased retention.

The 30-mil chlorinated polyethylene sheeting plot was the most effective treatment during 1969, averaging 96 percent runoff. The sheeting is slightly water repellent and has few wrinkles. As a result, there is very little retention on the plot. The 15-mil butyl sheeting averaged 89 percent runoff. The sheeting,

not water repellent, is severely chalking, and requires an appreciable quantity of rainfall before runoff occurs. The 1-mil aluminum foil, averaging only 81 percent runoff, is starting to develop pinholes, apparently as a result of corrosion by salty soil blown onto the plot by wind. Runoff from the vinyl-coated asphalt-fiberglass averaged only 85 percent for the year. The surface is in excellent condition, is slightly water repellent, and should yield 100 percent runoff. The standard gravel roofing covering averaged 74 percent runoff. The gravel retains an average of 2 mm of rainfall per storm. The total runoff from 32 separate storms was 60 mm less than the rainfall. A catchment of concrete averaged 71 percent runoff. The low efficiency is a result of lateral cracks in the concrete.

The sodium carbonate treatment on the ridge and furrow plot averaged only 91 percent of runoff from a similar untreated plot, showing that all effect of the salt treatment has disappeared in 3 years. Comparison of runoff from a cleared watershed to a similar uncleared watershed for the past 6 years indicated that regrowth of brush is starting to reduce the quantity of runoff. Runoff from three, smoothed untreated plots is less than measured in preceding years. This apparently results from variations in rainfall characteristics rather than deterioration of the smoothed soil surface. A regression analysis of runoff from one of the smoothed untreated plots vs. that from an uncleared watershed indicated that the rainfall-runoff relationship between the two plots has not changed significantly. Runoff from the water-repellent plot had decreased to 40 percent of the runoff. A detailed study of the degree of water repellency indicated approximately 70 percent of the plot showed no signs of water repellency on the soil surface compared to 8 percent 2 years ago. This plot was retreated with a silicone water repellent and

averaged 86 percent runoff after treatment. The original treatment produced approximately 850 liters of water per m^2 during the 52 month study at a cost of 28 cents per 1000 gallons.

Six commercially available materials were examined in the laboratory for erosion resistance, and in the laboratory and the field for penetration into soil. All of them are, or can be made, water repellent. All of them can impart reasonable stability to soil surfaces immediately after treatment. None of these materials soak into natural, undisturbed sandy loam soil rapidly enough for practical field application. Future work will be aimed at solving this problem

Laboratory studies of soap-salt solutions for creating hydrophobic soils showed that soil drying between solution applications was not desirable. The best treatment on Granite Reef soil appeared to be: (1) application of a solution containing 0.5 percent soluble stearate plus 2.0 percent polyvinyl alcohol, (2) immediate application of a 0.5 percent solution of an aluminum salt. Applying 1.7 liter m^{-2} of each solution resulted in good erosion resistance and a soil-water contact angle of 145^{o}.

To assist in the rational design of water harvesting structures, a computer program was developed which determines the relative sizes of catchment and storage to provide adequate water supplies at the lowest total cost.

PERSONNEL: L. E. Myers, G. W. Frasier and K. R. Cooley.

CURRENT TERMINATION DATE: December 1970.

Table 1. Watershed characteristics.

WATERSHED	AREA			CHANNEL			Max. Difference in Elevation
	Treated[1/]	Natural	Total	Main	Lined	Total	
#1	-	7.6 acres	330,000 ft^2 7.6 acres	290 ft	-	1220 ft	80'
#2	8200 ft^2	173,800 ft^2	182,000 ft^2 4.2 acres	-	820 ft	820 ft	70'
#3	7500 ft^2	272,500 ft^2	280,000 ft^2 6.4 acres	380 ft	750 ft	1300 ft	106'
#4	-	15.1 acres	656,000 ft^2 15.1 acres	1440 ft	-	1870 ft	120'

1/ Refers to lined ditches.

Table 2. Rainfall-runoff data.

Date	Watershed	Average Rainfall (mm)	Average Runoff		Runoff (mm)		% Runoff	
			%	(mm)	Watershed	Channel	Watershed	Channel
2-3 Oct. 1968	1	5.90	2	.14	.14	-	2	-
	2	5.93	44	2.59	.04	4.74	1	80
	3	6.89	64	4.43	2.63	5.86	38	85
31 Oct. 1968	1	2.24	19	.41	.41	-	19	-
	2	1.99	72	1.43	.59	1.59	30	80
	3	3.40	68	2.30	1.42	2.89	42	85
13-15 Nov. 1968	1	29.97	6	1.69	1.69	-	6	-
	2	28.72	56	16.09	3.91	22.98	14	80
	3	30.90	60	18.49	10.40	26.27	34	85

Table 3. Rainfall and runoff for Esso plots at Granite Reef.

Date	Total Rainfall	E-1 Runoff		E-2 Runoff		E-3 Runoff		E-4 Runoff	
	mm	mm	%	mm	%	mm	%	mm	%
1965	395.5	352.1	89.0	352.8	89.2	165.0	41.7	365.5	92.4
1966	228.2	182.2	79.8	174.6	76.5	101.2	44.3	196.5	86.1
1967	272.1	195.1	71.7	168.6	62.0	80.3	29.5	205.4	75.5
1968	152.3	103.8	68.2	87.6	57.5	46.8	30.7	104.3	68.5
1969	232.2	124.7	53.7	104.0	44.8	46.9	20.2	119.4	51.4

NOTE: Treatments applied 10 Dec 1967.

E-1 MC-800 Venezuelan asphalt, 1.95 kg asphalt m^{-2}.

E-2 RC-250 Venezuelan asphalt, 1.85 kg asphalt m^{-2}.

E-3 Smoothed untreated.

E-4 RC-250 Venezuelan asphalt with 2% butyl 2.2 kg asphalt m^{-2}.

Table 4. Treatments on paved or covered plots at Granite Reef.

Plot	Treatment Date	Treatment
L-1	8 Aug 1967	Basecoat. MC-250 at 1.5 kg asphalt m^{-2}
	22 Aug 1967	Topcoat. RSK asphalt emulsion at 0.7 kg asphalt m^{-2}
	20 May 1968	Top Sheeting. 30-mil chlorinated black polyethylene
L-4	30 Nov 1961	Butyl Rubber Sheeting. 15-mil
L-5	18 Sep 1962	Basecoat. S-1 at 1.04 kg asphalt m^{-2}
	16 Mar 1966	Topcoat. RSK asphalt emulsion at 0.6 kg asphalt m^{-2}
L-6	19 Apr 1963	Basecoat. RC-special at 1.5 kg asphalt m^{-2}
	8 May 1963	Topcoat South Half. SS-2 special asphalt emulsion at 0.65 kg asphalt m^{-2} with 3% butyl latex
	9 Jul 1963	Topcoat North Half. S-1 at 0.5 kg asphalt m^{-2} with 3% butyl latex
	17 Feb 1966	Top Spray. Aluminum coating TS-A-1 at 0.16 kg material m^{-2}
L-7	3 Aug 1967	Basecoat. MC-250 at 1.5 kg asphalt m^{-2}
	22 Aug 1967	Top Sheeting. 1-mil aluminum foil bonded with RSK asphalt emulsion at 0.7 kg asphalt m^{-2}
A-1	3 Aug 1967	Basecoat. MC-250 at 1.5 kg asphalt m^{-2}
	22 Aug 1967	Top Sheeting. 3/4 oz chopped fiberglass matting bonded with RSK asphalt emulsion at 1.4 kg asphalt m^{-2}
	Jan 1968	Top Spray. Vinyl aluminum coating at 0.1 gal yd^{-2}

Table 4. (continued) Treatments on paved or covered plots at Granite Reef.

Plot	Treatment Date	Treatment
A-2	3 Aug 1967	Basecoat. MC-250 at 1.5 kg asphalt m^{-2}
	12 Sep 1967	Top Sheeting. Standard rag felt-rock roofing treatment
A-5	Sep 1968	Concrete slab

Table 5. Rainfall and runoff for paved or covered plots at Granite Reef.

Date	Total Rainfall	L-1 Runoff		L-4 Runoff		L-5 Runoff		L-6 Runoff		L-7 Runoff		A-1 Runoff		A-2 Runoff		A-5 Runoff	
1969	mm	mm	%	mm	%	mm	%	mm	%	mm	%	mm	%	mm	%	mm	%
14/15 Jan	24.0	23.1	96.3	21.0	87.5	21.1	87.9	23.5	97.9	19.8	82.6	22.2	92.5	21.8	90.8	20.0	83.4
15 Jan	4.9	4.5	91.8	4.1	83.7	3.7	75.5	4.2	85.7	4.1	83.7	4.1	83.7	3.8	77.6	3.7	75.5
19/20 Jan	2.3	2.2	95.7	1.9	82.6	1.3	56.5	1.6	69.6	1.4	60.9	1.7	73.9	1.0	43.5	1.0	43.5
21 Jan	6.5	6.6	101.5	6.1	93.8	5.3	81.5	5.8	89.2	5.6	86.2	6.0	92.3	5.3	81.5	7.5	115.3
25/27 Jan	3.4	3.4	100.0	3.1	91.2	1.9	55.9	2.9	85.3	2.5	73.7	3.0	88.2	2.0	58.8	2.2	64.7
6/7 Feb	6.9	6.9	100.0	6.7	97.1	5.9	85.5	6.2	89.9	5.9	85.5	6.5	94.2	5.1	73.9	5.6	81.2
13 Feb	4.3	4.1	95.6	4.1	95.3	3.6	83.7	3.9	90.7	3.5	50.7	3.8	88.4	3.0	69.8	3.0	69.8
18 Feb	6.1	5.8	95.1	5.8	95.1	5.2	85.3	5.5	90.2	4.9	80.3	5.4	88.5	4.3	70.8	6.1	100.0
20 Feb	1.2	.8	66.7	.8	66.7	0.3	25.0	0.5	41.7	0.5	41.7	0.6	50.0	0.1	8.3	.3	25.0
22 Feb	4.5	4.3	95.6	4.2	93.3	3.5	77.8	3.9	86.7	3.3	73.3	3.9	86.7	2.6	57.8	3.4	75.6
10 Mar	16.0	15.8	98.8	16.7	104.4	15.0	93.8	18.2	113.8	15.1	94.4	14.3	89.4	13.3	83.1	20.0	125.6
10/11 Mar	9.9	8.1	81.8	8.5	85.9	7.2	72.7	8.9	89.9	7.9	79.8	8.1	81.8	8.6	86.9	7.9	79.8
23 Mar	1.5	1.6	106.7	1.5	100.0	0.9	60.0	1.0	66.7	1.2	80.0	1.2	80.0	0.1	6.7	.7	46.7
11 Apr	3.5	3.3	94.3	3.0	85.7	2.0	57.1	2.2	62.9	2.3	65.7	2.9	82.9	1.8	51.4	1.3	37.1
4 May	5.5	5.2	94.8	5.1	92.7	3.1	56.4	3.8	69.1	3.8	69.1	4.7	85.5	2.4	43.6	2.3	41.8
5 May	10.2	9.4	92.2	9.5	93.1	8.3	81.4	9.2	90.2	8.8	86.3	7.5 1/	73.5	7.8	76.5	7.7	75.5
17 Jul	2.5	1.9	76.0	1.8	72.0	1.2	48.0	1.1	44.0	1.4	56.0	1.6	64.0	.6	24.0	.7	28.0
18 Jul	1.5	1.2	80.0	1.1	73.3	.9	60.0	.8	53.3	.9	60.0	1.1	73.3	.4	26.7	.1	6.7

1/ Probable meter error.

Table 5. (continued) Rainfall and runoff for paved or covered plots at Granite Reef.

Date	Total Rainfall	L-1 Runoff		L-4 Runoff		L-5 Runoff		L-6 Runoff		L-7 Runoff		A-1 Runoff		A-2 Runoff		A-5 Runoff	
1969	mm	mm	%	mm	%	mm	%	mm	%	mm	%	mm	%	mm	%	mm	%
23 Jul	16.4	14.3	87.3	10.2	62.2	14.3	87.3	16.1	98.3	13.9	84.8	15.0	91.4	14.4	87.8	14.4	87.8
7 Aug	3.4	4.9	144.1	3.5	102.9	3.2	94.1	2.7	79.7	2.9	85.3	3.7	108.8	2.2	64.9	1.5	44.1
14 Aug	11.1	10.4	93.7	10.4	93.7	10.2	91.9	11.7	105.4	10.2	91.9	10.8	97.3	10.1	91.0	9.5	85.6
28 Aug	3.0	3.1	103.5	2.7	90.0	1.8	60.0	2.0	66.7	2.3	76.7	2.2	73.3	1.3	43.3	1.7	56.7
4 Sep	4.4	3.9	88.6	3.5	79.5	3.5	79.5	3.2	72.7	3.1	70.5	3.2	72.7	2.6	59.1	2.0	45.5
11/12 Sep	12.5	12.9	103.2	12.2	97.6	11.5	92.0	11.7	93.6	11.1	88.8	10.8	86.4	11.1	88.8	8.5	68.0
15 Sep	8.4	7.8	92.9	7.3	86.9	7.2	85.7	6.6	78.6	6.5	77.4	6.3	75.0	5.3	63.1	5.4	64.3
18 Oct	10.0	10.0	100.0	9.3	93.0	8.6	86.0	8.5	85.0	8.0	80.0	8.0	80.0	7.0	70.0	6.5	65.0
21 Oct	2.5	2.1	84.0	1.9	78.0	1.7	68.0	2.0	80.0	1.1	44.0	1.6	64.0	1.0	40.0	.4	16.0
9/10 Nov	6.7	6.7	100.0	5.9	88.1	5.3	79.1	4.5	67.2	4.5	67.2	4.9	73.1	3.0	44.8	2.6	38.8
10/11 Nov	5.8	5.8	100.0	5.6	96.6	5.3	91.4	5.3	91.4	4.7	81.0	5.1	87.9	5.5	94.8	3.8	65.5
15 Nov	5.5	5.5	100.0	4.8	87.3	4.7	85.5	4.5	81.8	3.9	70.9	3.9	70.9	3.6	65.5	2.7	49.3
3/4 Dec	9.6	9.7	101.0	8.6	89.6	8.4	87.5	7.4	77.1	7.5	78.1	7.6	79.2	6.2	64.6	5.0	52.2
28 Dec	18.2	18.5	101.6	16.6	91.2	15.7	86.3	17.6	96.5	15.1	82.7	15.6	85.7	15.0	82.4	9.8	53.9
Total	232.2	223.8	96.4	207.5	89.4	191.8	82.6	207.0	89.1	187.7	80.8	197.3	85.0	172.3	74.2	164.7	70.9

Table 6. Treatments on bare soil plots at Granite Reef.

Plot	Treatment Date	Treatment
L-2	30 Nov 1961	Smoothed soil, 14.14 m × 14.14 m plot
L-3	4 Aug 1965	Smoothed soil, 14.14 m × 14.14 m plot treated with R-9 at 0.057 kg m^{-2}
	6 Nov 1969	Retreated with R-9 at 0.04 kg m^{-2}
A-3	1 Aug 1967	Smoothed soil, 6 m × 30 m plot
E-3	10 Dec 1964	Smoothed soil, 7.6 m × 15.2 m plot
W-1	1 Dec 1963	Uncleared watershed
W-3	1 Dec 1963	Cleared watershed
R-2	1 Mar 1965	Ridge and furrow - 10% side slope
R-4	13 May 1966	Ridge and furrow - 10% side slope treated with 44.9 g m^{-2} sodium carbonate

Table 7. Rainfall and runoff for bare soil plots at Granite Reef.

Date	Total Rainfall	L-2 Runoff		L-3 Runoff		A-3 Runoff		E-3 Runoff		W-1 Runoff		W-3 Runoff		R-2 Runoff		R-4 Runoff	
1969	mm	mm	%	mm	%	mm	%	mm	%	mm	%	mm	%	mm	%	mm	%
14/15 Jan	24.0	2.1	8.8	9.3	38.8	2.6	10.8	2.1	8.8	0	0	.1	1.0	1.9	7.9	2.0	8.3
15 Jan	4.9	.8	16.3	1.8	36.7	1.0	20.4	1.5	30.6	.3	6.1	.4	8.2	1.2	24.5	1.0	20.4
19/20 Jan	2.3	0	0	0	0	.4	17.4	0	0	0	0	0	0	0	0	0	0
21 Jan	6.5	2.4	36.9	3.7	56.9	2.8	43.1	2.4	36.9	.4	6.2	.7	10.8	2.8	43.1	2.6	40.0
25/27 Jan	3.4	0	0	0	0	0	0	0	0	.4	11.8	.4	11.8	0	0	0	0
6/7 Feb	6.9	.5	7.2	4.0	58.0	1.8	26.1	1.4	20.3	0	0	.8	11.6	2.1	30.4	1.6	32.2
13 Feb	4.3	0	0	1.1	25.6	0	0	.6	14.0	0	0	.3	7.1	.2	4.7	0	0
18 Feb	6.1	.8	13.1	2.3	37.7	1.7	27.8	1.5	24.6	.6	9.8	.4	6.6	1.4	23.0	1.5	24.6
20 Feb	1.2	0	0	0	0	0	0	0	0	0	0	0	0	0	0	0	0
22 Feb	4.5	0	0	.8	17.8	.4	8.9	.6	13.3	0	0	0	0	0	0	0	0
10 Mar	16.0	8.6	53.7	11.5	71.8	9.2	57.5	9.6	60.0	8.4	52.5	8.8	55.0	9.6	60.0	9.7	60.6
10/11 Mar	9.9	.8	8.1	3.9	39.5	1.8	18.3	1.2	12.1	.2	2.0	.3	3.0	1.1	11.1	1.0	10.2
23 Mar	1.5	0	0	0	0	0	0	0	0	0	0	0	0	0	0	0	0
11 Apr	3.5	0	0	0	0	0	0	.3	8.6	.2	8.6	.3	8.6	0	0	0	0
4 May	5.5	0	0	0	0	0	0	.3	5.5	0	0	0	0	0	0	0	0
5 May	10.2	2.2	21.6	4.9	48.1	4.4	43.2	2.8	27.5	.8	7.9	.8	7.9	3.3	32.4	3.1	30.4
17 Jul	2.5	0	0	0	0	0	0	0	0	0	0	0	0	0	0	0	0
18 Jul	1.5	0	0	0	0	0	0	0	0	0	0	0	0	0	0	0	0

Table 7. (continued) Rainfall and runoff for bare soil plots at Granite Reef.

Date	Total Rainfall	L-2 Runoff		L-3 Runoff		A-3 Runoff		E-3 Runoff		W-1 Runoff		W-3 Runoff		R-2 Runoff		R-4 Runoff	
1969	mm	mm	%	mm	%	mm	%	mm	%	mm	%	mm	%	mm	%	mm	%
23 Jul	16.4	6.6[1/]	40.0	11.5[2/]	70.0	7.5	45.7	6.0	36.6	4.3	26.3	5.2	31.7	6.3	38.4	6.7	40.9
7 Aug	3.4	0	0	0	0	0	0	.4	11.8	0	0	0	0	0	0	0	0
14 Aug	11.1	5.3	47.7	7.6	68.5	7.0	63.1	6.5	58.6	4.0	36.1	5.3	47.7	6.9	62.2	6.0	54.1
28 Aug	3.0	0	0	.4	13.3	0	0	.6	20.0	0	0	0	0	0	0	0	0
4 Sep	4.4	0	0	.5	11.4	.7	15.9	.6	13.6	.2	4.5	.1	2.3	.6	13.6	.1	2.6
11/12 Sep	12.5	2.1	16.8	5.0	40.0	3.2	25.6	2.6	20.8	1.1	8.8	1.6	12.8	2.6	20.8	2.3	18.4
15 Sep	8.4	1.8	21.4	3.4	40.5	2.9	34.7	2.2	26.2	.4	4.7	.9	10.7	2.2	26.2	2.0	23.8
18 Oct	10.0	1.8	18.0	3.5	35.0	1.6	16.0	1.5	15.0	.3	3.0	.6	6.0	2.1	21.0	1.2	12.0
21 Oct	2.5	0	0	0	0	0	0	0	0	0	0	0	0	0	0	0	0
9/10 Nov	6.7	0	0	4.6[3/]	68.7	0	0	0	0	0	0	0	0	0	0	0	0
10/11 Nov	5.8	0	0	5.8	100.0	0	0	0	0	0	0	0	0	0	0	0	0
15 Nov	5.5	0	0	4.9	89.1	0	0	.4	7.3	0	0	0	0	0	0	0	0
3/4 Dec	9.6	1.2	12.5	8.0	83.3	1.9	19.8	1.5	15.6	1.6	18.9	.2	2.1	1.8	18.8	1.1	11.5
28 Dec	18.2	0	0	16.0	87.8	0	0	.3	1.6	0	0	0	0	0	0	0	0
Total	232.2	37.0	15.9	114.5	49.3	50.9	21.9	46.9	20.2	23.2	10.0	27.2	11.7	46.1	19.9	41.9	18.0

1/ Meter malfunction, runoff estimated at 40 percent by comparison with Plot A-3 and storm on 10 Mar 1969.

2/ Meter malfunction, runoff estimated at 70 percent by comparison with storm on 10 Mar 1969.

3/ Plot retreated on 6 Nov 1969.

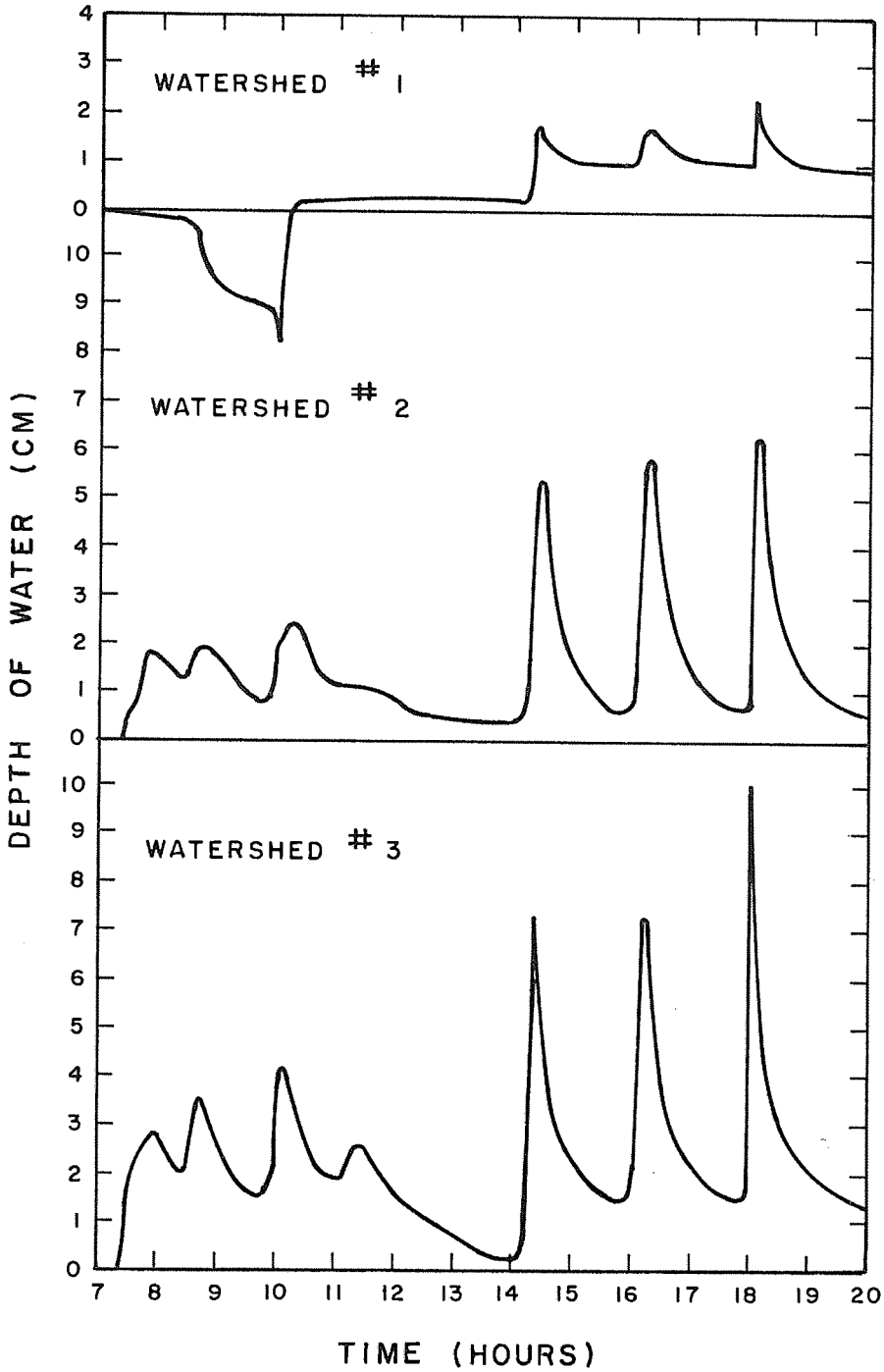

FIGURE 1. Stage vs. time for storm of Oct. 2, 1968 on three Monument Tank watersheds.

TITLE: CLAY DISPERSANTS FOR THE REDUCTION OF SEEPAGE LOSSES FROM RESERVOIRS.

CRIS WORK UNIT: SWC 018-gG-2 CODE NO.: Ariz.-WCL 64-3

INTRODUCTION:

Water loss observations and soil analyses were made on two ponds treated with sodium carbonate to reduce seepage. Because of increasing seepage losses, both ponds were retreated with sodium carbonate in the summer of 1968.

PROCEDURE:

Dick Mason. Treated in July 1965, this pond had maintained a low seepage rate (3 mm/day) through October 1968. Measurements in May 1969 showed that this rate had increased to 8 mm/day, and analysis of soil samples showed an ESP of 3.5 in the 0-10 cm depth. The pond was retreated in August 1969 with 800 pounds of sodium carbonate spread on 7250 ft^2 of pond soil for a design ESP of 14 in the top 10 cm of soil.

House Mountain No. 1. In July 1963 this pond was treated with sodium carbonate and was given a "booster shot" (sodium carbonate and sodium chloride added to the water) in November 1966 to maintain low seepage rates.

Seepage measurements in May 1969 showed an increase to 8 mm/day from its previous low rate of 3 mm/day. Soil analyses showed an ESP of 1-2 in the top 10 cm of soil. The pond was retreated in June 1969 with 2300 pounds of sodium carbonate spread on 17,950 ft^2 for a design ESP of 14 in the top 10 cm of soil. This treatment was not a booster shot but was a complete retreatment to restore the high sodium level in the soil.

RESULTS AND DISCUSSION:

Through October 1969 there was no runoff into either Dick Mason or House Mountain No. 1 ponds, and evaluation of the effectiveness of the retreatments could not be made. From our

experience, it appears that the initial treatment of a pond with sodium carbonate will maintain low seepage rates for about 3 years. The addition of a much less amount of salt to the pond water every other year seems to maintain the low rate for at least 2 years. Initial material cost is about $200 per acre, while each biyearly addition costs about $60 per acre. If booster shots are not given to the pond as required, complete retreatment of the pond may be necessary.

SUMMARY AND CONCLUSIONS:

The use of sodium carbonate (soda ash) to treat soil for reducing seepage from ponds has been shown to be highly successful. Enough soda ash is spread on the soil and mixed in to give an exchangeable sodium percentage of about 15 inches in the top 10 cm of soil. This initial treatment has lasted at least 3 years in field trials. After this 3-year period, soda ash and sodium chloride can be added to the water (much less than used in the initial treatment) every other year to maintain low seepage rates.

The average cost of material for the initial treatment is about $200 per acre with subsequent additions of about $60 every other year.

PERSONNEL: Robert J. Reginato and Lloyd E. Myers

CURRENT TERMINATION DATE: December 1970

TITLE: DISPERSION AND FLOCCULATION OF SOIL AND CLAY MATERIALS AS RELATED TO THE Na AND Ca STATUS OF THE AMBIENT SOLUTION.

CRIS WORK UNIT: SWC-018-gG-2 CODE NO.: Ariz-WCL-64-6

PART I. HYDROLYSIS OF $CaCO_3$, Na_2CO_3 AND $NaHCO_3$ AND THEIR COMBINATIONS IN THE PRESENCE AND ABSENCE OF EXTERNAL CO_2 SOURCE

INTRODUCTION:

In our program of water conservation, sodium salts have been used for sealing ponds and for increasing precipitation runoff (Annual Reports 1963-1968). The chemical property of the soil governs to a large degree the type of salt most suitable for treatment. With calcareous soils, we found that Na_2CO_3 works better than other sodium compounds in pond sealing, and in this case the salt serves a twofold purpose: The first is to supply the sodium necessary for creating an environment favorable for soil swelling and dispersion with consequent decrease in water permeability. The second is to inactivate the replaced and other sources of free calcium and magnesium by precipitating and/or complexing them. The salt addition will change the quality of the pond water, and thus an understanding of the chemical interaction of Na_2CO_3 with water and $CaCO_3$ in particular is necessary for providing useful predictors of salt treatment.

The pre- and post-salt treatment present a wide spectrum of hydrolysis conditions ranging from a strictly $CaCO_3$ to a $CaCO_3$-Na_2CO_3, to a Na_2CO_3 dominant system, all of which can occur in the presence or absence of atmospheric and other sources of CO_2. Similar situations occur naturally in alkali soils. A selected few of the preceding conditions have been theoretically treated by Garrels and Christ (6), Ponnamperuma (19), and Turner (20), but a complete description of the entire range of the hydrolysis process is not available.

Existing methods for predicting pH's over the wide range of conditions and combinations were found to be inadequate. A critical review of these techniques showed that the primary shortcoming has been the introduction of certain simplifying assumptions in the derivation of the equations which were necessary to make the computation amenable to straightforward numerical manipulation. Unfortunately, the reasons for making such assumptions are frequently overlooked and consequently no consideration is afforded any resultant limitation. Furthermore, these oversights become entrenched in the literature. In this section the hydrolysis of $CaCO_3$, Na_2CO_3, and $NaHCO_3$ will be reexamined individually and in combination with each other with computations based on unsimplified theoretical equations for predicting the hydrolytic ionic components in solution. The hydrolysis of Na_2CO_3 alone was superficially treated in the 1968 Annual Report. The treatment will be further expanded to include the "open" and "closed" systems, experimental measurements, and activity coefficient functions. The designation "closed" system indicates that no external source of CO_2 is present, and does not mean the total absence of CO_2 since it will be present in a carbonate solution in equilibrium with the other carbonate forms.

THEORY:

Na_2CO_3 "Closed" System. The mass and charge balance relations for describing the equilibrium condition of a Na_2CO_3 system at a total carbonate concentration C are as follows:

Mass:

$$C = [H_2CO_3] + [HCO_3^-] + [CO_3^{2-}] \quad (1)$$

$$[Na^+] = 2C \quad (2)$$

Charge:

$$[Na^+] + [H^+] = [HCO_3^-] + 2[CO_3^{2-}] + [OH^-] \quad (3)$$

The concentration of the different components can be described by their dissociation constants as

$$K_{1A} = (H^+)[HCO_3^-]\gamma_3/(H_2CO_3) \quad (4)$$

$$K_{2A} = (H^+)[CO_3^{2-}]\gamma_4/[HCO_3^-]\gamma_3 \quad (5)$$

$$K_w = (H^+)(OH^-) \quad (6)$$

where the bracket, [], represents concentration, the parenthesis, (), activity, and gamma, γ, the activity coefficient where $\gamma_1 = \gamma_{H^+}$, $\gamma_2 = \gamma_{OH^-}$, $\gamma_3 = \gamma_{HCO_3^-}$, $\gamma_4 = \gamma_{CO_3^{2-}}$.

By solving for $[H_2CO_3]$, $[CO_3^{2-}]$, and $[OH^-]$ in terms of (H^+) and $[HCO_3^-]$ in equations (4), (5), and (6) and substituting into (1) and (2), we have

$$C = \frac{(H^+)\gamma_3[HCO_3^-]}{K_{1A}} + [HCO_3^-] + \frac{\gamma_3[HCO_3^-]K_{2A}}{(H^+)\gamma_4} \quad (7)$$

$$2C + \frac{(H^+)}{\gamma_1} = \frac{K_w}{(H^+)\gamma_2} + [HCO_3^-] + \frac{2K_{2A}\gamma_3[HCO_3^-]}{(H^+)\gamma_4} \quad (8)$$

Solution of the pair of simultaneous linear equations (7) and (8) permits the calculation of (H^+), which is in the quartic form

$$F_1(H^+)^4 + F_2(H^+)^3 + F_3(H^+)^2 + F_4(H^+) + F_5 = 0 \quad (9)$$

where

$$F_1 = \gamma_3/\gamma_1 K_{1A} \quad (10)$$

$$F_2 = (2C\gamma_3/K_{1A}) + 1/\gamma_1 \quad (11)$$

$$F_3 = C + (\gamma_3 K_{2A}/\gamma_1\gamma_4) - (\gamma_3 K_w/\gamma_2 K_{1A}) \quad (12)$$

$$F_4 = -K_w/\gamma_2 \quad (13)$$

$$F_5 = -\gamma_3 K_w K_{2A}/\gamma_2\gamma_4 \quad (14)$$

$NaHCO_3$ "Closed" System. The $NaHCO_3$ system is solved in a manner similar to the Na_2CO_3 system, except that in the mass balance equation (2) $[Na^+] = C$ is used instead of $[Na^+] = 2C$. The equation for (H^+) computation has the same form as equation (9), but the F coefficients are now $F_1 = \gamma_3/\gamma_1 K_{1A}$, $F_2 = C\gamma_3/K_{1A} + 1/\gamma_1$, $F_3 = \gamma_3 K_{2A}/\gamma_1\gamma_4 - \gamma_3 K_w/\gamma_2 K_{1A}$, $F_4 = -(K_w/\gamma_2 + C\gamma_3 K_{2A}/\gamma_4)$, and $F_5 = -\gamma_3 K_w K_{2A}/\gamma_2\gamma_4$.

$CaCO_3$-Na_2CO_3 "Closed" System. A mixture of Na- and Ca-carbonates yields charges and carbonate masses as indicated by equations (3) and (7) of the preceding, but in addition, carbonate and charges represented by "S" arising from the $CaCO_3$ solid being hydrolyzed must be considered. This situation is related to its solubility product K_S as

$$K_S = (Ca^{2+})(CO_3^{2-}) \tag{15}$$

Thus, the mass and charge balance becomes, respectively

$$C + S = [HCO_3^-] + [CO_3^{2-}] + [H_2CO_3] \tag{16}$$

$$[Na^+] + [H^+] + 2[Ca^{2+}] = [OH^-] + [HCO_3^-] + 2[CO_3^{2-}] \tag{17}$$

Solving for (16) and (17) in terms of (H^+) and $[HCO_3^-]$ and letting $\gamma_5 = \gamma_{Ca^{2+}}$ leads to the relation

$$C + \frac{K_S(H^+)}{K_{2A}[HCO_3^-]\gamma_3\gamma_5} = [HCO_3^-] + \frac{K_{2A}[HCO_3^-]\gamma_3}{(H^+)\gamma_4} + \frac{(H^+)[HCO_3^-]\gamma_3}{K_{1A}} \tag{18}$$

$$2C + \frac{(H^+)}{\gamma_1} + \frac{2K_S(H^+)}{K_{2A}[HCO_3^-]\gamma_3\gamma_5} = \frac{K_W}{(H^+)\gamma_2} + [HCO_3^-] + \frac{2K_{2A}[HCO_3^-]\gamma_3}{(H^+)\gamma_4} \tag{19}$$

Equations (18) and (19), a pair of nonlinear simultaneous equations, can be solved for (H^+), $[HCO_3^-]$, $[CO_3^{2-}]$, $[Ca^{2+}]$, and $[OH^-]$ on the computer as a function of the Na_2CO_3 added to a saturated $CaCO_3$ solution. If Na_2CO_3 concentration is set to zero, we have a closed $CaCO_3$ system and a highly simplified condition which may be related to $CaCO_3$ equilibrium in groundwater. If "S" in equation (16) is equated to the dissolved carbonate content in rainwater in equilibrium with atmospheric CO_2 with consequent isolation, as would be the case of rapidly infiltrating rainwater, the component concentrations can also be calculated with these sets of equations. Turner (20) and Garrels and Christ (6) also have made estimates of the pH for this special case.

$CaCO_3$-$NaHCO_3$ "Closed" System. As noted in the $NaHCO_3$ "closed" system section, the pH for the $CaCO_3$-$NaHCO_3$ "closed" system is estimated in the same manner as the $CaCO_3$-Na_2CO_3 "closed" system. The "2C" term in equation (19) is replaced by "C" for the $NaHCO_3$-$CaCO_3$ combination, and equations (18) and (19) are solved simultaneously for (H^+) and $[HCO_3^-]$. The other carbonate constituents are obtained using equations (16) and (17).

Na_2CO_3-CO_2 "Open" System. The open system can be treated analogously to the closed system, except that an additional factor, the H_2CO_3 activity $(H_2CO_3 + CO_2)$, in equilibrium with gaseous CO_2 must be considered, which is

$$(H_2CO_3) = kP \qquad (20)$$

where k is Henry's law constant for the solubility of CO_2, and P is the partial pressure of CO_2. The charge balance in this case, using equation (3) and substituting $[HCO_3^-]$ and $[CO_3^{2-}]$ in terms of $[H^+]$, is

$$[H^+] + [Na^+] = \frac{K_w}{[H^+]\gamma_1\gamma_2} + \frac{K_{1A}kP}{[H^+]\gamma_1\gamma_3} + \frac{2K_{1A}K_{2A}kP}{[H^+]^2\gamma_1^2\gamma_4} \quad (21)$$

which can be rearranged to

$$[H^+]^3 + [Na^+][H^+]^2 - \left(\frac{K_w}{\gamma_1\gamma_2} + \frac{K_{1A}kP}{\gamma_1\gamma_3} \right) [H^+] - \frac{2K_{1A}K_{2A}kP}{\gamma_1^2\gamma_4} = 0 \quad (22)$$

Ponnamperuma (19) made a set of simplifications to reduce equation (22) to a quadratic form; then further simplified the resultant quadratic equation. Since the equations represented here were solved on a computer, there was no reason to defer to the simplified form. However, the two methods are compared in the Results and Discussion section.

$CaCO_3$-CO_2 "Open" System. The charge balance relation for the $CaCO_3$-CO_2 system is

$$2[Ca^{2+}] + [H^+] = [HCO_3^-] + 2[CO_3^{2-}] + [OH^-] \quad (23)$$

which when solved in terms of $[H^+]$ yields a quartic equation of the form

$$R_1[H^+]^4 + [H^+]^3 - (R_2 + R_4)[H^+] - R_3 = 0 \quad (24)$$

where

$$R_1 = 2\gamma_1^2 K_S / K_{1A} K_{2A} k \gamma_5 P \quad (25)$$

$$R_2 = K_{1A} k P / \gamma_1 \gamma_3 \quad (26)$$

$$R_3 = 2 K_{1A} K_{2A} k P / \gamma_1^2 \gamma_4 \quad (27)$$

$$R_4 = K_w / \gamma_1 \gamma_2 \quad (28)$$

Equation 23 can be simplified to a cubic equation which is more commonly presented for practical application as

$$pH = (\log 2 + pK_{2A} - pK_S)/3 + 2(pk + pK_{1A} - \log P)/3 + (\log \gamma_3 - \log \gamma_5)/3 \quad (29)$$

$\underline{CaCO_3\text{-}Na_2CO_3\text{-}CO_2}$ "Open" System. The addition of Na_2CO_3 to the $CaCO_3\text{-}CO_2$ system requires a modification of the charge balance in equation (23) to the form

$$[H^+] + [Na^+] + 2[Ca^{2+}] = [HCO_3^-] + 2[CO_3^{2-}] + [OH^-] \quad (30)$$

Replacement of $[Ca^{2+}]$, $[HCO_3^-]$, $[CO_3^{2-}]$, and $[OH^-]$ in terms of $[H^+]$ and $[H_2CO_3]$ leads to a quartic equation

$$R_1[H^+]^4 + [H^+]^3 + [Na^+][H^+]^2 - (R_2 + R_4)[H^+] - R_3 = 0 \quad (31)$$

This relation differs from the preceding equation (24) describing the $CaCO_3\text{-}CO_2$ system by the term $[Na^+][H^+]^2$.

$NaHCO_3$-CO_2 and $CaCO_3$-$NaHCO_3$-CO_2 "Open" Systems. The pH's for the $NaHCO_3$ system are computed in the same way as the Na_2CO_3 system using either equation (22) or (31) for the combination under consideration. If carbonate salt concentrations C are expressed in molar units, precaution must be taken to differentiate the two types of salts in terms of Na concentration as $[Na^+] = 2C$ for Na_2CO_3 and $[Na^+] = C$ for $NaHCO_3$.

PROCEDURE:

Experimental. The pH's of various concentrations of Na_2CO_3 and $NaHCO_3$ were measured in the "closed" and "open" system at 25^oC. For the closed system the reagent-grade sodium carbonate salt was dissolved in ultrasonically and N_2 deaerated-deionized water, and at the lower salt concentrations, in water further purified by distilling deionized water from dilute permanganate solution. pH's were measured as soon as the solution was made in a closed flask. With the closed $CaCO_3$ solution, nitrogen gas, first passed through ascarite, was bubbled into saturated $CaCO_3$ before the pH and Ca concentrations were determined.

The pH's for the open system were determined after CO_2-N_2 gas mixtures of different CO_2 composition were passed through the Na_2CO_3, $NaHCO_3$, saturated $CaCO_3$, and combinations of Na_2CO_3-$CaCO_3$, $NaHCO_3$-$CaCO_3$ solutions.

The glass-saturated calomel electrode system was used for the pH measurements. It was calibrated against standard buffers which were initially checked with NBS standards. Sodium correction for the glass electrode was unnecessary at the range of pH and Na concentrations encountered.

Computational. The component concentrations for all the preceding sets of solution combinations were calculated using a digital computer system. A reasonable initial "guess" of the equilibrium ionic strength was made for estimating the component

activity coefficients, using the extended Debye-Hückel (D-H) theory. This step was necessary because the component concentrations were not known at this stage. The initial activity coefficients in combination with the equilibrium constants and sodium concentration and necessary set of equations were used to compute the cation and anion concentrations. These values were then used to estimate a new ionic strength and, consequently, improved activity coefficients. This iteration procedure was continued until the concentrations remained unchanged.

The constants used were $K_{1A} = 4.34 \times 10^{-7}$, $K_{2A} = 4.69 \times 10^{-11}$, $K_w = 1 \times 10^{-14}$, $K_S = 5.0 \times 10^{-9}$, and $k = .0344 - .0084\ \mu$. The activity coefficients were calculated using the D-H relation

$$- \log \gamma = Az^2\sqrt{\mu}/(1 + aB\sqrt{\mu}) \qquad (32)$$

where z is the valence, and A, a, and B are constants for the specific ion in solution and were obtained from Kielland (15).

The partial pressures of the CO_2 were estimated from the CO_2 composition of the CO_2-N_2 gas mixture including corrections for barometric and water-vapor pressures.

RESULTS AND DISCUSSION:

Na_2CO_3 "Closed" and "Open" Systems. The theoretical computation and experimental results for the pH of Na_2CO_3 at different concentration and external CO_2 partial pressures are presented in Fig. 1. For the "closed" system, $P_{CO_2} \cong 0$, the theory represented by equation (9), predicts adequately the measured pH of the Na_2CO_3 solution. The experimental data are those of Lortie and Demer (16) who used a hydrogen electrode instead of the glass electrode. The simplified form (dashed line A merging into the solid line) is represented by the relation

$$pH = (pK_W + pK_{2A} + \log C)/2 \qquad (33)$$

and also predicts pH reliably at high carbonate concentration. However, this relation gives results which deviate from equation (9) below Na_2CO_3 concentration of 10^{-3} M. In the simplified derivation, it is assumed that $[CO_3^{2-}] = C$ (9), but since the hydrolytic form HCO_3^- becomes the predominating species at the lower Na_2CO_3 concentration the equation is no longer dependable in this range.

Reliable pH measurements could not be obtained below 10^{-4} M Na_2CO_3 for this closed system. The pH readings continued to drift to lower values without reaching equilibrium and were below the theoretical curve obtained from equation (9). However, despite the lack of adequate data, the good agreement between theory and experimental results in the succeeding examples would lead one to favor the use of the unsimplified equation (9) over equation (33) at the lower Na_2CO_3 concentrations for pH predictions.

The pH's were also computed on the assumption that the form $NaCO_3^-$ was present in solution. The pH values in this case were 2 and 1 per cent less than the pH's obtained with no $NaCO_3^-$ for the 1 and 0.1 M Na_2CO_3 concentration levels, respectively, whereas no difference in computed pH's was obtained with either models at the lower Na_2CO_3 concentrations. Whether the pH differences are significant remains an open question since the K_{1A} and K_{2A} constants used are based on the assumption that Na carbonate ion-pairs are absent.

For the "open" system at CO_2 partial pressures of 3.5×10^{-4} and 0.93 atmosphere, there is also good agreement with the theoretical (solid line) values based on equation (22) and the experimental results. It is interesting to note

the good agreement even at the high carbonate concentration, where the D-H theory would be expected to fail.

The dashed lines B and C extending from the solid theoretical lines for the "open" system at low carbonate concentrations and at the 3.5×10^{-4} and 0.93 atmospheres CO_2 represent the portion of the simplified equation (22) reduced from the cubic to quadratic stage following the method of Ponnamperuma (19), (his equation (8) with simplification). This quadratic relation is essentially adequate for predicting pH's even at the low Na_2CO_3 concentration and at the low CO_2 partial pressure of 3.5×10^{-4} atm., but is not so at the higher 0.93 CO_2 atm. and lower carbonate concentrations.

Theoretical values (asterisks) obtained from Ponnamperuma's (19) further simplification at the higher carbonate concentrations are also compared for the two CO_2 partial pressures at 0.5×10^{-3} and 0.5×10^{-2} moles per liter. The agreement is adequate for most purposes and the variation is caused primarily in the factor $.51\sqrt{\mu}$ and the change of the ionic strength in addition to the slight difference in the value for the constant $(pk + pK_{1A})$.

$NaHCO_3$ "Closed" and "Open" Systems. The experimental and theoretical results for the pH of $NaHCO_3$ as a consequence of its hydrolysis are presented in Fig. 2. Unlike the Na_2CO_3 solutions, the pH's of the "closed" ($P_{CO_2} \doteq 0$) decrease with increasing bicarbonate concentration above 10^{-3} M. The pH's in these ranges are also less than that for the $NaHCO_3$ solutions in equilibrium with 3.5×10^{-4} atm. CO_2.

In the "open" system the pH-$NaHCO_3$ relation is similar to the "open" Na_2CO_3 system, but displaced one-half mole units left of the Na_2CO_3 system in the graphical representation since its Na equivalent is one-half that of Na_2CO_3.

Ponnamperuma's simplified form for pH prediction of $NaHCO_3$ at 10^{-2} M (pH = 5.80 − log P) and 10^{-3} M (pH = 5.82 − log P), yields pH of 9.27 and 8.30 at CO_2 partial pressure of 3.5×10^{-4} atm. The exact version gives 9.14 and 8.25, whereas the experimental pH values are 9.03 and 8.23, respectively. At CO_2 partial pressure of 0.93 atm., the experimental pH's at 10^{-2} and 10^{-3} M equal 5.80 and 4.86, compared to the exact solution of 5.81 and 4.84, and the simplified form of 5.87 and 4.90. Therefore, the reduced version is a suitable method for predicting equilibrium pH's of carbonate solution for most practical situations.

$CaCO_3$-Na_2CO_3 and $CaCO_3$-$NaHCO_3$ "Open" and "Closed" Systems. The theoretical and experimental pH data for the $CaCO_3$-Na_2CO_3 and $CaCO_3$-$NaHCO_3$ combinations both in the presence and absence of external CO_2 are given in Fig. 3. Both experimental and theoretical sets of pH values compare well with each other. Equilibration of $CaCO_3$-Na_2CO_3 to CO_2 at a partial pressure of 3.5×10^{-4} atmosphere decreases the pH approximately 1.6 units at the lower Na_2CO_3 concentrations and about 1 pH unit at the higher Na_2CO_3 concentrations. At P_{CO_2} = 0.93 atm., the pH decrease from the "closed" Na_2CO_3-$CaCO_3$ system is in the order of 4 pH units.

The interesting results are those for the $CaCO_3$-$NaHCO_3$ "closed" system. Theory predicts a decrease in pH with increasing $NaHCO_3$ for this system and is substantiated by the experimental measurements. Furthermore, the pH's for the $CaCO_3$-$NaHCO_3$-CO_2 "open" system combination at bicarbonate concentrations greater than 10^{-2} M are higher than the "closed" system.

The computed pH of the saturated $CaCO_3$ in absence of CO_2 and Na_2CO_3 or $NaHCO_3$ is 9.96. Garrels and Christ (6) state that this value should lie between pH 9.9 and 10. A pH value of 9.76 was obtained for a similarly defined condition in this experiment.

It is not known at present whether some atmospheric CO_2 leaked into the system or that complete equilibrium was not attained. When rainwater in equilibrium with CO_2 at 3.5×10^{-4} atmosphere is mixed with $CaCO_3$ with consequent isolation from external CO_2 source, the resultant predicted pH is 9.79. Turner (20) using slightly different values for K_{1A}, K_{2A}, K_S, and P_{CO_2} reported a pH of 9.93.

The pH's computed for the $CaCO_3$-CO_2 system without any Na-carbonates are 8.31 and 6.08 at $P_{CO_2} = 3.5 \times 10^{-4}$ and $P_{CO_2} = 0.93$, respectively, using the unsimplified quartic equation (24). With the simplified equation (29), the pH's at the equivalent CO_2 partial pressures are 8.30 and 6.02. The comparison thus shows that a pH difference exists for the two equations, but is not of significance for most practical applications.

Using the computed pH, total dissolved Ca and ionic strength computation for the $CaCO_3$-Na_2CO_3-CO_2 system, a further breakdown of the Ca forms were made. In this case the dissociation constants for $CaHCO_3^+$, $CaCO_3^o$, and $CaOH^+$ of .0564, 3.29×10^{-5}, and 0.040, respectively, were used. The computational results are presented in Tables 1 and 2. The increase in Na_2CO_3 not only causes a pH increase and Ca decrease, but a drastic reduction in the $[Ca^{2+}]$ in solution and a large increase in $[CaCO_3^o]$ form. Even without Na_2CO_3 present, the $[Ca^{2+}]$ species is approximately 80 percent of the total solution calcium. The $[CaOH^+]$ form in solution is much less relative to the Ca bicarbonate and carbonate forms.

PART II. SODIUM BICARBONATE AND CARBONATE ION-PAIRS

INTRODUCTION:

An accurate knowledge of the dissociation constants of carbonic acid is necessary for computing the constituent carbonate concentration in the CO_2-HCO_3-CO_3 systems of soil and water. The classical reports of Harned and co-workers (11, 12, 13) have been cited frequently for the first ($\underline{K}_{1A}$) and second ($\underline{K}_{2A}$) dissociation constants of carbonic acid. Thermodynamically defined $\underline{K}_{1A}$ and $\underline{K}_{2A}$ were obtained by a method of extrapolation to zero ionic strength. This procedure appears reasonable since the calculated apparent K's were essentially a linear function of the ionic strength, but if all the factors comprising the theoretical relation for obtaining $\underline{K}_{1A}$ and $\underline{K}_{2A}$ could be accounted for, computed ionization constants could be made independent of ionic strength. The ionic strength in their experiments was varied directly by changing the concentration of NaCl, $NaHCO_3$, or Na_2CO_3, and indirectly but to a minor extent only by changing the partial pressure of CO_2.

In addition to the ionic strength dependence of $\underline{K}_{1A}$, a distinct effect of $NaHCO_3$ concentration upon the computed dissociation constants was shown by the results of Harned and Bonner (11). At a constant NaCl concentration of 0.1 M, the dissociation constant increased with increasing $NaHCO_3$ concentration. We have observed that the pH of the H_2CO_3-NaCl system, as measured with the glass-saturated KCl calomel electrode system, decreased systematically as the ionic strength was increased by the increase in NaCl concentration. The change was close to the order of magnitude of the junction potential, but a possibility existed that the Na^+ was interacting with the HCO_3^- to form undissociated $NaHCO_3^o$ with the attendant increase in H^+ concentration, i.e., decreasing pH. The systems of Harned and co-workers did not

involve any liquid junction, but the direction in the change of the dissociation constant with HCO_3-Na change further indicated evidence of interaction between Na^+ and HCO_3^-, and Na^+ and CO_3^{2-}.

The existence of the forms $NaHCO_3^o$ and $NaCO_3^-$ has been suggested, and values for their dissociation constants $\underline{K}_{NaHCO_3^o}$ and $\underline{K}_{NaCO_3^-}$ are available (5, 7, 8). If these forms are present, the variability in the computed apparent carbonic acid dissociation constants could possibly be related to changes in the amounts of $NaHCO_3^o$ and $NaCO_3^-$ in solution as the Na, HCO_3 and CO_3 concentrations are changed experimentally, and not to the ionic strength factor <u>per se</u>. The purpose of this section is to explore the possibility for the presence of $NaHCO_3^o$ and $NaCO_3^-$ in Na-carbonate solutions and to reevaluate the carbonic acid dissociation constants based on these species.

THEORY:

The first and second dissociation constants of carbonic acid are defined as

$$\underline{K}_{1A} = \frac{(H^+)(HCO_3^-)}{(H_2CO_3)} = \lim_{P_{CO_2} \to 0} \left(\frac{[H^+][HCO_3^-]}{[CO_2] + [H_2CO_3]} \right) \tag{1a}$$

$$\underline{K}_{2A} = \frac{(H^+)(CO_3^{2-})}{(HCO_3^-)} \tag{1b}$$

where the ( ) represents activities and [ ] concentration.

First Dissociation Constant. $\underline{K}_{1A}$ is determined by the electrometric measurement of cell $Pt;H_2,CO_2|NaHCO_3,NaCl,CO_2|AgCl;Ag$ and a knowledge of the various constituents making up the following relation:

$$\left[-\log \underline{K}_{1A}\right]_{\mu=0} = \frac{(\underline{E} + \underline{E}_c - \underline{E}^o)\underline{F}}{2.303\underline{RT}} + \log \gamma_{CO_2} \underline{SP}_{CO_2} + \log \frac{[Cl^-]}{[HCO_3^-]}$$

$$+ \log \frac{\gamma_H \gamma_{Cl}}{\gamma_H \gamma_{HCO_3}} \qquad (2)$$

where $\underline{E}$ = emf of the cell, $\underline{E}_c = (-\underline{RT}/2\underline{F}) \ln \underline{P}_{H_2}$, $\underline{E}^o$ = standard potential of reference electrode, R = gas constant, $\underline{T}$ = Kelvin temperature, $\underline{F}$ = Faraday, $\underline{S}$ = Henry's law constant, $\underline{P}$ = partial pressure, γ = activity coefficient. Alternately, the γ relation can be transferred to the left side of the equation and the apparent dissociation constant $\underline{K}'_{1A}$ defined according to Harned and Davis (12).

If the species $NaHCO_3^o$ is assumed to be present, the mass balance relationships for Na and HCO_3 are written as

$$[Na]_{total} = [Na^+] + [NaHCO_3^o] \qquad (3)$$

$$[HCO_3]_{total} = [HCO_3^-] + [NaHCO_3^o] \qquad (4)$$

Consequently, the $[HCO_3^-]$ term in equation (2) will not be equal to the stoichiometric bicarbonate concentration, but to a value less than this. This condition would not be apparent by the extrapolation or activity coefficient adjustment techniques which have been used previously. The dissociation constant for $NaHCO_3^o$ is defined as

$$\underline{K}_{NaHCO_3^o} = (Na^+)(HCO_3^-)/(NaHCO_3^o) \quad (5)$$

The charge balance relation for the constituents in the cell system remains the same with or without $NaHCO_3^o$ and is

$$[H^+] + [Na^+] = [Cl^-] + [HCO_3^-] \quad (6)$$

The OH^- and CO_3^{2-} forms are neglected since the pH of the system can be adjusted to levels where these are insignificant.

By substituting the definition for $NaHCO_3^o$ from equation (5) into equations (3) and (4) we have

$$[Na]_{total} = [Na^+] + \gamma_{Na}[Na^+]\gamma_{HCO_3}[HCO_3^-]/\underline{K}_{NaHCO_3^o} \quad (7)$$

$$[HCO_3]_{total} = [HCO_3^-] + \gamma_{Na}[Na^+]\gamma_{HCO_3}[HCO_3^-]/\underline{K}_{NaHCO_3^o} \quad (8)$$

and $[HCO_3^-]$, $[Na^+]$, and $[NaHCO_3^o]$ may be computed from the simultaneous solution of equations (6), (7), (8) if the γ's and $\underline{K}_{NaHCO_3^o}$ are known. The activity coefficient is derived from one form of the extended Debye-Hückel theory

$$-\log \gamma_i = \underline{A}z_i^2\mu^{1/2}/(1 + \underline{B}a_i\mu^{1/2}) \quad (9)$$

where i is the specified ion, μ the ionic strength, z_i the valence, and $\underline{A}$, $\underline{B}$, and $\underline{a}_i$ are constants.

$\underline{K}_{NaHCO_3^o}$ is obtained indirectly from measured (H^+) values of $NaHCO_3$-NaCl solutions of different concentrations. The procedure is to make various systematic selections of $\underline{K}_{NaHCO_3^o}$, from which the actual $[HCO_3^-]$ can be computed, and consequently $\underline{K}_{1A}$

can be obtained from equation (2). When the proper value of $\underline{K}_{NaHCO_3^o}$ is chosen, the computed $\underline{K}_{1A}$ values should be the same at the different ionic strengths in which the concentrations of NaCl and $NaHCO_3$ are different. The ionic strength, $\mu = ([H^+] + [HCO_3^-] + [Na^+] + [Cl^-])/2$, is also systematically adjusted in the computational process to account for the $NaHCO_3^o$ concentration which affects the Na^+ and HCO_3^- concentrations.

The $NaHCO_3^o$ concentration in a different and simpler system at lower HCO_3^- concentration, such as H_2CO_3-NaCl solutions, can also be computed from their solution pH's. The addition of equation (3) and (6) yields

$$[Na]_T + [H^+] = [Cl^-] + [HCO_3^-] + [NaHCO_3^o] \qquad (10)$$

and since $[Na]_T = [Cl^-]$, equation (10) becomes

$$[NaHCO_3^o] = [H^+] - [HCO_3^-] \qquad (11)$$

Thus, with a knowledge of pH, $\underline{K}_{1A}$, partial pressure of CO_2, Henry's law constant for the solubility of CO_2 in NaCl solutions, and using an iterative procedure for ionic strength computation, $[H^+]$ and $[HCO_3^-]$ can be calculated, and consequently, $[NaHCO_3^o]$ and its dissociation constant.

Second Dissociation Constant. $\underline{K}_{2A}$ is determined from an electrochemical cell system $Pt;H_2|NaHCO_3,NaCl,Na_2CO_3|AgCl;Ag$ in conjunction with the relation

$$\left[-\log \underline{K}_{2A}\right]_{\mu=0} = \frac{(\underline{E} - \underline{E}^o)\underline{F}}{2.303\underline{RT}} + \log \frac{[HCO_3^-][Cl^-]}{[CO_3^{2-}]} + \log \frac{\gamma_{HCO_3}\gamma_{Cl}}{\gamma_{CO_3}} \qquad (12)$$

If $NaHCO_3^o$ and $NaCO_3^-$ are present in solution, the ratio $[HCO_3^-]/[CO_3^{2-}]$ in equation (12) may not be equal to the stoichiometric ratio except by coincidence and instead related to one governed by the degree of association of Na^+ with HCO_3^- and CO_3^{2-}. Thermodynamic $\underline{K}_{2A}$ has been obtained through extrapolation to zero ionic strength to circumvent the inability of knowing the amount of Na-carbonate association.

The mass and electroneutrality relations when the ion-pairs are taken into account are

$$[Na]_{total} = [Na^+] + [NaHCO_3^o] + [NaCO_3^-] \quad (13)$$

$$[Carbonate]_{total} = [HCO_3^-] + [CO_3^{2-}] + [NaHCO_3^o] + [NaCO_3^-] \quad (14)$$

$$[Na^+] + [H^+] = [HCO_3^-] + 2[CO_3^-] + [OH^-] + [NaCO_3^-] \quad (15)$$

and the dissociation constant for $NaCO_3^-$ is

$$\underline{K}_{NaCO_3^-} = (Na^+)(CO_3^{2-})/(NaCO_3^-) \quad (16)$$

With the $\underline{K}_{NaHCO_3^o}$ value obtained from the determination of the first dissociation constant $\underline{K}_{1A}$, $\underline{K}_{NaCO_3^-}$ is computed in an analogous manner as $\underline{K}_{NaHCO_3^o}$. Different concentration combinations of HCO_3^-, CO_3^{2-}, and Na^+ are computed by the simultaneous solution of equations (13), (14), and (15) by systematically changing preselected values for $\underline{K}_{NaCO_3^-}$. The ionic strength factor is also corrected iteratively to account for the nonionic $NaHCO_3^o$, the $NaCO_3^-$, and the hydrolysis of CO_3^{2-} to form HCO_3^- and OH^-. This latter hydrolysis presented difficulties for MacInnes and Belcher (17) and Harned and Scholes (13) in their estimation of $\underline{K}_{2A}$, and it had to be treated separately

with additional extrapolations which sometimes were made on curvilinear portions of the graphical plots.

Equation (12) is then solved for $\underline{K}_{2A}$ using the various computed HCO_3^-, CO_3^{2-}, and ionic strength combinations corrected for $NaHCO_3^o$ and $NaCO_3^-$. If the same $\underline{K}_{2A}$'s are obtained with the different Na^+, HCO_3^-, and CO_3^{2-} levels and ionic strengths, the supposition for the presence of $NaHCO_3^o$ and $NaCO_3^-$ forms is essentially substantiated and this $\underline{K}_{2A}$ is equivalent to a thermodynamic value derived without extrapolation to zero ionic strength.

Experimental. The excellent experimental electrometric data of Harned and co-workers (11, 12, 13) for the $NaHCO_3$-$NaCl$-CO_2 and $NaHCO_3$-$NaCl$-Na_2CO_3 mixtures with the H_2-Ag;AgCl electrode system ($\underline{E}^o$ = .22234 V) without liquid junction were used to test for the presence of $NaHCO_3^o$ and $NaCO_3^-$. pH's were computed from the cell described by Bates (1) which is applicable to this set of experimental data. Henry's law constant, $\underline{S}$, for CO_2 solubility in NaCl solutions was recomputated from Harned and Davis (12) as $\underline{S}$ = .0344 - .00805 μ + .000192 μ^2.

pH's of the H_2CO_3-NaCl were determined with the glass-saturated KCl calomel electrode system at 25 $\pm$ .1°C. The electrode system was calibrated with NBS standard potassium phthalate. Premoistened, research-grade (99.999%) CO_2 was passed through NaCl solutions which were prepared from reagent-grade NaCl and redistilled water. CO_2 partial pressure was obtained from the barometric pressure and corrected for vapor pressure of water.

A digital computer was used to solve the equations by a method of successive approximation. The effect of $NaHCO_3^o$ and $NaCO_3^-$ on the ionic strength, since its formation results in a change in ionic species, was taken into account. The activity

coefficient for the undissociated species CO_2 and $NaHCO_3^o$ was assumed to be unity and that for $NaCO_3^-$, equal to HCO_3^-. The constants for the Debye-Hückel relation were obtained from the tabulation of Kielland (15).

RESULTS AND DISCUSSION:

The recomputed first dissociation constants of carbonic acid at 25°C for the $NaHCO_3$-NaCl-CO_2 system with associated results are presented in Tables 3 and 4. The dissociation constants of $NaHCO_3^o$ based on the glass electrode-saturated KCl, calomel electrode measurements of the NaCl-CO_2 system are listed in Table 5. Dissociation constants for HCO_3^- corrected for $NaHCO_3^o$ and $NaCO_3^-$ species are given in Table 6.

The example of computational results for $\underline{K}_{1A}$ and $\underline{K}_{NaHCO_3^o}$ shown in Table 3 is for only three of the eight series of data sets given by Harned and Davis (12). One, their series 4, was out of line with the other seven sets and was not used to estimate the $\underline{K}$'s which are $\underline{K}_{NaHCO_3^o} = .690 \pm .096$ and $\underline{K}_{1A} = (4.407 \pm .036) \times 10^{-7}$. By introducing the form $NaHCO_3^o$ and using the "true" $[Cl^-]/[HCO_3^-]$ ratio in equation (2) instead of the stoichiometric ratio, it was possible to make $\underline{K}_{1A}$ independent of ionic and $NaHCO_3$ concentration. The $NaHCO_3^o$ form relative to HCO_3^- amounts to only about 0.5% at the lowest NaCl-$NaHCO_3$ solution concentration of 2.182×10^{-3}, but reaches a magnitude of 15% at the highest concentration of 1.0391×10^{-2}. The $\underline{K}_{1A}$ value of 4.41×10^{-7} compares favorably with that of 4.45×10^{-7} obtained by Harned and Davis through an extrapolation process. The assumptions and computational techniques presented in this section avoid extrapolation or the need to adjust the parameters in the Debye-Hückel type relation for estimating the ion activities in order to achieve linearity between $\underline{K}_{1A}$ and μ.

This approach appears to work at the higher ionic strengths as illustrated in Table 4. In a solution of constant 0.1 M NaCl and $NaHCO_3$ concentration varying from 5×10^{-3} to 3×10^{-2} M, essentially similar -log K_{1A} values are computed. Harned and Bonner's results (11) are HCO_3^- dependent (also their Figure 1) and involve a double extrapolation technique to get K_S for carbonic acid in NaCl. The $K_{NaHCO_3}^o$ = (.460 ± .063) and K_{1A} = (4.176 ± .078) x 10^{-7} for all the four data sets are smaller than those computed for the series in Table 3, and since the data in Table 3 are based on lower concentrations more reliance is being placed on the results from them.

The possibility of Na^+ and HCO_3^- interaction at even lower HCO_3^- concentrations was examined in the NaCl-CO_2 system. By use of CO_2 partial pressure of approximately one atmosphere, HCO_3^- concentrations in the order of 10^{-4} M were attained. The resultant $K_{NaHCO_3}^o$ in this case, as shown in Table 5, is .308 ± .018. This is about one-half that of .690 obtained by recomputation of Harned and Davis' data (12). The discrepancy may be caused by the presence of significant liquid junction in the measurement system of the glass-calomel electrodes and analytical inaccuracies due to the low HCO_3^- concentrations. While the agreement of $K_{NaHCO_3}^o$ between the two methods is not favorable, the fact that $K_{NaHCO_3}^o$ can be established at the lower HCO_3^- concentration strongly supports the possibilities for the presence of $NaHCO_3^o$ in bicarbonate solutions.

A $K_{NaHCO_3}^o$ of 1.78 was reported by Garrels and Thompson (7) compared to .690, but a critical evaluation to explain this discrepancy could not be made because the experimental data and measurement technique were not available in their paper.

The dissociation constant of HCO_3^- when computed on basis of the presence of $NaHCO_3^o$ and $NaCO_3^-$ was essentially independent

of HCO_3^- and CO_3^{2-} concentrations, and also ionic strength of up to 0.08 (Table 6). The slightly different value for $-\log \underline{K}_{1A}$ at $\mu = 0.123$ appears to be due to experimental error. Harned and Scholes' (13) results and their recomputation of MacInnes and Belcher's data (17) (their Figures 1 and 2) show $\underline{K}_{2A}$ dependence on concentration even when the hydrolysis of CO_3^{2-}, which they thought caused much of the nonlinearity, was taken into account. They placed greater reliance upon the apparent $\underline{K}_{2A}$'s at the higher ionic strength levels because of smaller variations when extrapolating to zero ionic strength to derive a thermodynamic $\underline{K}_{2A}$. A $\underline{K}_{2A}$ of $(4.652 \pm .480) \times 10^{-7}$ was obtained for this study compared to 4.69×10^{-11} reported by Harned and Scholes (13) and 4.79×10^{-11} reported by Näsänen (18). The extrapolation method apparently gives values of sufficient accuracy at this temperature.

The $NaHCO_3^o$ and $NaCO_3^-$ relative to the HCO_3^-, CO_3^{2-}, and Na^+ concentrations become proportionately larger as the latter concentrations are increased, and in highly concentrated alkali-brine solutions they could possibly become the dominant species in solution.

The dissociation constant for $NaCO_3^-$ of $\underline{K}_{NaCO_3^-} = .282$ compares with one of 0.054 given by Garrels, et al. (8), who obtained it with a glass-calomel electrode system at very much higher (1 to 5) ionic strengths. Butler and Huston (2), measuring Na activity with the Na-amalgam and Na-selective glass electrodes at 1 to 2 ionic strengths in carbonate solutions, reported a $\underline{K}_{NaCO_3^-}$ of .45. Both groups did not take into account the $NaHCO_3^o$ species in the calculation of $\underline{K}_{NaCO_3^-}$. The data in Table 6 show that the concentrations of $NaHCO_3^o$ and $NaCO_3^-$ are of comparable magnitudes in these Na-carbonate solutions. By combining $NaHCO_3^o$ with the $NaCO_3^-$ concentration to give presumably similar

computational conditions as Garrels et al. (8) and Butler and Huston (2), $\underline{K}_{NaCO_3^-}$ becomes .171, still approximately midway in value between these investigations. Regardless of the differences in $\underline{K}_{NaHCO_3^o}$ and $\underline{K}_{NaCO_3^-}$, the different measuring techniques and carbonate model used, the computations indicate strongly the possibility for the presence of $NaHCO_3^o$ and $NaCO_3^-$ forms in Na-carbonate type solutions.

PART III. POTASSIUM BICARBONATE AND CARBONATE ION-PAIRS

INTRODUCTION:

The preceding study showed evidence for the presence of the bicarbonate and carbonate ion-pairs of Na, i.e. $NaHCO_3^o$ and $NaCO_3^-$. The conclusion was based on the observation that the bicarbonate and carbonate concentrations or ionic strength dependency of the apparent dissociation constants of H_2CO_3 and HCO_3^-, $\underline{K}'_{1A}$ and $\underline{K}'_{2A}$, could be eliminated by introducing the Na-bicarbonate and -carbonate ion-pairs into the computation of these constants. So far there is no positive proof for the existence of the species $KHCO_3^o$ and KCO_3^-. However, the results of MacInnes and Belcher (17), who used K- instead of Na-carbonates to get $\underline{K}'_{1A}$ and $\underline{K}'_{2A}$, give strong indication for the presence of K-carbonate ion-pairs, since the data do appear to behave in a similar manner as the Na-carbonate results. Therefore, experimental results and computations are presented here to show the possibility of the existence of these ion-pairs. The determination of the dissociation constants of $KHCO_3^o$ and KCO_3^- depends upon the estimation of $\underline{K}_{H_2CO_3}$ and $\underline{K}_{HCO_3^-}$ which is in turn based on the electrometric potential measurements of bicarbonate and bicarbonate-carbonate solutions and the use of the following equations:

$$-\log \underline{K}_{H_2CO_3} = \frac{(\underline{E}-\underline{E}^o)\underline{F}}{2.303\underline{RT}} + \log \frac{[Cl^-][CO_2]}{[HCO_3^-]} + \log \frac{\gamma_{CO_2}\gamma_H\gamma_{Cl}}{\gamma_H\gamma_{HCO_3}} \qquad (1)$$

$$-\log \underline{K}_{HCO_3^-} = \frac{(\underline{E}-\underline{E}^o)\underline{F}}{2.303\underline{RT}} + \log \frac{[HCO_3^-][Cl^-]}{[CO_3^{2-}]} + \log \frac{\gamma_H\gamma_{HCO_3}\gamma_{Cl}}{\gamma_H\gamma_{CO_3}} \qquad (2)$$

where $\underline{E}$ = emf of the cell, $\underline{E}^{o}$ = standard potential reference cell, $\underline{F}$ = faraday, $\underline{R}$ = gas constant, $\underline{T}$ = Kelvin temperature, γ = ion activity.

The usual method in both cases for obtaining the thermodynamic $\underline{K}$'s was to use the stoichiometric concentrations for HCO_3^- and CO_3^{2-} and extrapolate to zero ionic strength. Subsequent treatment indicated that this procedure can be improved when alkali carbonate ion-pairs are taken into account. In which case the computed $\underline{K}$'s become independent of other ionic strengths or carbonate concentrations.

PROCEDURE:

Experimental. The glass electrode -AgCl;Ag emf measurements of the $KHCO_3$-KCl-CO_2 and the H_2;Pt-AgCl;Ag determination of the $KHCO_3$-K_2CO_3-KCl solutions of MacInnes and Belcher (17) were used. In a separate experiment, the pH's of KCl-CO_2 solutions were measured with the glass electrode-saturated KCl, calomel electrode system at 25 $\pm$ .1°C. The 99.999% pure research-grade CO_2 gas was premoistened and passed through various concentrations of KCl solutions. The glass electrode was calibrated against NBS buffer standards.

Computational--First dissociation constant of carbonic acid and dissociation constant of $KHCO_3^o$. The various constituents and equilibrium constants making up the $KHCO_3$-KCl-CO_2 or KCl-CO_2 system were represented by the following equations of mass and charge balance:

$$[K]_{total} = [K^+] + [KHCO_3^o] \quad (3)$$

$$[HCO_3]_{total} = [HCO_3^-] + [KHCO_3^o] \quad (4)$$

$$[K^+] + [H^+] = [HCO_3^-] + [Cl^-] \quad (5)$$

$$\underline{K}_{KHCO_3^o} = (K^+)(HCO_3^-)/(KHCO_3^o) \quad (6)$$

$$[CO_2] = \underline{SP}_{CO_2} \quad (7)$$

$$-\log(H^+) = \frac{(\underline{E}-\underline{E}^o)\underline{F}}{2.303\underline{RT}} + \log(Cl^-) \quad (8)$$

The bracket [ ] represents concentration and parenthesis ( ) activity. Henry's law constant, $\underline{S}$, was obtained from recomputation of Harned and Davis' (12) data for CO_2 solubility in NaCl solution and is

$$\underline{S} = .0344 - .00805\ \mu + .000912\ \mu^2 \quad (9)$$

The activity coefficient, γ, is defined by the Debye-Hückel relation

$$-\log\ \gamma = -Az_i^2\mu^{1/2}/(1 + Ba_i\mu^{1/2}) \quad (10)$$

where A, B, a_i are constants which were obtained from Kielland (15), and the ionic strength, μ, defined by

$$\mu = ([HCO_3^-] + [K^+] + [Cl^-])/2 \quad (11)$$

The computational procedure involved making systematic changes in the value of $\underline{K}_{KHCO_3^o}$ and solving simultaneously for $[HCO_3^-]$, $[K^+]$, $[KHCO_3^o]$ using equations (3) through (11), and equation (1) for $\underline{K}_{1A}$ after $[HCO_3^-]$ is obtained. When the proper $\underline{K}_{KHCO_3^o}$ value is attained, the computed or apparent

K'_{1A} should be essentially the same at the different bicarbonate and chloride concentrations, i.e. K'_{1A} independent of ionic strength. Thus, by this technique both $K_{KHCO_3^o}$ and $K_{H_2CO_3}$ values are obtained concurrently.

Computational--Second dissociation constant of carbonic acid and dissociation constant of KCO_3^-. In addition to the preceding equations (2), (6), (8), and (10), the following relations are used to get $K_{HCO_3^-}$ and $K_{KCO_3^-}$:

$$[K]_{total} = [K^+] + [KHCO_3^o] + [KCO_3^-] \quad (12)$$

$$[Carbonate]_{total} = [HCO_3^-] + [CO_3^{2-}] + [KHCO_3^o] + [KCO_3^-] \quad (13)$$

$$[K^+] + [H^+] = [HCO_3^-] + 2[CO_3^{2-}] + [KCO_3^-] + [Cl^-] + [OH^-] \quad (14)$$

$$K_{KCO_3^-} = (K^+)(CO_3^{2-})/(KCO_3^-) \quad (15)$$

$$K_W = (H^+)(OH^-) \quad (16)$$

$$\mu = ([H^+] + [K^+] + [HCO_3^-] + [OH^-] + 4[CO_3^-] + [KCO_3^-])/2 \quad (17)$$

The computational procedure in this case is similar to the preceding one for getting K_{1A}, but since the value for $K_{KHCO_3^o}$ has been established, only K_{2A} and $K_{KCO_3^-}$ must be determined. Values of $K_{KCO_3^-}$ were systematically chosen and $[HCO_3^-]$, $[K^+]$, $[KHCO_3^o]$, $[HCO_3^-]$, $[CO_3^{2-}]$, $[KCO_3^-]$ computed from the simultaneous solution of equations (8), (10), (12), (13), (14), (15), (16), and (17); and, with a knowledge of $[HCO_3^-]$, and $[CO_3^{2-}]$ and the other factors, $K_{HCO_3^-}$ obtained with equation (2). The correct choice of $K_{KCO_3^-}$ should then give K_{2A}'s which are independent of μ, and K and carbonate concentrations.

RESULTS AND DISCUSSION:

The computed dissociation constants of $\underline{K}_{1A}$ and the concentration of K^+, $KHCO_3^o$, and HCO_3^- are presented in Table 7 relative to the KCl and $KHCO_3$ concentration and ionic strength. The pK_{1A}'s for this study and that from MacInnes and Belcher (17) are compared graphically in Figure 4. In this study the $\underline{K}_{1A}$'s remain essentially constant, being independent of either HCO_3^- concentration or ionic strength when the $KHCO_3^o$ is assumed to be present in solution. Thus this method avoids the need for extrapolation and removes the uncertainty associated with any type of extrapolation.

The $\underline{K}_{KHCO_3^o}$ value of .809 permitted the computations which yielded constant $\underline{K}_{1A}$'s. The $\underline{K}_{1A}$ in this case was (4.437 $\pm$ .022) x 10^{-7} or pK_{1A} = 6.353 $\pm$ .002 and compared with that of $\underline{K}_{1A}$ = 4.54 x 10^{-7} (pK_{1A} = 6.343) reported by MacInnes and Belcher (17). A $\underline{K}_{1A}$ of 4.41 x 10^{-7} was obtained for Harned and Davis' (12) data in which the form $NaHCO_3^o$ was assumed to be present compared to the extrapolated $\underline{K}_{1A}$ of 4.45 x 10^{-7}. Thus the recomputed $\underline{K}_{1A}$'s of 4.44 x 10^{-7} and 4.41 x 10^{-7} (vs. extrapolated 4.54 x 10^{-7} and 4.45 x 10^{-7}) become more comparable when the HCO_3 ion-pair of K^+ and Na^+ are taken into consideration in these two types of carbonate solutions.

The $\underline{K}_{1A}$ and $\underline{K}_{KHCO_3^o}$ values for the simpler KCl-CO_2 system are presented in Figure 5. Again, when the $KHCO_3^o$ form is taken into account the $\underline{K}_{1A}$'s are essentially independent of the ionic strength. For this system $\underline{K}_{1A}$ is (4.52 $\pm$ .04) x 10^{-7} and $\underline{K}_{KHCO_3^o}$ is .964. These values are slightly different than that $\underline{K}_{1A}$ of 4.44 x 10^{-7} and $\underline{K}_{KHCO_3^o}$ of .809 obtained with the preceding $KHCO_3$-KCl-CO_2 system and is probably due to uncorrected junction potential effects of the calomel reference system. In addition, the HCO_3^- concentrated in the KCl-CO_2

combination was in the order of 1×10^{-4}, whereas that in the $KHCO_3$-KCl-CO_2 was greater by a factor of 100 and thus led to greater experimental error.

The dissociation constant of HCO_3^- is $(5.001 \pm .111) \times 10^{-11}$ when values of $K_{KHCO_3}^o = .809$ and $K_{KCO_3^-} = 1.18$ were used in the computation. The constituent concentrations of potassium and carbonates are listed in Table 8. The pK_{2A}'s are also compared in Figure 4 with that reported by MacInnes and Belcher (17). Their plots show a definite curvature which is somewhat exaggerated in the plot. In their study the extrapolation was made on basis of the pK_{2A} vs. $\mu^{1/2}$ relationship. The pK_{2A}'s as seen in Table 8 and Figure 4 are independent of ionic strength and essentially fall within the value of $10.300 \pm .009$.

As the K^+ and carbonate concentrations are increased, the $KHCO_3^o$ form (Table 7) and $KHCO_3^o + KCO_3^-$ forms (Table 8) become increasingly important in the computation of K_{1A} and K_{2A}. Thus the $[HCO_3^-]$ in equation (1) and $[HCO_3^-]/[CO_3^{2-}]$ ratio in equation (2) cannot be the stoichiometric values. Admittedly, at low concentrations they will approach stoichiometry, but then the analytical techniques become the predominant error-producing factor.

MacInnes and Belcher (17) reported $K_{2A} = 5.69 \times 10^{-11}$ for the $KHCO_3$-K_2CO_3-KCl system and Harned and Scholes (13) $K_{2A} = 4.69 \times 10^{-11}$ for the $NaHCO_3$-Na_2CO_3-NaCl system. With the accounting for $KHCO_3^o$ and KCO_3^- and $NaHCO_3^o$ and $NaCO_3^-$, the K_{2A}'s become $K_{2A} = 5.00 \times 10^{-11}$ and $K_{2A} = 4.65 \times 10^{-11}$, respectively, and which thus improves the agreement in K_{2A}'s obtained with the two different types of carbonate systems.

A usual laboratory observation is that the pH of the K_2CO_3 solution is slightly higher than a similar concentration of Na_2CO_3 and this has been also documented in the literature

(16). The explanation generally accepted is simply that the K-carbonate hydrolyzes to a greater extent than the Na-carbonate and also to differences in the activity coefficients of K and Na ions. An examination of the dissociation constants of $KHCO_3^o$, KCO_3^-, $NaHCO_3^o$, and $NaCO_3^-$ forms, however, leads to a better alternative method to explain differences in solution pH. Since the association of K^+ with HCO_3^- and CO_3^{2-} is less than Na^+, the H^+ concentration is expected to be less in K- than Na-carbonate solution, and consequently, the pH of the K solution will be greater than that in the Na-carbonate solution.

PART IV. SODIUM SULFATE AND HYDROGEN SULFATE ION-PAIRS

The sulfate and sodium ions may be present in significant amounts in certain soil solutions, and surface and groundwaters. In this case Na^+ and also H^+ may associate with SO_4^{2-} to form the ion-pairs $NaSO_4^-$ and HSO_4^-. The dissociation constant for these forms can be determined in a manner similar to that presented in Parts II and III for $NaCO_3^-$ and HCO_3^- dissociation.

THEORETICAL:

The dissociation constants of HSO_4^- and $NaSO_4^-$ are determined simultaneously in the cell $Pt;H_2|NaHSO_4,NaCl,Na_2SO_4|AgCl;Ag$ and the relations

$$-\log \underline{K}_{HSO_4^-} = \frac{(\underline{E}-\underline{E}^o)\underline{F}}{2.303\underline{RT}} + \log \frac{[HSO_4^-][Cl^-]}{[SO_4^{2-}]} + \log \frac{\gamma_{Cl}\gamma_{HSO_4}}{\gamma_{SO_4}} \qquad (1)$$

$$\underline{K}_{NaSO_4^-} = \frac{(Na^+)(SO_4^{2-})}{(NaSO_4^-)} \qquad (2)$$

The mass balances for Na and SO_4 are, respectively

$$[Na]_T = [Na^+] + [NaSO_4^-] \qquad (3)$$

$$[SO_4]_T = [NaSO_4^-] + [SO_4^{2-}] + [HSO_4^-] \qquad (4)$$

and the charge balance is

$$[Na^+] + [H^+] = [HSO_4^-] + 2[SO_4^{2-}] + [HSO_4^-] + [Cl^-] \quad (5)$$

Equation (1) is solved for $K_{HSO_4^-}$ at different Na and SO_4 concentrations at various preselected values of $K_{NaSO_4^-}$ until $K_{HSO_4^-}$ remains constant for a specific $K_{NaSO_4^-}$ value.

Experimental. The electrometric measurements of Hamer (10) for the NaCl, $NaHSO_4$, Na_2SO_4 solution using the H_2 and Ag-AgCl electrodes without liquid junction at 25°C were used. Since the ionic strengths of the solutions were high, the Davies et al. (3) relation $\log \gamma = -Az^2\mu^{1/2}/(1 + \mu^{1/2}) - .2\ \mu$ was used instead of the extended Debye-Hückel equation for activity coefficient.

RESULTS AND DISCUSSION:

The component concentrations of the Na and SO_4 species are presented in Table 9. The dissociation constants obtained are $K_{HSO_4^-} = .0102 \pm .0003$ and $K_{NaSO_4^-} = .189$, which compare well with the value of $K_{HSO_4^-} = .0103$ reported by Davies et al. (3) and $K_{NaSO_4^-} = .190$ by Jenkins and Monk (14) using different experimental and computational procedures.

SUMMARY AND CONCLUSIONS:

Complete theoretical equations were developed and solved for predicting the pH's of carbonate systems in the presence and absence of external carbon dioxide source. The single salts and carbonate combinations of $NaHCO_3$-$CaCO_3$ and Na_2CO_3-$CaCO_3$ at CO_2 partial pressures from .03 to 1 atmosphere were included in the study. The equation developed here gives theoretical pH values comparable to the experimental results, whereas the simplified versions previously used fail particularly at the low carbonate concentrations. At high carbonate concentrations a large fraction of the total Ca exists in the nonionic ion-pair form.

Theoretical and computational methods were also initiated for determining the existence of Na-carbonate and -sulfate ion-pairs in solution and dissociation constants of carbonic acid ($K_{H_2CO_3}$) and bicarbonate ion ($K_{HCO_3^-}$). This treatment yielded simultaneously the dissociation constant of the ion-pair and its associated acid. In the case of the acid, the constant was independent of ionic strength or carbonate and sulfate concentrations and thus avoided the need and the uncertainty associated with extrapolation to zero ionic strength for obtaining the thermodynamic dissociation constants.

The dissociation constants at 25°C are as follows:

$K_{NaHCO_3^o} = .690$; $K_{NaCO_3^-} = .282$

$K_{KHCO_3^o} = .809$; $K_{KCO_3^-} = 1.18$

$K_{H_2CO_3} = 4.41 \times 10^{-7}$; $K_{HCO_3^-} = 4.61 \times 10^{-9}$

$K_{NaSO_4^-} = .189$; $K_{HSO_4^-} = .0103$

A comparison of the dissociation constants of Na- and K-carbonates indicates greater Na than K association with the carbonate and gives a good explanation as to why Na-carbonate solutions have lower pH's than K-carbonate solutions. The treatment developed here also improved the agreement of the $\underline{K}_{H_2CO_3}$ and $\underline{K}_{HCO_3^-}$ values obtained from the Na-carbonate and K-carbonate systems.

REFERENCES:

1. Bates, R. G. Determination of pH. Theory and Practice. John Wiley & Sons, Inc., N.Y. 1965. p. 24.

2. Butler, J. N. and Huston, R. Activity coefficients and ion-pairs in the systems $NaCl-NaHCO_3-H_2O$ and $NaCl-Na_2CO_3-H_2O$. Abst. 158th Natl. Meeting Amer. Chem. Soc., Div. Water, Air and Waste Chem., N.Y., Sept. 1969. pp. 113-114.

3. Davies, C. W., Jones, H. W., and Monk, C. B. E.M.F. studies of electrolytic dissociation, Part I. Sulfuric acid in water. Trans. Faraday Soc. 48:921-928. 1952.

4. Davis, R., Jr. The ionization constant of carbonic acid and the solubility of carbon dioxide in water and sodium chloride solution from 0° to 50°C. Unpub. Ph.D. Thesis. Yale Univ., New Haven, Conn. 1942.

5. Distèche, A. and Distèche, S. The effect of pressure on the dissociation of carbonic acid from measurements with buffered glass electrode cells. J. Electrochem. Soc. 114:330-340. 1967.

6. Garrels, R. M. and Christ, C. L. Solutions, Minerals and Equilibria. Harper and Row, New York. pp. 74-92. 1965.

7. Garrels, R. M. and Thompson, M. A chemical model for sea water at 25°C and one atmosphere total pressure. Amer. J. Sci. 260:57-66. 1962.

8. Garrels, R. M., Thompson, M., and Siever, R. Control of carbonate solubility by carbonate complexes. Amer. J. Sci. 259:24-45. 1961.

9. Gucker, F. T., Jr., and Meldrum, W. B. Physical Chemistry. American Book Company, N.Y. 1944. pp. 358-359.

10. Hamer, W. J. The ionization constant and heat of ionization of the bisulfate ion from electromotive force measurements. J. Amer. Chem. Soc. 56:860-864. 1934.

11. Harned, H. S. and Bonner, F. T. The first ionization of carbonic acid in aqueous solutions of sodium chloride. J. Amer. Chem. Soc. 67:1026-1031. 1945.

12. Harned, H. S. and Davis, R., Jr. The ionization constant of carbonic acid in water and the solubility of carbon dioxide in water and aqueous salt solutions from 0 to 50°, J. Amer. Chem. Soc. 65:2030-2037. 1943.

13. Harned, H. S. and Scholes, S. R., Jr. The ionization constant of HCO_3 from 0 to 50°. J. Amer. Chem. Soc. 63:1706-1709. 1941.

14. Jenkins, I. L. and Monk, C. B. The conductances of sodium, potassium and lanthanum sulfates at 25°. J. Amer. Chem. Soc. 72:2695-2698. 1950.

15. Kielland, J. Individual activity coefficients of ions in aqueous solutions. J. Amer. Chem. Soc. 59:1675-1678. 1937.

16. Lortie, L. and Demer, P. Physico-chemical studies of alkaline carbonates. I. Studies of the activity of hydrogen ions in aqueous solutions of alkali carbonates. Canadian J. Res. 18:160-167. 1940.

17. MacInnes, D. A. and Belcher, D. The thermodynamic ionization constant of carbonic acid. J. Amer. Chem. Soc. 55:2630-2646. 1933.

18. Näsänen, R. The second dissociation constant of carbonic acid in NaCl and KCl solutions. Suom. Kemistibehti B. 19:89-93. 1946.

19. Ponnamperuma, F. N. A theoretical study of aqueous carbonate equilibria. Soil Sci. 103:90-100. 1967.

20. Turner, R. C. A theoretical treatment of the pH of calcareous soils. Soil Sci. 86;32-34. 1958.

PERSONNEL: F. S. Nakayama and B. A. Rasnick

CURRENT TERMINATION DATE: August 1974

Table 1

Calcium constituents of $CaCO_3$-Na_2CO_3-CO_2 system: $P_{CO_2} = 3.5 \times 10^{-4}$ atm.

$[Na_2CO_3]$	pH	Ca total	$[Ca^{2+}]$	$[CaHCO_3^+]$	$[CaCO_3^o]$	$[CaOH^+]$	Fraction $[Ca^{2+}]$
M		M	M	M	M	M	
1	10.58	3.22×10^{-7}	6.80×10^{-10}	1.96×10^{-10}	3.21×10^{-7}	2.01×10^{-12}	2.11×10^{-3}
1×10^{-1}	9.94	9.51×10^{-7}	5.89×10^{-9}	1.92×10^{-9}	9.43×10^{-7}	5.67×10^{-12}	6.20×10^{-3}
1×10^{-2}	9.39	5.87×10^{-6}	2.17×10^{-7}	3.30×10^{-8}	5.62×10^{-6}	8.98×10^{-11}	3.69×10^{-2}
1×10^{-3}	8.60	1.57×10^{-4}	7.85×10^{-5}	2.49×10^{-6}	7.61×10^{-5}	6.75×10^{-9}	4.99×10^{-1}
1×10^{-4}	8.34	5.13×10^{-4}	3.89×10^{-4}	6.94×10^{-6}	1.17×10^{-4}	1.87×10^{-8}	7.59×10^{-1}
1×10^{-5}	8.32	5.70×10^{-4}	4.43×10^{-4}	7.50×10^{-6}	1.19×10^{-4}	2.02×10^{-8}	7.77×10^{-1}
1×10^{-6}	8.31	5.76×10^{-4}	4.49×10^{-4}	7.56×10^{-6}	1.20×10^{-4}	2.04×10^{-8}	7.79×10^{-1}
1×10^{-7}	8.31	5.77×10^{-4}	4.50×10^{-4}	7.56×10^{-6}	1.20×10^{-4}	2.04×10^{-8}	7.79×10^{-1}

Table 2

Carbonate constituents and activity coefficients of $CaCO_3$-Na_2CO_3-CO_2 system:

$P_{CO_2} = 3.5 \times 10^{-4}$ atm.

$[Na_2CO_3]$ M	$[HCO_3^-]$ M	$[CO_3^{2-}]$ M	$\gamma_{Ca^{2+}}$	$\gamma_{HCO_3^-}$	$\gamma_{CO_3^{2-}}$	γ_{H^+}	γ_{OH^-}
1	1.02×10^{-1}	9.48×10^{-1}	.1594	.5390	.1028	.7112	.5084
1×10^{-1}	6.13×10^{-2}	6.95×10^{-2}	.3003	.6966	.2524	.7827	.6833
1×10^{-2}	1.48×10^{-2}	2.61×10^{-4}	.5806	.8632	.5618	.8840	.8605
1×10^{-3}	2.21×10^{-3}	4.87×10^{-5}	.8124	.9479	.8086	.9512	.9475
1×10^{-4}	1.19×10^{-3}	1.39×10^{-5}	.8446	.9577	.8420	.9599	.9574
1×10^{-5}	1.13×10^{-3}	1.24×10^{-5}	.8453	.9579	.8427	.9601	.9576
1×10^{-6}	1.12×10^{-3}	1.23×10^{-5}	.8453	.9579	.8427	.9601	.9576
1×10^{-7}	1.12×10^{-3}	1.23×10^{-5}	.8453	.9579	.8427	.9601	.9576

Table 3. First Dissociation Constant of Carbonic Acid at Different Bicarbonate Concentrations and Ionic Strengths at 25°C.[a/]

	$[NaHCO_3]=[NaCl]$, M×10²	E, V	I, ×10²	$-\log K_{1A}$	$-\log K_S$	pH	$[Na^+]$, M×10²	$[HCO_3^-]$, M×10²	$[NaHCO_3^o]$, M×10³
(A)	.2182	.67236	.436	6.356	6.354	5.248	.435	.218	.012
	.3951	.67271	.787	6.364	6.360	5.502	.786	.392	.038
	.7177	.67243	1.424	6.361	6.355	5.744	1.424	.706	.117
	2.859	.67209	5.572	6.363	6.350	6.295	5.572	2.713	1.46
	3.687	.67192	7.144	6.362	6.347	6.392	7.144	3.457	2.30
	10.391	.67106	19.42	6.360	6.332	6.779	1.942	9.037	13.5
(B)	.4271	.66438	.850	6.355	6.350	5.484	.850	.423	.044
	.6684	.66460	1.327	6.360	6.353	5.673	1.327	.658	.102
	1.005	.66433	1.988	6.357	6.349	5.835	1.988	.983	.218
	1.646	.66427	3.238	6.358	6.348	6.034	3.238	1.592	.540
	2.360	.66423	4.616	6.360	6.347	6.177	4.616	2.256	1.04
	3.137	.66382	6.102	6.355	6.340	6.283	6.102	2.965	1.72
(C)	.4271	.69075	.850	6.358	6.355	5.685	.850	.423	.041
	.6684	.69079	1.327	6.360	6.355	5.871	1.327	.659	.096
	1.005	.69046	1.990	6.356	6.350	6.032	1.989	.985	.205
	1.646	.69050	3.241	6.359	6.350	6.232	3.241	1.595	.509
	2.360	.69034	4.622	6.358	6.348	6.373	4.622	2.262	.978
	3.137	.69025	6.111	6.359	6.346	6.484	6.111	2.974	1.63

A: 78.8% CO_2 - 22.2% H_2, $K_{NaHCO_3^o}$ = .677

B: 84.4% CO_2 - 14.6% H_2, $K_{NaHCO_3^o}$ = .679

C: 54.58% CO_2 - 45.42% H_2, $K_{NaHCO_3^o}$ = .722

(a) Data in columns 1 and 2 from Harned and Davis (12) and in column 5 from Davis (4).

Table 4. First Dissociation Constant Carbonic Acid in 0.1 M NaCl and varying Bicarbonate Concentrations at 25°C.[a/]

	$[NaHCO_3]$, M×10^2	E, V	μ, ×10^1	$-\log K_{1A}$	$-\log K_S$	pH	$[Na^+]$, ×10^1	$[HCO_3^-]$, ×10^2	$[NaHCO_3^o]$, ×10^3
(A)	.5035	.61238	1.045	6.378	6.117	5.656	1.045	.4455	.58
	.7478	.62234	1.066	6.375	6.112	5.824	1.066	.6601	.88
	1.000	.62994	1.088	6.378	6.113	5.951	1.088	.8809	1.19
	1.497	.64105	1.131	6.376	6.108	6.122	1.131	1.314	1.84
	1.999	.64765	1.175	6.378	6.107	6.247	1.175	1.747	2.52
	2.994	.65781	1.260	6.376	6.099	6.415	1.260	2.598	3.96
(B)	.5035	.61217	1.045	6.370	6.115	5.652	1.045	.4513	.52
	.7478	.62245	1.066	6.372	6.116	5.824	1.067	.6689	.79
	1.000	.62978	1.089	6.370	6.112	5.947	1.089	.8927	1.07
	1.497	.64019	1.133	6.372	6.110	6.121	1.133	1.332	1.65
	1.999	.64768	1.177	6.374	6.109	6.246	1.177	1.772	2.27
	2.994	.65772	1.264	6.369	6.099	6.412	1.264	2.636	3.58

A: 751.8 mm Hg b.p., $K_{NaHCO_3^o} = .469$

B: 755.8 mm Hg b.p., $K_{NaHCO_3^o} = .528$

(a) Data in columns 1, 2, and 5 from Harned and Bonner (11) for 2 of 4 series; 44.09% H_2, 55.91% CO_2.

Table 5. Dissociation Constant of $NaHCO_3^o$ in $NaCl-CO_2$ System at 25°C ($\underline{K}_{1A} = 4.41 \times 10^{-7}$).

[NaCl] $\underline{M}x10^1$	pH	P_{CO_2}, atm	μ, $x10^1$	$\underline{K}_{NaHCO_3^o}$	$[Na^+]$, $\underline{M}x10^1$	$[NaHCO_3^o]$, $\underline{M}x10^5$	$[H^+]$, $\underline{M}x10^4$	$[HCO_3^-]$, $\underline{M}x10^4$
.25	3.906	.9198	.251	.226[a/]	.2499	1.06	1.4090	1.3028
.50	3.896	.9219	.501	.286	.4998	1.55	1.4878	1.3323
.75	3.886	.9218	.751	.292	.7498	2.14	1.5526	1.3382
1.00	3.880	.9236	1.001	.320	.9998	2.49	1.5965	1.3475
1.25	3.873	.9217	1.251	.323	1.2497	2.95	1.6405	1.3450
1.50	3.866	.9202	1.501	.319	1.4997	3.45	1.6822	1.3373

(a) Not used in computing average $\underline{K}_{NaHCO_3^o} = .308 \pm .018$.

Table 6. Dissociation Constant of HCO_3^- at 25°C Based on the Presence of $NaHCO_3^o$ and $NaCO_3^-$ Species.[a/]

[NaCl] = $[Na_2CO_3]$, M x 10^2	$[NaHCO_3]$, M x 10^2	E, V	μ, x10^1	-log K_{2A}	pH	$[Na^+]$, M x 10^1	$[NaHCO_3^o]$, M x 10^3	$[NaCO_3^-]$, M x 10^3	$[HCO_3^-]$, M x 10^2	$[CO_3^{2-}]$, M x 10^2
.3940	.3956	.96680	.1926	10.335	10.119	.1559	.069	.118	.4037	.3671
.5606	.5628	.95746	.2733	10.338	10.104	.2209	.132	.220	.5645	.5237
.5821	.5843	.95647	.2837	10.339	10.102	.2293	.141	.235	.5851	.5437
1.156	1.160	.93700	.5571	10.335	10.047	.4504	.482	.750	1.126	1.067
1.660	1.666	.92693	.7930	10.341	10.019	.6419	.913	1.355	1.588	1.511
2.230	2.239	.91302	1.056	10.250	9.899	.8559	1.525	2.172	2.097	2.002
2.620	2.630	.91808	1.233	10.417	10.047	1.001	2.018	2.794	2.443	2.326
3.241	2.254	.90620	1.514	10.321	9.929	1.230	2.901	3.892	2.975	2.840

(a) $K_{NaHCO_3^o} = .690$; $K_{NaCO_3^-} = .282$, Data in columns 1 to 3 from Harned and Scholes (13).

Table 7. Dissociation constant H_2CO_3 and constituent concentrations in $KHCO_3$-KCl system at 25°C ($\underline{K}_{KHCO_3^o}$ = .809).

[KCl] = [$KHCO_3$], $\underline{M}x10^2$	μ $x10^2$	-log $\underline{K}_{H_2CO_3}$	pH	[K^+] $\underline{M}x10^2$	[HCO_3^-] $\underline{M}x10^2$	[$KHCO_3^o$] $\underline{M}x10^4$
.1090	.2192	6.348	4.846	.2177	.1102	.027
.1810	.3622	6.352	5.060	.3613	.1812	.071
.2140	.4278	6.356	5.138	.4270	.2138	.098
.2329	.5051	6.355	5.203	.5045	.2522	.135
.3407	.6795	6.353	5.329	.6790	.3588	.238
.5545	1.103	6.350	5.527	1.103	.5488	.601
1.065	2.110	6.353	5.794	2.110	1.045	2.04
1.064	2.108	6.354	5.794	2.108	1.044	2.03
1.072	2.124	6.353	5.795	2.123	1.052	2.06
1.075	2.129	6.354	5.798	2.129	1.054	2.07
2.010	3.955	6.355	6.049	3.955	1.945	6.51
3.097	6.053	6.353	6.212	6.053	2.956	14.11
5.030	9.730	6.352	6.400	9.730	4.700	32.99

Table 8. Dissociation constant HCO_3^- and constituent concentration in $KHCO_3$-K_2CO_3-KCl system at 25°C (K_{KHCO_3} = .809, $K_{KCO_3^-}$ = 1.18).

[KCl], M x 10^2	[$KHCO_3$], M x 10^2	[K_2CO_3], M x 10^2	μ x 10^1	-log $K_{HCO_3^-}$	pH	[K^+], M x 10^2	[HCO_3^-], M x 10^2	[CO_3^{2-}], M x 10^2	[$KHCO_3^o$], M x 10^4	[KCO_3^-], M x 10^4
.2512	.2512	.2201	.1146	10.281	10.039	.9391	.2610	.2068	.24	.11
.4447	.4451	.4403	.2182	10.291	10.078	1.760	.4516	.4229	.73	.36
.5704	.5704	.4999	.2608	10.306	10.034	2.125	.5721	.4826	1.09	.47
.6276	.6282	.6214	.3079	10.303	10.072	2.478	.6284	.6009	1.37	.65
.9412	.9420	.9318	.4610	10.307	10.050	3.705	.9272	.9051	2.84	1.31
1.154	1.154	1.011	.5259	10.304	9.986	4.275	1.127	.9833	3.89	1.58
1.358	1.358	1.190	.6181	10.312	9.981	5.023	1.318	1.157	5.20	2.07
1.593	1.594	1.577	.7707	10.309	10.010	6.237	1.535	1.532	7.21	3.16
3.001	3.001	2.630	1.352	10.297	9.896	10.980	2.804	2.544	20.75	7.55
4.718	4.718	4.134	2.107	10.295	9.851	17.100	4.281	3.970	44.68	15.42

Table 9. Sodium and sulfate constituents of the $NaHSO_4$-Na_2SO_4-NaCl system. ($K_{NaSO_4^-} = .189$)

[NaCl] = [$NaHSO_4$]	[Na_2SO_4]	μ	$K_{HSO_4^-}$	pH	[Na]	[$NaSO_4^-$]	[HSO_4^-]	[SO_4^{2-}]
$M\times10^2$	$M\times10^2$	$M\times10^1$	$M\times10^2$		$M\times10^1$	$M\times10^3$	$M\times10^2$	$M\times10^2$
.09713	.09798	.0655	1.02	3.102	.03876	.00264	.0108	.1816
.1947	.1957	.1280	1.04	2.844	.07719	.00892	.0338	.3477
.2926	.2956	.1890	1.01	2.703	.1158	.0179	.0656	.5048
.4871	.4913	.3059	1.01	2.532	.1915	.0414	.140	.7970
.6815	.6874	.4194	1.01	2.424	.2667	.0709	.226	1.0718
.9724	.9776	.5841	1.02	2.311	.3776	.124	.367	1.4594
1.957	1.968	1.1187	1.04	2.097	.7489	.360	.912	2.6527
2.931	2.946	1.6257	1.09	1.971	1.1092	.662	1.49	3.7244
4.975	5.018	2.6274	1.07	1.826	1.8536	1.45	2.89	5.6532
6.934	6.994	3.5144	.97	1.757	2.5512	2.34	4.44	7.1412

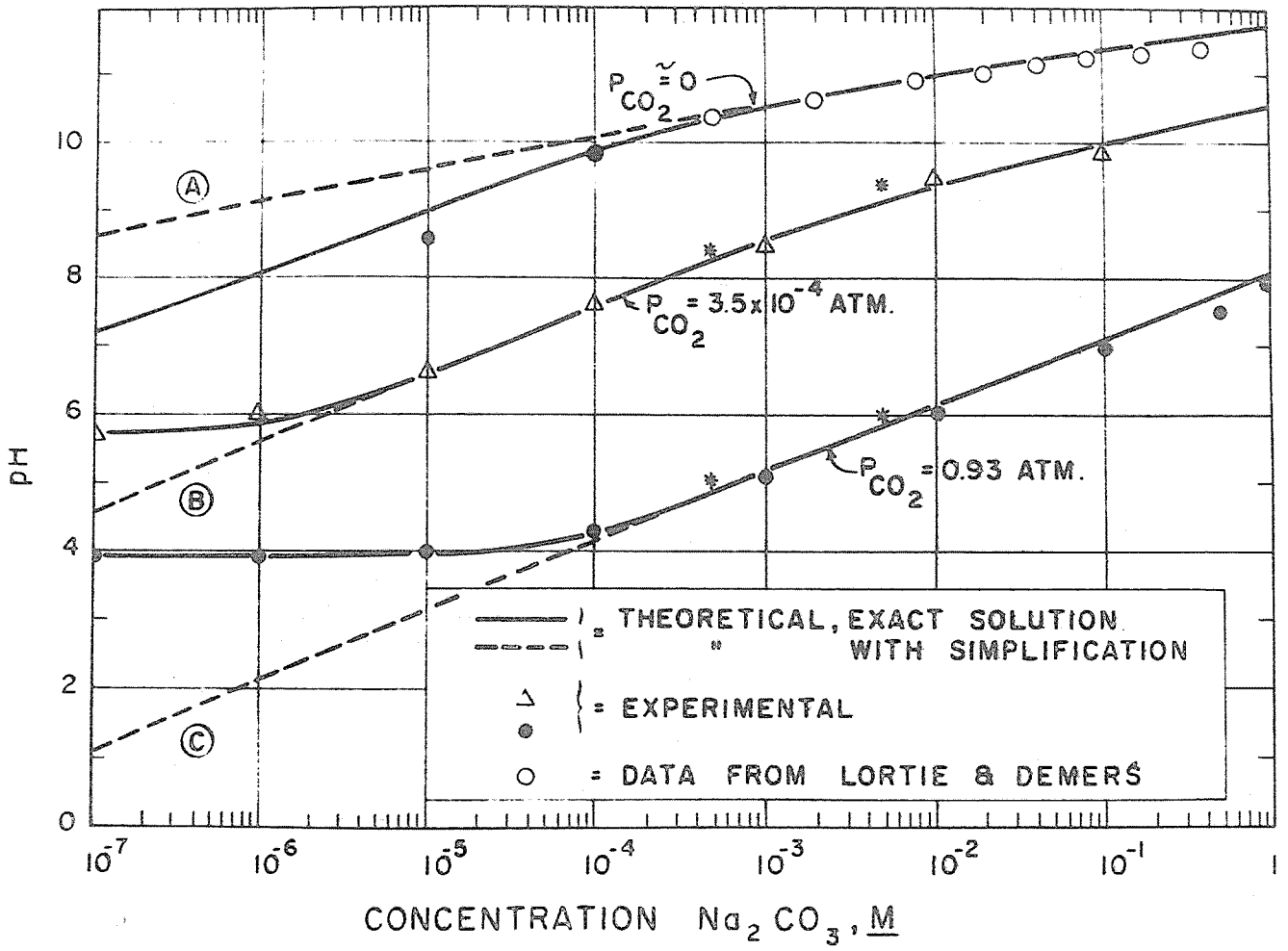

Figure 1. Comparison of theoretical and experimental pH values for Na_2CO_3 solutions at different CO_2 partial pressures (See text for description of asterisks).

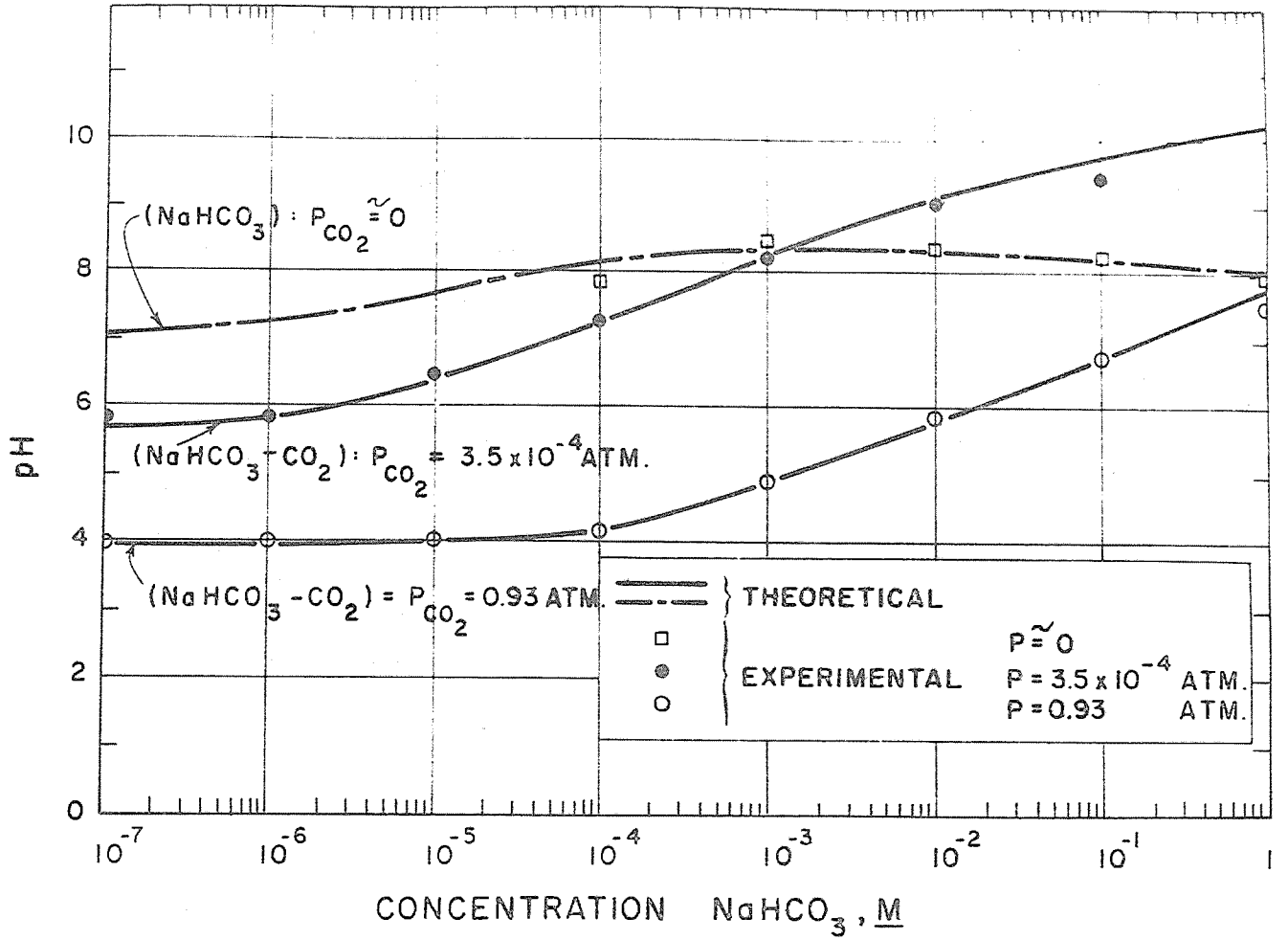

Figure 2. Comparison of theoretical and experimental pH values for $NaHCO_3$ solutions at different CO_2 partial pressures.

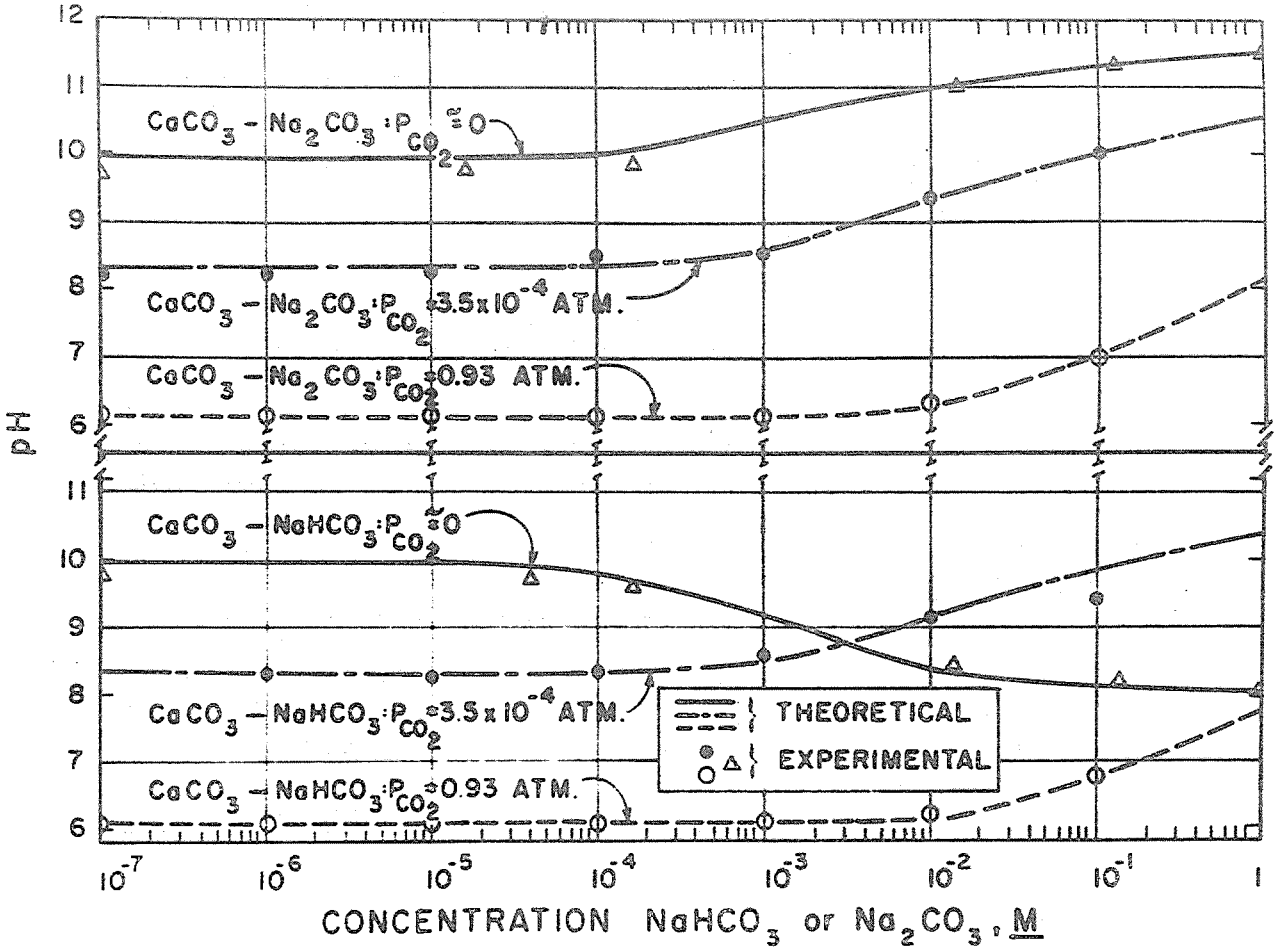

Figure 3. Comparison of theoretical and experimental pH values for the $CaCO_3$-Na_2CO_3 and $CaCO_3$-$NaHCO_3$ combinations at different CO_2 partial pressures.

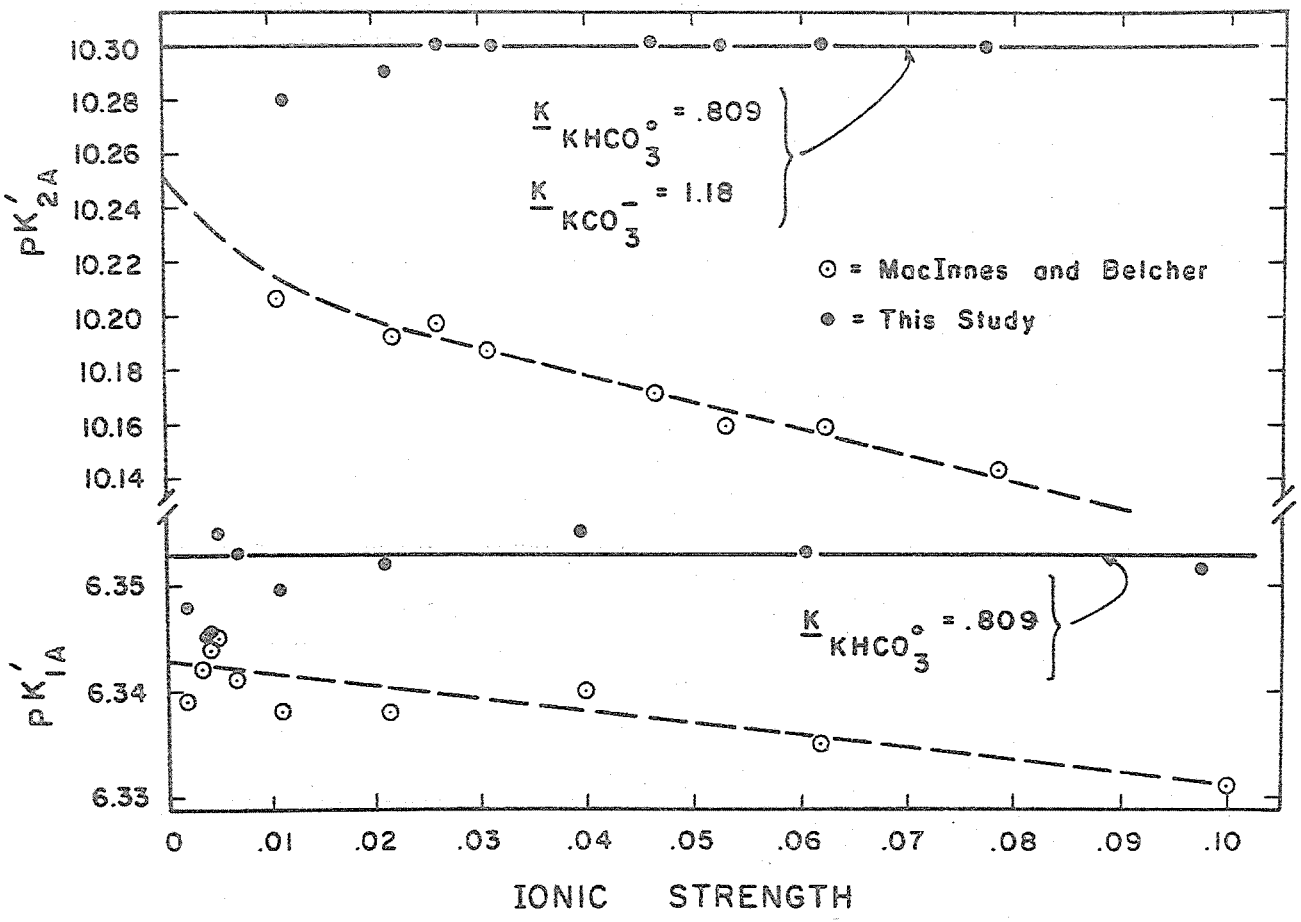

Figure 4. First and second dissociation constants of carbonic acid as related to ionic strength and K-carbonate ion-pairs in the $KHCO_3$-KCl-CO_2 and $KHCO_3$-K_2CO_3-KCl systems at 25°C.

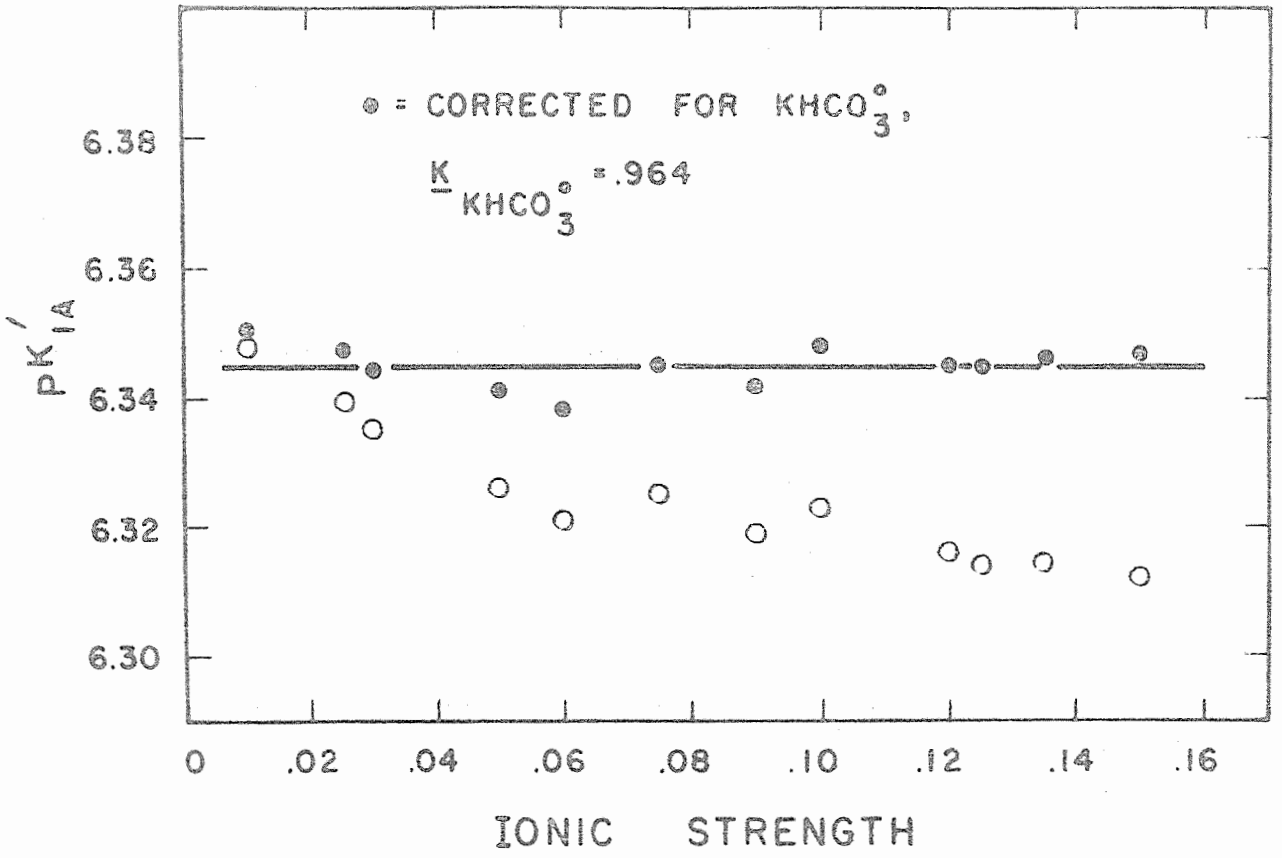

Figure 5. First dissociation constant of carbonic acid in the H_2CO_3-KCl system at 25°C.

TITLE: MATERIALS AND METHODS FOR WATER HARVESTING AND WATER STORAGE IN THE STATE OF HAWAII

CRIS WORK UNIT: SWC-018-gG-2 CODE NO.: Ariz.-WCL 65-2

INTRODUCTION:

A description of the Maui and Hawaii water harvesting test facilities is given in previous Annual Reports. Both sites were inspected in June 1969. The Maui site was revisited in September 1969 at which time a new water measuring system was installed on all plots including the Hypalon sheeting plot. The asphalt plot was covered with asphalt-fiberglass and an experimental ditch lining of asphalt-fiberglass was installed.

PROCEDURE:

The system for measuring water collected by the Maui plots was changed from the critical depth flumes and water stage recorders to a combination of two rotary-turbine, recording water meters, 1 inch and 2 inch diameter, connected in parallel. The original critical depth flumes, with an aluminum bulkhead bolted to the discharge end, act as a head box for the meters. Outlets are at the bottom and 4 inches above the bottom of the V-shaped headbox for the 1 and 2-inch meters respectively. Low flows are measured by the small meter and both meters operate to handle high flows. The meters are connected to 3 inch plastic drain lines which run to a ditch at the edge of the test area. By dropping the ends of the discharge lines approximately 18 inches down into the ditch, with an elbow on the lower end to cause the pipe to run full, a total discharge head of approximately 4 feet was obtained to operate the meters. All meters were precalibrated in pairs at the Laboratory using a full scale mock-up. Over a flow range of 40 to 200 liters min^{-1}, which is the flow range previously recorded by the flumes, the maximum measurement error of the two-meter system was $\pm$ 2 percent.

A detailed description of the retreatment of the asphalt plot and the installation of the experimental ditch lining with asphalt fiberglass is given in the Annual Report section titled "Fabricated-in-Place, Reinforced Reservoir Linings." The lined ditch section was 100 feet long and had a perimeter of 24 feet. The area is heavily infested with a sedge commonly called nutgrass. The ditch had been scraped and, prior to lining, polyborachlorate was spread on the soil and sprinkled with water to carry the sterilant into the soil surface.

The recording raingage at the plots was replaced with a 550 mm capacity storage raingage. The water meters and raingages are read at monthly intervals by East Maui Irrigation Company personnel and the data forwarded to the U. S. Water Conservation Laboratory for evaluation.

RESULTS AND DISCUSSION:

Kukaiau Catchment. The storage reservoir was full and the reservoir lining material was in excellent condition when inspected in June 1969. The catchment material is still intact but more of the seams are showing signs of possible failure. A few holes, about 2 to 5 mm in diameter, are developing in the sheeting. For the period of 1 January 1969 through 31 December 1969 a total of 4033 mm of rainfall was recorded. During the year a total of approximately 10 million liters of water was collected from the combined catchment and reservoir. This is sufficient water for 200 head of cattle for a full year.

Maui Catchments. For a description of the plots, see previous Annual Reports. Inspection in September 1969 revealed that several seams on the Hypalon sheeting Plot No. 1, were starting to fail. It was found the sheeting's tear resistance in the longitudinal direction was quite low. Longitudinal tear resistance was not checked prior to original installation and so is not known whether

the existing low tear resistance is a result of deterioration or a result of the manufacturing process. The sheeting showed no other signs of deterioration.

Plot No. 2 covered with butyl sheeting showed no visible changes over the past year. Retention of water by cross-slope wrinkles in the sheeting is a definite undesirable factor.

The two-phase asphalt treatment on Plot No. 3 has lasted much longer than was originally expected. In June 1969, grass encroachment from the plot edges was considered to be a serious problem and there were a few plants growing on the interior of the plot. Prior to installation of asphalt-fiberglass in September, the grass was cut down to the plot surface. With removal of the grass it was found that the plot was in good condition. The damaged portions of the pavement could have been easily repaired. It is now apparent that the plant growth problem was not serious and could have been corrected by a small amount of maintenance. Deterioration of the pavement surface occurred at a much lower rate than has been experienced on similar test plots in Arizona.

Analysis of the runoff data collected from the critical-depth flumes is not completed. A partial summary of the runoff by weeks for the period 13 February 1968 to 4 July 1968 is presented in Table 1. The weeks of 7 March and 17 April to 14 May are not included in the table. During the week of 7 March, 318 mm of rainfall was recorded but the measured runoff from the two treated plots was unquestionably in error. It is believed that runoff occurred for sufficient time to completely exhaust the batteries on the water-stage recorder clocks, making them inoperative at the end of the week. The totals in Table 1 do not include the period 17 April to 14 May 1968 when the raingage was inoperative.

For the 5 month period represented in Table 1 when all equipment was operative, a total of 564 mm of rainfall was recorded. The

rainfall runoff in percent was: butyl 88, asphalt 91 and grass 13. Water was retained by grass on the asphalt plot and there was some seepage loss through patches for deteriorated asphalt. As previously mentioned, water was retained in cross-slope wrinkles on the butyl plot. The data emphasize the desirability of eliminating any form of retention in catchments made from any type of material.

The weekly rainfall totals are relatively high but weekly rainfall occurs in from 5 to 50 individual storms consisting primarily of light showers. Most individual storms precipitate less than 3 mm of rain. As an example, rainfall totalling 40.6 mm during the week of 6 June 1969 fell in 30 individual storms as follows.

Rainfall in mm	No. of Storms
0.0 - 0.5	9
0.5 - 1.0	4
1.0 - 2.0	9
2.0 - 3.0	5
3.0 - 4.0	3

Analysis of rainfall vs. runoff is difficult for small rains because of measurement accuracy. The recording raingage charts can only be read to $\pm$ 0.2 mm, for example. Despite these errors, examination of data collected to date indicates that both the asphalt and butyl plots can collect essentially 100 percent of the water from small rain showers when retention of water on the plot is eliminated.

Data from the plots since installation of the new water measuring system is limited. Preliminary analysis shows the system is working. This system reduced labor of instrument reading and maintenance by more than 75 percent. The old system required weekly changing of four recorder charts, plus changing batteries and other maintenance, in order to obtain rainfall and runoff records for individual storms. Reasonably adequate information of this type has been obtained. The

new system requires reading eight meter dials and one storage rain-gage once a month, and maintenance should be limited to cleaning trash screens. Monthly rainfall and runoff totals will be sufficient for continued evaluation of catchment performance.

Experimental Ditch Lining. The experimental asphalt fiberglass ditch lining was installed to evaluate the flexible membrane lining in an area where nutgrass is a problem. The site selected had a heavy growth of nutgrass. The growing tip of the plant is sharp and is capable of penetrating many materials. Within two days after installation of the lining, the grass was starting to grow through. Three months after installation, a large number of plants 2 to 6 inches tall had grown through the lining. It is hoped that water seeping through holes made by the grass in the lining will carry the sterilant to the plant roots and kill the grass. The top growth of the plants can then be burned off and a sealcoat applied to make an impermeable lining.

SUMMARY AND CONCLUSIONS:

The Kukaiau catchment and storage unit on the island of Hawaii was in excellent condition when inspected in June 1969. Rainfall records from the site during the year show approximately 10 million liters of water was collected from the unit. This is sufficient water for 200 head of cattle for a full year.

Preliminary analysis of runoff data collected from the Maui test plots for the period of 13 February 1968 to 4 July 1968 when all equipment was operative, show rainfall runoff in percent was: butyl 88, asphalt 91 and grass 13, from a total rainfall of 472 mm. Water retention in cross-slope wrinkles is a problem on the butyl plot. Examination of runoff on an individual storm basis shows the treatments can be effective in collecting water from light showers.

New water measuring systems using two turbine-type water meters connected in parallel were installed on all four Maui plots in September 1969. This system reduced maintenance requirements and gives quantitative monthly rainfall and runoff data.

An experimental lining of asphalt-fiberglass was installed in an operational ditch. Nutgrass started growing through the lining within two days after installation. It is hoped that soil sterilant applied under the lining will eventually kill the grass, permitting it to be burned off. A final sealcoat will then be applied to the lining.

PERSONNEL: L. E. Myers and G. W. Frasier.

CURRENT TERMINATION DATE: December 1970.

Table 1. Rainfall runoff by weeks from 15 × 24 meter plots at the Maui test site.

Date	Total rainfall	Butyl Plot runoff		Asphalt Plot runoff		Grass Plot runoff	
1968	mm	mm	%	mm	%	mm	%
13 Feb	33.5	29.3	87.5	29.9	89.3	0	0
21 Feb	10.9	10.7	98.2	10.4	95.4	0	0
1 Mar	61.5	52.8	85.9	46.0	74.8	9.5	15.5
17 Mar [1/]	8.9	10.6	119.1	7.9	88.8	0	0
21 Mar	88.9	80.1	90.1	83.5	93.9	25.0	28.1
29 Mar	33.5	29.4	87.8	27.3	81.5	0	0
4 Apr	47.0	30.4	64.7	49.5	105.3	10.3	21.9
11 Apr	58.4	42.5	72.8	48.2	82.5	17.1	29.3
14 May	6.4	6.2	96.9	5.3	82.8	0	0
23 May	11.6	12.6	108.6	12.2	105.2	0	0
31 May	0.8	1.6	200.0	1.3	162.5	0	0
6 Jun	40.6	43.7	107.6	39.9	98.3	0	0
14 Jun	49.0	41.6	84.9	49.4	100.8	0	0
21 Jun	18.8	18.9	100.5	16.5	87.8	0	0
27 Jun	2.5	3.1	124.0	2.3	92.0	0	0
	472.3	413.5 [2/]	87.6	429.6 [2/]	91.0	61.9 [2/]	13.1

1/ The week of 7 Mar omitted because of battery failure on waterstage recorders. Rainfall for week was 317.5 mm.

2/ Does not include runoff for period of 17 Apr to 14 May.

TITLE: PHYSICAL AND CHEMICAL CHARACTERISTICS OF HYDROPHOBIC SOILS

CRIS WORK UNIT: SWC-018-gG-2 CODE NO.: Ariz.-WCL 67-2

PART I. BONDING OF ORGANIC MOLECULES TO INORGANIC SOIL AND CLAY SURFACES

INTRODUCTION:

The surfaces of the crystalline and amorphous inorganic constituents of soil are extremely active chemically and are capable of adsorbing organic molecules through a variety of bonding sites and mechanisms. Bonding between organics and these inorganics may be classified as being either physical or chemical, the former denoted by low adsorption energies compared to the strong chemical bond. The physical bonds range from weak, nonspecific London dispersion, to H-bonding, to permanent dipole-exchangeable cation interaction types. Chemical bonds are of two types: (1) organic-inorganic cation exchange (including acid-base neutralization), and (2) covalent bonding.

To permanently alter the physical and chemical properties of a soil by coating its surfaces with organic materials, the materials must remain adsorbed under the prevailing environmental conditions. This stringent, but academic requirement normally precludes the weak, physically bonded organic monomer units from consideration, and permits a focus of attention in the search either toward monomers capable of chemically bonding to the soil surfaces, or else toward polymeric organics with strong adhesive characteristics derived from multi-bonding sites per polymer unit.

The overall objective of the present phase of the study is to quantitatively characterize the bonding between organic monomers and inorganic-soil and -clay surfaces.

OBJECTIVES:

The specific objectives of the present work phase of Part I are to (1) establish the presence of chemical bonding between

certain organic molecules and inorganic-clay and -soil surfaces, (2) determine the functional groups involved, (3) locate the active sites on the inorganic phase, and (4) compare hydration properties of the untreated and treated inorganic surfaces in hopes of finding treatments which significantly lower the surface energy of the inorganic phase.

EQUIPMENT:

Adsorption isotherms can be used to differentiate between physical and chemical bonding; under specific conditions they can be used to locate the active adsorbing sites; and they are uniquely well suited to evaluate and compare the hydration properties of surfaces having radically different free energies. The first procedural step thus was to design and build a suitable apparatus for running adsorption isotherms.

The adsorption apparatus presently in use is diagramed in Figure 1. In essence, it consists of three integrated systems: a gas flow system, an electro-balance, and a temperature controlling system.

A gas flow system was selected for controlling the relative vapor pressure of the adsorbate phase rather than the more conventional vacuum system primarily because some means was needed to continually flush the contemplated, reactive gases away from the electronics of the electro-balance.

Bottled nitrogen gas which serves as the carrier (N_2 at room temperature is essentially non-reactive, non-adsorbing) is split into three lines: the N_2 in line I is saturated with the vapor of the adsorbate phase as it passes through the three bubblers; the N_2 of line II serves strictly as a dilutent; line III serves to keep reactive adsorbate gases and reaction products out of the balance chamber. The gases from lines I and II are combined, then flowed past the adsorbent sample which is suspended from the balance. Relative vapor pressure of the gas flowing past the

sample is controlled by regulating the relative flow rates of N_2 in lines I and II with the two needle valves.

The actual flow rate in each of these two lines is determined by measuring the pressure drop (ΔP_I and ΔP_{II}) across the two glass capillaries using water manometers read with a cathetometer, then, relating this ΔP to flow with a previously obtained calibration equation. Gas flows for lines I and II can be determined with less than 2% error throughout the range of 1 to 100 ml per minute. A computer program has been prepared which gives the relative vapor pressure of the adsorbate phase using input data of ΔP_I, ΔP_{II}, the atmospheric pressure, and the saturation vapor pressure of the adsorbate gas phase at the temperature of the water bath.

The equation describing the relative vapor pressure of the gas flowing past the adsorbent sample is:

$$P/P_o = \frac{ZQ_I}{Q_{II} + ZQ_I} = \frac{Zf(\Delta P_I)}{f(\Delta P_{II}) + Zf(\Delta P_I)}$$

where P/P_o is the relative vapor pressure, Q_I and Q_{II} are the flow rates of the dry N_2 gas in the two lines, $f(\Delta P)$ represents the calibration equations relating gas flow to pressure drop across the two capillaries, and Z is a correction term describing the pick up of vapor as the N_2 passes through the bubblers:

$$Z = P_a/(P_a - P_o)$$

where P_a is the atmospheric pressure and P_o is the saturation vapor pressure at the temperature of the bath.

The system as presently designed should be able to use most adsorbates which are liquids at atmospheric pressure and at or within the temperature range limits of the temperature bath

(presently 0-50° C), and whose saturation vapor pressures (P_o) are approximately within the limits of 1 to 400 mm Hg. The primary limitation is that the saturation vapor pressure P_o of the liquid be low enough to obtain relative vapor pressures (P/P_o) down to or even below $P/P_o = 0.05$.

The balance is a Cahn RG Electrobalance which has a sensitivity capability as great as 10^{-7} gram. This roughly corresponds to a monolayer of water covering an area only 6 centimeters squared. The balance as presently used can accomodate samples as large as 1 gram, and can detect weight changes as large as 0.2 gram. This wide range permits considerable latitude in sample selection. The temperature bath, which was designed and built at this laboratory can control temperature to better than 0.02° C.

RESULTS:

The apparatus is still in a testing phase; therefore, the results reported here are strictly preliminary in nature. Adsorption isotherms and their respective BET plots for water on two soil materials appear in Figures 2 and 3. The adsorption plots are typical Type II isotherms (1), thus permitting them to be used for BET surface area determination (2).

The BET equation is normally written in the form:

$$\frac{X}{W(1 - X)} = \frac{1}{CW_m} + \frac{C - 1}{CW_m} X$$

where $X = P/P_o$, W is the weight of adsorbate adsorbed at a respective P/P_o, W_m represents the weight of adsorbate necessary to form a monolayer and C relates to the net heat of adsorption of the adsorbate on the adsorbent. For Type II isotherms, plots of $X/W(1 - X)$ versus X will normally produce a straight line portion over part of the P/P_o range of 0.05 - 0.5, from which C and W_m may be obtained from the slope and intercept.

For the Na-Otay bentonite in Figure 2: $C = 4.2$ and $W_m = 92.6$ mg/g. Using $14.8A^2$/molecule (1) as the surface area of a water molecule, and then assuming each water molecule in interlayer position is associated with two adjacent surfaces, and that the external surface area on this clay is 50 m^2/g, the internal surface area becomes 816 m^2/g.

For the Lloyd soil in Figure 3: $C = 8.2$ and $W_m = 10.6$ mg/g. This represents a surface area of 52.5 m^2/g, assuming that this soil has no 2:1 type expandable clay.

SUMMARY:

An adsorption isotherm apparatus has been built to study the bonding of organic molecules to soil and clay materials. The apparatus was designed to handle highly reactive as well as the relatively inert adsorbates; it can be used for BET surface area determination, and it can be used for studying bonding energies, as well as soil surface energies before and after treatment with organic coatings. The system can handle most adsorbates which are liquid at standard temperatures and pressures. The apparatus currently is undergoing testing.

PART II. Na-Ca-DEMIXING IN FREE-SWELLING MONTMORILLONITE

INTRODUCTION:

The introduction and model theory of free-swelling in clay-water systems containing mixtures of Na and Ca on the exchange complex were presented in the 1968 Annual Report. As pointed out in that report, the preliminary data were not in agreement with any of the several models presented.

RESULTS:

Efforts in 1969 were directed at attempting to explain the apparent impass, and have led to the following two possibilities: (1) faulty X-ray diffraction data; (2) the original models were incorrect or inadequate.

Some additional X-ray data points taken in 1969 on the same samples used previously, but run on a different diffraction unit, were not in agreement with the original data. The rather large discrepancy between these two data sources graphically illustrates the necessity for having correct diffractometer and sample alignment - especially at the low angles encountered in this type study. Diffraction work thus has been stopped until this problem can be satisfactorily resolved.

The original swelling models for the mixed cation system were based on the assumption of a salt-free solution phase; however, small amounts of salt were found to have been inadvertently left in the samples. This undoubtedly altered the clay-swelling characteristics, thus preventing any meaningful comparison with the several models as originally conceived.

Salt is known to suppress double-layer type expansion in clay-water systems. Nevertheless, plots of d-spacing versus increasing water content seem to be straight lines, even for the cases where small quantities of salt are present. The following proposed mathematical relations may serve to describe this type

of expansion:

$$d = 9.4 + u[W_t - (a + bW_t)]/S_i$$

where d is the d-spacing, 9.4 is the thickness of the individual platelets, W_t is the total water present, S_i is the internal surface area, u is a constant equal to 2×10^4 A·m^2/g, and the term $(a + bW_t)$ equals W_e the external water in the system. The constant a is thought to relate to the initial hydration of the external surfaces and is thought to remain constant as W_t increases; the constant b has more interesting possibilities - it implies that the amount of water in the external regions of these clay systems increases linearly as the total water in the system increases, thus, b may relate to the salt distribution between the internal and external solutions.

SUMMARY:

The free-swelling of a clay-water system containing mixtures of sodium and calcium on the exchange complex did not fit proposed model theory. Two possible explanations are: (1) X-ray equipment was not critically aligned to meet the exacting requirements imposed by these highly expanded materials, i.e., as great as 100 Å; (2) excess salt in the system may have suppressed swelling to such an extent that the original model theory was inadequate. This is turn has led to the following proposed theory to explain free-swelling of a 2:1 type clay in acqueous dilute salt solutions:

$$d = 9.4 + u[W_t - (a + bW_t)]/S_i$$

where d is d-spacing of the expanded platelets, W_t is total water present, S_i is internal surface area, u is a constant equal to 2×10^4 A·m^2, and $(a + bW_t)$ represents the water associated with the

external surfaces and voids. The constant a is thought to represent the initial hydration of the external surfaces and is assumed to remain constant as W_t increases; the term bW_t would represent a constant build-up of externally associated water as the total water in the system (W_t) increases. The constant b should relate to the salt distribution between the internal and external solution phases, e.g. the osmotic potential.

REFERENCES:

1. Gregg, S. J., and Sing, R. S. W. Adsorption, Surface Area, and Porosity. Academic Press Inc., New York, N.Y. 1967.

2. Brunauer, S., Emmett, P. H., and Teller, E. Adsorption of gases in multimolecular layers. J. Amer. Chem. Soc. 60:309-319. 1938

PERSONNEL: D. H. Fink

CURRENT TERMINATION DATE: December 1970

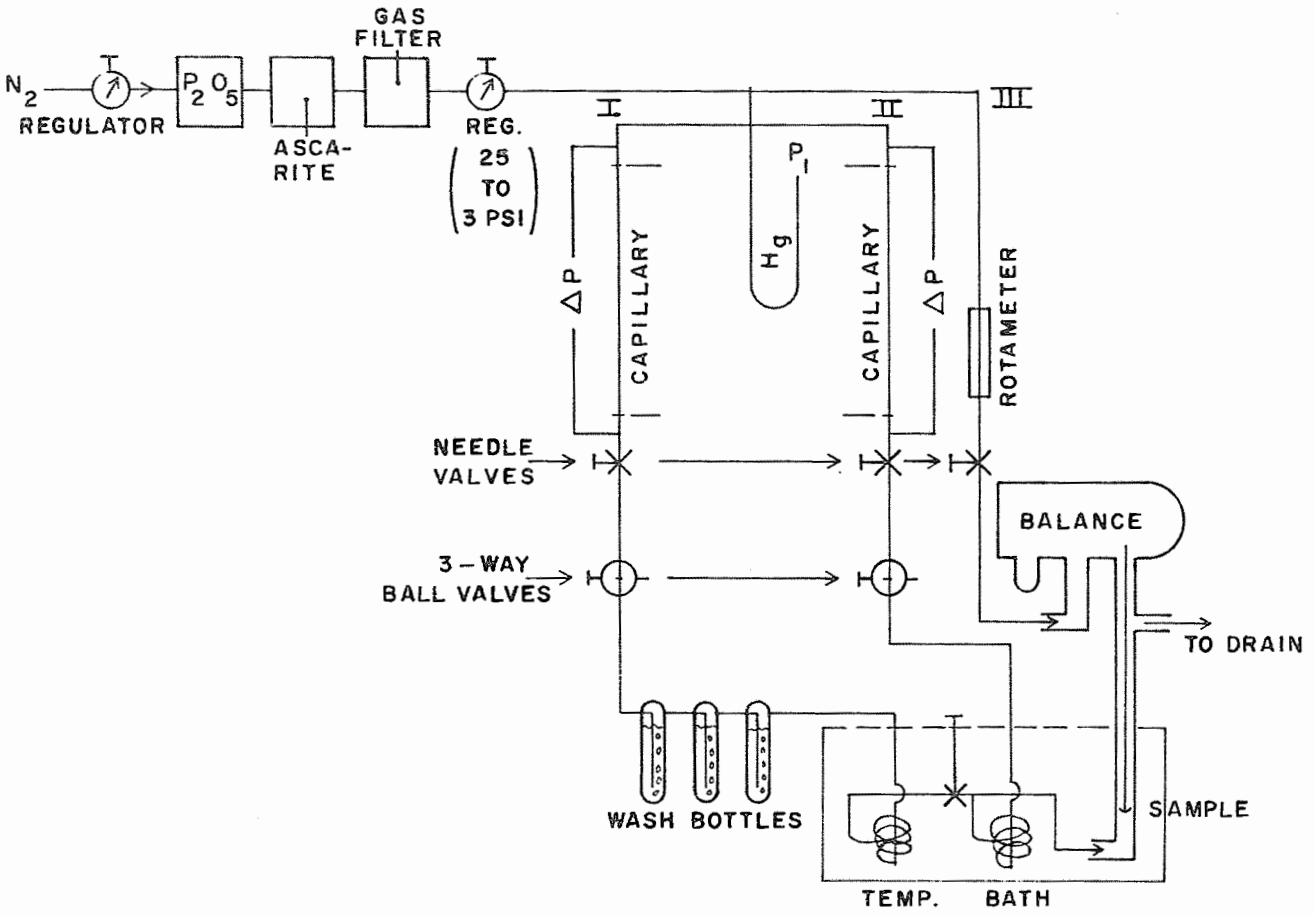

Figure 1. Adsorption isotherm apparatus using a gas flow system to control P/P_o, and an electro-balance to record adsorption.

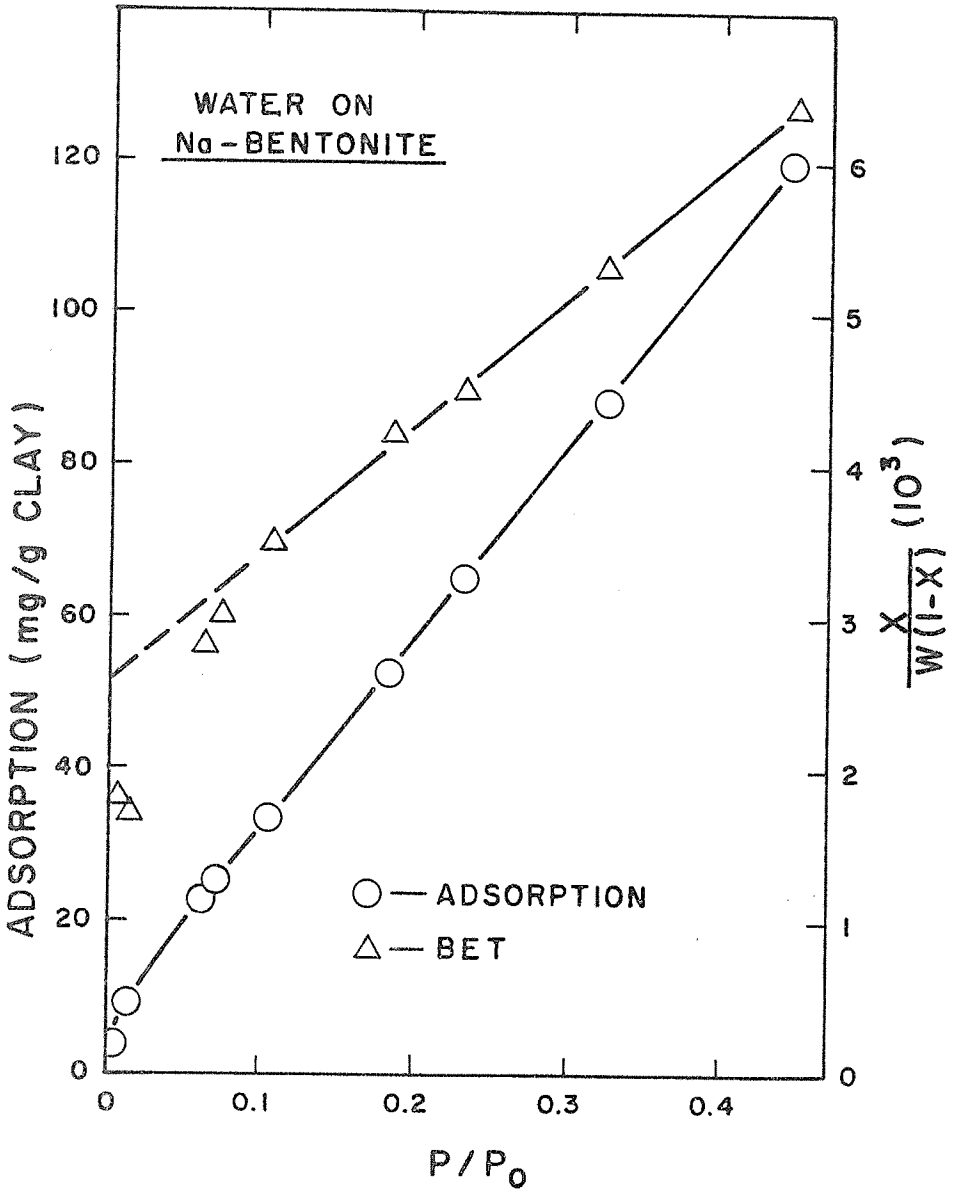

Figure 2. Adsorption isotherm and BET plot of water adsorption on Na-Otay bentonite at 20 C.

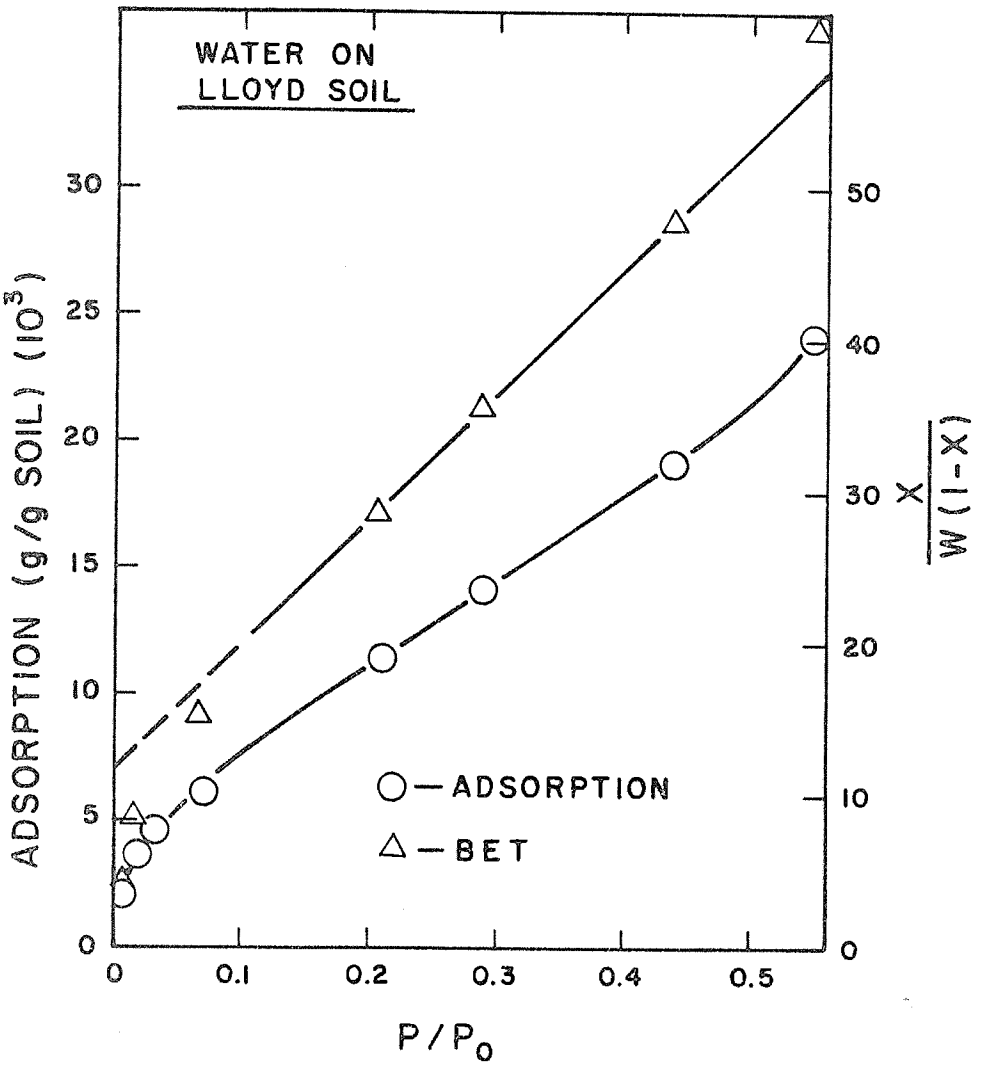

Figure 3. Adsorption isotherm and BET plot of water adsorption on Lloyd soil at 20 C.

TITLE: THE USE OF FLOATING SOLID AND GRANULAR MATERIALS TO REDUCE EVAPORATION FROM WATER SURFACES

CRIS WORK UNIT: SWC-018-gG-2 CODE NO.: Ariz.-WCL 67-3

INTRODUCTION:

A study of the complete heat budget of partially covered tanks provided considerable insight into the most important factors to consider when designing floating covers for evaporation reduction (see 1968 Annual Report, WCL 67-3). Further insight was provided from a theoretical analysis of the energy equation for a partially covered body of water. This analysis revealed that materials with high emittance and high reflectance will be the most efficient in reducing evaporation if other factors such as size and permeability are equal. White materials best satisfied the requirement that emittance and reflectance be as high as possible and should therefore be the most efficient. The relative efficiencies of other colors could be determined by their radiative properties. However, due to the unknown and dependent terms in the energy equation, experiments are necessary to determine absolute values of efficiency for a given material and color.

PROCEDURE:

The experiment was conducted during May and June on four insulated evaporation tanks. One tank was left open and used as a reference throughout the experiment. Covers of white, green and black butyl rubber, supported by means of a plastic pipe attached around their perimeter, were placed on the other three tanks. Each cover was approximately 1.8 meters in diameter, and covered about 80 percent of the water surface area. The green and black covers were approximately 1.5 mm thick, being made of a foamed butyl. The white cover was common butyl painted white on top, and 0.7 mm thick.

RESULTS AND DISCUSSION:

The results of the experiment involving three butyl covers of different colors are presented in Table 1. The data presented

represent the actual evaporation from each tank, the percent of evaporation reduction of the covered tanks as compared to the open tank, and the percent of surface area covered in each case. These results show the importance of using white or light colored materials when designing covers to provide maximum evaporation reduction efficiency.

The white cover, which covered 80 percent of the surface area as compared to 82 and 81 percent for the green and black covers, respectively, reduced evaporation by 75 percent as compared to 68 and 62 percent for the green and black covers, respectively. In other words, the white cover actually covered slightly less surface area than the other two, but was 13 percent more efficient than the black cover and 7 percent more efficient than the green cover. The same relative efficiencies of these three covers could have been deduced from handbook values of reflectance and emittance; however, actual efficiencies can only be obtained by experiments.

SUMMARY AND CONCLUSIONS:

The color of material used to reduce evaporation losses from open water surfaces is an important factor to consider when designing covers for maximum efficiency. The relative efficiencies of various colors of a given material can be obtained from analysis of the energy relationships of a partially covered body of water using handbook values of reflectance and emittance. Experimental methods are required to provide absolute values of evaporation reduction efficiency.

An experiment, designed to compare absolute values of evaporation reduction efficiency for three covers of the same material and size but different colors, was conducted for a two week period in late May and early June. Approximately 80 percent of the surface area of three insulated evaporation tanks was covered with covers made of white, green and black butyl rubber. A fourth tank (from which evaporation exceeded 9 cm during the study period) was left open

and used as a reference. The absolute values of evaporation reduction efficiency obtained during this study were 75, 68 and 62 percent for the white, green and black covers, respectively.

PERSONNEL: Keith R. Cooley

CURRENT TERMINATION DATE: December 1970.

Table 1. Evaporation reduction efficiency of butyl rubber covers.

Cover	Open	White			Green			Black		
Period	Evap. (cm)	Evap. (cm)	% Red.	% Area Covered	Evap. (cm)	% Red.	% Area Covered	Evap. (cm)	% Red.	% Area Covered
29 May-9 Jun	6.14	1.53	75	80	1.99	68	82	2.40	61	81
9 Jun-13 Jun	3.35	0.80	76	80	1.07	68	82	1.24	63	81
Total	9.49	2.33	75	80	3.06	68	82	3.64	62	81

TITLE: EVAPORATION OF WATER FROM SOIL

CRIS WORK UNIT: SWC-018-gG-2 CODE NO.: Ariz.-WCL 68-1

OBJECTIVE:

To describe the evaporation of water from the soil surface that occurs under natural conditions and to relate evaporation to pertinent physical processes in the soil.

NEED FOR RESEARCH:

Evaporation of water from soil generally may be regarded as wasteful. Modification of the soil surface for the purpose of reducing evaporation has been tried with mulches, frequently with contradictory and ambiguous results. The inconclusive results are probably a result of insufficient knowledge of physical and chemical processes that occur in the layers of soil in which evaporation occurs. These processes include moisture flow in liquid and vapor form as a result of moisture and temperature gradients, heat flow by conduction, by latent heat transfer, and salt accumulation at the surface.

Many studies, both theoretical and experimental have been made of surface evaporation. Theoretical studies have often been too simplifying, assuming predominance of one form of water movement in the soil over another, assuming isothermal conditions, and assuming a constant evaporative demand. Even so, the solutions provided are not straightforward and defy ready application in practice.

Experimental work has been mainly carried out with columns of soil in artificial, controlled environments bearing small resemblance to the atmosphere close to the natural soil surface. It is considered necessary to conduct experimental studies under natural conditions where evaporative demand is periodic and where soil temperatures in the surface layers vary periodically and with depth. If such observations do not conform sufficiently to available theoretical prediction it will be necessary to find different

models. An accurate model of surface evaporation would permit prediction of evaporation rates as well as the associated effect on soil temperatures. Furthermore, it would indicate which physical process is most important as drying proceeds and which changes in soil or surface properties may be effective in modifying the evaporation process to suit a particular purpose.

EXPERIMENTAL:

Preliminary work on this project has entailed laboratory and field development of gamma ray transmission equipment for measuring water content of soil in situ in thin layers.

Laboratory:

The gamma ray transmission method for measuring water content of soil in situ can give results unattainable by other methods in terms of accuracy, resolution, and absence of time lag and site disturbance. This nuclear method has been used successfully to measure density and water content of soil under controlled laboratory conditions. Recent tests of the equipment under field conditions have been only partially successful because of electronic drift problems. The electronic drift probably was caused by multiplier phototube gain changes and scintillation crystal light output and resolution changes resulting from temperature fluctuations. The temperature dependency of these components has been reported elsewhere. Current methods that utilize gamma emitters for stabilizing nuclear counting equipment require two detector assemblies, and the equipment, designed for laboratory experiments, is not readily adaptable to field use.

Our objective for this portion of the general research project was to develop an improved method of stabilizing gamma ray transmission equipment against temperature fluctuations, thereby permitting use of this equipment in the changing temperature environment of a field soil.

Accurate determination of soil density or water content depends only upon counting primary photons transmitted from the source to the detector. Electronic discrimination against scattered radiation is preferred for field equipment, as collimating with lead is impractical.

An example of the effect of temperature on the energy spectrum of ^{137}Cs is illustrated in Figure 1. Ideally, the baseline voltage and window width, set at appropriate values for which the system was calibrated, should not change during the measurement period. Figure 1 shows that a system calibrated at 20 C with the baseline voltage and window width set to count only primary photons would detect essentially none if the system were operated at 30 C.

Equipment and Procedure. General details of the experiment and experimental setup are reported in the 1962 Annual Report. In 1969 the following equipment was purchased from the Hamner Electronics Company:

Scaler	NS-11
Ratemeter	N-780A
High voltage supply	NV-13P
Amplifier	NA-12
Single channel analyzer	NC-11
Spectrum stabilizer	NC-20
Timer	NT-11

The recently designed spectrum stabilizer provides the means of stabilizing against temperature changes.

The detector assembly, ^{137}Cs gamma ray source, glass plate sample tray, and soil cylinder were placed in a controlled temperature room. The detector assembly was connected to the counting equipment (located outside the controlled room, at ambient temperature of 23 $\pm$ 2 C) with a 45-meter cable. Even though laboratory

counting equipment is necessary, the 45-meter cable (and longer, if necessary) should allow the detector and source to be used remotely in an experimental field.

The primary source of gamma rays, 5 mCi of ^{137}Cs, was located about 30 cm from a NaI(Tl) scintillation crystal (1.27 cm thick by 4.81 cm diameter) mounted on an RCA 6199 multiplier phototube. The window width of the single channel analyzer was set at 0.2 volt. Glass plates were used as standard absorbers. A 26.6-cm-long sample holder was designed so that the plates could be easily inserted or removed from the beam path. Density measurements were made at 22, 5.5, 20, 33, 5, 26 and 13 C, in that sequence.

Stabilization. One method for stabilization utilizes the NC-20 spectrum stabilizer. This unit is a special single channel analyzer which detects shifts in the spectral peak of interest. When a shift is detected, a compensating signal is generated which causes an external high voltage power supply to change its output voltage to correct for the shift. Our first choice was to use the 0.66 MeV ^{137}Cs photopeak which is transmitted through the absorber. However, as the absorber thickness (density) changes, the low energy side of the ^{137}Cs photopeak becomes skewed because of small angle Compton scattering. Under these conditions the electronics used to stabilize the spectrum are unable to accurately track the photopeak in the desired manner. Figure 2 shows count rate versus glass density for a "stabilized" and unstabilized system at 33 ± 0.5 C. The nonlinearity of the stabilized system is evidence that the transmitted ^{137}Cs photopeak cannot be used for stabilizing purposes. This clearly shows that density changes cause variations in the spectrum shape to the degree that the electronic spectrum stabilizer fails.

Our alternative approach was the use of another reference source on which the system could be stabilized. The source was

located so that it was not affected by density changes. Theoretical considerations limit this secondary source to gamma emitters, such as ^{60}Co, which have the same energy spectrum response to temperature variations as the primary ^{137}Cs source. A 0.4μCi ^{60}Co gamma ray source was incorporated into the detector assembly by attaching it to the bottom of the scintillation crystal. The photopeak of this secondary source, tracked by the electronic spectrum stabilizer, varied with temperature, but was independent of density changes. Although Compton scattering from the ^{60}Co in the region of the ^{137}Cs photopeak gives a relatively high and uniform background count (15 cps), it does not interfere with the density measurements.

Results and Discussion: Count rate as a function of glass density at seven temperatures from 5 to 33 C is presented in Figure 3. The experimentally determined count rates are designated by the open circles while the solid line was obtained from a linear regression analysis of log count versus density for all densities at all seven temperatures. The linearity of the data demonstrates the high degree of stability achieved even with a wide variation in temperature and density.

Field:

With the temperature stabilization technique discussed above comes the necessity of designing auxiliary equipment which will facilitate the field measurement of water content. Our objective was to develop equipment which could be programmed to automatically move a source of gamma rays and a scintillation detector assembly within the soil profile and record the count rates and soil depths. From these data, water contents would then be calculated.

Previous work with field equipment used a single source of gamma rays with a single detector. However, to increase the

sampling area, and to increase the count rate for better counting statistics, we designed a system which uses a scintillation detector surrounded by three 5 mc ^{137}Cs gamma ray sources, 120^{o} apart, each 30 cm from the center of the detector.

The active portion of each cesium source is a cube, 0.2 cm on a side, and is housed in a 0.47 cm diameter stainless steel rod. The detector assembly and nuclear counting equipment were the same as reported under Laboratory. The soil sampling volume with this equipment is composed essentially of three solid angles with the face of the 0.2 x 0.2 cm gamma ray source on one end and the scintillation crystal face of 0.5 cm x 4.8 cm at the other end.

Sources and detector are connected by rods to a mounting plate, which in turn is connected with a gear rack to a gear motor. This motor is mounted on a tripod which stands over the source and detector access tubes. The sources and crystal are in the same plane, so as the mounting plate is moved down and up, the water content profile is measured in nearly 0.5 cm increments. To control and program this vertical movement, an electronic control system was designed and interfaced with the nuclear counting equipment.

Connected to the main driveshaft of the gear motor is a 7.6 cm diameter disk with five 0.3 cm diameter holes equally spaced on a 2.9 cm radius. On one side of the disk is a photoelectric (PE) cell and on the other a lamp. The PE is connected to an electronic counter in the control box. For this particular system, 10 counts registered by the PE is equal to a vertical movement of 0.1 cm by the source and detector assembly.

The system operates as follows. The sources and detector are initially positioned so that the scintillation crystal "sees" the 0 to 0.5 cm layer of surface soil, with the sources at the 0 to 0.2 cm depth. When the system rezero button is activated, all

counters are reset to zero. With the timer set for a preset time (say, 2 minutes), the system start switch is activated. Counts are accumulated on the scaler for the preset time. At the end of the counting period a command is given to the digital printer to print the depth (000.5 cm) and the counts (up to 999999 total counts). After printing, a command is sent to reset the timer, scaler, and increment counter to zero and start the gear motor. The motor then runs until the increment counter reaches its preset value, stops, and the scaler begins counting that increment.

With the four increment counters (which correspond to 0.5, 1.0, 5.0, and 10.0 cm increments) are four totalizing counters. These counters accumulate the counts from their appropriate increment counters and switch to the next increment counter when the preset total count is reached. For instance, count rate determination (water content measurements) can be made in 0.5 cm increments for the 0 to 10 cm soil depth, then switched to 1 cm increments for the 10 to 30 cm depth. The next increments could then be 10 cm for the 30 to 150 cm soil depth. Other combinations than these mentioned can also be programed.

After the last increment is measured, the total depth counter activates the system reset switch which reverses the motor, bringing the sources and detector back to the zero reference, and initiates the scanning procedure again.

In addition to this automatic mode is a manual mode, which allows the operator to manually switch the motor on to move the probes down or up. The probes can be stopped at any depth by engaging the system stop switch. The probe depth is visually displayed on the front of the control panel as well as on the printed tape. Depressing the system start switch starts the probes moving from the position where they were manually stopped.

Field Installation of Access Tubes. Installing the three source and one detector access tubes in the field must be done

carefully to insure proper alignment of the tubes. A 24 x 24 x ½ inch thick steel plate with holes and guide tubes in the proper arrangement is placed in the field where measurements are to be made. A bullseye level on the plate is used to insure that the access tubes will be placed in the soil at right angles to the surface. The access tubes, 2 inch OD x 0.049 inch wall thickness detector tube and 0.75 inch OD x 0.043 inch wall thickness access tubes, are placed in the guides in the alignment jig.

An auger is put into one of the access tubes and soil removed from a 5-cm depth increment. The soil sample is used for gravimetric water content analysis. The access tube is then pushed into the soil this 5-cm increment and this procedure is repeated in all the tubes until the predetermined depth is reached.

The alignment jig is then removed leaving 30 cm of access tubes exposed above the soil surface. Leveling of the sources and the detector is facilitated by using the tops of the tubes as a reference point.

Calibration. The equation used to describe the number of monoenergetic gamma rays that pass through an absorber (in our case, a soil-water system) is

$$\ln I = \ln I_o - x\mu_s P_s - x\mu_w P_w \qquad (1)$$

where I is the count rate of the rays passing through the absorber, I_o is the count rate with no absorber, x is the distance between source and detector, μ_s the mass attenuation coefficient for dry soil, μ_w the attenuation coefficient for water, P_s and P_w are the masses of dry soil and water per unit volume of the soil water system. The term P_w, when divided by the density of water, is the volumetric water content of the soil.

The primary interest in using a gamma transmission technique in a soil-water system is to measure the volumetric water content P_w (assuming the density of water to be 1.00). This term can be calculated if I is measured and all other terms are known. It is assumed that the term ln I_o, $x\mu_s$, $x\mu_w$ and P_s remain constant during an experiment. One limitation of the method is that the soil bulk density P_s may change due to shrinking and swelling of the soil.

The four constants, I_o, $x\mu_s$, $x\mu_w$, and P_s must be obtained by experiment, with the exception that an empirical relation between theoretical values of μ_s and μ_w can be used to simplify the calculation of P_s. The term I_o is obtained by inserting an absorber between the source and detector access tubes whose density can be changed in a known way and the count rate obtained for different densities. In practice this is achieved by placing a tray containing 10¼ x 2 x 2 inch steel plates between the source and detector access tubes. Count rates are obtained and a plate removed and the count rate taken again. This is repeated until all but one plate is removed. The logarithm of the count rate is plotted versus the number of steel plates. If all assumptions are met and the equipment is working properly, a linear relation is obtained. The intercept of this relation is the term ln I_o.

The volumetric water content can be expressed as

$$P_w = P_s \theta_w \tag{2}$$

where θ_w is the gravimetric water content and P_w is again implicitly divided by the density of water (1.00). If we can assume that the experimentally determined values of μ_s and μ_w will always be in the same ratio to each other as the theoretical values, then

$$\mu_s = 0.9\ \mu_w \tag{3}$$

substituting (2) and (3) into (1) yields

$$P_s = \frac{\ln I_o - \ln I}{x\mu_w(.9 - \theta_w)} \quad . \tag{4}$$

Of the terms in the right hand side of (4) only $x\mu_w$ and θ_w remain to be evaluated.

If the soil within the experimental area is horizontally uniform, the water content θ_w can be measured by sampling and weighing at the soil depths of interest. This is done at the same time that the gamma apparatus is scanning the various depths. The term $x\mu_w$ can be measured during an irrigation. If several centimeters of water is ponded above the soil and the count rate taken, $x\mu_w$ is merely the difference $\ln I_o - \ln I$. Knowing $x\mu_w$ and $\ln I_o$, and measuring I and θ_w at each depth, the bulk density for each depth can be calculated using equation (4).

Assuming that the bulk density P_s does not change with time, once P_s is evaluated the volumetric water content can be calculated for each depth using

$$P_w = .9\ P_s - (\ln I_o - \ln I)/x\mu_w \quad . \tag{5}$$

A check can be made on equation (3) by scanning and taking gravimetric samples at two different times when the soil water contents at the two times are quite different. When this is done, the bulk density can be calculated using

$$P_s = \frac{\ln I_{t1} - \ln I_{t2}}{x\mu_w\ (\theta_{wt2} - \theta_{wt2})} \quad . \tag{6}$$

All terms in equation (1) are now known except $x\mu_s$ which can be calculated. With this value of $x\mu_s$ and the measured value of $x\mu_w$ the ratio $x\mu_s/x\mu_w$ will indicate the degree of validity of (3).

Background Radiation. When the ^{60}Co source is used in the stabilization technique, a significant background count is obtained. This background will be constant (within its counting statistics) and must be subtracted from both I_o and I before any calculations, discussed under Calibration, are made.

SUMMARY:

Laboratory and field experiments have been conducted to develop a gamma ray transmission technique to measure water content profiles in situ. The output from electronic components in the gamma ray detector assembly is highly temperature dependent. A recently available spectrum stabilizer compensates for output changes due to temperature fluctuations by adjusting the high voltage supply. Laboratory experiments showed that, when a spectrum stabilizer was locked on to a ^{60}Co peak (1 microcurie of ^{60}Co was taped to the detector assembly) the corrected output from the detector did not change when exposed to temperatures ranging from 5 to 33 C.

For field use a tripod assembly was constructed to house a motor and gear mechanism which would lower and raise the source and detector assembly on command from an electronic controller. The controller is programable and will automatically position the source detector assembly at a preset depth, start the scaler, count for a preset time, stop the scaler, print the depth and number of counts, lower the source and detector to the next preset depth, and repeat the counting-positioning sequence. Upon reaching the lowest preset depth the assembly is raised to the zero depth and the sequence is repeated.

In the field, it is desired to measure water contents in thin increments in order to obtain well defined water content profiles.

Detector assemblies containing scintillation crystals 0.5 and 1 cm thick were obtained. The particular assemblies have proven unstable and have been returned to the factory for repair. Upon receipt of satisfactory detector assemblies, extensive field experiments will be conducted with this equipment.

PERSONNEL: Ray D. Jackson and Robert J. Reginato

CURRENT TERMINATION DATE: December 1970.

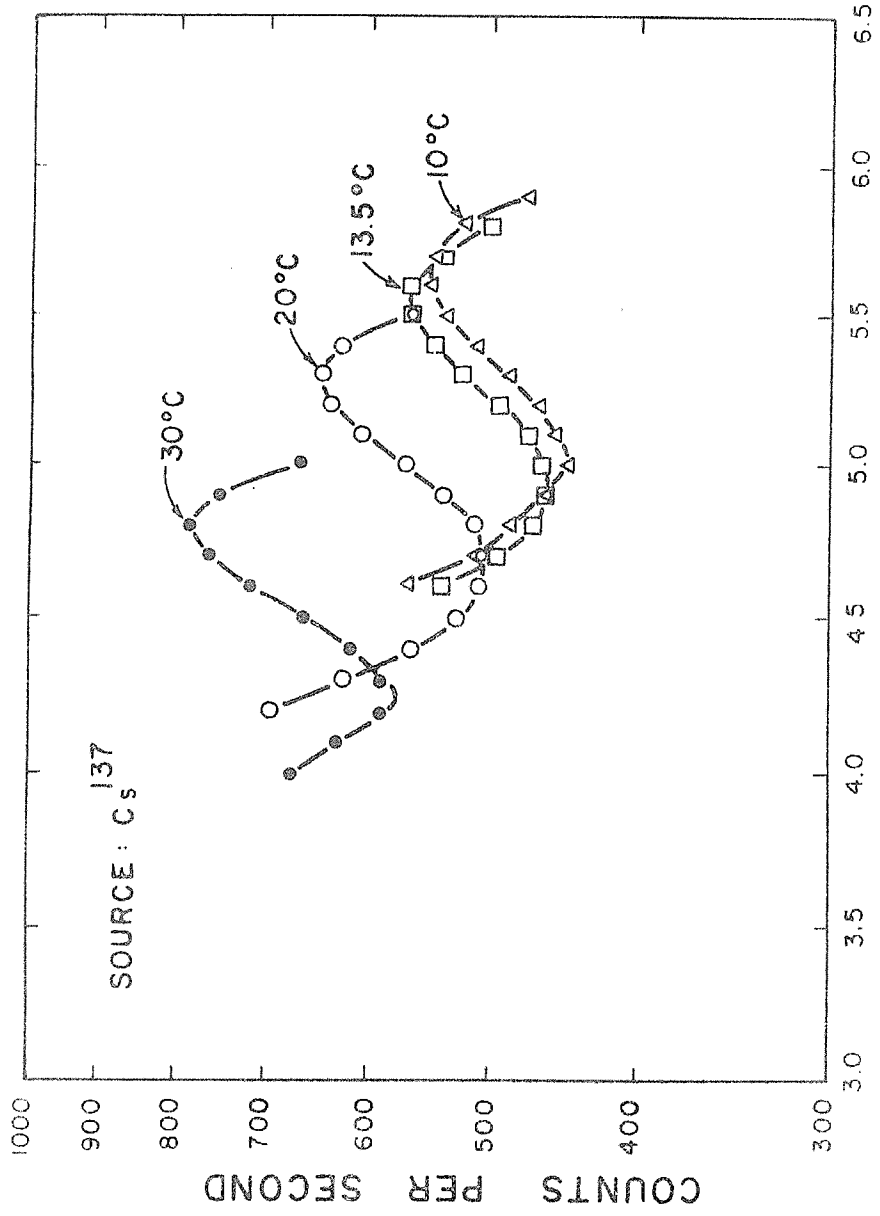

Fig. 1 — Cs^{137} gamma ray energy spectrum shift as a function of temperature.

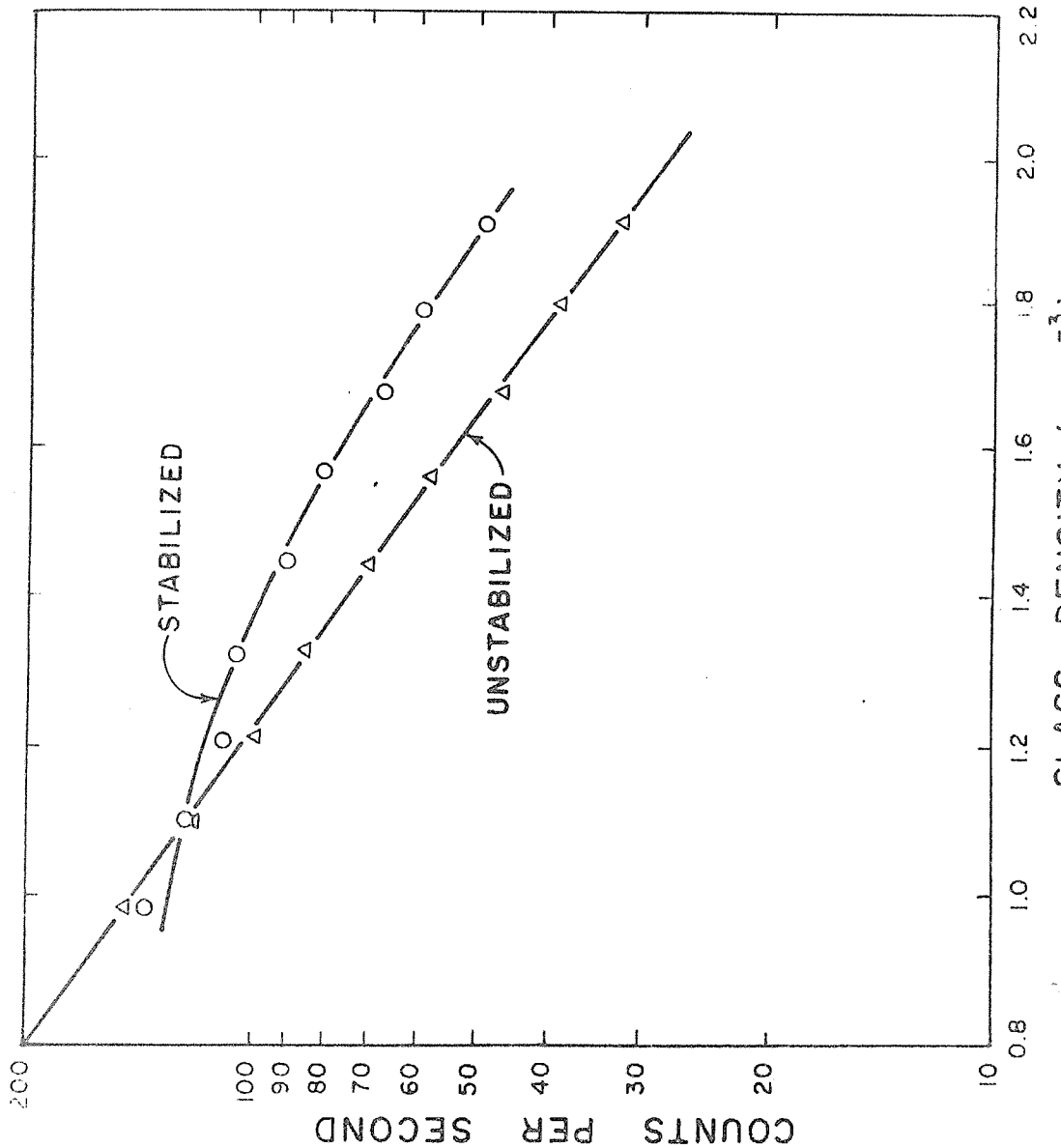

Fig. 2--Count rate versus glass density for unstabilized and "stabilized" conditions using ^{137}Cs for reference photopeak at 33 C.

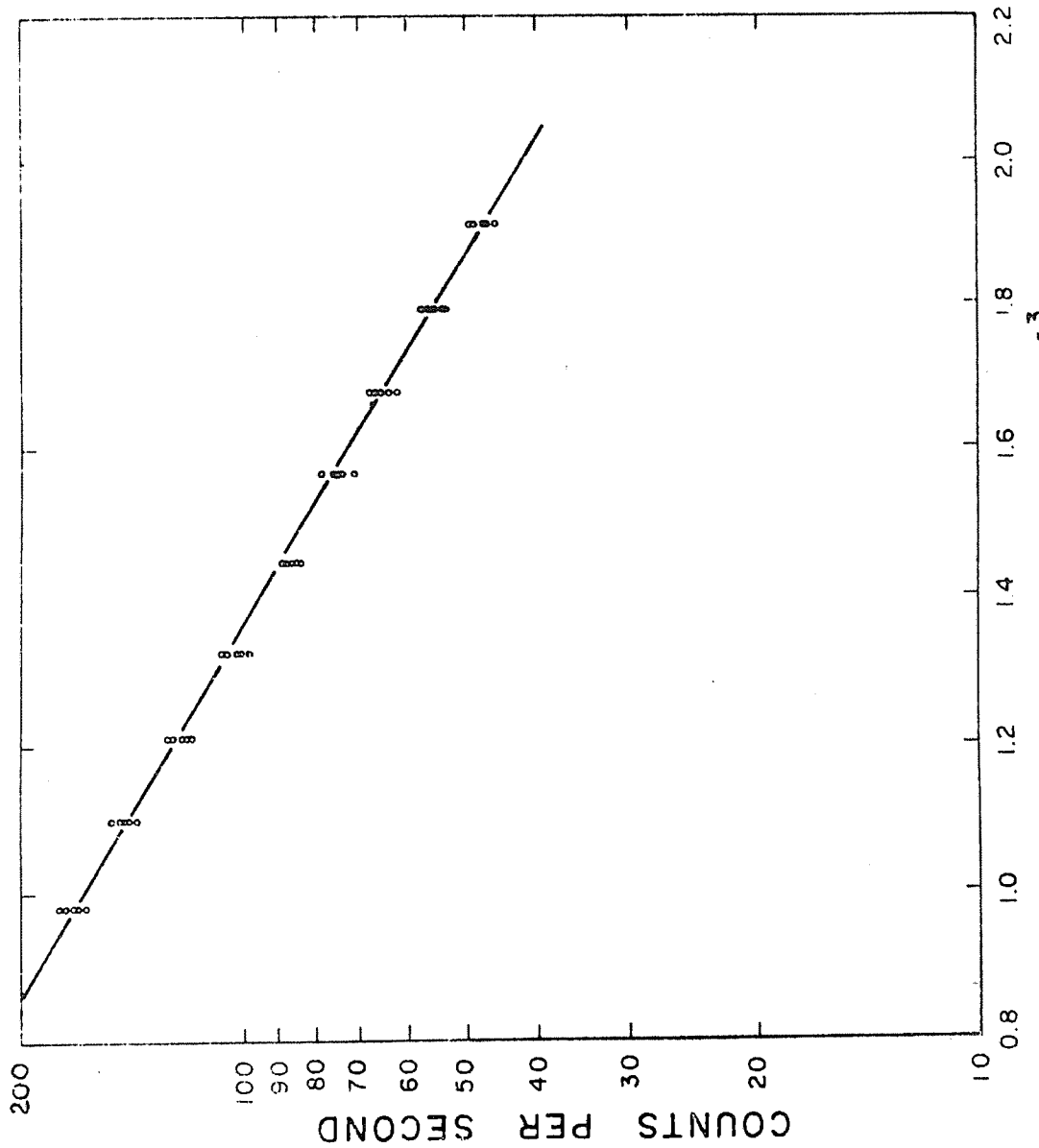

Fig. 3--Count rate versus glass density for stabilized condition using ^{60}Co for reference photopeak at temperatures from 5 to 33 C.

TITLE: FABRICATED-IN-PLACE, REINFORCED LININGS AND GROUND COVERS.

CRIS WORK UNIT: SWC-018-gG-2 CODE NO.: Ariz.-WCL 68-2

INTRODUCTION:

Research on soil treatment to increase precipitation runoff has reduced the cost of materials from over $2 per square yard to less than 50 cents per square yard. While these reductions in cost enhance the potential use of water harvesting techniques, the high cost of present storage structures is still a deterrent factor. Construction site conditions often require the use of expensive, high strength materials such as steel tanks, butyl bags, or reinforced butyl linings for reservoirs. While the structures are durable, they also cost about $80 per 1,000 gallons storage for an average sized structure of 25,000 gallons capacity. Materials for these structures are relatively bulky, increasing transportation costs to the construction sites, which often can be reached only in four-wheel drive vehicles. There is an urgent need for materials and installation procedures which permit lower cost construction of durable water storage structures.

In June 1962 a 120,000 gallon reservoir was constructed on the Hualapai Indian Reservation in cooperation with the Bureau of Indian Affairs (see previous Annual Reports titled "Soil treatment to reduce infiltration and increase precipitation runoff"). The reservoir was lined by laying 1 oz per ft^2 chopped fiberglass mat and spraying with two coats of asphalt emulsion. Thirty months later a sealcoat of asphalt-clay emulsion was mopped on the lining. In June 1964 a similar reservoir lining was installed on the Ft. Apache Indian Reservation in cooperation with the Bureau of Indian Affairs. Periodic inspection of the two reservoirs has found that the linings have excellent weathering and durability

characteristics with essentially no maintenance. Animal traffic has not punctured the linings. Deer often puncture reinforced butyl linings with their relatively sharp hooves. During the 8 and 6 years, respectively, since installation of the reservoirs, the linings have remained in excellent condition.

A study was initiated in July 1968 to investigate improved materials and methods for the construction of asphalt-fiberglass reservoir linings, ditch linings and precipitation catchments. The variables under consideration are: type of reinforcing material, sealing material, and protective coating; site preparation methods and costs; and lining installation methods and costs.

PROCEDURE:

Selection of materials is initially done on basis of information supplied by manufacturers. The potential toxicity of the materials is of primary consideration. The initial work is being done with fiberglass matting sealed with asphaltic materials. The studies consist of a concurrent laboratory and field evaluation.

PROCEDURE:

Pressure-Plate Studies: Primary laboratory studies consist of determining the maximum head of water that various treatments on different types of reinforcing materials are capable of supporting without leakage. These studies are conducted on a pressure-plate assembly. The assembly consists of two cup-shaped plates, 11 inches in diameter and 1 inch deep. The bottom plate can be filled with different subgrade materials. The lining sample to be tested is clamped between the two plates and air pressure is applied to the top plate. A flexible outlet tube from the bottom plate is submerged in a beaker of water. The air pressure in the top plate is increased by 2 psi increments at not less than two hour intervals. When air bubbles from the outlet tube indicate air

passing through the lining, the lining is considered to have failed and the pressure is recorded. The samples are cut from larger segments of lining material that have been treated and cured with the same equipment and procedures used in the field. Samples are allowed to equilibrate to room temperature before testing.

Field Studies: The field studies consist of installations of different linings under operational conditions to develop installation techniques and to observe performance under actual field conditions. Experimental installations constructed in 1969 consist of: an experimental ditch lining in Hawaii; an operational catchment installed in cooperation with the Bureau of Land Management in Arizona, and a small water harvesting test plot in Hawaii.

RESULTS AND DISCUSSION:

Pressure-Plate Studies: Cutback asphalts were not satisfactory for the asphalt-fiberglass lining. The asphalt would flow and fail at pressure heads of 2 psi until all solvent had evaporated. This can take more than two months of curing time under field conditions.

Either cationic or anionic asphalt emulsions satisfactorily bonded the glass fibers together and bonded lap joints when sprayed on top of the glass mat. The emulsions do not seal all holes in the mat and a second sealcoat is necessary. Emulsions break rapidly and a sealcoat can be applied one day after spraying the emulsion. There is a possibility that the sealcoat can be applied immediately after the emulsion is applied.

Roofing type asphalt-clay emulsion and rubberized asphalt emulsions have received preliminary examination as sealcoats. Pinholes in the sealcoats have been a serious problem. Some

pinholes result from entrained air bubbles, and anti-foaming agents should correct this. Other pinholes result from the fact that a fresh, non-oxidized asphalt surface is hydrophobic and tends to repel water-based asphalt emulsions applied as sealcoats. The pinhole problem has not been observed in field application of sealcoats to oxidized asphalt surfaces. Future laboratury studies will be aimed at solving the pinhole problem through the use of surfactants and/or modified application techniques.

Field Studies: An experimental section of asphalt-fiberglass ditch lining was installed near Puunene, Maui, Hawaii, to obtain information on nutgrass penetration and labor requirements. The nutgrass problem is discussed in the Annual Report on "Materials and methods for water harvesting and water storage in the state of Hawaii." The ditch section was 100 ft. long and had a wetted perimeter of 24 ft. Surface weed growth was removed by scraping, and trenches about 4 x 6 inches were dug along the upper banks to bury the lining edges. A soil sterilant was applied to the soil surface. Sheets of 1-1/2 oz per ft^2 fiberglass matting 60 inches wide and 26 ft. long were laid across the ditch, starting at the lower end so that lap joints were shingled in a downstream direction. Anionic asphalt emulsion was sprayed on the mat at a rate of 0.6 gal. per yd^2 as it was laid. A sealcoat of asphalt-clay roofing emulsion was applied with hand brooms at a rate of 0.3 gal. per yd^2 three days after initial installation of the mat. Laying the mat and spraying emulsion took 5 men 1-3/4 hours. Sealcoat application was done in 45 minutes by 4 men. Labor requirements for the lining installation, excluding ditch preparation done by machine, was less than 2.7 man-minutes per square yard.

Asphalt-fiberglass was installed on top of the existing 40 x 80 ft. asphalt catchment at the Maui, Hawaii, test site. Construction procedure was the same as for the ditch lining except that soil sterilant was applied only around the edges and the sealcoat was spread two days after initial application of asphalt emulsion. Light rain fell during the initial spraying but did not interfere with the application. The sealcoat cannot be applied during rain. Laying and spraying fiberglass required 1-1/4 hours by 6 men. The sealcoat was put on by 3 men in 1-3/4 hours. Labor requirement was less than 2.2 man-minutes per square yard.

An operational asphalt-fiberglass catchment was installed on Whitlock Peak, in southeastern Arizona, in cooperation with the Bureau of Land Management. The site is accessible only in 4-wheel drive vehicles. Numerous partially buried rocks, up to 3 ft. in diameter, covered the catchment site and could not be removed. Butyl rubber, or any other elastomeric or plastic materials could not have been installed under these conditions. Asphalt-fiberglass conforms to the shape of the rough surface, does not develop localized stresses, and is highly resistant to damage by animal traffic or wind. The 100 x 100 foot catchment was laid and sprayed by 7 men in 3 hours. Application of the sealcoat was done by BLM personnel at a later date.

SUMMARY AND CONCLUSIONS:

Research is reducing the cost of water harvesting catchments but storage costs are still too high for most potential users. The initial cost of a 25,000 gallon steel tank or elastomeric bag has averaged about $80 per 1,000 gallons. To reduce costs, linings of fiberglass matting sprayed with asphalt emulsion were installed at catchments on the Haulapai and Ft. Apache Indian

Reservation, in cooperation with the Bureau of Indian Affairs, in 1962 and 1964, respectively. These linings have remained in excellent condition, with little maintenance, and have not been damaged by cattle or deer walking on them.

Laboratory and field studies were initiated in 1969 to investigate improved materials and construction methods for fabricated-in-place, reinforced linings and ground covers. Laboratory studies showed that cutback asphalts are not satisfactory because of the long curing time required. Asphalt emulsions cure relatively rapidly, bond the glass fibers together, and make excellent lap joints, but do not seal all holes in the glass mat. A second sealcoat is required. Pressure-plate studies showed that pinholes, caused by entrained air or the hydrophobic characteristics of fresh asphalt surfaces, can be a problem.

An experimental section of asphalt-fiberglass ditch lining was installed near Puunene, Maui, Hawaii, to obtain information on nutgrass penetration and labor requirements. The ditch section was 100 ft. long and had a wetted perimeter of 24 ft. The lining was made with 1-1/2 oz per ft^2 chopped fiberglass matting bonded with anionic asphalt emulsion. A sealcoat of asphalt clay emulsion was applied with hand brooms three days after initial installation. Total labor requirements, excluding ditch preparation by machine, were less than 2.7 man-minutes per yd^{-2}.

Asphalt fiberglass was installed on top of the existing 40 x 80 ft. asphalt catchment at the Maui, Hawaii test site, using the same procedure as for the ditch lining. The initial installation was done during a light rain that did not interfere with the installation. The sealcoat was applied two days later. Total labor requirements were less than 2.2 man-minutes per yd^2.

An operational asphalt-fiberglass catchment was installed in cooperation with the Bureau of Land Management in southeastern

Arizona. The catchment site, accessible only in 4-wheel drive vehicles, is so rough that butyl rubber, or any other elastomeric or plastic materials could not have been installed. The asphalt-fiberglass conforms to a rough surface, eliminating local stress and is highly resistant to damage by animals or wind.

PERSONNEL: G. W. Frasier and L. E. Myers

CURRENT TERMINATION DATE: July 1971.

TITLE: CONSUMPTIVE USE OF WATER BY CROPS IN ARIZONA

PART I. UP-DATING CONSUMPTIVE USE ESTIMATES FOR WHEAT AND BARLEY.

CRIS WORK UNIT: SWC-019-gG-3 CODE NO.: Ariz.-WCL 58-2

INTRODUCTION:

Consumptive use studies were conducted several years ago on wheat and barley planted with a grain drill on the flat. The varieties were the commercial ones used at that time. Within the last two years, several new varieties of barley and wheat have been released for commercial use. These new varieties are higher producers, can be planted earlier, and with new, modern equipment, can be precision planted on beds as well as in rows or on the flat. These new varieties of wheat are yielding considerably more than the old varieties, but the straw is shorter and possibly there is less leaf area.

Previous measurements of consumptive use for wheat and barley were published in Tech. Bul. 169. New measurements of the consumptive use by these new varieties under the new cultural practices should be made, to update the previous information.

Very little wheat has been produced in Arizona; however, the high-yield potential of the new varieties will cause a considerable increase in wheat acreage. This consumptive use data is used in planning cropping systems, design of irrigation systems, and as an aid in developing irrigation schedules.

OBJECTIVES:

1. To measure the consumptive use for the new varieties of wheat and barley.

2. To check the need for a fall irrigation or late irrigation near harvest, resulting from earlier planting dates and variety changes.

3. To make Piche evaporimeter measurements for possible correlation with consumptive use.

PROCEDURE:

The experiment was located on two borders, H60 and H61, (0.42 acres), at the University of Arizona Mesa Experiment Farm, Mesa, Arizona. Three varieties of wheat -- Sonora 64, Maricopa, and Siete Cerros -- and three varieties of barley -- Arimar, Hembar, and Arivat -- were planted 22 November 1968 in a randomized, split plot, six-replication design. A precision planter was used, planting in rows 12 inches apart. Each plot was 6 rows wide and 44 ft long. Seed was planted at a rate of 35 lbs to the acre. The seed bed had previously been fertilized with 140 lbs of nitrate, 80 lbs of phosphate, and irrigated about 10 days before planting. Soil moisture samples were obtained at the planting date, harvest date, about every 10 days, and before and after irrigations. Yields were measured on the two inside rows of each plot on 20 ft of row. Heads were hand cut and threshed.

Timing of irrigations was based mainly on previous studies and close observation of the soil moisture measurements.

RESULTS AND DISCUSSION:

A good stand was obtained, except on Sonora 64. No additional irrigation water was given until 25 February. The stand on Sonora 64 was only fair, and very little tillering was observed; however, all other varieties tillered well.

No rain was reported after the planting date until 21 December, when 1/10 inch was reported. On 26 and 27 December, 0.54 inch and 0.42 inch, respectively, were reported. There was 1.44 inch in January, 0.47 inch in February, and 0.95 inch in March for a total of 3.92 inches during the growing season. The first irrigation was given on 25 February, then two additional irrigations were given on 21 March and 12 April.

No insects were observed; however, the Hembar barley lodged, partly because of a wind storm. The Hembar straw was very weak,

and because of the randomization within the study, it caused some lodging of the other two varieties of barley. Since the windstorm occurred during the blossoming stage, yield was undoubtedly reduced, especially on Hembar. Wheat varieties did not lodge from this windstorm. There was some reason to believe an additional light irrigation might have been beneficial, but because of the lodging, it was not accomplished.

SUMMARY AND CONCLUSIONS:

Table 1 shows that yields of wheat can be expected to be more than 100 bu to the acre. Though Sonora 64 yielded only about 80 bu to the acre, a heavier seeding rate or better tillering should make it comparable in yield to the other two varieties. The water use by wheat would appear to be at least 5 inches more than the 22.9 inches as reported in Tech. Bul. 169 (Fig. 1). An additional late irrigation might have been slightly beneficial, increasing the consumptive use. An additional year of study should be made, increasing the seeding rate for Sonora 64, adding the Inia variety, and checking the benefits of a late, light irrigation.

Table 2 shows the barley yields. The yields of Arimar and Arivat can be compared, but the Hembar yield was drastically reduced because of premature lodging, and thus should not be considered as being typical. Consumptive use for the three varieties compares very closely with the 25.3 inches as reported in Tech. Bul. 169. If there is any change involved, it would probably be on the plus side. An additional year of study should be conducted to confirm this.

PERSONNEL: L. J. Erie and O. F. French

CURRENT TERMINATION DATE: December 1970.

Table 1. Yield -- Wheat (gms. per plot) [a]

Replications[b]	Variety		
	Sonora 64	Sieta Cerros	Maricopa
2	1849	2838	2715
3	1928	3103	2225
4	1768	2692	2646
5	2029	2750	2396
Average	1894	2845	2496

[a] Multiply gms. X 2.40 to get pounds per acre.

[b] Some samples in Reps. 1 and 6 were accidentally destroyed.

Table 2. Yield -- Barley (gms. per plot) [a]

Replications[b]	Variety		
	Arimar	Arivat	Hembar[c]
2	2092	1647	1120
3	1871	1752	852
4	2395	2097	1843
5	2252	2388	1408
Average	2153	1971	1306

a. Multiply gms. X 2.40 to get pounds per acre.

b. Some samples in Reps. 1 and 6 were accidentally destroyed.

c. Barley lodged early, partly because of wind. Yield was drastically reduced.

Table 3. Consumptive Use (inches) -- Wheat and Barley

WHEAT		BARLEY	
Variety	Inches	Variety	Inches
Sonora 64	26.0	Hembar	25.7
Siete Cerros	28.4	Arimar	27.3
Maricopa	27.3	Arivat	26.7

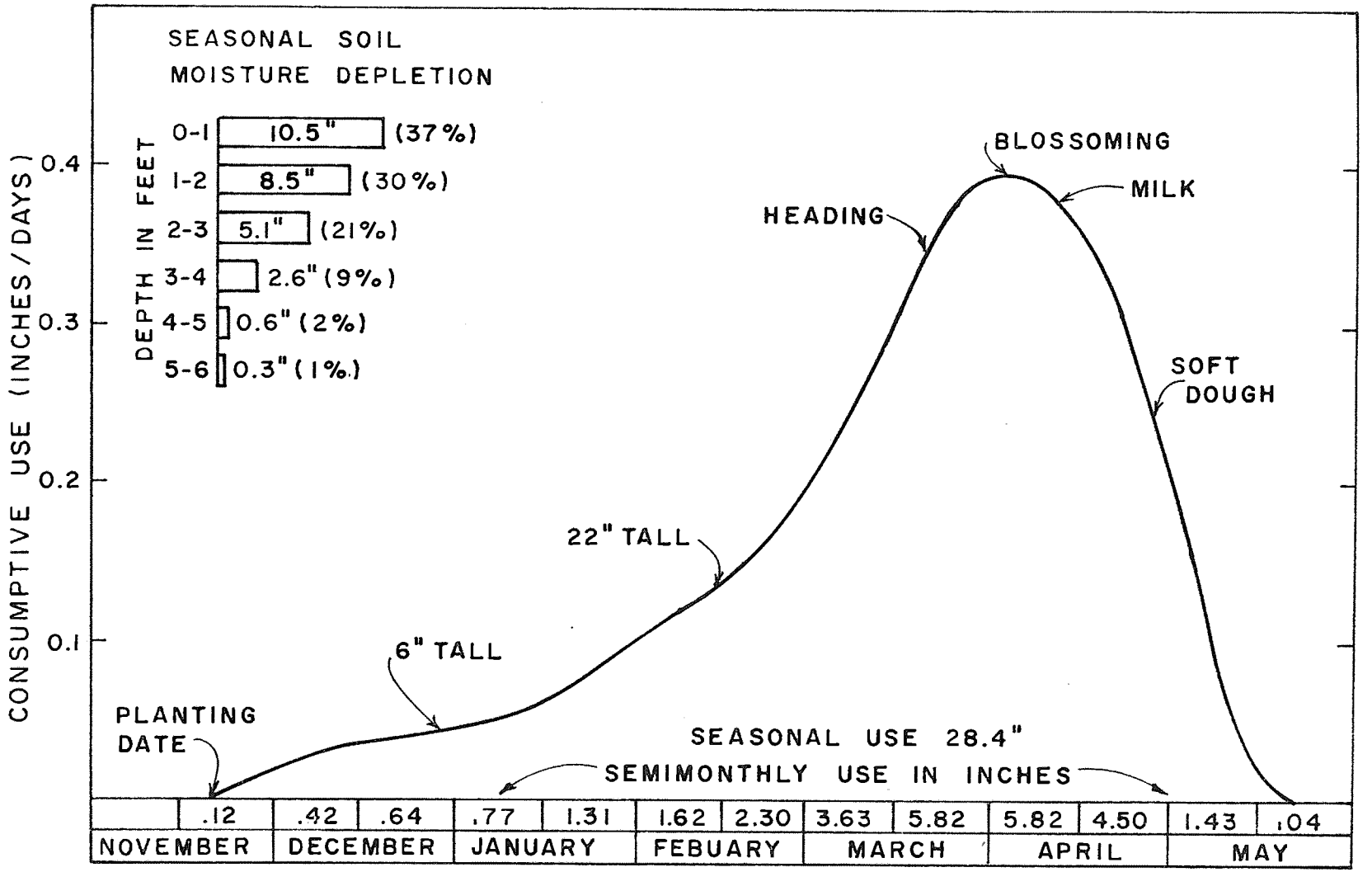

Fig. 1. Consumptive Use for Wheat (Siete Cerros) at Mesa, Arizona. 1968-1969.

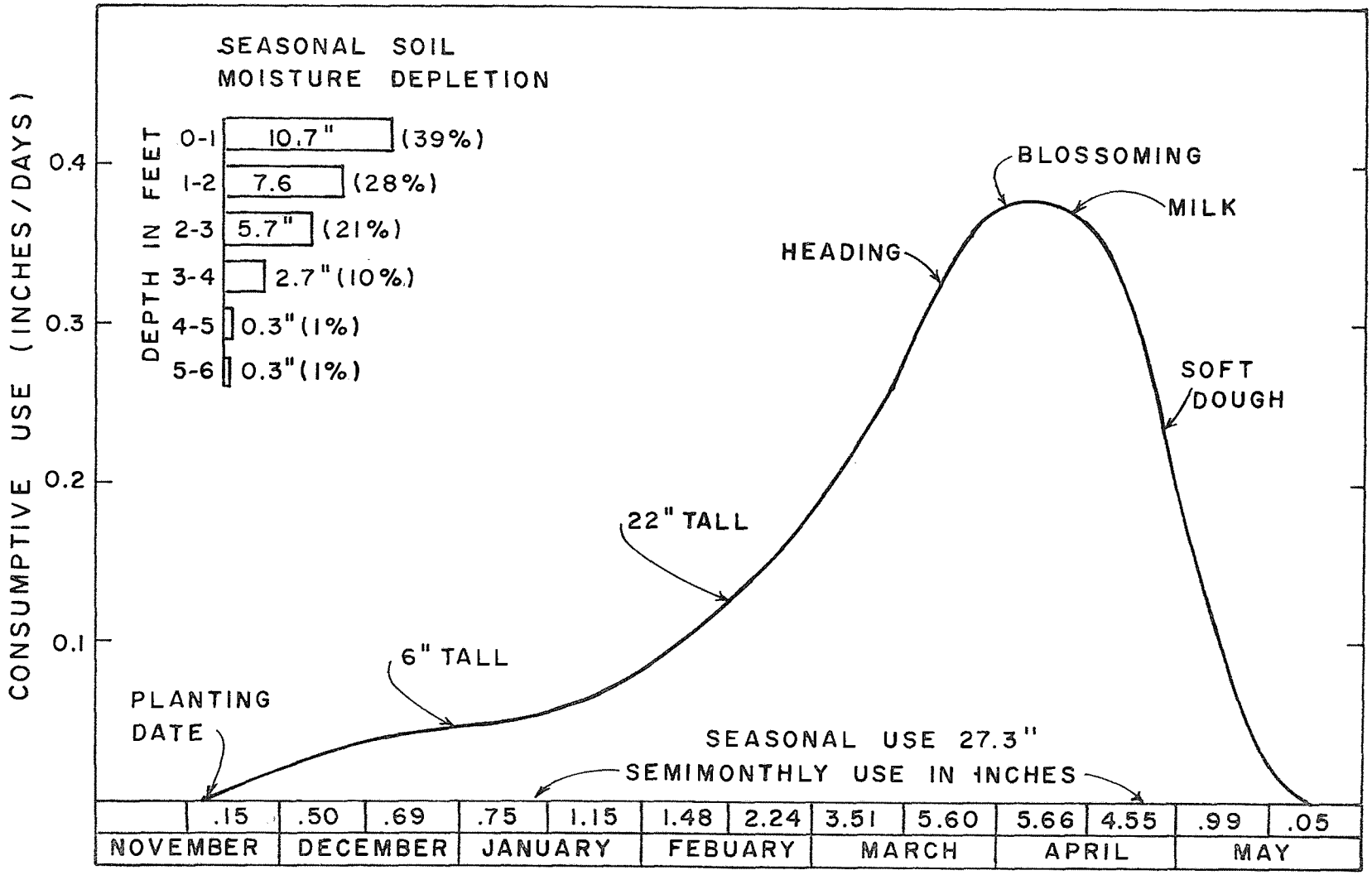

Fig. 2. Consumptive Use for Barley (Arimar) at Mesa, Arizona. 1968-69.

PART II: WATER MANAGEMENT ON NEW, PRESENT-DAY VARIETIES OF COTTON

INTRODUCTION:

For need of study, see Annual Reports for 1957, 1958, and 1966. This year's report is a continuation of the study reported in the 1968 Annual Report as Ariz. WCL 58-2.

OBJECTIVES:

1. To correlate certain meteorological measurements with water management on cotton.

2. To check three irrigation schedules on three present-day cotton varieties.

3. To obtain data on accumulative production of blossoms, bolls, and yield on three varieties of cotton, as affected by three irrigation regimes and an early irrigation cut-off date.

PROCEDURE:

The experiment is located on Field C-1 at the University of Arizona Cotton Research Center, Phoenix, Arizona. The field has been in cotton for the past three years, and alfalfa for two years prior to the cotton.

Cotton stalks from the 1968 crop were plowed under, fertilizer (150 lb/acre of 21-53-0) was applied, and Arivat barley was planted. This was used as a green manure crop to iron out residual effects, as an aid to pink bollworm control, to add organic matter, and to improve intake rates.

Urea was applied to the field on 5 Feb 1969, at the rate of 300 lb/acre, and the barley was plowed under. The field was furrowed out into 40-inch furrows and the pre-plant irrigation was given on 8 March.

On 27 March, a buffer area of 12 rows of Deltapine-16 was planted, beginning on the west side of the field. After the buffer

zone was planted, DPL-16, Hopicala, and Pima S-4 were planted in 4-row plots in a random block design, replicated four times. Within each replication, there were three moisture treatments; 65% (medium) and 50% (wet) moisture used from the top 3 ft. The third moisture treatment (frequent) was given the same quantity of water as the medium treatment, but applications were one-half as much given twice as often. The last 24 rows on the east side were planted equally to Pima S-3 and Pima S-4.

Timing of irrigations on the medium treatment was based on soil moisture determinations. Irrigations on the wet and frequent treatments were also based on these soil moisture samples, but with visual plant symptoms and calendar schedule also entering into the picture.

Two 30-ft lengths of row, beginning 80 ft from the north end of the field in each 4-row plot on replications 1, 2, and 3, were used for tagging of blossoms. Four 12-ft lengths of row, each comprising 16 plants, were selected and designated as quadrants 1, 2, 3, and 4. Blossoms in Quadrant 2 were tagged daily from 15 June until 20 September. Quadrants 2 and 3 were in the upper half of the field.

On 15 August, a border dike was built through the entire study area but specifically through the middle of the tagging area. This was to facilitate an early season cutoff of irrigation water to the lower portion of the field. On 17 August, tagging was begun in Quadrants 1 and 3, and continued in Quadrant 2.

Machine-picked yield measurements were made on 75 ft of the two inside rows of the 4-row plots, on both sides of the border dike which divided the field in half, creating the areas referred to as "upper" and "lower". Additional yield and boll count measurements were made on Quadrants 1, 3, and 4 tagging areas by hand picking.

Atmographs, net radiometers, anemometers, and a hygro-thermograph were installed in a 4-row area between reps. 3 and 4, about 10 June.

Soil moisture depletion measurements were made in two replications of the medium soil moisture treatment on all three varieties.

RESULTS AND DISCUSSION:

A good stand was attained, temperatures were slightly above normal in April and May, and good vegetative growth occurred. Blossoming began around the 15th of June.

On the medium treatment, all irrigations were given when the soil moisture depletion was somewhat greater than the 65% point, actually averaging 81% used, for the four irrigations starting 25 June. However, visual plant symptoms did not indicate that the plants were in a state of severe stress at the time irrigations were given. Specific quantities of irrigation water were applied at each irrigation (Table 4), principally measured with a Sparling meter.

Insect populations were low in the early season, with some lygus damage in late July. Leaf perforator buildup began about three weeks later than in 1968, and was not as prevalent. Some pink bollworm damage was noted late in the season. The field was defoliated twice, on October 1 and 8. This early defoliation affected the late-season boll size, and therefore, overall total yield.

SUMMARY AND CONCLUSIONS:

The original plan was to maintain the medium "M" treatment at a 65% moisture depletion level. The end of the year soil moisture data show that this treatment was irrigated when 81% of the available water was used, thus the medium treatment is really a dry treatment. Defoliation and insect control were discontinued too early to best satisfy this study. This probably did not affect blossom production, but late boll size could have been reduced, especially on the Pima S-4 variety.

A single machine bulk picking was made on 16 December after two defoliations. An additional picking and salvage of cotton from the ground would have probably resulted in an additional

1/4 to 1/2 bale of cotton. Table 5 shows the yields in seed and lint cotton, and the lint percentages. The consumptive use was measured for the "M" plots only. Table 6 shows the lint weights for each half of the field designated by upper and lower. The lower half did not receive irrigation water after 8 August. The upper half did receive one additional irrigation. Inspection of the lint percentages shows there was no difference in lint percentage between different moisture regimes or between the upper and lower half of the field. Lint percentages were down at least 10% for all varieties as compared to other years. Yield differences between moisture levels were very small. If any trend existed, it was toward a lower "M" (81% used) treatment yield; this was especially true for the Pima variety. Plant heights also showed this relationship, i.e. "M" irrigation plots were shortest and "F" plots were tallest.

Upper half yields were always higher than lower half for all varieties and irrigation regimes. These differences reflect the benefit achieved by giving a late August or early September irrigation. Less benefit was achieved by the late irrigation on the wet treatment, probably because this treatment had a greater amount of stored water on 8 August when the last irrigation was given the lower half. The medium treatment (81% used) was very dry on 8 August, therefore, the irrigation given then did not last long enough to completely mature the bolls. The early defoliation could be expected to do more damage to the upper half, thus differences between upper and lower might have been greater if the defoliation had been delayed.

Consumptive use measurements were made only on the medium treatments. For all varieties the consumptive use of 34.4 inches was lower than the long time average for maximum production. If irrigations had been given when 65% had been used from the top 3 feet, a higher consumptive use would have resulted and possibly a higher yield.

Table 7 shows the weight in grams of seed cotton for all tagging quadrants. Q_2 and Q_3 are in the top half and Q_1 and Q_4 are in the lower half, or the half that did not receive the normal September irrigation. This data shows that yields were increased about 22% for the Hopi and Pima by giving an early September irrigation. The Deltapine was increased 10.2%. Less increase was noted for the wet treatment suggesting that an early cut-off may be economically feasible if a wet regime has been maintained or if soils are such that a large amount of water can be stored in early August. Though the medium was overstressed (81% used), it was quite competitive yieldwise. If it had been kept slightly wetter - more like our recommended 65% used - a better boll size would have resulted.

Table 8 shows the blossoms and bolls as counted for the entire flowering season in Quadrant 2. This quadrant was given a late irrigation. The figures are the mean number of blossoms and bolls from 3 replications consisting of 16 plants in 12 lineal feet per plot. The medium treatment (81% used) resulted in the largest number of blossoms for all varieties. The efficiency of bolls from blossoms varied between varieties and irrigation levels. The number of bolls on the sort staple varieties was greater for the medium irrigation level. For the Pima variety, the number of bolls for the frequent irrigation level was less than the other two irrigation levels mainly because there were less blossoms and there were only minor differences in efficiency.

Tables 9 and 10 show the blossoms and bolls after 17 August. Quadrant 2 (Q_2) and Q_3 are in the upper half, while Q_1 is in the lower half (which did not receive a September irrigation). The efficiency of bolls from blossoms was always low for Q_1 or the lower or late season stressed plots. The medium (M) irrigation level resulted in a greater number of blossoms after 17 August than the other irrigation levels (Table 10). The frequent (F)

irrigated treatment had the fewest blossoms. The efficiency of bolls from blossoms was significantly reduced by the stress resulting from the 8 August irrigation cutoff as shown by the lower efficiencies on Q_1 as compared to Q_3. The number of blossoms produced in the two halves of the field were not effected by the late season stress placed on the lower half (Table 10).

It is of importance to know when blossoms open, and how many, to intelligently assess answers to the economics associated with prolonging the cotton growing season. Table 11 shows the flower production up to 17 August, the beginning of the cut-out period, and the flower yield for the remainder of the year, generally referred to as the second set or late season set.

The data shows that differences in number of flowers up to 17 August were not significantly different for any varieties tested. After 17 August the medium treatment put on more flowers than other irrigation regimes. When all varieties under the medium moisture level are added together, the blossoms after 17 August represent over one-fourth of the total blossoms. Though the late season bolls are smaller, a one-fourth increase in the number of pickable bolls could be expected to be significant.

Tables 12 and 13 show the relationship between the bolls from flowers before and after 17 Autust. The number of bolls before 17 August was short 7 days during the cut-out period. Again the number of bolls up to 17 August are nearly equal when comparing quadrants 1 and 3 for all varieties. Moisture levels did not alter the number of bolls opening before 17 August.

The size of bolls seems to be very sensitive to moisture levels. The data in Table 14 show that bolls were smaller for the medium treatment (stressed 81% used) for all moisture levels and varieties in the upper half of the field. The wet treatment had larger bolls in both upper and lower positions of the field

for all varieties. The boll size was reduced by the late season moisture stress on the lower half of the field for all varieties and moisture levels.

PERSONNEL: Leonard J. Erie and Orrin F. French

CURRENT TERMINATION DATE: December 1970

Table 4. Irrigation Schedule for Cotton - 1969

Irrigation Treatments	Irrigation Dates											
	5/26	6/11	6/25	7/3	7/8	7/15	7/22	7/28	8/7	8/19[a]	8/26[a]	9/3[a]
Wet	4[b]	3	5		6		5		6		5	
	W[c]	W	R[d]		R		W		R		W	
Medium	4		6			6			6			6
	W		R			R			R			W
Frequent	4	3	3	3		3		3	3	3		3
	W	W	R	W		R		W	R	W		W

(a) Upper half of field irrigated, only.

(b) Numbers refer to inch/application.

(c) Well (W)

(d) River (R)

Table 5. Yield and Consumptive Use of Water by Cotton, 1969

Varieties & Regimes	Irrigations	Seed[a]	Lint	Lint[a]		Consumptive Use
	No.	lb/plot	%	lb/plot	bales/acre	Inches
Hopi						
Wet (U)[b]	7	27.44	35.9	9.85	1.72	----
Wet (L)[c]	6	26.44	36.5	9.65	1.68	----
Medium (U)	5	27.31	35.5	9.70	1.69	33.8
Medium (L)	4	23.81	35.8	8.52	1.48	----
Frequent (U)	9	28.94	36.0	10.40	1.81	----
Frequent (L)	7	26.50	36.0	9.54	1.64	----
DpL-16						
Wet(U)	7	42.25	36.2	15.29	2.66	----
Wet (L)	6	39.88	36.0	14.36	2.50	----
Medium (U)	5	42.31	35.9	15.19	2.65	33.3
Medium (L)	4	34.38	35.9	12.34	2.15	----
Frequent (U)	9	43.17	36.4	15.71	2.74	----
Frequent (L)	7	39.00	35.4	13.81	2.41	----
Pima S-4						
Wet (U)	7	26.00	34.0	8.84	1.54	----
Wet (L)	6	25.38	33.4	8.48	1.48	----
Medium (U)	5	24.06	32.8	7.89	1.37	33.3
Medium (L)	4	19.88	33.2	6.60	1.15	----
Frequent (U)	9	25.63	33.4	8.56	1.49	----
Frequent (L)	7	22.63	32.8	7.42	1.29	----

[a] Mean of 4 replications

[b] Upper half of field

[c] Lower half of field

Table 6. Lint Cotton Weight Difference Between Upper and Lower Halves of Plots. (Average of Four Replications).

Moisture Level	Upper [a] (Pounds)	Lower [b] (Pounds)	Increase Due to Extra Irrigation (Percent)
		Hopi	
Wet	9.85	9.65	2.1
Medium	9.70	8.52	13.8
Frequent	10.40	9.54	9.0
		Dpl-16	
Wet	15.29	14.36	6.5
Medium	15.19	12.34	23.1
Frequent	15.71	13.81	13.8
		Pima S-4	
Wet	8.84	8.48	4.2
Medium	7.89	6.60	19.5
Frequent	8.56	7.42	15.4

[a] Late irrigation given.

[b] Early irrigation cut-off.

Table 7. Weight (grams) of Seed Cotton for All Tagging Quadrants.
(3 replications, 16 plants/12 lineal feet per plot)

Irrigation Regimes	Upper		Total Upper	Lower		Total Lower	Percent Increase Due to Extra Irrigations
	Q_3	Q_2		Q_1	Q_4		
				Hopi			
Wet	3579.8	3984.2	7564.0	3469.5	3605.8	7075.3	6.9
Medium	3733.4	4399.6	8133.0	3350.0	3315.1	6665.1	22.0
Frequent	3668.8	3787.4	7456.2	3363.9	3260.3	6624.2	12.6
				DpL-16			
Wet	4958.9	4713.8	9672.7	4638.3	4643.1	9281.4	4.2
Medium	5425.7	4996.9	10422.6	4670.9	4790.5	9461.4	10.2
Frequent	4984.6	5064.8	10049.4	4527.7	4402.0	8929.7	12.5
				Pima S-4			
Wet	3194.3	3413.3	6607.6	3126.6	2969.0	6095.6	8.4
Medium	3275.6	3298.9	6574.5	2777.2	2629.7	5406.9	21.6
Frequent	3125.1	3196.1	6321.2	2905.0	2859.3	5764.3	9.7

Table 8. Number of Blossoms and Bolls in Quadrant Two for the Period 15 June to 20 September (3 replications, 16 plants/12 lineal feet per plot)

	Wet (7 Irrigations)[a]			Medium (5 Irrigations)[a]			Frequent (9 Irrigations)[b]		
	Hopi	DpL-16	Pima S-4	Hopi	DpL-16	Pima S-4	Hopi	DpL-16	Pima S-4
Blossoms	2605	2653	2713	2933	2713	2795	2481	2564	2566
Bolls	760	1065	1371	849	1136	1339	730	1108	1254
Efficiency	29.2	40.1	50.5	28.9	41.9	47.9	29.4	43.2	48.9

[a] Tagging of blossoms not accomplished for 6 days due to insecticide spray.

[b] Tagging of blossoms not accomplished for 7 days due to insecticide spray.

Table 9. Blossoms and Bolls After 17 August
(3 replications, 16 plants/12 lineal feet per plot)

	Wet			Medium			Frequent		
	Blossoms	Bolls	Efficiency	Blossoms	Bolls	Efficiency	Blossoms	Bolls	Efficiency
Hopi									
Q_1	620	194	31.3	772	210	27.2	472	184	39.0
Q_2	670	227	33.9	966	358	37.1	657	205	31.2
Q_3	547	179	32.7	833	273	32.8	547	188	34.4
DpL-16									
Q_1	469	161	34.3	607	188	31.0	356	96	27.0
Q_2	547	251	45.9	562	239	42.5	328	164	50.0
Q_3	428	190	44.4	759	305	40.2	401	130	32.4
Pima S-4									
Q_1	540	285	52.8	688	280	40.7	499	246	49.3
Q_2	516	301	58.3	598	300	50.2	383	205	53.5
Q_3	578	340	58.8	711	382	53.7	491	264	53.8

[a] Quadrant 1 (Q_1) in lower and Q_2 and Q_3 in upper half of field

Table 10. Number of Blossoms After 17 August
(3 replications, 16 plants/12 lineal feet per plot)

Irrigation Level	Q_1 [a]	Q_3 [b]	Q_2 [b]
	Hopi		
Wet	620	547	670
Medium	772	833	966
Frequent	472	547	657
Total	1864	1927	2293
	DpL-16		
Wet	469	428	547
Medium	607	759	562
Frequent	356	401	328
Total	1432	1588	1437
	Pima S-4		
Wet	540	578	516
Medium	688	711	598
Frequent	499	491	383
Total	1727	1780	1497

[a] Quadrant 1 in lower half of field

[b] Quadrants 2 and 3 in upper half of field

Table 11. Total Blossoms for Quadrant Two

Variety	Wet	Medium	Frequent
	Before 17 August[a]		
Hopi	1913	1932	1824
Deltapine-16	2070	2112	2236
Pima S-4	2152	2134	2183
	After 17 August		
Hopi	670	966	657
Deltapine-16	547	562	328
Pima S-4	516	598	383
	Total Season[a]		
Hopi	2583	2898	2481
Deltapine-16	2617	2674	2564
Pima S-4	2668	2732	2566

[a] Seven days were not tagged during this period

Table 12. Bolls From Blossoms Opening Before 17 August[a]
(3 replications, 16 plants/12 lineal feet per plot)

Irrigation Level	Quadrant	
	Q_1	Q_3
	Hopi	
Wet	568	572
Medium	549	514
Frequent	575	609
Total	1692	1695
	DpL-16	
Wet	908	922
Medium	948	997
Frequent	968	1009
Total	2824	2928
	Pima S-4	
Wet	1038	1050
Medium	1016	1051
Frequent	1017	1098
Total	3071	3199

[a] Information for Q_2 not included for comparison because tagging was not accomplished for 7 days

Table 13. Bolls from Blossoms Opening After 17 August
(3 replications, 16 plants/12 lineal feet per plot)

Irrigation Level	Quadrant		
	Q_1	Q_3	Q_2
	Hopi		
Wet	194	179	227
Medium	210	273	358
Frequent	184	188	205
Total	588	640	790
	DpL-16		
Wet	161	190	251
Medium	188	305	241
Frequent	96	130	164
Total	445	625	656
	Pima S-4		
Wet	285	340	301
Medium	280	382	300
Frequent	246	264	205
Total	811	986	806

Table 14. Boll Size Comparing Quadrant One with Quadrant Three (grams)

	Wet	Medium	Frequent
		Hopi	
		Total Growing Season[a]	
Upper (Q_3)	4.61	4.49	4.47
Lower (Q_1)	4.44	4.32	4.38
		Pre- 17 August[b]	
Upper (Q_3)	4.92	4.77	4.47
Lower (Q_1)	4.86	4.57	4.38
		DpL-16	
		Total Season[a]	
Upper (Q_3)	4.37	4.09	4.32
Lower (Q_1)	4.23	4.07	4.20
		Pre- 17 August[b]	
Upper (Q_3)	4.73	4.52	4.52
Lower (Q_1)	4.57	4.39	4.38
		Pima S-4	
		Total Season[a]	
Upper (Q_3)	2.28	2.25	2.26
Lower (Q_1)	2.34	2.12	2.24
		Pre- 17 August[b]	
Upper (Q_3)	2.37	2.38	2.26
Lower (Q_1)	2.50	2.25	2.38

[a] Each figure an average of over 1000 bolls

[b] Each figure an average of approximately 850 bolls

TITLE: DYNAMIC SIMILARITY IN ELBOW FLOW METERS

CRIS WORK UNIT: SWC 019-gG-3 CODE NO.: Ariz.-WCL 60-2

INTRODUCTION:

See Annual Report for 1968.

The project is now completed. The results have been analyzed and reported in two publications and a discussion. The first paper, "Evaluation of pipe elbows as flow meters" (September 1966), was published in the Journal of the Irrigation and Drainage Division, ASCE, Vol. 72, No. 3. Discussions by J. M. Robertson and M. A. Gill followed in Vol. 93, No. IR1:158-161 and No. IR3:75-76. A reply to the discussions was prepared and published in Vol. 94, No. IR3: 335-339.

A second manuscript, "Modifications of elbow meters to totalize flow," has been submitted to the same jounral.

PROCEDURE:

No new data was collected. Analysis of previous data was completed and reviewed in the process of preparing the second manuscript mentioned above.

RESULTS AND DISCUSSION:

The manuscript on "Modification of elbow meters to totalize flow" presents the same basic mathematical analysis of shunt meters as flow totalizers for elbow meters that was previously given (see Annual Report, 1968). It outlines the expected sources and magnitudes of error, describes how to select the proper size of shunt meter to match the elbow pressure range, offers suggestions on preparing the elbow pressure taps, and outlines the field calibration techniques in detail.

Laboratory evaluation of the meter indicates that an accuracy equal to the accuracy of the elbow meter itself ($\pm$ 3%) is possible. It is probable that $\pm$ 5% is more realistic under field conditions.

SUMMARY AND CONCLUSIONS:

The project has been completed and the results have been analyzed. During the process of this investigation, a number of flanged, 90^{o}, commercial elbows of several sizes ranging from 3 inches to 12 inches in diameter were calibrated as elbow flow meters. The accuracy to which a calibration equation can be predicted using only the nominal elbow size and the average calibration results of several similar elbows was determined to be $\pm$ 5%. The accuracy can be improved to $\pm$ 3% if precise measurements of the elbow diameter and radius of bend are obtained and incorporated into the calibration equation. A relatively simple and inexpensive method for accurately determining the radius of bend with casting plaster was used.

The effects of installing the elbow downstream from other piping components was studied. In general, 20 diameters of straight pipe upstream from the elbow was sufficient to reduce the effects of other components on the calibration to less than 1%. Components downstream from the elbow produced insignificant effects on the calibration.

A second phase of the study involved the conversion of the elbow meter, which is basically a rate meter, into a flow totalizing meter. Recently available inexpensive water meters of the turbine-type intended for municipal use in household metering are well suited for use as shunt meters across differential head devices such as elbow meters. This permits low-cost conversion of a rate meter into a totalizing meter. Methods and techniques for properly selecting the elbow size and preparing it to produce a shunt-flow rate compatible with the working range of the shunt meter were developed. The result is an inexpensive totalizing meter with an

error less than ± 5%. The metering system is most suited to clean flows such as those normally pumped from wells.

PERSONNEL: J. A. Replogle

CURRENT TERMINATION DATE: December 1970

TITLE: PLANT RESPONSE TO CHANGES IN EVAPORATIVE DEMAND AND SOIL WATER POTENTIAL, AS SHOWN BY MEASUREMENTS OF LEAF RESISTANCE, TRANSPIRATION, LEAF TEMPERATURE, AND LEAF WATER CONTENT

CRIS WORK UNIT: SWC-019-gG-3 CODE NO.: Ariz.-WCL 62-10

PART I. THE WATER USE EFFICIENCY OF AGAVE AND OPUNTIA PLANTS IN THE DESERT

INTRODUCTION:

The Annual Report for 1968 outlined the procedure for the field experiment with two succulent species. The objective was "to measure the water use efficiency under two levels of soil water content: (a) a low level, as governed by the natural rainfall and perhaps by a minimal amount of supplementary irrigation, and (b) a higher level provided by a somewhat greater amount of irrigation, sufficient to promote rapid growth." At present, only part (b) has been attained, since the overall growth has not been considered sufficient to initiate the dry treatment.

RESULTS AND DISCUSSION:

Irrigation. At planting, a heavy irrigation was given, 75 mm of water pumped from the reservoir which is at the north edge of the experimental area. This was to firm the soil around the plants, to help leach salt downward, and to store moisture in the soil for encouragement of adequate rooting. This first irrigation was followed in two weeks by a 40-mm irrigation on 28 October 1968.

During the year a total of 16 irrigations (including the two just mentioned) added 435 mm of water to the 251 mm of accumulated rainfall (through 9 October 1969) for agave; there were two less irrigations for opuntia. This resulted in a total water application of 686 mm for agave and 626 mm for opuntia. Monthly distribution of irrigation and rain is shown in Table 1. Most irrigations consisted of a 20-mm application from a garden hose, measured with

an accurate water meter (400 liters applied to a plot area of 20 m^2, with a measurement precision of 1 liter). Such a small amount at a time minimized deep percolation, but necessitated moving the hose to different locations within each plot to obtain uniform water spreading during the 10-minute application period.

Preliminary observations indicate that the root systems of both species have remained quite shallow, many roots not being any deeper than 15 cm below the soil surface. It would further enhance water use efficiency if an individual irrigation were reduced to a mere 10-mm application. Plans are being made to utilize sprinkler irrigation in order to make such a reduction possible and still apply water homogeneously. However, this is with the proviso that no salinity or specific ion effects appear. In recent weeks five stem segments from three different plants have fallen off, after having developed a surface necrosis. The sodium-adsorption ratio (SAR) of the saturation extract from soil near the base of the affected plants was high enough to be a possible cause of concern. Appropriate leaching may have to be carried out.

The potential development of a salinity or sodium problem due to the minimal level of irrigation, and consequent negligible amount of deep percolation, may impose a limit as to how much reduction can be achieved in total application per year.

Soil Water Content. Weekly measurements were made with a neutron meter in an access tube at the center of each of the four plots. Readings were taken at the following depths: 4, 24, 44, 64, 84, 104, 124, and 144 cm. Although the first depth was much too shallow to give a true reading of the soil water content, the readings varied in the expected direction with changes in soil moisture. Most emphasis was placed on the data from the 24-cm depth, where root activity would be most likely. Here the soil water content, θ_v, percent by volume, tended to remain at 12.5%, due to rains and timely irrigations. However, in April θ_v

ranged down to the minimum for the whole year, despite 20-mm irrigations on 09 and 24 April, an amount usually sufficient to restore θ_v to about 20%. This minimum, 8%, was equivalent to a soil water tension (SWT) of 8 bars, as read from the soil water characteristic curve for a composite sample of soil taken from the experimental site. The standard pressure plate - pressure membrane method was used to develop the curve. Conversion of percentages by weight to a volume basis was by means of bulk density (B.D.) taken in plot nos. 1 and 2. An Alabama sampler was used to measure B.D. in 15-cm increments from the surface to a maximum depth of 60 cm. The average B.D. for the 8 samples was 1.80 g cm^{-3}.

The 1/3-bar percentage was 22.9, a value somewhat higher than the maximum θ_v measured immediately after the irrigation water receded from the soil surface. The most prevalent water content at the 24-cm depth, θ_v = 12%, corresponded to a SWT of 1.3 bars. At such a water content 66% of the available water has been depleted. Although this regime brought about good growth during the first year, it is believed feasible to maintain a somewhat higher soil water content by increasing the irrigation frequency. If θ_v could be maintained at no less than 15%, tensiometers could be used without going off scale. Such a regime might be attempted for a "wet" treatment, to contrast with a "dry" treatment wherein SWT attained the 15-bar value (θ_v = 7.8 percent) before irrigation.

Plant Growth. A. Agave: When transplanted, on 10 and 11 October 1968, the agaves had from 10 to 20 leaves and an average fresh weight of 1100 g. At this time the spine at the tip of each leaf was clipped off, thus facilitating recognition of new growth, as indicated by the presence of a spine. In the 38 weeks from planting until 24 July 1969, the 24 agaves in plot no. 1 developed 118 new leaves, those in plot no. 4 122 leaves, giving a

growth rate of 3.1 and 3.2 leaves per week per plot, respectively. From 24 July to 16 October the rate increased to 5 leaves per week per plot in plot no. 1 versus 3.9 for plot no. 4. Paradoxically, the two rows constituting the half of the plot in which the plants were set out with no roots developed 41% more leaves than those with roots initially. For the whole year the agaves formed 173 new leaves in plot no. 1 and 165 in plot no. 4. Unfortunately there is no means of converting the increase in leaf numbers to a gain in fresh or dry weight. Obtaining the dry weight increment will have to be deferred until a later date, when the plants are large enough to be thinned out by removal of alternate plants. A few senescent or dead leaves at the base of the plants were trimmed off on 16 October and retained for a future cumulative value for dry weight production per plot. The oven-dry weight of these leaves ranged from 2 to 50 grams.

Plant Growth. B. Opuntia: Ten of the 12 plants originally transplanted in each of two plots on 9 and 10 October 1968 were cuttings without roots or buds. The other two were established plants with the original stem segment (pad) and two additional pads. The initial average fresh weight of the plants in plot no. 2 was 684 g, and for plot no. 3 674 g. In a year the plants in plot no. 2 developed 32 new pads, as compared to 43 in plot no. 3.

Four plants were damaged somewhat by rodents until a fence was built. Also, later in the year one or two pads on each of three plants developed a necrosis which has been correlated with a high level of sodium in the saturation extract of soil taken near the base of the affected plants. The necrosis apparently was severe enough in two instances to cause the pad to drop off the plant. However, these difficulties resulted in only a small loss in total growth. When the buds form again, growth should occur geometrically in comparison to the beginning of the previous season, when only a single pad was present (at 10 of the 12 locations per plot).

Increasing the frequency of irrigation may alleviate the excess sodium condition in the opuntia plants. Special attention will be given to maintenance of a low SWT when buds are enlarging.

SUMMARY AND CONCLUSIONS:

The agaves made good growth during the past year, having produced 169 new leaves (mean of two plots) from the 24 plants in the 20-m^2 plot. This was accomplished with the comparatively small quantity of 686 mm of water added to the plot in the form of rainfall and irrigation water. Timely irrigations succeeded in maintaining a low soil water tension (SWT) in the root zone in all four plots (two each for agave and opuntia), the prevalent value being 1.3 bars, rising to about 8 bars only in April. The SWT was inferred from weekly measurements of soil water content by a neutron meter, by reference to the soil water characteristic curve for the Granite Reef sandy loam soil from the experimental area.

The opuntias also grew well, and on 60 mm less water than the agaves. The single pad initially present at 10 of the 12 locations per plot increased to an average of 4 pads in one year. This was in spite of the loss of several pads due to rodent damage and an apparent excess of sodium in the soil around a few plants.

It is concluded that during the next year essentially the same procedure should be followed as before, except for increasing the frequency of irrigation somewhat, while reducing the amount per irrigation from 20 mm to 10 mm whenever feasible. If the growth rate continues to be adequate, it is anticipated that the "dry" treatment can be started in 2 or 3 months, wherein SWT will be allowed to reach 15 bars before irrigation in one plot each of agave and opuntia. In contrast, the "wet" treatment will not be permitted to attain a SWT greater than 1 bar. These treatments will determine the effect of plant water stress on water use efficiency of two succulent plant species.

PART II. THE TRANSPIRATION RATIO OF AGAVE AND CORN PLANTS AS AFFECTED BY LOW SOIL WATER POTENTIAL

INTRODUCTION:

A previous greenhouse experiment demonstrated a water use efficiency of agave twice that of corn, when soil water was freely available (the transpiration ratio being 70 vs. 136, respectively). It was of interest to find out whether this high efficiency could be further enhanced by imposing a plant water deficit due to soil drought.

PROCEDURE:

Six agave offshoots (Agave americana) weighing about 150 g each were transplanted to 1-gallon glazed pots of a standard soil mixture. The plants were grown for 11 months, during which time sufficient leaf development occurred to increase the transpiration rate from 10 to 125 g/plant/day. Watering, maintenance of soil fertility, avoidance of salt accumulation, and estimation of the total soil water potential, ψ_T, were in accordance with a modification of the standard technique described in the 1967 Annual Report. For 11 months all pots were treated as a "wet" series, in which the soil matric potential, ψ_M, as measured with a tensiometer, ranged from 0.02-0.04 bar at "pot capacity" to 0.2 bar at irrigation, when 64% of the available water had been depleted. In this report the negative sign will be omitted for values of ψ_M and ψ_T, so that the drier the soil, the greater the numerical value of potential.

On 19 December 1969, 10-day old corn seedlings (Zea mays cv. Mexican June) were transplanted into six 1-gallon pots and treated in the same manner as the agaves, except for a shorter establishment period, two months. Measurements of the growth rate were started on 4 February. The "dry" treatment began four days later for three pots of corn, at which time the cumulative transpiration per pot had attained 717 g, a loss corresponding to ψ_M = 0.2 bar. When cumulative transpiration had attained 972 g/pot, a loss corresponding to

ψ_M = 1 bar, the plant was reirrigated. Depending on the leaf area and evaporative demand, the drying cycle lasted for from 4 to 36 hours. In the 1-month treatment period there was a total of 10 such cycles.

The corn was harvested shortly after tassels had emerged, at which time measurements were made of fresh and dry weights of leaves, stalks, and roots. Two days before harvest hourly measurements were taken of the transpiration rate, followed at harvest by determination of the leaf area per plant.

For agave, the dry treatment began at the same water loss as for corn, 717 g/pot, but extended to and much beyond the 15-bar percentage soil water content. After the drying cycle was started, there was no further watering of the agaves for several weeks. The one irrigation that broke the long period of soil drought again was followed by a 2-month drought, after which the plants were harvested. Fresh and dry weight of shoot and roots were obtained, in addition to measurements of the total water potential of plant and soil.

RESULTS:

Corn. As shown in Figure 1, the growth rate of corn plants, as measured by increase in height, was slowed down due to plant stress induced by a soil matric potential of 1 bar. This was equivalent to a total soil water potential of 3 bars. The general downward trend became more pronounced with time, although undergoing transient reversals following irrigations.

Although interpretation of the results is complicated by intervals of cloudy weather, it appears that both growth and transpiration were affected simultaneously by a soil water deficit. However, growth was more responsive than transpiration, undergoing wider fluctuations due to changing stress. At the end of the experiment both processes were depressed more than 50% due to the dry treatment.

Such a depression of transpiration was due partly to stunting, since the final leaf area of plants on the dry treatment was 19% below that of the control. That plant stunting was not the only factor responsible for depressed transpiration is shown by Figure 2. The 23% transpiration reduction in the dry treatment occurred even on an equal leaf area basis, leading one to implicate stomatal closure as the mechanism for reduced water loss. Apparently stomatal closure was not sufficient to negate the powerful influence of solar radiation on transpiration, since there was no significant difference between the correlation coefficients for the wet and dry treatments in the regression of transpiration on irradiance (0.94 vs. 0.86 respectively). This probably would not be true if a greater soil water deficit had been allowed to develop.

On the dry treatment corn made less efficient use of water than on the wet one (Table 2). The transpiration ratio for plants with freely available water, 134, is quite low, and in excellent agreement with the value (136) obtained in a previous greenhouse experiment carried out under quite comparable conditions. A soil water deficiency encompassing only 10 drying cycles in which ψ_M = 1 bar, generally for only a short time at each cycle, nevertheless depressed the dry weight gain by 50%. However, transpiration was reduced only 40%; hence - the higher transpiration ratio, 161.

Since dry weight gain, a function of photosynthesis, was reduced more than transpiration, it appears that stomatal closure was not the only means by which dry soil reduced water use efficiency. Photosynthesis may have been reduced not only by decreased absorption of carbon dioxide through partially closed stomates, but also by protoplasmic dehydration occurring even with open stomates.

Agave. Plants on the dry treatment gradually depleted the available soil water, and transpired progressively less than those on the wet treatment, although starting at a slightly higher rate (Figure 3). By early March all available soil water had been

depleted; yet relative transpiration at that time had fallen only to 0.29. The plants maintained a slow transpiration rate for several more weeks, the relative rate finally falling to its minimum of 0.03. The absolute rate at this time was 3-5 g/plant/day. The vapor barrier over the soil surface was considered sufficiently good to eliminate evaporation as a component of the weight loss, but this cannot be certified, in view of such small losses and a weighing precision of $\pm$ 1 gram.

At this time the plants on the dry treatment had lost a total weight of 1568, 1523, and 1513 g respectively, for a mean weight loss of 1535 g. If this is considered to represent the amount of transpiration, it exceeds the available water in the soil by 417 g, provided the 15-bar soil matric potential value is used as the lower limit of available water. Even if the 200-bar value is assumed to represent a more realistic lower limit, this would provide only 182 g more water to the plant. The conclusion is reached that at least 235 g of water was removed from the plant's own tissues.

On 21 April the three pots of the dry treatment were irrigated to the pot capacity value (ψ_M = 0.02-0.04 bar) and then were put on another drying cycle lasting until harvest in early July. The remarkable recovery is shown in Figure 3, where relative transpiration rises rapidly from 0.05 to 0.84 in three days. A value of 1.0 was not achieved presumably because of the stunting that occurred during the first drying cycle. However, sufficient growth had taken place even in the dry treatment for the absolute rate to be 69 g/plant/day after the drought-breaking irrigation, as compared to 45 g/plant/day at the start of the first drying cycle.

At harvest three full-length core samples from each pot were taken from the soil of the dry treatment, composited, and measured for the equilibrium relative humidity (R.H.) with an Aminco wide-range hygrometer. From the measured R.H. values ψ_T was calculated. The same type of measurements was made with the agave leaves, too,

but without success, due to sensor insensitivity in the high range of R.H.

Determination of the gravimetric water content of the soil at harvest permitted an alternate measurement of ψ_T, by later calibration of known low soil water contents against R.H. as measured with the hygrometer. This calibration procedure extended the soil water characteristic curve from the 15-bar value obtained on the pressure membrane to 887 bars, the value for air-dry soil. Use of this extended curve established that ψ_T at harvest, when relative transpiration had remained rather steady at 0.03 was as follows: 102, 128, and 182 bars for the three dry soil treatments. Even in the case of the pot having the lowest ψ_T, 102 bars, the additional water extracted from the soil amounted to 138 g beyond the conventional wilting point value. However, calculations show that this total available water still lacked 267 g of balancing the total cumulative loss. Presumably the difference came from the plant's own tissues. As confirmation of this hypothesis, the percentage water, on a fresh weight basis, was as follows: leaves, wet treatment 84-87; dry treatment, 74-77; roots, wet, 81-83; dry, 35-37.

The transpiration ratio was almost identical for the agaves, regardless of treatment, 114 for the wet vs. 116 for the dry (Table 3). The reason is that both transpiration and dry weight gain were reduced 54% by the extended period of soil water depletion. This is in contrast to the results for corn.

SUMMARY AND CONCLUSIONS:

A greenhouse experiment verified previous results: (1) With freely available soil water the transpiration ratio (TR) for corn was low, 136 vs. 134 in two experiments, (2) The TR for agave was even lower, 70 and 114, respectively. The second part of the most recent experiment extended these data to determining the effect of a dry treatment on TR. Soil water depletion reduced water use efficiency in corn (raised TR from 134 to 161) but caused no change

in agave. The dry treatment for corn consisted of 10 cycles of soil water stress wherein ψ_M reached 1 bar (ψ_T 3 bars) before reirrigation restored low stress conditions (ψ_M = 0.02-0.04 bar). For agave the dry treatment lasted for 5 months, except for one drought-relieving irrigation near the middle of the period.

Gradual soil water depletion occurred until ψ_T reached 100^+ bars, at which time the relative transpiration (dry treatment as a fraction of the wet treatment) sank to its minimum of 0.03. Extension of the soil water characteristic curve all the way to the air-dry value, 887 bars, enabled the soil water content in the agave pots in the dehydrated state to be converted into equivalent ψ_T values. These data showed that in addition to extracting water to a point at which $\psi_T = 100^+$ bars, agave plants partially dehydrated their own tissues as they adapted to and survived the long drought. The rapid recovery from the dehydrated condition was demonstrated by an increase in relative transpiration from 0.05 immediately before irrigation to 0.84 in three days.

Since the dry treatment reduced the dry weight gain of corn more than transpiration, it appears that a soil-induced tissue dehydration may impair photosynthesis not only by partly closing stomates and thus reducing the supply of carbon dioxide, but also by desiccating the photosynthetic apparatus or associated tissues.

PART III. PLANT RESPONSE TO SOIL WATER DEPLETION UNDER A CONSTANT EVAPORATIVE DEMAND

INTRODUCTION: The 1967 Annual Report describes in detail a standard procedure developed for studying the mechanism of transpiration control under carefully regulated environmental conditions. The hypothesis underlying the research is that there are ecologically important species differences in a plant's ability to limit transpiration losses, and that an understanding of these differences may lead to a greater water use efficiency than now exists in the important agronomic crops. The 1967 report gave results for the bean plant; the present report deals with a similar experiment carried out with the lemon plant.

PROCEDURE: The standard technique was utilized. Briefly, it consists of growing the plant in the greenhouse in a 2-ℓ pot of standard soil mixture to a stage at which there is adequate leaf area to sustain a high transpiration rate, and at which root permeation of the substrate is thorough. The plant is taken to a controlled environment room, irrigated to "pot capacity," equilibrated overnight, then subjected to gradual illumination, and permitted to deplete the available soil water by continued transpiration until a deficiency begins to activate stomatal closure. Various sensors are used to monitor the plant's drought responses. One long day of such a test essentially duplicates a field experiment requiring three or four weeks. Environmental factors held steady are light, air temperature, humidity and carbon dioxide content, and wind speed.

The two experimental plants had five and eight branches, respectively, five of which were monitored on each plant. Five leaves, one from each branch, had thermocouples installed in the leaf midrib; the leaves were about 40 cm up from the pot lid, near the top of the plant, where illumination was 90 kilolux, (well over the saturation value for stomatal opening). Leaf temperature was

recorded on a 16-point recorder every eight minutes. The temperature of one of the five leaves from each plant was duplicated on another recorder, which gave alternate 1-minute readings that could be followed visually on a strip chart. On the plant in soil the same five leaves having thermocouples also were monitored periodically for leaf resistance (R_L) readings by means of a meter. Each plant was on a balance; half-hourly weight loss determinations gave the transpiration rate, the soil or water surface being covered to minimize evaporation. Air temperature was controlled at 30 $\pm$ 0.3° C, vapor pressure 15 $\pm$ 0.2 mb, carbon dioxide level of the air 350 $\pm$ 10 ppm, irradiance 1.04 $\pm$ 0.01 ly min^{-1}. The measurements were continued until the transpiration rate of the plant in soil was reduced by 50% of the initial rate in well watered soil. A mercury manometer tensiometer installed 1 cm off the bottom of the pot permitted periodic readings of the rise in soil matric potential (ψ_M) as soil water depletion progressed.

RESULTS AND DISCUSSION:

Transpiration. The plant in nutrient solution was the reference plant for comparing the rise in leaf temperature under two contrasting conditions, one in which water always was freely available, and one in which prolonged transpiration depleted the available soil water. The hypothesis was that transpiration of the plant in nutrient solution would continue at the potential rate indefinitely, and with no increase in leaf temperature. On the other hand, it was expected that as the plant in soil depleted the available water, leaf temperature would rise at the same time that transpiration declined. In order for this hypothesis to be valid, however, both plants should not be exposed to abrupt changes in illumination. Since the mercury vapor lamps were turned on gradually over the period from 0500 to 0800, the plants were exposed to the increased light level in about the same manner as in nature. As shown in Figure 4, however, apparently not all the stomates were

open until 0900, at which time the potential rate of water loss was first attained. This rate did last for many hours, as hypothesized. At 1330, however, a rate about 5% lower set in, without any change in the aerial environment. From 1500 on a further slight decline ensued. Verification of this is given by the leaf temperature (T_L) of the plant in nutrient solution (Figure 7A). From 1345 to 1445 T_L rose one degree from the rather stable value of 35 C that had prevailed during the previous five hours. It is possible that the steady rise in the temperature of the nutrient solution (T_S) might have impaired water absorption, since T_S rose from 31 C at 0820 to 35 C at 1330. However, it is rather unlikely that 35 C is high enough to affect water absorption of citrus roots significantly. It may be that an autonomic rhythm in stomatal aperature was responsible for the change. If stomatal aperture tends to narrow in early afternoon, the consequent lesser evaporative demand in the presence of a high radiant load would cause a rise in T_L.

The plant in soil started to transpire at the potential rate at 0730, one-half hour before there was full illumination. This is confirmation of the statement made earlier, that the light level of this experiment (90 to 104 kilolux, depending on the amount of shading by other leaves) was more than the saturation value for stomatal opening. The potential rate continued for three hours, after which the first indication of plant control of water loss was evident (Figure 5), as shown by the deviation of the actual rate from the straight line course followed earlier. At 1030 ψ_M had risen only to the low value of 148 mb. However, it should be kept in mind that the evaporative demand was high, and that all of the roots were contained in a rather small volume. The potential rate for the plant in soil, 49 g/hour, was not significantly different from that of the plant in nutrient solution, when compared on a leaf area basis (236 vs. 231 $g/m^2/hr$, respectively), thus verifying the statement that a soil at a high water potential (well watered) can supply

water fully as well as a water culture.

At 1400, when transpiration had declined 50% due to soil water depletion, ψ_M had climbed to 319 mb, a value equivalent to a total soil water potential of 1.4 bars.

Reirrigation at 1400 threw the plant into a cyclic behavior, in which the stomates opened and closed with a vigor not usually apparent. These oscillations continued for many hours, finally being brought to a halt when the lights were turned off. As shown in Figure 6, the rate during this period was only 45% of the potential rate, even though enough water had been added at 1400 to restore the soil water content to the value at the start of the experiment (ψ_M = 40 mb). This was due to the very complete stomatal closure during approximately one-half the time of cycling.

Leaf Temperature. The slight rise in T_L of the plant in nutrient solution has already been mentioned. Although this was unexpected, it still was small in comparison to the 4-degree rise occurring in the plant in soil. Significantly, most of the rise in T_L of the soil-grown plant took place after 1030, the time at which transpiration first began to decline below the potential rate. The rise in T_L is interpreted as an indirect consequence of partial stomatal closure, where lesser evaporative flux from the stomates dissipates less of the constant heat load, and thus leads to a rise in T_L. Soil temperature rose 5.5 degrees over the whole period, despite heavy insulation around the pot. This was unfortunate, but probably does not constitute sufficient interference to invalidate the above results and conclusions. When the lights were turned off, T_L of both plants rapidly plunged to lower levels, thus demonstrating the overwhelming importance of radiant load on T_L (Figure 7B).

Leaf Resistance. R_L readings were not taken until just after the plant had begun to limit transpiration. Therefore, the value, 3 sec/cm, may be somewhat higher than could be expected as a reference for evaluating subsequent closure. Nevertheless, R_L

increased from 3 to 8 sec/cm over the period in which transpiration fell to one-half the potential rate (Figure 8). This response objectively evaluates stomatal closure due to leaf dehydration as soil water became more limiting, and covers a range of R_L readings almost identical with the amplitude found earlier with the bean plant subjected to the same percentage decrease in potential transpiration. Later, during the most violent of the prolonged cyclic behavior induced by irrigation, three separate R_L measurements were taken which show much more pronounced opening as well as closing than during non-cyclic responses.

SUMMARY AND CONCLUSIONS:

If there is a circadian rhythm in stomatal aperture, as seems to be indicated by the data from the plant in nutrient solution, interpretation of the effect of a lack of available water is made more difficult. Nevertheless, the results with lemon generally confirm those from the earlier experiment with bean: Under a high evaporative demand only a small rise in the total soil water potential (the term being used without the negative sign) ψ_T, can cause leaf tissues to dehydrate sufficiently to initiate stomatal closure. For both species ψ_T was only about 1 bar when leaf resistance (R_L) started to rise above the 3 sec/cm value prevailing while the plant still was transpiring at its potential rate. A mere increase in ψ_T from 1.0 to 1.1 bar (bean) or 1.4 bar (lemon) resulted in a 50% decrease in the transpiration rate as R_L rose to around 8 sec/cm. It is significant that the soil osmotic potential, often neglected in "non-saline" soils, accounted for 70^+% of ψ_T, yet the conductivity of the saturation extract was only 1.2 millimhos/cm in these experiments. In other words, the osmotic potential was too important to neglect, even in a non-saline soil.

An important species difference brought out in this study is that the lemon plant, in spite of exposure to a radiant level almost double that given the bean plant (1.04 vs. 0.55 ly/min), and

consequently having an initial leaf temperature 5 degrees rather than 2 degrees above air temperature, transpired at only about half the rate (236 vs. 450 $g/m^2/hr$). This is due to the almost complete lack of functional stomates on the upper epidermis of lemon, and the resulting very high R_L values, regardless of the illumination level. Such behavior has obvious implications for water conservation by crops.

PERSONNEL: W. L. Ehrler

CURRENT TERMINATION DATE: December 1970

Table 1. Monthly amounts of water received by the two agave plots at Granite Reef from 09 Oct 1968 to 10 Oct 1969, in millimeters

Month	By irrigation	By rainfall	Total
Oct	135	-	135
Nov	-	45.6	45.6
Dec	20	32.6	52.6
Jan	-	41.7	41.7
Feb	-	22.7	22.7
Mar	-	26.5	26.5
Apr	40	3.5	43.5
May	60	15.8	75.8
Jun	60	-	60
Jul	40	20.3	60.3
Aug	40	17.8	57.8
Sep	40	24.8	64.8
Yearly Total	435	251.3	686.3

Table 2. The transpiration ratio of corn as affected by soil moisture.

Treatment	Pot No.	Water Loss (G)	Dry Wt. Gain (G)	Transp. Ratio	Mean
Wet	7	22,528	158.3	142	
	9	16,381	119.1	138	134
	12	22,237	182.4	122	
Dry	8	13,899	82.6	168	
	10	10,378	81.1	128	161
	11	12,290	65.9	186	

Table 3. The transpiration ratio of agave as affected by soil moisture.

Treatment	Pot No.	Water Loss (G)	Dry Wt. Gain (G)	Transp. Ratio	Mean
Wet	1	18,754	165.4	113	
	2	15,654	145.6	108	114
	3	20,682	172.3	120	
Dry	4	10,150	67.1	151	
	5	7,379	76.0	97.1	116
	6	7,957	80.0	99.5	

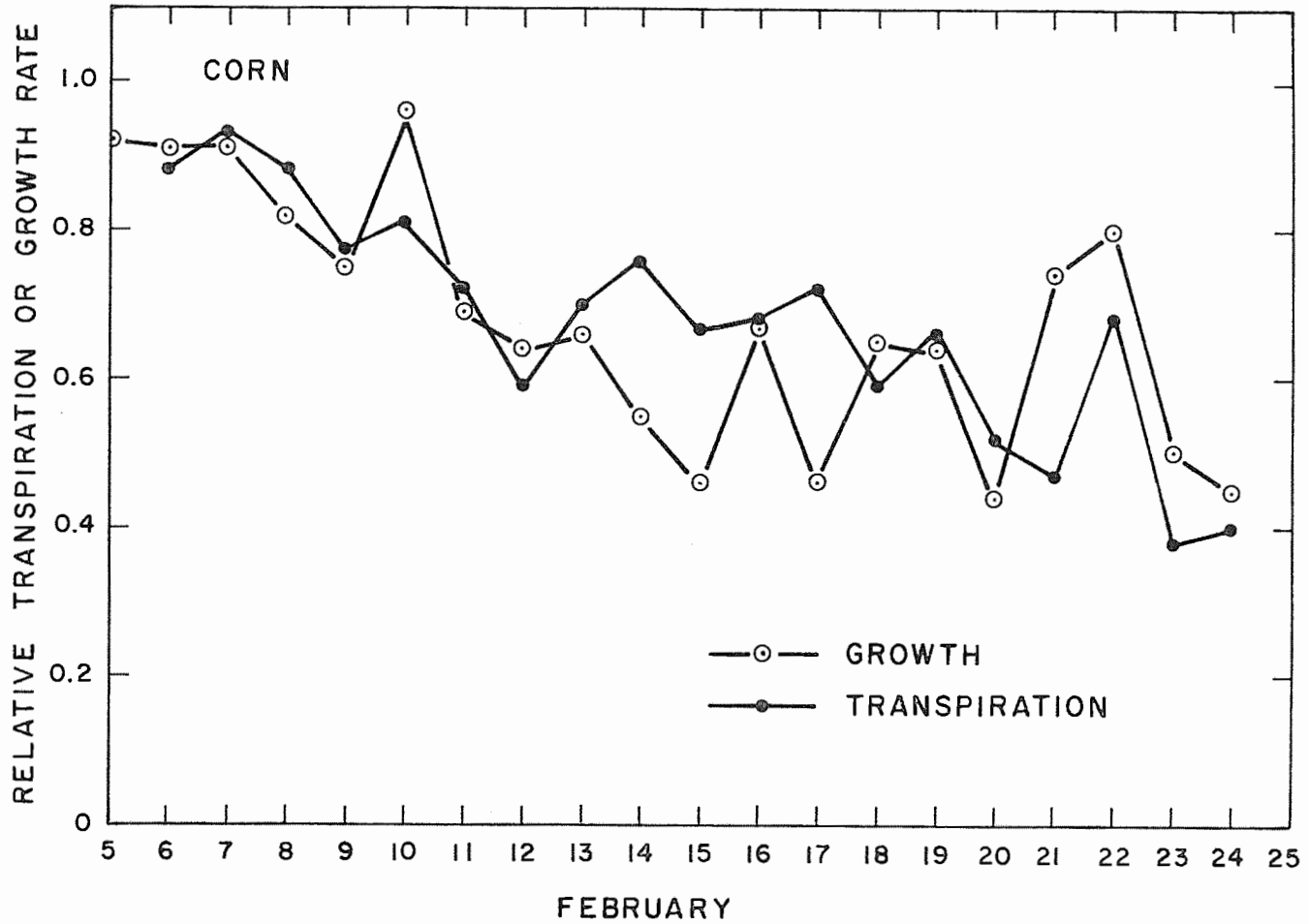

Figure 1. Rate of growth and transpiration of corn plants on a dry treatment (soil matric potential, ψ_M 0.05-1.0 bar) as a fraction of the respective values on a wet treatment (ψ_M 0.05-0.20 bar), mean of three replications.

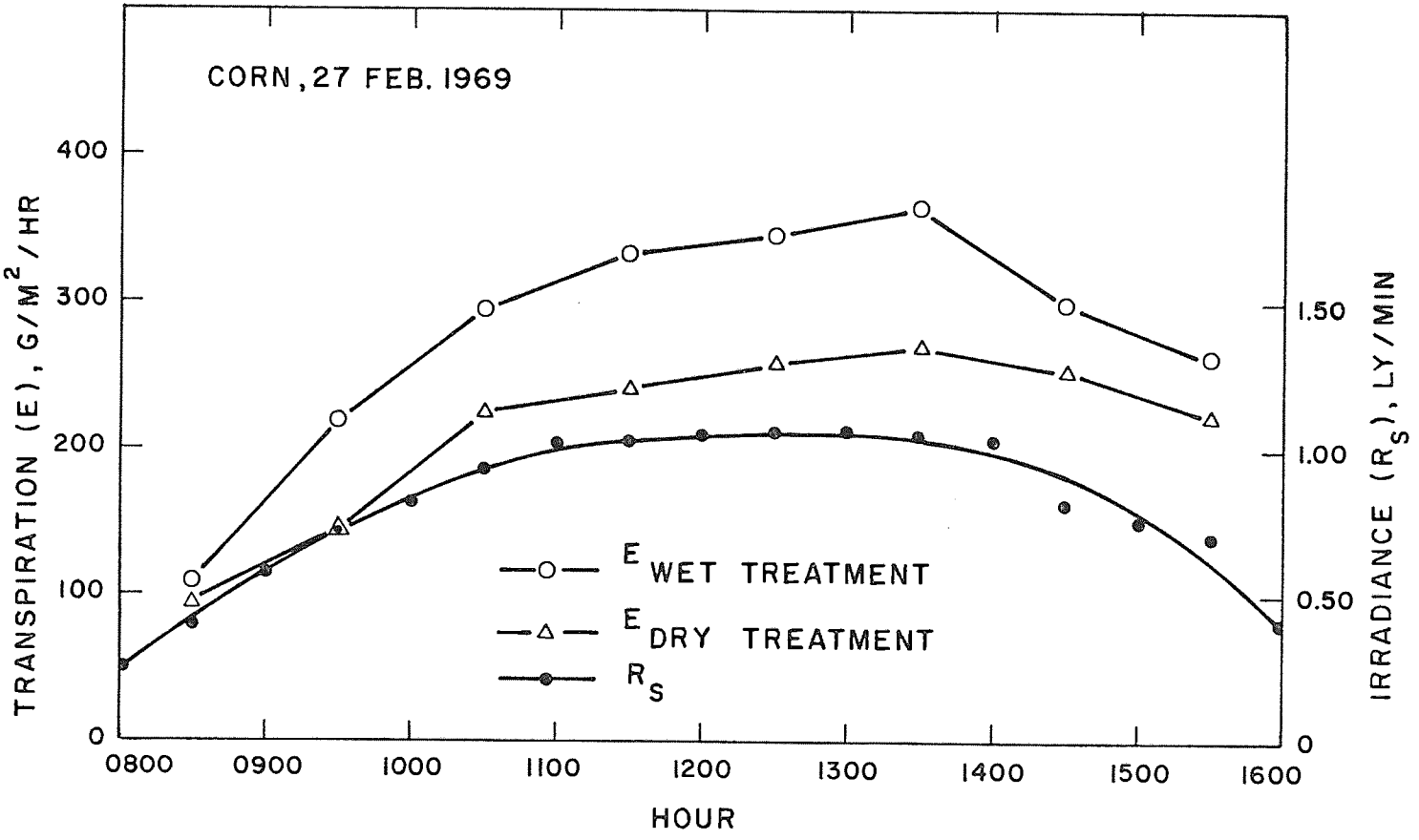

Figure 2. Hourly transpiration rate of mature corn plants as affected by a dry treatment and illumination (mean of three replications).

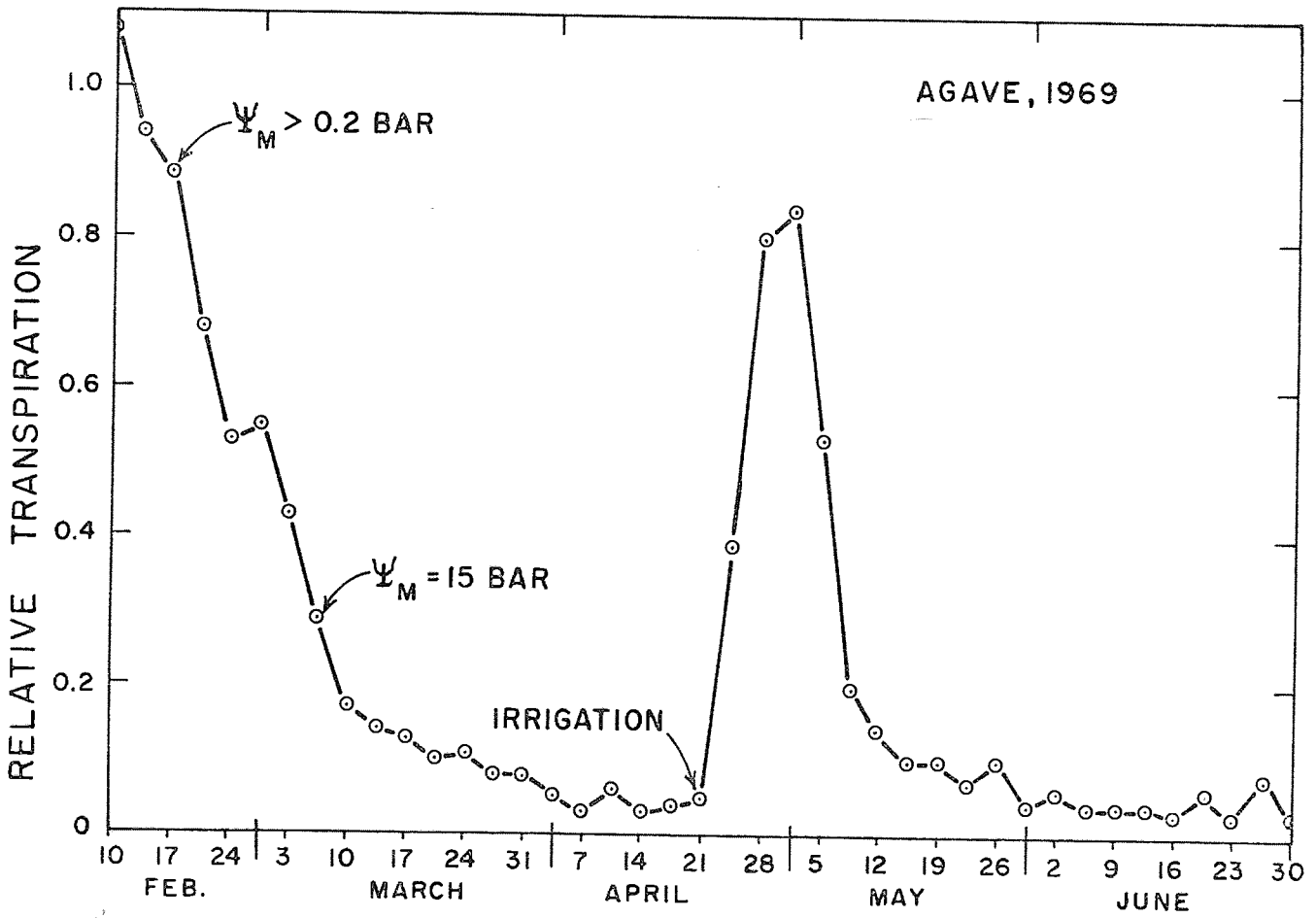

Figure 3. Transpiration from agave plants (mean of three replications) on a dry soil treatment (soil matric potential, ψ_M, >> 0.2 bar) as a fraction of that from plants on a wet treatment (ψ_M 0.05-0.2 bar). On 21 April the plants on the dry treatment were given sufficient water to restore ψ_M to 0.05 bar, without any further irrigations until harvest.

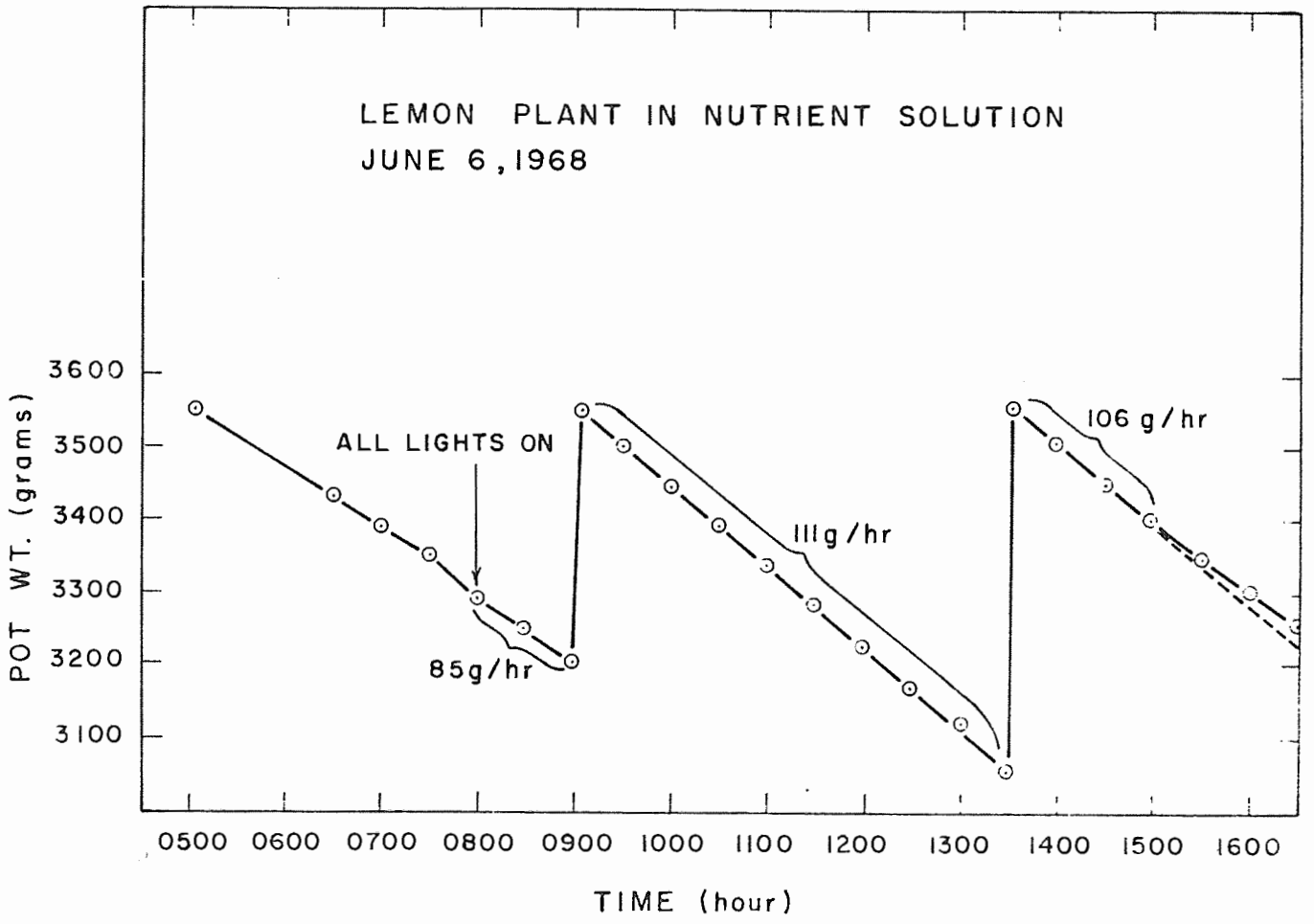

Figure 4. Weight loss (transpiration) of a lemon plant in nutrient solution in a controlled environment.

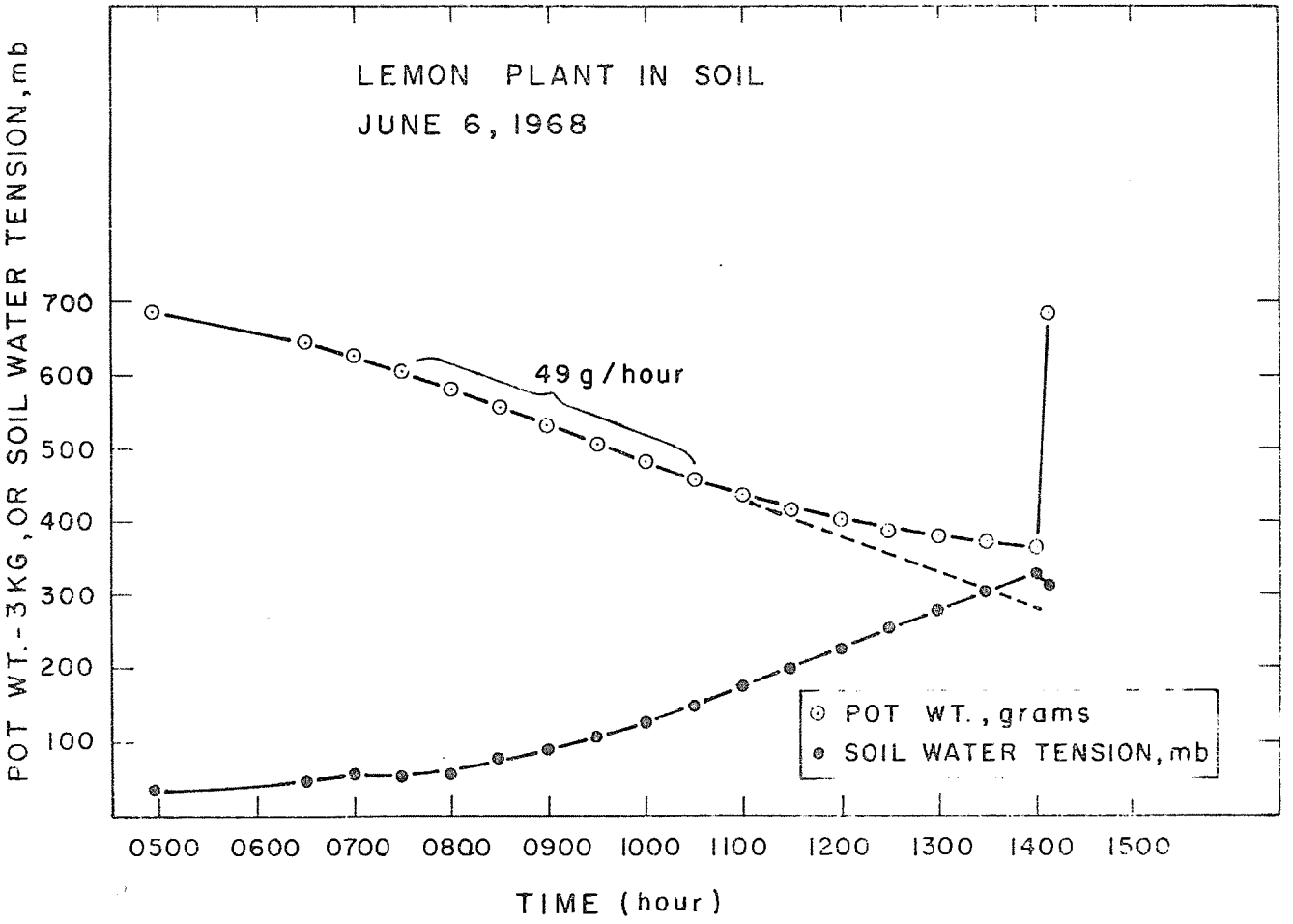

Figure 5. Transpiration (by weight loss) and change in soil water tension as a lemon plant gradually depletes the soil of available water.

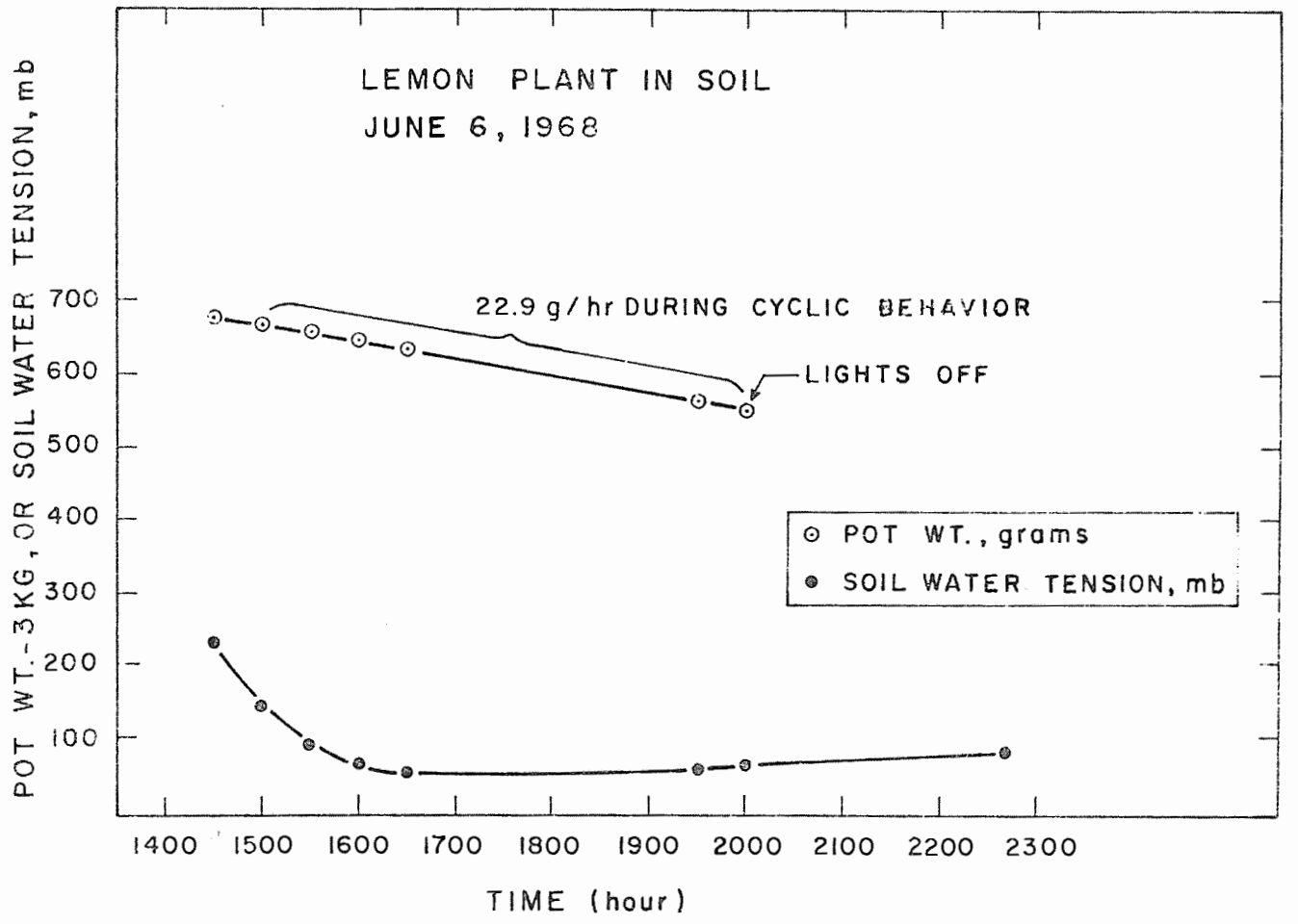

Figure 6. Lemon plant transpiration occurring during pronounced cyclic opening of stomates.

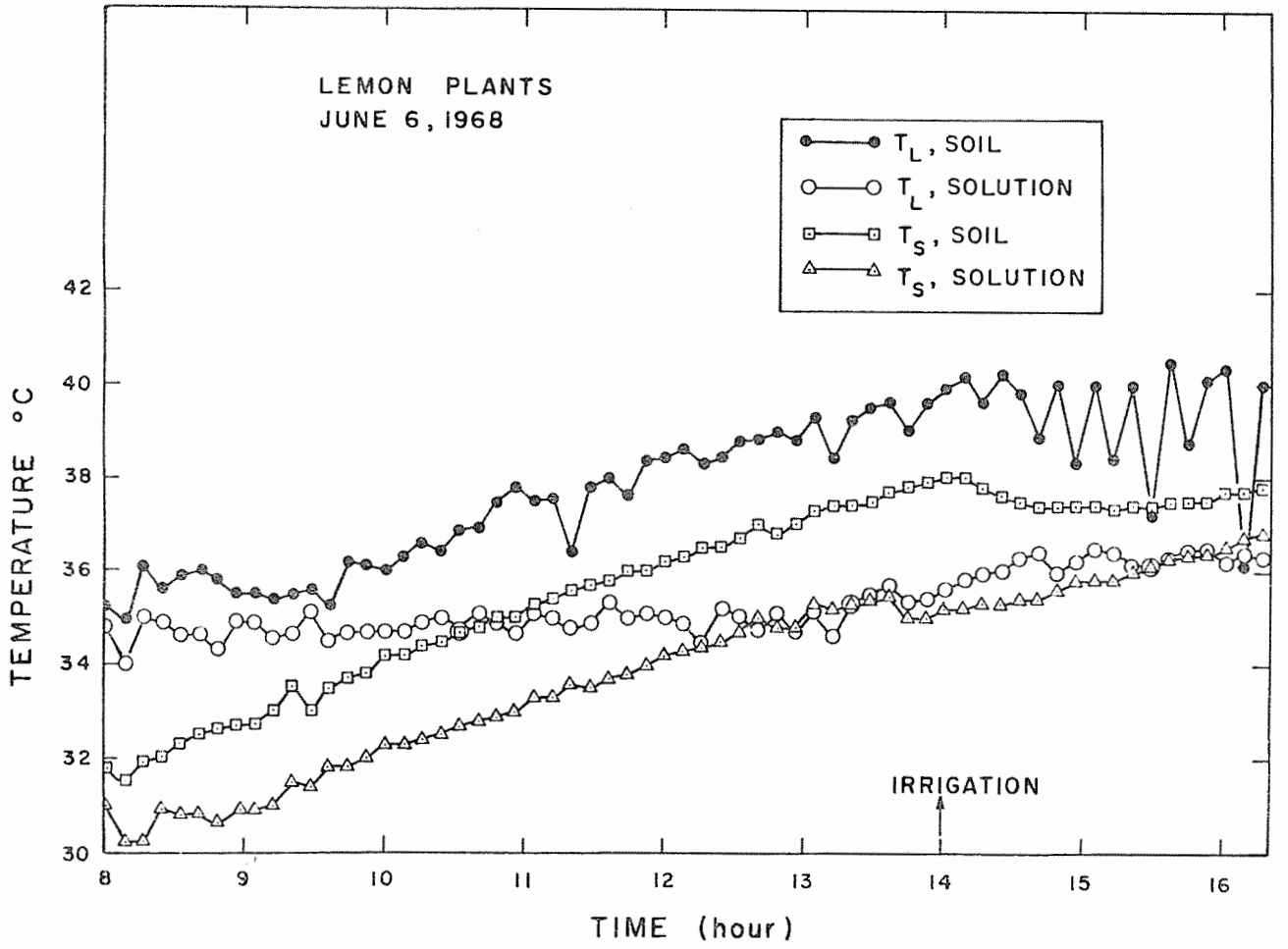

Figure 7A. Comparative changes in leaf temperature (T_L) and substrate temperature (T_S) of lemon plants in nutrient solution and soil, occurring in a controlled environment. The plant in soil was gradually depleting the available water, whereas the one in nutrient solution always had freely available water.

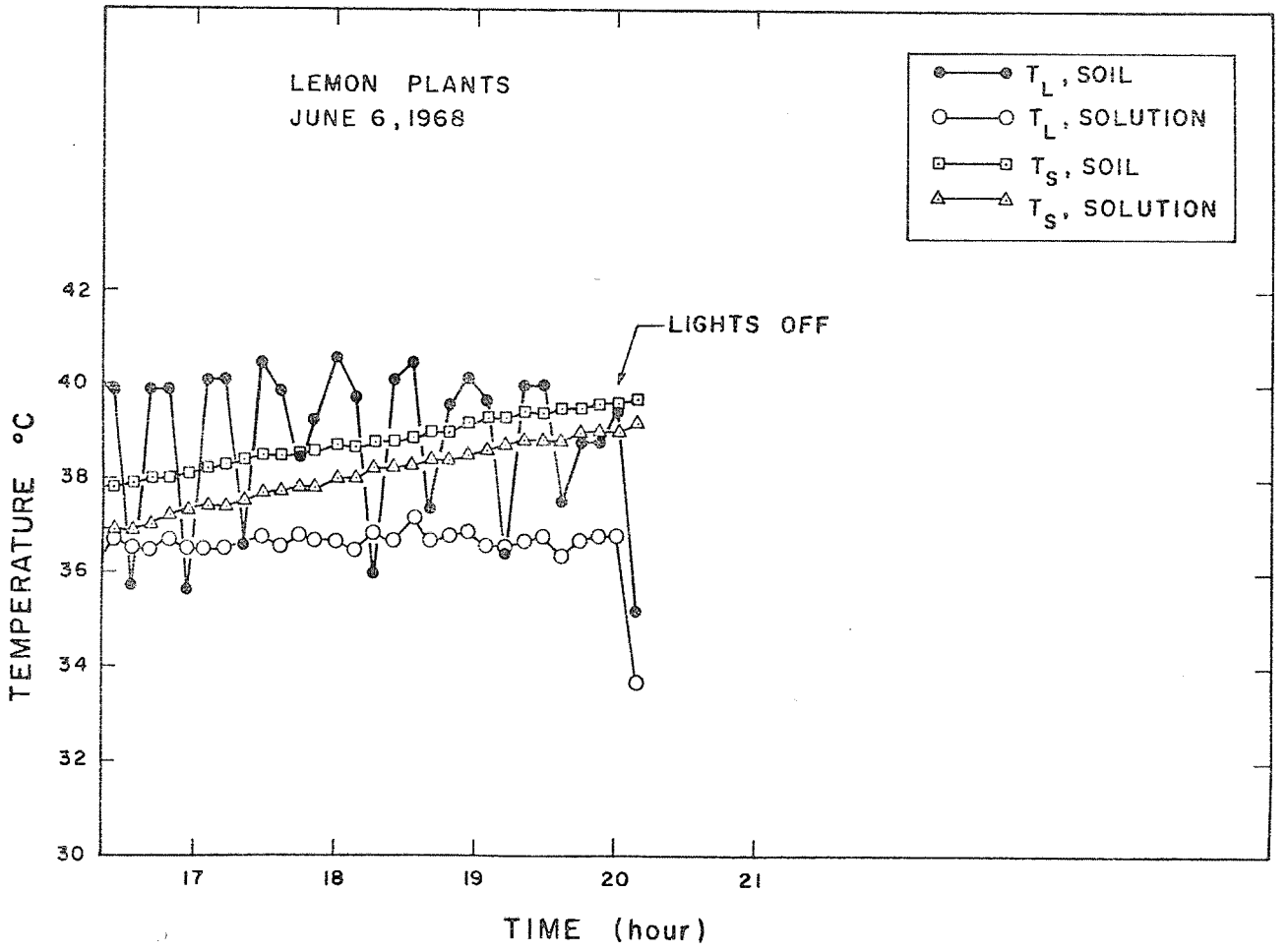

Figure 7B. Same legend as for Figure 4A. In addition, this demonstrates the abrupt effect that instantaneous removal of a high radiant load (ly/min) has on leaf temperature of plants, whether they are in soil or nutrient solution.

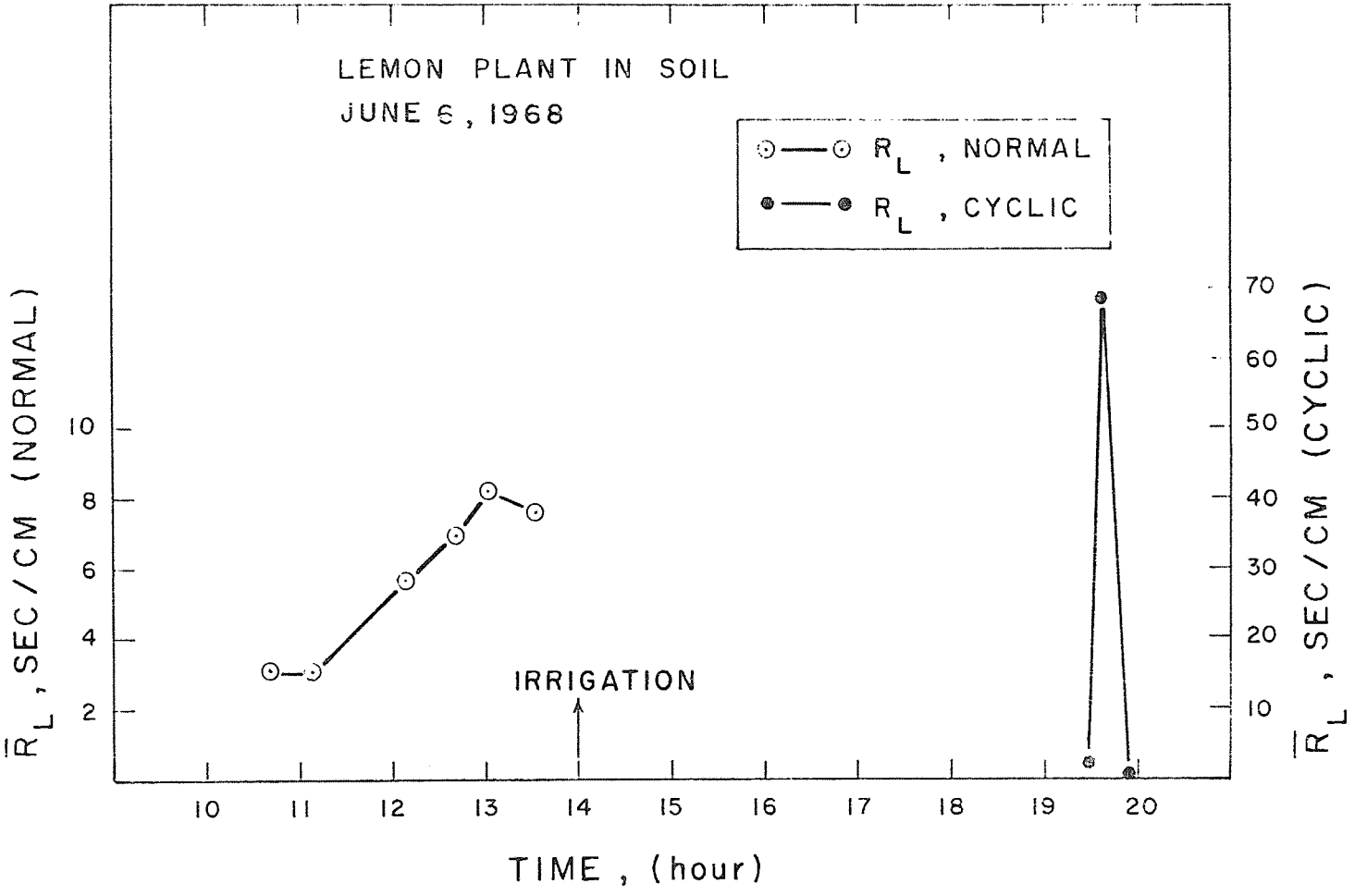

Figure 8. Response of leaf diffusion resistance (R_L) of a lemon plant in soil being gradually depleted of available water, and later, when adequate soil water is present, but when cyclic stomatal opening is occurring.

TITLE: IRRIGATION OUTLET STRUCTURE TO DISTRIBUTE WATER ONTO EROSIVE SOILS.

CRIS WORK UNIT: SWC-019-gG-3 CODE NO.: Ariz.-WCL 66-2

INTRODUCTION:

For need of study, see Annual Report, 1966.

OBJECTIVES:

1. To obtain design criteria for low-cost irrigation outlets that will distribute large streams of water without excessive erosion.

PROCEDURE:

The major activity on this project has been to construct outlets at farm sites where erosion problems exist, observe their operation, determine their weaknesses, then repair or reconstruct them and continue to observe. About 30 structures remained after the 1968 growing season. Several of these were repaired and others were replaced. The SS-2 asphalt structures on the Spencer and Spencer Ranch were rebuilt and covered with a clay emulsion.

A new figuration for the lip part of the box, resembling a fan, was built on the Taubman and Parker Ranch. Several new structures were made on this ranch by constructing the dissipator boxes in the field with our portable forms designed for this purpose. It is estimated that two boxes per hour can be built with two forms. Two of the structures made on the Taubman and Parker Ranch were attached to 12-inch tile from a high railroad fill in such a way as to be models for future construction on a continuous ½-mile ditch. Tile and field elevations were provided by their field foreman. Several changes were made in the portable forms to make them better adapted to field use. They were also painted, in order to allow easier extraction of the inner form and a decrease in the amount of labor necessary to oil them.

SUMMARY AND CONCLUSIONS:

Structure inspections this year complement last year's results, showing that a square dissipator box, when properly attached with appropriate components, will discharge a non-erosive stream of water.

The failures observed were not due to faulty design, but to breakage by machinery and cracking caused by bermuda grass. In a few instances, a thicker concrete structure would have prevented the need for repairs.

The use of fiber glass, SS-2 and clay emulsion has not proved successful so far. On the Spencer and Spencer Ranch, the weed problem caused the failure of both SS-2 and clay emulsion. Using a permanent weed killer probably would have eliminated this problem. The material does not have great strength, and can be destroyed if an irrigator or animal should step on the back or shoulder. A failure such as this happened at the Taubman and Parker Ranch. These materials will again be tested in new structures, but weeds will be eliminated first. We may apply two coats of clay emulsion with fiber-glass reinforcement, or perhaps try some less costly type of reinforcement. Since we now have a new modeling tank at the laboratory, several different figurations will be tested.

PERSONNEL: L. J. Erie and J. A. Replogle.

CURRENT TERMINATION DATE: December 1970.

TITLE: FLOW MEASUREMENT IN OPEN CHANNELS WITH CRITICAL DEPTH FLUMES

CRIS WORK UNIT: SWC-019-gG-3 CODE NO.: Ariz.-WCL 67-1

INTRODUCTION:

Previous reports (see Annual Reports for 1966-1968) summarized the results of studies on several critical-depth flumes with throat sections that were trapezoidal, triangular or circular. The technical paper titled "Flow Measurement with Critical-Depth Flumes" was presented before the VII Congress of the International Commission on Irrigation and Drainage, Mexico City, April, 1969. The report presents the theoretical aspects for predicting the calibration results for flumes and summarizes the effects of installation anomolies. These include effects of torsional twist of the flume, deflection of the sides, elevating or lowering the outlet end, sedimentation in the flume, approach conditions, the removal or addition of diverging sections at the outlet, and submergence.

Several flumes have been designed for other agencies and two more sizes built, but only one has been calibrated, a rectangular flume described in Table 1.

PROCEDURE:

The laboratory calibration was accomplished as previously described using a weighing system to determine discharge rate. Head in the flumes was referenced to the bottom of the outlet end of the throat section, but measured in the approach section of the flume with a point gage mounted in the stilling well.

The computer study tested several concepts that might serve to explain the behavior of the flumes. The most logical of these is described below.

RESULTS AND DISCUSSION:

The computation of the calibration equation for flumes is based on energy concepts using idealized flow. It is readily recognized that real fluids can be expected to deviate from the idealized flow behavior. The manner in which they deviate cannot be easily measured in such a way as to eliminate all doubt about the process involved. For example, small corrections must be made for the velocity distribution in both the approach section and the throat section. Although the exact magnitudes of the velocity distribution coefficients are not known, and even though they could be measured, their evaluation is thought to be unimportant since the total correction they can be expected to contribute is in the order of 0.5 to 1.0%. Thus, this correction is included using estimated values approximated from other works.

The friction loss, on the other hand, is difficult to measure accurately enough to absolutely define its characteristics, even though the possible correction it can contribute might be several percent. Thus, a trial and error study of possible friction-loss mathematical models was conducted to attempt a universal correlation of all flume data.

Several mathematical models were contrived based on computing a friction loss between the location of the critical section and the point where the head is measured. These models failed to work for all flume shapes and all construction materials. Although the concept of an energy loss seems well founded, the resulting computations based on friction factor charts caused too much correction at some flow depths and too little at others. Also, the results did not transfer well from flume shape to flume shape. A probable conclusion was that the energy losses were not as great as expected and that the decrease in discharge was actually due to some other characteristic of the flowing fluid. After all,

even with an energy loss, the fluid was still essentially assumed to be an ideal flow with uniform velocity distribution. If friction loss were to predict the correct result, it would have to be correlated accurately with the correct phenomenom, whatever it may be.

A more likely phenomenom is that first suggested for broad-crested weirs by Ippen (3) and later by Harrison (2). For negligible boundary shear, the idealized equations hold. With boundary shear along the walls and bottom, a boundary layer with a displacement thickness δ is formed that effectively reduces the flow area of the opening and also changes the reference elevation for the flow depth measurement. For purposes of this calculation it is sufficiently accurate to assume the velocity to be equal to the critical velocity over the entire length of the flume throat. Thus, the throat width is reduced by 2 δ and the head H, originally referenced to the throat bottom is reduced by δ. In the case of the triangular-throated flumes, H is necessarily reduced by the mathematical effect of moving the side walls together a distance of 1 δ applied to each wall or $\delta \sqrt{1 + Z^2}/Z$. In trapezoidal throats the width B is similarly treated by a reduction of $2\delta \sqrt{1 + Z^2}$ where Z is the side slope, horizontal/vertical.

Other energy losses not accounted for in the head required for the main flow to "climb" over the boundary layer would be an internal turbulent loss. No clear way to estimate this loss is available, but it is probably at least one or two magnitudes below the boundary shear losses and is negligible.

The estimation of boundary layer displacement thickness is by no means a simple task. It is well known that surface roughness affects the rate of growth of the turbulent boundary layer and also affects transition. In fact, a roughness strip is

commonly used to assure the early advent of a turbulent boundary layer.

Another problem involves the virtual origin of the turbulent layer. Prandtl's 1927 simplification used the leading edge of a flat plate, but the location of this virtual origin really depends on several factors, the sharpness of the leading edge, the turbulence of the flow, and the roughness of the plate.

In the present boundary layer concept for flumes, the drag on flat surfaces is not as important as the displacement thickness, although the two are certainly related. Another simplification is that the maximum δ in the throat for each flow rate becomes the controlling factor. Still further, this maximum must occur at or before the apparent location of the critical section in the flume throat. Thus, if transition occurs before this location, the control is governed by a turbulent boundary layer; if after, then by a laminar boundary layer. As suggested by Prandtl (see Schlichting (7) p 538), the turbulent boundary layer is assumed to behave as if it were turbulent from the leading edge of a flat plate or more precisely, following Robertson (6), from a virtual origin upstream of the flat plate. With enough roughness at the joint connecting the throat section of the flume to the converging section, the virtual origin may be as far upstream as that measured by Klebanoff and Diehl (4) who obtained Reynolds numbers, R_{xo}, based on the distance, xo, upstream from the leading edge of -0.66×10^6 to -3.06×10^6. Other experiments with rounded edges have indicated values of R_{xo} of -0.086×10^6 and $+ 0.5 \times 10^6$.

Translated in terms of flumes, this means that the virtual origin can be upstream several feet from the inlet of the flume throat. The origin is not simple or obvious. A rough approximation is to assume it to be at the midpoint of the converging section.

The next point to ponder is the very act of transition itself. How can an estimate of the point of transition be established so that the correct thickness can be applied? Recourse here is to the concept of admissible roughness (Schlichting (7) p 557). The amount of roughness which is considered "admissible" in engineering applications is that maximum height of individual rougness elements, K, which causes no increase in drag compared to a smooth wall. The assumption is that the boundary layer will have undergone transition to a turbulent condition if the admissible roughness, K, computes to be less than the roughness of the flume throat. The relation in terms of throat-length Reynolds number (the throat length, L, is taken as the physical length of the throat plus the distance to the virtual origin) is given by

$$R_L < 100 \frac{L}{K}$$

Laminar boundary layers are assumed to exist when the relation is satisfied and turbulent boundary layers assumed to exist otherwise.

Continuing the conjecture a step further, if the critical section migrates upstream with increasing discharge in a flume with free outfall, the length L would be reduced and the increase of the boundary layer beyond this point probably has little effect on discharge. However, it is likely that the virtual origin also moves upstream keeping the value of L nearly constant for the free discharging flume. Suppose that a divergent section is added to the flume or that partial submergence exists. In these cases the curved water surface profile of the free overfall is changed to nearly parallel flow to the end of the throat, so that the control section is probably at the outlet end of the throat. This is the case usually assumed even for the free overfall situation, but evidence appears to favor a migrating of the point of critical depth.

If the above concepts are true, the length L should be increased by an amount equal to the critical depth. The net result is that free discharging flumes will discharge slightly less if partly submerged or if divergent sections are added to the downstream end. On smooth flumes the amount should be small, on rough flumes the amount may be easily detected.

This might explain why some researchers note changes in discharge at theoretically minor submergences or when free overfall is eliminated, while others report no effects.

Finally, with the correct boundary layer size determined, the discharge that it contributes must be added to the total Q. Although the shape of the velocity profile in the boundary layer is probably logarithmic, it is simpler to assume a parabolic profile with the maximum velocity equal to the average velocity in the flume throat. Great accuracy in this quantity is not required since this quantity is small compared to the total discharge.

The computer program was designed to compute the discharge rating curves applying all of the above corrections for five flumes representing three basic shapes and three roughness conditions. Two more flumes using data from Bondurant, et al. (1) and from Neogy (5) are also compared bringing the total to seven flumes, four roughness conditions and three basic shapes - triangular, rectangular, and trapezoidal. Table 1 compares the laboratory calibrations with the computed calibration. The idealized discharge is also shown to illustrate the magnitudes of error that can occur if corrections are not included. Subtracting this latter value from 100% would represent the discharge coefficient that would have to be applied to the idealized flow. Only for the rectangular flume is it a fairly constant value, 0.95 or 0.96, and then only for heads greater than about 0.4 foot.

The concrete flume was calibrated by Bondurant, et al. (1). Its throat is too short to conform to the stated requirements for parallel flow when the head is greater than about 0.6 foot. The broad-crested weirs of Neogy (5) are not predicted well. The boundary-layer thickness is obviously not well enough defined. The correct prediction is closely approximated by the average of assuming a laminar boundary layer and then assuming a turbulent boundary layer, however, this is probably just fortuitous.

Another way to look at the boundary layer effects is to consider the total drag caused by the flume boundaries between the point of measurement and the critical depth. This is similar to the original concept of friction loss except that the loss is calculated with provision that a portion of the length of the boundary layer can be laminar while the rest is turbulent. The corresponding shear forces acting through a distance constitute work being done on the flow and can be included in the energy equation being solved.

Although the above concept has not been tested it would appear to offer advantages where the flow depth is small compared to the throat length, perhaps a ratio of 1 to 20. It is obvious that the reduced-area concept offers only two alternatives, either a completely laminar or a completely turbulent boundary layer. The problems that this oversimplified concept can produce is illustrated by the poor predictions on the long-throated broad-chested weirs and at the low flows on several other flumes, Table 1.

Modeling. Laboratory facilities are limited in capacity so that proving large-sized flumes directly is not convenient. Existing calibrations on small flumes may, however, be projected to large sizes by modeling techniques. The resulting calibrations can then be compared to direct computations for the large prototype. Since smooth fiberglass will model the roughness of good

quality concrete at a modeling ratio of 1 to 7, the calibration for a fiberglass flume was projected to a concrete flume 7 times as large. For a Froude model the velocity ratio, V_r, is equal to the square root of the length ratio, L_r, and the area ratio, A_r, is equal to L_r^2. By the continuity equation the discharge ratio Q_r, is given by $Q_r = A_r V_r = L_r^2 L_r^{0.5} = L_r^{2.5}$. The multiplication factor between the discharge in the fiberglass model, Q_m, and the discharge in a concrete prototype, Q_p, which is seven times larger then becomes $7^{2.5} = 129.6$, or $Q_p = 129.6\ Q_m$.

The results of such a projection are compared in Table 2 to directly calculated values using the energy equations corrected for boundary layer development. The predicted calibration is slightly below the model-derived calibration by less than 1% except at the lowest modeled flow which has a prototype flow depth of 2.1 feet that is predicted with an error of -2.44%. The idealized discharge is also shown. The percent differences here are identical to the corresponding values of Table 1 for the fiberglass flume (the Flushing Meadows flume) except for rounding errors. As expected, the predicted discharge rates for large concrete flumes at high flow rates is predicted to within $\pm$ 2% by the idealized flow equation but is predicted better throughout its flow range by the prediction method that corrects for boundary layer thickness.

A listing of the current version of the computer program in the Basic language is attached as Appendix A.

SUMMARY AND CONCLUSIONS:

Theoretical equations for predicting the discharge through critical depth flumes have been developed. The equations have been extended to real flows by computing the thickness of the boundary layer that forms in the throat of the flumes and serves to reduce the effective area for flow. The bottom elevation of the flume is also corrected for the thickness of the boundary

layer and finally the flow discharging by way of the boundary layer itself is added to the computed discharge. Although the discharge through the boundary layer is small it can amount to 1 to 5% depending on the roughness of the flume walls and hence the thickness of the boundary layer. The detailed computations required are done with the aid of electronic computers. With all corrections applied, the prediction is accurate to within $\pm$ 2% through a flow range of 1:10 for all flumes calibrated. The flumes include triangular, rectangular, and trapezoidal cross-sectional shapes. Three roughness conditions were included, smooth fiberglass, galvanized sheet metal, and aluminum sheet metal.

High accuracy in the prediction of the boundary layer thickness does not appear necessary for flumes with flow depths greater than about 1/20 the throat length. More refinement appears necessary before the results can be applied routinely to very long throated flumes or to low flows through flumes or over broad-crested weirs.

REFERENCES:

1. Bondurant, James A., Humpherys, Allan S., and Robinson, A. R. Cast in Place Concrete Trapezoidal Measuring Flumes. USDA ARS 41-155, November 1969.

2. Harrison, A. J. M. The Streamlined Broad-Crested Weir. Proc. Institution of Civil Engineers (London), 38:657-678, 1968.

3. Ippen, A. T. "Channel Transitions and Controls," Chapter VIII of Rouse, H. (Editor), "Engineering Hydraulics." John Wiley and Sons, Inc. New York. 1950. pp 525-528.

4. Klebanoff, P. S. and Diehl, Z. W. Some Features of Artificially Thickened Fully Developed Turbulent Boundary Layers Fully Developed Turbulent Boundary Layers with Zero Pressure Gradient. NACA (Presently NASA) Report 1110, Washington, D.C., 1952.

5. Neogy, Birendra Nath. Tests on Broad-Crested Weir of Trapezoidal Cross-Section. (Thesis submitted in partial fulfillment of the requirement for the degree of Master of Science in Civil Engineering) University of Wisconsin, Madison, Wis., 1960.

6. Robertson, James M. Discussion of "Boundary Layer Displacement Thickness" by A. J. Harrison, Journal of the Hydraulics Division, Amer. Soc. of Civil Eng., 93(HY3): 79-91, July, 1967. Discussion is in 94(HY3):768-771, May, 1968.

7. Schlichting, Hermann. Boundary Layer Theory. McGraw-Hill Book Company, Inc. New York, 4th Edition, 1960.

PERSONNEL: J. A. Replogle

CURRENT TERMINATION DATE: December, 1970.

Table 1. Comparison of laboratory calibrations and computed calibrations.

Flume Description	Flow Depth Ft	Laboratory Calibration cfs	Predicted Calibration cfs	% Diff.	Idealized Discharge -No Corr.- cfs	% Diff.
Name: Flushing Meadows Flume						
Triangular: B1 = .667 ft	.3	.0633	.06224	-1.67	.06591	+ 4.12
z1 = z3 = .57735 (60°)	.5	.232	.2314	-0.26	.2389	+ 2.93
Fiberglass, K = .00005 ft	.7	.555	.5482	-1.23	.5603	+ 0.95
Throat Length = 3.0 ft	1.1	1.756	1.751	-0.29	1.775	+ 1.08
	1.5	3.872	3.899	+0.70	3.936	+ 1.65
Name: Brawley Flume						
Triangular: B1 = .667 ft	.2	.0184	.01753	-4.72	.02077	+12.88
z1 = z3 = .50404 (53.5°)	.4	.110	.1095	- .45	.1184	+ 7.64
Galv. Sheet Metal, K = .0008 ft	.6	.312	.3124	+ .13	.3294	+ 5.58
Throat length = 2.0 ft	.8	.653	.6557	+ .41	.6830	+ 4.59
	1.0	1.160	1.165	+ .43	1.205	+ 3.88
Name: Small Flume						
Triangular: B1 = .167	.1	.00386	.003729	-3.39	.00425	+10.10
z1 = z3 = .57735 (60°)	.2	.0234	.02323	-0.73	.02459	+ 5.08
Alum. sheet, K = .00005	.3	.0671	.06679	-0.46	.0693	+ 3.28
Throat Length = 1.0 ft	.4	.1418	.1414	-0.35	.1452	+ 3.13
	.5	.253	.2529	-0.39	.2585	+ 2.17
Name: Rectangular						
Rectangular: B1 = 1.5 ft	.2	.286	.2839	-0.73	.3115	+ 8.92
B3 = 1 ft, z1 = z3 = 0	.4	.835	.8339	-0.13	.8812	+ 5.53
Galv. Sheet Metal, K = .0008 ft	.6	1.550	1.551	+0.06	1.619	+ 4.45
Throat Length = 3 ft	.8	2.398	2.403	+0.21	2.492	+ 3.92
	1.0	3.33	3.370	+1.20	3.483	+ 4.59

Table 1. Comparison of laboratory calibrations and computed calibrations. (continued) -

Flume Description	Flow Depth ft	Laboratory Calibration cfs	Predicted Calibration cfs	% Diff.	Idealized Discharge -No Corr.- cfs	% Diff.
Name: U.S.B.R. Flume						
Trapezoidal: B1 = .833 ft	.2	.129	.1266	- 1.86	.1388	+ 7.60
B3 = .333 ft, z1 = Z3 = 1	.4	.504	.4966	- 1.47	.5247	+ 4.11
Varnished Fiberb'd, K = .00005 ft	.6	1.183	1.170	- 1.10	1.217	+ 2.87
Throat Length = 3 ft	.8	2.23	2.208	- 0.99	2.276	+ 2.06
	1.0	3.69	3.666	- 0.65	3.757	+ 1.82
Name: Concrete (Bondurant)						
Trapezoidal: B1 = 1 ft	.2	.16	.1496	- 6.50	.1576	- 1.58
B3 = .4 ft, z1 = z3 = 1	.4	.54	.5444	+ 0.81	.5759	+ 6.648
Concrete, Steel Form, K = .0005	.6	1.24	1.251	+ 0.89	1.307	+ 5.40
Throat Length = 1 ft*	.8*	2.35*	2.322	- 1.19	2.408	+ 2.47
*Throat length shorter than required	1.0*	3.91*	3.811	- 2.53	3.93	+ 0.51
Name: Broad-Crested Weir (Neogy)						
Trapezoidal: B1 = 3.75 ft	.3	.541	.5744	+ 6.17	.6116	+13.05
B3 = 1 ft, z1 = 0, z3 = 1	.4	.911	.8628	- 5.29	.9968	+ 9.41
Weir Height = 2.052 ft	.5	1.37	1.295	- 5.47	1.4711	+ 7.38
Painted Wood, K = .00005 ft	.6	1.90	1.816	- 4.42	2.038	+ 7.26
Throat Length = 12.1 ft	.7	2.52	2.429	- 3.61	2.700	+ 7.14
Name: Broad-Crested Weir (Neogy)						
Trapezoidal: B1 = 3.75 ft	.3	.501	.5614	+12.06	.6116	+22.08
B3 = 1 ft, z1 = 0, z3 = 1	.4	.858	.7718	-10.04	.9968	+16.18
Weir Height = 2.052 ft	.5	1.302	1.178	- 9.52	1.471	+12.98
Painted Wood, K = .00005 ft	.6	1.83	1.671	- 8.69	2.038	+11.37
Throat Length = 24.2 ft	.7	2.44	2.254	- 7.62	2.700	+10.65

Table 2. Comparison of model derived calibration and direct computed calibration.

Flume Description	Flow Depth ft	Model Derived Calibration cfs	Predicted Calibration cfs	% Diff.	Idealized Discharge -No Corr.- cfs	% Diff.
Model flume is the Flushing						
Meadows flume of Table 1.	2.1	8.21	8.010	-2.44	8.545	4.08
Prototype is taken to be a	3.5	30.1	29.79	-1.03	30.97	2.89
concrete flume 7 times larger	4.9	72.0	70.62	-1.92	72.64	0.89
Triangular: B1 = 4.67 ft	6.3	136.4	134.7	-1.25	137.74	0.98
z1 = z3 = .57735 (60^{o})	7.7	228.	225.8	-0.96	230.1	0.92
Concrete, K = .0005	9.1	348.	347.5	-0.14	353.1	1.46
Throat Length = 21 ft	10.5	502.	503.1	+0.22	510.2	1.63

APPENDIX A

```
TRAP21     14:40    FRI.    01-23-70

99 READ K3
100 DATA .666667
109 READ B1,B3
110 DATA .666667,0
119 READ Z1,Z3
120 DATA .57735,.57735
129 READ S,I,L0
130 DATA .1,.2,1.5
139 READ K
140 DATA .00001
149 READ L
150 DATA 3
159 READ Y8
160 DATA 0
169 READ T
170 DATA 0
179 READ A1,A3
180 DATA 1,1
189 READ R2,G,V1
190 DATA 6,32.16,1.228E-5
200 LET J=0
210 LET L1=0
220 LET E=1E-5
230 LET Y0=S-I
240 LET Q=0
250 LET Y0=Y0+I
260 LET Y1=Y0
270 LET K1=1
280 LET Y2=Y1
290 GOSUB920
300 LET F=Q/(A0*SQR(G*A0/T0))
310 LET F= INT(F*10↑4+.5)/10↑4
320 LET Q=INT ( Q*10↑R2+ .5 ) / 10↑R2
330 IF K1=1 THEN 380
340 LET Q4=Q
350 LET Y5=INT(Y3*10↑4+.5)/10↑4
360 LET F4=F
370 GO TO 480
380 LET Q1=Q
390 LET Y6=INT(Y3*10↑4+.5)/10↑4
400 LET Y4 = Y0 + 45*I
410 LET F1=F
420 IF Y4>L0 THEN 460
430 LET K1=4
440 LET Y2=Y4
```

```
450 GØ TØ 290
460 LET Q4=0
470 DEF FNR(X)=INT(X*10↑D0+.5)/10↑D0
480 LET D0=5
481 IF K=0 THEN 490
482  IF R>(100*L/K)/1E5 THEN 490
483 IF T=1 THEN 490
484 LET H1=FNR(H1+9)
487 GØ TØ 500
490 LET H1=FNR(H1)
500 LET C1 = FNR(C1)
520 LET R=FNR(R)*100000
525 IF K=0 THEN 539
530 LET L9=FNR(L/K)
538 GØ TØ 540
539 LET L9=0
540 LET L1=L1+1
550 IF L1 =1 THEN 570
560 GØ TØ 740
570 LET J=J+1
580 PRINT"FLUME:  SILL=";Y8;"   B1=";TAB(22);B1;TAB(33);"B3=";
590 PRINT TAB(36);B3;TAB(45);"Z1=";TAB(48);Z1;TAB(60);"Z3=";
600 PRINT TAB(63);Z3
610 PRINT TAB(1);"ALPHA 1=";A1;TAB(16);"ALPHA 3=";A3;
620 PRINT TAB(34);"K=";K;TAB(44);"L=";L;TAB(54);"L/K=";L9;TAB(69);J
630 IF Q4>0 THEN680
640 PRINT"   Y         Q     CRITICAL  FRØUDE "
650  PRINT"   FT.      CFS   DEPTH-FT NØ.AT Y ";
660 PRINT TAB(38); " Q--B.L.     DELTA      R"
670 GØ TØ 720
680PRINT"   Y         Q     CRITICAL  FRØUDE *";
690 PRINT TAB(38);"Y-F       Q     CRITICAL  FRØUDE"
700 PRINT"   FT.      CFS   DEPTH-FT NØ.AT Y *";
710 PRINT TAB(38);"FT.      CFS   DEPTH-FT  NØ.AT Y"
720 PRINT "==================================*";
730 PRINT "=================================="
740 IF Q4=0 THEN 780
750 PRINTTAB(1);Y1;TAB(8);Q1;TAB(17);Y6;TAB(26);F1;TAB(34);"*";
760 PRINT TAB(36);Y4;TAB(43);Q4;TAB(52);Y5;TAB(61);F4
770 GØ TØ 800
780 PRINTTAB(1);Y1;TAB(8);Q1;TAB(17);Y6;TAB(26);F1;TAB(34);
790 PRINT TAB(36);C1;TAB(47);H1;TAB(57);R
800 IF (L1/5)-INT(L1/5)=0 THEN 820
810 GØ TØ 830
820 PRINT
830 IF L1=45 THEN 850
840 GØ TØ 900
850 FØR P1=1TØ7
860 PRINT
870 NEXT P1
```

```
880 LET L1=0
890 LET Y0=Y4
900 IF Y0>=L0-1 THEN 1570
910 GØ TØ 240
920 LET H1=0
930 LET M=0
940 LET C2=0
945 LET Y7=Y8+Y1
950 LET   H   =   Y2 + A1 * Q*Q / (2*G*Y7*Y7* (B1+Z1*Y7)↑2)
960 LET X=(4*Z3*H)-3*B3
970 LET C = (SQR(X*X+40*Z3*B3*H)+X)/10
980 LET X =((B3+C)/(3*B3+5*C))↑(3/2)
990 LET X=H↑(3/2)*SQR(2*G/A3)*(2*B3+4*C)*X
1000 LET E3=ABS(X-Q)
1010 LET C2=C2+1
1020 IF C2<1000 THEN 1050
1030 PRINT"NØT CØNVERGING AFTER 1000 CYCLES, CURRENT DIFFERENCE=";E3
1040 GØ TØ 1070
1050 LET Q = X
1060 IF E3>E THEN 950
1070 IF Z3=0 THEN1100
1080 LET Y3=C/Z3
1090 GØ TØ 1110
1100 LET Y3=2*H/3
1110 IF M=1 THEN 1530
1120 LET Y=Y3
1130 LET B=B3
1140 LET A=Y*(B3+Z3*Y)
1150 LET V=Q/A
1155 LET R=(V*L/V1)*1E-5
1160 IF K=0 THEN 1540
1161 IF R>(100*L/K)/1E5 THEN 1165
1162 IF T=1 THEN 1165
1163 LET C1=1.72/SQR(R*1E5)
1164 GØ TØ 1450
1165 IF L/K<400 THEN 1565
1170 IF L/K<1000 THEN 1221
1180 IF L/K<4000 THEN 1230
1190 IF L/K<10000 THEN 1280
1200 IF L/K<=30000THEN 1330
1210 GØ TØ 1380
1221 LET C9=.89984+(.0676/R)
1222 LET C0=.65040+(.11872/R)
1223 LET K0=1000
1224 LET K9=400
1225 GØ TØ 1420
1230 LET C9=.65040+(.11872/R)
1240 LET C0=.43031+(.20879/R)
1250 LET K0=4000
1260 LET K9=1000
1270 GØ TØ 1420
```

```
1280 LET C9=.43031+(.20879/R)
1290 LET C0=.34731+(.28032/R)
1300 LET K0=10000
1310 LET K9=4000
1320 GØ TØ 1420
1330 LET C9=.3473+(.28032/R)
1340 LET C0=.48949*(R↑-.14314)
1350 LET K0=30000
1360 LET K9=10000
1370 GØ TØ 1420
1380 LET C9=.48949*(R↑-.14314)
1390 LET C0=.50793*(R↑-.19831)
1400 LET K0=1E6
1410 LET K9=30000
1420 GØ TØ 1430
1430 LET C1=C0+((LØG((L/K)/K0)/LØG(K9/K0))*(C9-C0))
1440 LET C1=C1/100
1450  LET H1=C1*L
1460 IF B3=0 THEN 1500
1470 LET Y2=Y2-H1
1480 LET B3=B-2*H1*(1+Z3*Z3)↑.5
1490 GØ TØ 1510
1500 LET Y2=Y2-(H1*(Z3*Z3+1)↑.5)/Z3
1510 LET M=1
1517 LET C1=Q3
1520 GØ TØ 940
1530 LET B3=B
1540 LET T0=B1+2*Y7*Z1
1550 LET  A0 = Y7*(B1+Y7*Z1)
1556 LET P3=B3+2*Y3*(1+Z3*Z3)↑.5
1557 LET V3= Q/(Y3*(B3+Y3*Z3))
1558 LET Q3= K3*V3*P3*H1
1559 LET Q=Q+Q3
1560 RETURN
1565 PRINT"L/K VALUE IS TØØ LØW, L/K=";L/K
1570 END
```

TITLE: ASSESSING THE ENERGY ENVIRONMENT OF PLANTS

CRIS WORK UNIT: SWC-019-gG-3 CODE NO.: Ariz.-WCL-68-5

INTRODUCTION:

The prime forcing function in the energy environment of plants, and the ultimate source of all energy derived from foodstuffs, is the stream of solar radiation emitted from the sun. This factor was singled out for intensive study this year in regard to its transmittance through the earth's atmosphere. In particular, three aspects of this phenomenon were studied in the Phoenix area: 1) long-term averages of the atmospheric transmittance for solar radiation, 2) the transmittance of the atmosphere for solar radiation on individual clear days, and 3) variations of the transmittance function with altitude and season.

PROCEDURE:

Long-term Averages of Atmospheric Transmittance. Eighteen years of clear-day solar radiation data accumulated at Phoenix, Arizona, were analyzed to yield monthly averages of the transmittance of the atmosphere for solar radiation. These figures served as a basis against which theoretical calculations of the atmospheric transmittance were compared. The calculations employed are described in detail by Idso (2). Briefly, they were carried out as follows.

An expression developed by McDonald (5) for the absorption of solar radiation by water vapor was used in conjunction with the product of daily weighted mean optical path length and precipitable water (determined from surface vapor pressure) to yield the fractional depletion of the solar beam by water vapor absorption. The further depletion of this fraction by dust was then calculated by the formula of Houghton (1), expressible solely in terms of optical path length. Half of this depleted energy flux was considered to reach the earth as diffuse radiation. The Houghton (1) relations for solar radiation

transmission in the presence of scattering water vapor and the basic atmospheric constituents (derived from Smithsonian Institution data) then yielded, based upon precipitable water and optical path length, a final transmittance of the direct beam and a second scattered component. The sum of half of this scattered component, the fractional transmittance of the direct beam, and the component scattered downward by dust then yielded the total atmospheric transmittance.

Atmospheric Transmittance on Individual Clear Days. An entire year of individual clear-day solar radiation data was obtained for Phoenix, Arizona, and converted into a total of 100 individual daily transmittance values. The procedure of Idso (2) was used to determine to what accuracy calculations of these individual values could be made, utilizing only surface vapor pressure as a meteorological parameter.

Seasonal and Altitudinal Variations in Atmospheric Transmittance. For the same year period as the previous study, solar radiation data were also obtained at two different altitudes (Δ elevation = 464 meters) with a matched pair of Yellott Sol-A-Meters. From these measurements, the transmittance difference between the Valley Floor and the top of nearby South Mountain was obtained. The procedure of Idso (2) was used to compute the theoretical difference and its trend over the year; and supplementary meteorological data were acquired to explain the mechanism responsible for the distinctive results.

RESULTS AND DISCUSSION:

Long-term Averages of Atmospheric Transmittance. Table 1 contains the results of the measured mean monthly clear-day atmospheric transmittance, plus the analogous calculated results of three variations of the basic Idso (2) procedure. The first set of results is for the complete set of Houghton (1) attenuation coefficients; the second set is for the McDonald (5) water

vapor absorption curve together with the remaining Houghton (1) coefficients; and the third set is identical to the second, but with an assumed seasonal dust variability. The latter two procedures both agree to within better than 0.5% of the measured values on a yearly basis, while the pure Houghton (1) results are off by 2.6%. On a monthly basis, the dust-corrected results are also seen to be better than the McDonald results for an atmosphere of assumed constant dust content.

Atmospheric Transmittance on Individual Clear Days. A comparison of the calculated and measured atmospheric transmittances for the 100 clear days experienced at Phoenix over the year period July 1968 through June 1969 is shown in Figure 1. Included in this figure is a solid 45 degree or "1 to 1 correspondence" line and two dashed lines depicting a departure of $\pm$ 1.5% from this line. Only 17 of the 100 total points, or 17% of them, fall outside of this interval, and even these points do not lie very far from it. A least squares analysis of the data yields a line of slope 1.003 and zero intercept of 0.002, with a correlation coefficient of 0.921. The standard error of estimate is further calculated to be only 0.009. Since these calculations were made under the assumption of a constant dust load in the atmosphere, the results show that this assumption, although not necessarily true, is operationally valid.

Seasonal and Altitudinal Variations in Atmospheric Transmittance. The differential solar radiation transmittance measurements yielded mean differential transmittance differences over the 464 meter surface air layer of 0.012 for the summer period May-August and 0.066 for the winter period November-February. The theoretical transmittance calculations yielded very similar results, assuming that most of the atmospheric dust in winter is confined to this surface layer, as opposed to summer when it is assumed to be more evenly distributed to about 3,000 meters.

Local meteorological data indicated that this assumption regarding seasonal changes in the vertical distribution of atmospheric dust is well justified. Although the inversion heights are essentially invariant over the year and generally lie within the first 500 meters above the ground, they are much more frequent in the winter. Furthermore, calculations of the mean monthly maximum mixing height indicate that when the inversions do break, the surface generated dust can rise only slightly above the 500 meter level in winter, while in summer it can ascend to 3,000 meters and generally be removed from the city. In the winter, however, it remains trapped in the surface layer for greater periods of time.

SUMMARY AND CONCLUSIONS:

A method for calculating the transmittance of the atmosphere for solar radiation was developed. Assuming a constant dust load in the atmosphere, it was found to be equally as accurate for individual clear days as it was for long-term monthly averages. The use of the method in conjunction with differential transmittance measurements made at the ground surface and 464 meters aloft confirmed the existence of a surface generated dust layer which is statistically stagnant in the winter, but rises and is generally moved laterally away from the city in summer. Local meteorological data also supported this conclusion.

REFERENCES:

1. Houghton, H. G. On the annual heat balance of the northern hemisphere. J. Meteorol., 11:1-9. 1954.

2. Idso, S. B. Atmospheric attenuation of solar radiation. J. Atmos. Sci., 26:1088-1095. 1969.

3. Idso, S. B. The transmittance of the atmosphere for solar radiation on individual clear days. J. Appl. Meteorol., 9: In press. 1970.

4. Idso, S. B., and Kangieser, P. C. Seasonal changes in the

vertical distribution of dust in the lower troposphere. J. Geophys. Res. Submitted. 1970.

5. McDonald, J. E. Direct absorption of solar radiation by atmospheric water vapor. J. Meteorol., 17:319-328. 1960.

PERSONNEL: Sherwood B. Idso

CURRENT TERMINATION DATE: October 1971

Table 1. Mean monthly clear-day values of atmospheric transmittance for solar radiation, as calculated by three different methods and as measured at Phoenix, Arizona.

Month	Houghton	McDonald	Dust Corrected	Measured
Jan	0.731	0.754	0.772	0.768
Feb	0.757	0.778	0.790	0.798
Mar	0.777	0.796	0.797	0.805
Apr	0.787	0.806	0.799	0.800
May	0.796	0.813	0.802	0.795
June	0.789	0.809	0.797	0.789
July	0.748	0.778	0.765	0.758
Aug	0.739	0.770	0.759	0.757
Sep	0.756	0.782	0.776	0.771
Oct	0.759	0.782	0.784	0.773
Nov	0.737	0.760	0.772	0.766
Dec	0.727	0.750	0.768	0.752
Year	0.758	0.781	0.782	0.778

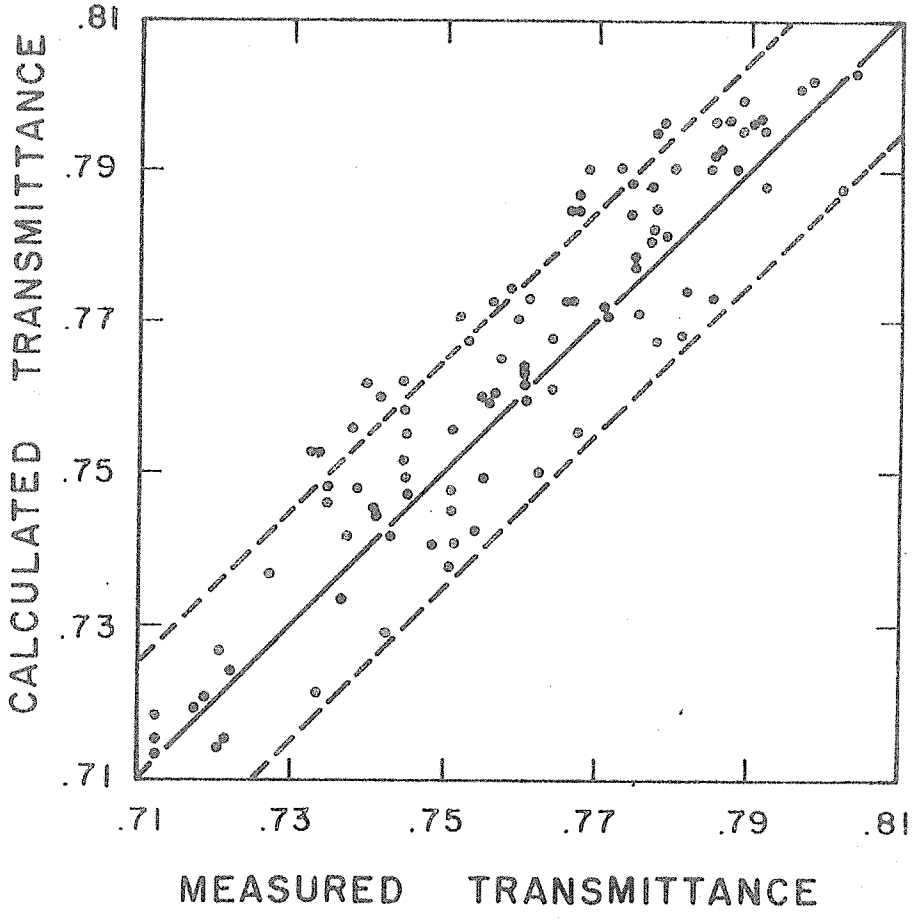

Figure 1. Calculated versus measured atmospheric transmittance for solar radiation for every clear day of the year period July 1968 - June 1969 at Phoenix, Arizona.

APPENDIX I

SUMMATION OF IMPORTANT FINDINGS

SWC-012-gG-1 METHODS FOR WATER QUALITY IMPROVEMENT AND ITS STORAGE UNDERGROUND

Nitrogen removal rates of 80% continued to occur with 2-3 week inundation periods at the Flushing Meadows Project where Phoenix sewage is reclaimed by ground-water recharge with infiltration basins. Grassed basins not only yielded higher infiltration rates than nonvegetated or gravel covered basins, they also yielded higher nitrogen removal. The nitrogen removal patterns in the field could be duplicated in laboratory columns. Gas chromatography studies on the columns and analysis of the soil from the recharge basins indicated that a significant amount of the nitrogen removed was stored in the soil, probably due to a reaction of ammonia with organic matter under anaerobic conditions. Nitrogen removal in the columns became less effective with inundation longer than 1 month and ceased completely after three months continuous inundation. Soil percolation at Flushing Meadows gave essentially complete removal of biochemical oxygen demand and fecal coliforms. Phosphates were reduced by 90% and fluorides by 60%. Cost of reclaiming water in a full-scale recharge system is estimated to be $5 per acrefoot. (WCL 67-4, 68-3)

An equation has been developed from basic flow theory that predicts experimentally observed drainage-time relationships better than previously published equations. Its upper limit is the familiar Young's equation, and its lower limit is a two-parameter equation. This latter equation was first found when statistically fitting drainage-time relationships. It is useful in predicting the hydraulic conductivity and total volume of drainage from soil columns. (WCL 66-1).

Field studies have demonstrated the importance of asphalt sources in determining the durability of sprayed asphalt catchments for water harvesting. Three plots near Phoenix, Arizona, treated with a single application of sprayed Venezuelan asphalt, are still producing 45% rainfall runoff 5 years after installation. Similar catchments constructed with California asphalt have always failed in less than 2 years. (WCL 60-7)

Exact mathematical solutions to equations used for estimating the pH's of Na- and Ca-carbonate solutions and their combinations gave more reliable results than the simplified versions. By further extension of the theoretical formulations and computational techniques, the assocation of Na and K cations in forming ion-pairs with anions commonly found in water was demonstrated. The chemical status of surface, irrigation and groundwater relative to sodium, potassium, calcium bicarbonate, carbonate and sulfate ions can now be defined more adequately with the theoretical model and experimental constants developed in this study. (WCL 64-6)

Substantiating theory, white covers were shown to be more effective in reducing evaporation than green or black covers of the same size and material. Approximately 80% of the surface area, of three 2.1-m diameter insulated evaporation tanks, was covered with white, green, and black butyl rubber during June 1969 at Phoenix, Arizona. The white, green, and black covers suppressed evaporation by 75, 68, and 62%, respectively, as compared to an open tank. These results demonstrate the importance of considering color when designing covers to reduce evaporation. (WCL 67-3)

SWC-019-gG-3 EFFICIENT IRRIGATION AND AGRICULTURAL WATER USE

Water metering flumes can now be designed by computer to accommodate many channel shapes and flow rates without conformance to arbitrary standard sizes. The flumes are proportioned so that the resulting flow will conform to rigorous mathematical analysis. Originally limited to flumes constructed from hydraulically smooth materials, the computer computations can now account for rough-surfaced materials, such as concrete. The flexibility in size, shape, and construction materials will permit flow measurements of irrigation deliveries, storm drainage and sewerage discharge at nominal cost with an accuracy within $\pm$ 2%. (WCL 67-1)

APPENDIX II

LIST OF PUBLICATIONS PUBLISHED AND MANUSCRIPTS PREPARED IN 1969

SWC-012-gG-1 Methods for water quality improvement and its storage underground.

Published:

	MS No.
Bouwer, Herman. Salt balance, irrigation efficiency, and drainage design. Jour. Irrig. & Drain. Div., Amer. Soc. Civil Engin. Proc. 95(IR 1):153-170. 1969.	248
Bouwer, Herman. Water quality improvement by ground-water recharge. Second Seepage Symposium Proc., Phoenix, Ariz., 25-27 March 1968. ARS 41-147. Pp. 23-27. April 1969.	255
Bouwer, Herman. Putting waste water to beneficial use - The Flushing Meadows project. 1968 Arizona Watershed Symposium Proc., Phoenix, Ariz. 18 Sept. 1968. Pp. 25-30. 1969.	268
Bouwer, Herman. Infiltration of water into nonuniform soil. Jour. Irrig. & Drain. Div., Amer. Soc. Civil Engin. Proc. 95(IR 4):451-462. 1969.	276

Prepared:

Bouwer, Herman. Ground-water recharge design for renovating waste waters. Jour., Sanitary Engin. Div., Amer. Soc. Civil Engin. Proc. (In press)	285

MS No.

SWC-018-gG-2 Increasing and conserving farm water supplies.

Published:

Bouwer, Herman. Theory of seepage from open channels. Chap. in 'Advances in Hydroscience', Vol. V. (V. T. Chow, Ed.) Academic Press, New York, 1969. Pp. 121-170. 197

Bouwer, Herman. Planning and interpreting soil permeability measurements. Jour. Irrig. & Drain. Div., Amer. Soc. Civil Engin. Proc. 95(IR 3):391-402. 1969. 219

Bouwer, Herman, and Rice, R. C. Review of methods for measuring and predicting seepage. Second Seepage Symposium Proc., Phoenix, Ariz., 25-27 March 1968. ARS 41-147. Pp. 115-120. April 1969. 254

Cooley, Keith R. and Myers, L. E. Water harvesting and storage. Proc., Seminar on Modifying the Soil and Water Environment for Approaching the Agricultural Potential of the Great Plains. Kansas State Univ., Manhattan, Kansas. March 17-19, 1969. Pp. 23-33. 282

Fink, Dwayne H., and Myers, L. E. Synthetic hydrophobic soils for harvesting precipitation. Symposium on Water-repellent Soils Proc., Univ. of Calif. at Riverside, May 6-10, 1968. Edited by L.F. DeBano and John Letey. Pp. 221-240. 1969. 261

Frasier, Gary W., and Myers, L. E. Digest: Stable Alkanol Dispersion to Reduce Evaporation. Trans., Amer. Soc. Civil Engin. 134:131. 1969. 293

Lagerwerff, J. V., Nakayama, F. S., and Frere, M. H. Hydraulic conductivity and swelling of soils. Soil Sci. Soc. Amer. Proc., 33(1):3-11. 1969. 216

MS No.

Myers, Lloyd E. Precipitation runoff inducement. Symposium on Water Supplies for Arid Regions Proc., Tucson, Ariz., 1-2 May 1967. CODAZR, AAAS, Contribution No. 10, Pp. 22-30. 1969. 210

Myers, Lloyd E. Saving water with asphalt. Div. of Petroleum Chem.,Inc., Amer. Chem. Soc. Symposium Proc., Atlantic City, N.J., 8-13 Sept 1968. Sect. C - New Uses for Asphalt. (C170-C173). 1969. 258

Myers, Lloyd E., Gen. Chairman & Editor. Second Seepage Symposium Proc., Phoenix, Ariz., 25-27 March 1968. ARS 41-147. (Agric. Res. Serv., USDA) April 1969. 264

Myers, Lloyd E., and Frasier, Gary W. Creating hydrophobic soil for water harvesting. Jour. Irrig. & Drain. Div., Amer. Soc. Civil Engin. Proc. 95(IR 1): 43-54. 1969. 227

Myers, Lloyd E., and Reginato, Robert J. Current seepage reduction research. Second Seepage Symposium Proc., Phoenix, Ariz., 25-27 March 1968. ARS 41-147. Pp. 75-78. April 1969. 251

Nakayama, F. S. Theoretical consideration of the calcium sulfate-bicarbonate-carbonate interrelation in soil solution. Soil Sci. Soc. Amer. Proc. 33(5):668-672. 1969. 277

Nakayama, F. S., and Rasnick, B. A. Bicarbonate complexes of barium and strontium. Jour. Inorg. & Nuclear Chem. 31(11):3491-3494. 1969. 278

MS No.

Nielsen, D. R., and Jackson, Ray D. Changes in water quality during seepage. Second Seepage Symposium Proc., Phoenix, Ariz., 25-27 March 1968. ARS 41-147. Pp. 8-13. April 1969. 252

Rice, Robert C. A fast response field tensiometer system. Trans., Amer. Soc. Agric. Engin. 12(1):48-50. 1969. 234

Van Bavel, C. H. M. Physical factors determining water use by crops. First Pan American Soil Conserv. Cong. Proc., Sao Paulo, Brazil, April 1966. Pp. 579-584. 1969. 162

Van Bavel, C. H. M. The three-phase domain in hydrology. UNESCO Symposium on "Water in the Unsaturated Zone" Proc., Wageningen, Holland, June 1966. (P. E. Rijtema and H. Wassink, Eds.) Vol. I, Pp. 23-32. 1969. 168

Van Bavel, C. H. M. Summary of papers presented in Section I-b of UNESCO Symposium on "Water in the Unsaturated Zone", Wageningen, Holland, June 1966. Symposium Proceedings (P. E. Rijtema and H. Wassink, Eds.) Vol. I, Pp. 287-291. 1969. 183

Watson, K. K., and Whisler, Frank D. A semi-numerical approach for determining the hydraulic conductivity of unsaturated porous material. Third Australasian Conf. on Hydraulics and Fluid Mechanics Proc., Sydney, Aust. 1968. Pp. 46-50. 1969. 266

Whisler, Frank D. Analyzing steady-state flow in an inclined soil slab. Soil Sci. Soc. Amer. Proc. 33(1):19-25. 1969. 217

Whisler, Frank D., and Watson, K. K. Analysis of infiltration into draining porous media. Jour. Irrig. & Drain. Div., Amer. Soc. Civil Engin. Proc. 95(IR 4): 481-491. 1969. 273

Prepared: MS No.

Cooley, Keith R. Energy relationships in the design of floating covers for evaporation reduction. Water Resources Research. (Submitted for publication). 302

Cooley, Keith R. Evaporation from open water surfaces in Arizona. Univ. of Ariz. Ext. Serv. Bul. (Approved for publication) 304

Fink, Dwayne H. Water repellency and infiltration resistance of organic-film coated soils. Soil Sci. Soc. Amer. Proc. (In press). 290

Frasier, Gary W., and Myers, Lloyd E. Protective spray coatings for water harvesting catchments. Trans., Amer. Soc. Agric. Engin. (In press). 274

Jackson, Ray D., and Whisler, Frank D. Approximate equations for vertical non-steady state drainage: I. Theoretical approach. (Approved for publication). 291

Myers, Lloyd E. Opportunities for water salvage. Civil Engineering. (In press). 283

Myers, Lloyd E. Water conservation for food and fiber production in arid lands. Chap. In "Food, Fiber and the Arid Lands." Amer. Assoc. Adv. Sci. and the Univ. of Ariz. Press. (In press). 300

Myers, Lloyd E., and Frasier, Gary W. Evaporation reduction with floating granular materials. Jour. Irrig. & Drain. Div., Amer. Soc. Civil Engin. Proc. (Submitted for publication). 295

Myers, Lloyd E., and Frasier, Gary W. Digest: Creating hydrophobic soil for water harvesting. Trans., Amer. Soc. Civil Engin. (Submitted for publication) 297

MS No.

Myers, Lloyd E., Frasier, Gary W., and Griggs, John R. Digest: Sprayed asphalt pavements for water harvesting. Trans., Amer. Soc. Civil Engin. (Approved for publication). 289

Nakayama, F. S. Hydrolysis of $CaCO_3$, Na_2CO_3 and $NaHCO_3$ and their combinations in the presence and absence of CO_2. Soil Sci. (In press). 294

Nakayama, F. S. Sodium bicarbonate and carbonate ion-pairs and their relation to the estimation of the first and second dissociation constants of carbonic acid. Jour. Phys. Chem. (Submitted for publication). 305

Reginato, Robert J., and Stout, Karl. Temperature stabilization of Gamma Ray transmission equipment. Soil Sci. Soc. Amer. Proc. (NOTE). (In press). 288

Whisler, Frank D., and Bouwer, Herman. Comparison of methods for calculating vertical drainage and infiltration for soils. Jour. Hydrol. (In press). 280

Whisler, Frank D., and Jackson, Ray D. Approximate equations for vertical non-steady state drainage: II. Statistical and empirical approach. (Submitted for approval). 292

Whisler, Frank D., Klute, Arnold, and Millington, Richard J. Analysis of radial, steady-state solution and solute flow. Soil Sci. Soc. Amer. Proc. (Submitted for publication). 298

MS No.

SWC-019-gG-3 Efficient irrigation and agricultural water use.

Published:

Erie, Leonard J., and French, O. F. Growth, yield, and yield components of safflower as affected by irrigation regimes. Agron. Jour. 61(1):111-113. 1969. 237

Erie, Leonard J., and French, O. F. Water management on fall-planted sugar beets in the Salt River Valley of Arizona. Trans., Amer. Soc. Agric. Engin. 11(6):792-795. 1968. 250

Haise, Howard R., Kruse, Gordon E., and Erie, Leonard J. Automating surface irrigation. Agric. Engin. 50(4):212-216. 1969. 257

Hilgeman, R. H., Ehrler, W. L., Everling, C. E., and Sharp, H. O. Apparent transpiration and internal water stress in Valencia oranges as affected by soil water, season and climate. First Internatl. Citrus Symp. Proc., March 1968, Riverside, Calif. Vol. 3, Pp. 1713-1723. 1969. 259

Idso, Sherwood B., A holocoenotic analysis of environment-plant relationships. Univ. of Minn. Agric. Expt. Sta. Tech. Bul. 264. 147 pp. 1968. 230

Idso, Sherwood B. A theoretical framework for the photosynthetic modeling of plant communities. Advan. Front. Plant Sci. (India) 23:91-118. 1969. 270

Idso, Sherwood B. Atmospheric attenuation of solar radiation. Jour. Atmos. Sci. 26(5):1088-1095. 1969. 281

MS No.

Idso, Sherwood B., Baker, D. G., and Blad, B. L. Relations of radiation fluxes over natural surfaces. Qtrly. Jour. Royal Meteorol. Soc. 95(404:244-257. 1969. 232

Idso, Sherwood B., and Jackson, Ray D. Comparison of two methods for determining infrared emittance of bare soils. Jour. Appl. Meteorol. 8(1):168-169. 1969. 260

Idso, Sherwood B., and Jackson, Ray D. Thermal radiation from the atmosphere. Jour. Geophys. Res. 74(23):5397-5403. 1969. 275

Jackson, Ray D., and Idso, Sherwood B. Ambient temperature effects in infrared thermometry. Agron. Jour. 61(2):324-325. 1969. 253

Replogle, John A. Target meters for velocity and discharge measurements in open channels. Trans., Amer. Soc. Agric. Engin. 11(6):854-856. 1968. 236

Replogle, John A. Flow measurement with critical depth flumes. Internatl. Comm. on Irrig. and Drainage, 7th Cong. Proc., Mexico City, April 1969. Ques. 24, R. 15. Pp. 24.215-24.235. 256

Prepared:

Erie, Leonard J. Digest - Management: A key to irrigation efficiency. Trans., Amer. Soc. Civil Engin. (In press). 286

Idso, Sherwood B. The transmittance of the atmosphere for solar radiation on individual clear days. Jour. Appl. Meteorol. (In press). 287

MS No.

Idso, Sherwood B. The relative sensitivities of polyethylene-shielded net radiometers for short- and long-wave radiation. Rev. Sci. Instruments. (Submitted for publication). 301

Idso, Sherwood B., and De Wit, C. T. Light relations in plant canopies. Appl. Optics. (In press). 279

Idso, Sherwood B., and Kangieser, P. C. Seasonal changes in the vertical distribution of dust in the lower troposphere. Jour. Geophys. Res. (In press). 296

Replogle, John A. Modifying elbow meters to totalize flow. Jour. Irrig. and Drain. Div., Amer. Soc. Civil Engin. Proc. (Submitted for publication). 299

Replogle, John A. Flow meters for water resources management. 5th Amer. Water Resources Conf. Proc., San Antonio, Tex. 24-30 Oct 1969. (Approved for publication). 306

APPENDIX III

SUMMARY TABLE OF STATUS OF RESEARCH OUTLINES

	Title	Code
SWC-012-gG-1	Methods for water quality improvement and its storage underground	
Ariz-WCL-66-1	Experimental and analytical studies of the flow and oxygen regimes in soil intermittently inundated with low quality water	B
Ariz-WCL-67-4	Waste-water renovation by spreading treated sewage for groundwater recharge	B
Ariz-WCL-68-3	Column studies of the chemical, physical and biological processes of wastewater renovation by percolation through the soil	B

	Title	Code
SWC-018-gG-2	Increasing and conserving farm water supplies	
Ariz-WCL-60-7	Soil treatment to reduce infiltration and increase precipitation runoff	B
Ariz-WCL-61-4	Measurement and calculation of unsaturated conductivity and soil-water diffusivity	C
Ariz-WCL-64-3	Clay dispersants for the reduction of seepage losses from reservoirs	B
Ariz-WCL-64-4	Water-borne sealants to reduce seepage losses from unlined channels and reservoirs	D
Ariz-WCL-64-6	Dispersion and flocculation of soil and clay materials as related to the Na and Ca status of the ambient solution	B
Ariz-WCL-65-2	Materials and methods for water harvesting and water storage in the State of Hawaii	B
Ariz-WCL-66-3	Study of unsaturated, two-dimensional soil water flow using an analog computer	C
Ariz-WCL-67-2	Physical and chemical characteristics of hydrophobic soils	B
Ariz-WCL-67-3	Use of floating solid and granular materials to reduce evaporation from water surfaces	B
Ariz-WCL-68-1	Evaporation of water from soil	B
Ariz-WCL-68-2	Fabricated-in-place, reinforced reservoir linings	B

	Title	Code
SWC-019-gG-3	Efficient irrigation and agricultural water use	
Ariz-WCL-58-2	Consumptive use of water by crops grown in Arizona	B
Ariz-WCL-60-2	Dynamic similarity in elbow flow meters	B
Ariz-WCL-62-10	Plant response to changes in evaporative demand and soil water potential, as shown by measurements of leaf resistance, transpiration, leaf temperature, and leaf water content	B
Ariz-WCL-65-3	Integrating velocity profile meters	C
Ariz-WCL-66-2	Irrigation outlet structures to distribute water onto erosive soils	B
Ariz-WCL-66-4	Automation of water distribution systems for surface irrigation	C
Ariz-WCL-67-1	Flow measurement in open channels with critical depth flumes	B
Ariz-WCL-68-4	Water stresses in plants	C
Ariz-WCL-68-5	Assessing the energy environment of plants	B
Ariz-WCL-68-6	Simulation of plant communities for determining water use efficiency	C

	Title	Code
PL 480 Projects		
A10-SWC-20	Biology and consumptive water use of range plants under desert conditions	C
A10-SWC-36	Runoff inducement in arid lands	C
A10-SWC-54	Optimum utilization of surface and subsurface water facilities in water resources systems	C
A10-SWC-75	Infiltration and rainfall runoff as affected by natural and artificial surface crusts	C